Impact of chronic liver inflammation on adaptive immune responses to viral infection

Lisa Mareike Assmus

ORCID ID:

0000-0002-4859-8334

Submitted in total fulfillment of the requirements of the joined degree of

Doctor of Philosophy (PhD)

of the Medical Faculty

The Rheinische Friedrich-Wilhelms-Universität Bonn

and

The Department of Microbiology and Immunology

The University of Melbourne

Bonn/Melbourne, 2020

from Holzminden, Germany

Performed and approved by the Medical Faculty of The Rheinische Friedrich-Wilhelms-Universität Bonn and The University of Melbourne

1. Supervisor: Prof. Natalio Garbi

2. Supervisor: Prof. Nicole La Gruta

Date of submission: September 2019

Date of oral examination: January 2020

Institute of Experimental Immunology, Bonn
Director: Prof. Dr. med. Christian Kurts

Department of Microbiology and Immunology, University of Melbourne,
Melbourne, Australia

Table of contents

Abbreviations

A		
	ALT	Alanine aminotransferase
	APC	Antigen-presenting cell
	a-SMA	Alpha-smooth muscle actin
	AST	Aspartate transaminase
	ATP	Adenosine tri-phosphate
B		
	BAL	Bronchoalveolar lavage
	BDL	Bile duct ligation
	BEC	Biliary epithelial cell
	BM	Bone Marrow
	BT	Bacterial translocation
C		
	CD	Cluster of differentiation
	cDC	Conventional dendritic cell
	CDR	Complementary determining region
	CFSE	Carboxyfluorescein succinimidyl ester
	CMV	Cytomegalovirus
	CTL	Cytotoxic T lymphocyte
	CTLA4	Cytotoxic T-lymphocyte-associated antigen 4
	CTV	Cell trace violet
D		
	DAMP	Danger-associated molecular pattern
	DC	Dendritic cell
	DG	Dystroglycan
	DNA	Deoxyribonucleic acid
E		

ECM	Extracellular matrix
ETC	Electron transport chain

F

FAO	Fatty acid oxidation

G

GI	Gastrointestinal
GP	Glycoprotein

H

HA	Hemagglutinin
HAV	Hepatitis A Virus
HBV	Hepatitis B Virus
HCMV	Human cytomegalovirus
HC	Hepatocyte
HCV	Hepatitis C Virus
HIV	Human immunodeficiency virus
HSC	Hepatic stellate cell

I

IAV	Influenza A Virus
ID	Immunodominance
IFN	Interferon
IFNAR	Interferon-a/b receptor
IL	Interleukin
ISG	Interferon-stimulated genes

K

KC	Kupffer cell

L

LAG3	Lymphocyte activating-gene 3
LC	Langerhans cells
LCMV	Lymphocytic choriomeningitis virus
LN	Lymph node

	LPS	Lipopolysaccharide
M		
	M1	Matrix protein 1
	MAPK	Mitogen-activated proteinkinase
	MCMV	Murine cytomegalovirus
	MDA-5	Melanoma differentiation-associated protein 5
	MHC	Major histocompatibility complex
	MPEC	Memory-precursor effector cell
	MTDR	Mitotracker deep red
	MTG	Mitotracker green
N		
	NA	Neuraminidase
	NASH	Non-alcoholic steatohepatitis
	NFAT	Nucelar factor of activated T cells
	NF-kB	Nuclear factor kappa-light-chain-enhancer of activated B cells
	NK	Natural killer cell
	NP	Nucleoprotein
O		
	OVA	Ovalbumin
	OXPHOS	Oxidative phosphorylation
P		
	PA	Polymerase acidic protein
	PAMP	Pattern-associated molecular pattern
	PBS	Phosphate buffered saline
	PCR	Polymerase chain reaction
	pDC	Plasmacytoid dendritic cell
	PD-1	Programmed death 1
	PFA	Paraformaldehyde

PGC1-α	Peroxisome proliferator-activated receptor-gamma coactivator-1 alpha
PI3K	Phophatidylinositaol-3-triphosphate
PKC	Protein kinase C
PRR	Pattern recognition receptor
R	
RIG-I	Retinoic-acid inducible gene I
ROS	Reactive oxygen species
RNA	Ribonucleic acid
S	
SLEC	Short-lived effector cell
SPF	Specific pathogen free
STING	Stimulator of interferon genes
T	
TCA	Tricarboxylic acid
TCR	T cell receptor
TF	Transcription factor
TGF	Transforming growth factor
TIM3	T-cell immunoglobulin and mucin domain-containing protein 3
TLR	Toll-like receptor
TNF	Tumor necrosis factor
TRAIL	TNF related apoptosis inducing ligand

List of tables

List of figures

Abstract

A common complication in patients suffering from chronic liver inflammation and fibrosis is the enhanced susceptibility to viral infections and weak responses to vaccination, which are associated with significant co-morbidities. To unravel the cellular and molecular mechanisms underlying the impaired adaptive immune response during liver fibrosis, we investigated the T cell-mediated immune responses to lymphocytic choriomenigitis virus (LCMV) infection, as well as in response to OVA/PolyI:C vaccination. Using the bile duct ligation (BDL) murine model of chronic liver inflammation and fibrosis, we found that chronic liver damage is associated with persistence of infection, recapitulating the clinical situation in humans. Hallmarks of the defective anti-viral immunity in these mice were reduced expansion of LCMV-specific CD4+ and CD8+ T cells, decreased expression of IFNγ and TNFα, as well as an elevated co-expression of the exhaustion marker PD1 together with LAG3 and TIM3 in virus-specific T cells from the spleen and liver. The reduced number of LCMV-specific CD4+ and CD8+ T cells are due to decreased proliferation as well as increased apoptosis among SMARTA T cells. Additionally, LCMV-specific CD4+ and CD8+ T cells display reduced mitochondrial fitness, characterized by a higher proportion of cells containing depolarized (i.e. dysfunctional) mitochondria, and producing high levels of superoxide among SMARTA and P14 T cells from mice with liver fibrosis. After OVA/PolyI:C vaccination antigen-specific CD4+ and CD8+ T cells were similarly reduced in numbers in mice with liver fibrosis and displayed reduced production of IFNγ, TNFα and IL-2. Interestingly, endogenous OVA-specific CD8+ T cells, as well as transferred OT-I T cells also show severe signs of exhaustion after vaccination, which manifested in elevated levels and co-expression of PD-1 and LAG3, as well as PD-1 and TIM3 in mice with liver fibrosis. The future goal of this project is to identify key molecular pathways induced by chronic liver damage that can be therapeutically modulated to promote anti-viral immunity and to improve

vaccination responses in patients suffering from chronic liver inflammation and fibrosis.

Declaration

The work presented in this thesis was conducted both at The Rheinische Friedrichs-Wilhelms-Universität Bonn, in the laboratory of Dr Zeinab Abdullah and at Monash University, in the laboratory of Professor Nicole La Gruta. The research work was funded by grants from the Deutsche Forschungsgemeinschaft (GRK2168) and the National Health and Medical Research Council (NHMRC) and Australian Research Councli (ARC). I was supported by the Melbourne International Fee Remission Scholarship.

This is to certify that,

I) the thesis comprises only my original work towards the joined PhD from The Rheinische Friedrich-Wilhelms-Universität Bonn and The University of Melbourne, except where indicated in the preface;

II) due acknowledgement has been made in the text to all other material used; and

III) this thesis is fewer than the maximum word limit in length, exclusive of tables, maps, bibliographies and appendices.

Lisa Mareike Assmus

Preface

My contribution to the experiments described in the results chapters of this thesis was as follows:

Chapter 3: 80%
Chapter 4: 100%
Chapter 5: 85%

I gratefully acknowledge the contribution of others to the experiments presented within this thesis:

Chapter 3: Dr Zeinab Abdullah, Dr Philipp Hackstein, Patrick Schuhmachers

Chapter 5: Xavier Sng

Acknowledgements

The completion of this thesis is nothing less than a collaborative effort and evidence to the fact that I had an absolutely amazing support network that enabled me to complete this work. I had the pleasure of working with and be supported by an incredible group of friends, colleagues and supervisors, as well as an incredible supportive and understanding family. All of you have my deepest gratitude.

Firstly, a big thanks goes to Zeinab, who not only gave me an amazing project to work on throughout the last years, but also never falls short of providing advice and support. Thank you for not only being a great supervisor, but also always believing in me (even when I sometimes struggled to do so myself). Thank you for giving me the opportunity to spend a year in Melbourne; it will always stay one of the most educating experiences in my life, which allowed me to grown not only at a personal level, but also as a scientist.

A big thanks also goes to Nicole, who made me feel immensely welcome, when I was the farthest from home I had ever been. Thank you for giving me such an amazing second project, when things didn't go according to plan. It proved to be an amazing opportunity to learn something new and exciting and I greatly appreciate it. Thanks to all your lab members, Xavier, Claerwen, Kylie, Pirooz and all the others, who made me feel welcome and were always there if I needed help.

Another big thanks goes to my colleagues and friends in the lab in Bonn. Philipp, Alisa, Helena, Giannis, Sara, Kostas, Celia, Salie and all the others, who make the lab an exciting and fun place to be. Thanks for the lively discussions, your support and always having a minute to spare, if I just needed to talk. I look forward to continue working with you.

Rebecca – everything I could write, would probably fall short of truly expressing my gratitude for your friendship. You are not only one of the best colleagues a person could wish for, but also one of my dearest friends. I know you went above and beyond for me during the last 3 years. Thank you for your continuous help, your advice and your friendship. You are one of the kindest persons I have ever met. Don't ever change!

David – I can't thank you enough for your love and support since the day we met. You continue to be my calming influence and always bring me back to reality, when I lose my head in the clouds once again or get lost in the science of it all. Thank you for staying by my side, even when I was half a world away in Australia. Thank you for understanding what it means to sometimes work odd hours as a scientist and thank your for never once complaining, while always being there for me no matter what. I love you.

Last but not least, my family. Mama, Papa, Lukas und Hanna, danke für alles! Danke, dass ihr mir zu jeder Tages- und Nachtzeit zugehört habt, wenn ich euch gebraucht habe und danke, dass ihr euch meine Erzählungen angehört habt, wenn ich wieder leidenschaftlich von der Wissenschaft und neuen Projekten berichtet habe. Mama, danke, dass du mich überzeugt hast den Schritt zu wagen nach Australien zu gehen. Die Lebenserfahrung war es mehr als wert. Ohne euch hätte ich diese Doktorarbeit bestimmt nicht durchziehen können, deshalb ist sie teilweise auch euer Verdienst. Ich bin froh, euch als Familie zu haben und mich immer auf euch verlassen zu können! Danke!

List of publications

Hackstein* C.-P., Assmus* L. M., Welz M., Klein S., Schwandt T., Schultze J., Förster I., Gondorf F., Beyer M., Kroy D., Kurts C., Jonel T., Kastenmüller W., Knolle# P. A., Abdullah# Z., 2016, Gut microbial translocation corrupts myeloid cell function to control bacterial infection during liver cirrhosis, *Gut*, 0:1–12. doi:10.1136/gutjnl-2015-311224

Namineni S., O'Connor T., Faure-Dupuy S., Johansen P., Riedl T., Liu K., Xu H., Shinde P., Li F., Pandyra A., Sharma P., Ringelhan M., Muschaweckh A., Borst K., Blank P., Lamapl S., Durantel D., Farhat R., Weber A., Lenggenhager D., Kundig T. M., Staeheli P., Protzer U., Wohlleber D., Holzmann B., Binder M., Breuhahn K., Assmus L. M., Nattermann J., Abdullah Z., Rolland M., Dejardin E., Lang P. A., Lang K. S., Karin M., Lucifora J., Kalinke U., Knolle P., Heikenwaelder M., 2019; A dual role for hepatocyte-intrinsic canonical NF-κB signaling in virus control, *Journal of Hepatology*, accepted

*Equal contribution
Senior authors

Chapter 1

Literature Review

1 Introduction

1.1 Liver fibrosis

Chronic liver inflammation can arise from many different insults to the liver such as viral infections like hepatitis B and C, alcoholism, NASH (non-alcoholic steatohepatitis) or drug induced injury (Henderson and Iredale, 2007). Persistent liver inflammation always precedes the development of liver fibrosis, which is a wound healing response initiated upon hepatocyte injury, during which the liver parenchyma is continuously replaced by scar tissue in order to enable the liver to heal (Bataller and Brenner, 2005) (Marra, 1999). Scar tissue formation is characterized by the deposition of extracellular matrix (ECM) components such as α-smooth muscle actin (a-SMA), collagen type-I, proteoglycans and fibronectin, by activated hepatic stellate cells (HSCs) and represents a key characteristic of liver fibrosis, which is for the most part reversible once the stimulus inducing hepatocyte death ceases (Hernandez-Gea and Friedmann, 2011) (Zhou et al. 2014). In addition, the pathological inflammation associated with liver fibrosis disrupts liver homoestasis and its tolerogenic properties, which involve the filtration of microbial products arriving from the gut via the portal vein (Robinson et al. 2016) (Knolle and Thimme, 2014). As a consequence of the extensive scarring of the liver during fibrosis and cirrhosis, patients develop portal hypertension promoting bacterial translocation (BT) from the gut lumen (Teltschik et al. 2012). The translocation of bacterial products brings about the release of pro-inflammatory cytokines (cytokine storm), which further exacerbates the inflammatory condition of the liver and contributes to the increased susceptibility to infections observed in cirrhotic patients (Fernandez and Gustot, 2012) (Teltschik et al. 2012). The sustained inflammation leads to the abolishment of the liver's tolerogenic properties, which in turn promotes inflammation and causes the recruitment of a myriad of immune cells such as neutrophils and inflammatory monocytes into the liver from the circulation (Robinson et al. 2016) (Heymann et al. 2015). The release of pro-

inflammatory cytokines such as IL-1, IL-6 and TNFα, as well as the pro-fibrotic cytokine transforming growth factor beta (TGF-β) produced by infiltrating leukocytes and liver resident Kupffer cells (KCs), are key activators of HSCs in the liver (Robinson et al. 2016) (Seki and Schnabl, 2012). Upon activation, HSCs start proliferating and trans-differentiating into myofibroblasts, which are responsible for the deposition of ECM components such as α-SMA and type-I collagen, resulting in scarring of the liver and its loss of function (Robinson et al. 2016) (Henderson and Iredale, 2007). If hepatocyte injury persists and scar tissue continues to form, liver cirrhosis develops as a result (often over a time period of 20 to 40 years), which is irreversible in the majority of cases and associated with severe morbidity and mortality in patients (Hernandez-Gea and Friedmann, 2011) (Schuppan and Afdhal, 2008). Hence, liver cirrhosis marks the end-stage of liver diseases and necessitates a liver transplant in order to maintain liver function and prevent death (Bataller and Brenner, 2005) (Henderson and Iredale, 2007). At a global level liver diseases in general and liver cirrhosis in particular, account for 2 million and 1.16 million deaths respectively, each year and thereby constitute a severe health burden worldwide with an incidence that is continuously rising (Asrani et al. 2019) (Henderson and Iredale, 2007).

1.2 Chronic liver inflammation is associated with immune dysfunction

Liver cirrhosis has been well established as a risk factor for increased morbidity and mortality; however, its effects on the susceptibility to infection are just beginning to be understood (Nusrat et al. 2014). In the hospital setting, but also at the community level, cirrhosis patients are more likely to contract and suffer from bacterial, viral and fungal infections (Cheruvattath and Balan, 2007) (Fernández et al. 2002). Liver cirrhosis is associated with the disability of the immune system to protect against and to clear bacterial and viral infections (Avaniti et al. 2010). The immunosuppressive state of cirrhosis patients increases their morbidity and mortality in response to bacterial infections by a factor of four, of

which a total of 30% die within one month of infection (Arvaniti et al. 2010). Bacterial infections mark the primary cause of death in patients with liver cirrhosis, which seems to be due to impaired innate immune responses that fail to contain and eliminate the invading pathogens (Fernandez and Gustot, 2012). Previous studies suggested that the increased susceptibility in cirrhosis patients is due to the so-called immunoparalysis mediated by increased systemic levels of the pro-inflammatory cytokines such as IL-6 and TNFα in response to the translocation of bacteria from the gut (Fernandez and Gustot, 2012). The increased levels of pro-inflammatory cytokines such as IL-6 and TNFα, which are also seen during sepsis, can subsequently cause a so called compensatory anti-inflammatory syndrome, which describes a response to a severe inflammatory state that is thought to provide normal tissue homeostasis with a change to heal from inflammation induced damage (Byl et al. 1993) (Bone et al. 1997) (Ward et al. 2008). Hence, patients are much more susceptible to nosocomial infections and show increased mortality rates, which is due in part to impaired lymphocyte effector functions, as well as increased IL-10 production by KCs and decreased phagocytic activity of neutrophils in the context of liver cirrhosis (Rajkovic and Williams, 1986) (Abe et al. 2004) (Hackstein et al. 2016). Liver cirrhosis has a profound impact on the entire immune system, including the lymphocyte compartment and the production of effector molecules such as IFNγ, as well as the entire complement system, of which the majority of complement factors is synthesized by hepatocytes (Abe et al. 2004) (Homann et al. 1997) (Propst-Graham et al. 2007). The immunosuppressive phenotype associated with liver cirrhosis does also appear to negatively impact the development of long-lasting immune protection after vaccination against viral infections such as hepatitis B and A virus (Dumot et al. 1999) (Jacobs et al. 2005). The majority of data available on vaccine efficacy suggests that they lose their effectiveness with progression of liver disease, which would be in line with the immunosuppressive phenotype of liver cirrhosis patients and their increased susceptibility to infection (Leise and Talwalker, 2012). Likewise, latent viral

infections such as human cytomegalovirus (HCMV) are also often reactivated in immunocompromised patients resulting in severe disease and increased overall patient morbidity and mortality (Tanaka et al. 1992) (Lepiller et al. 2011) (Bayram et al. 2009).

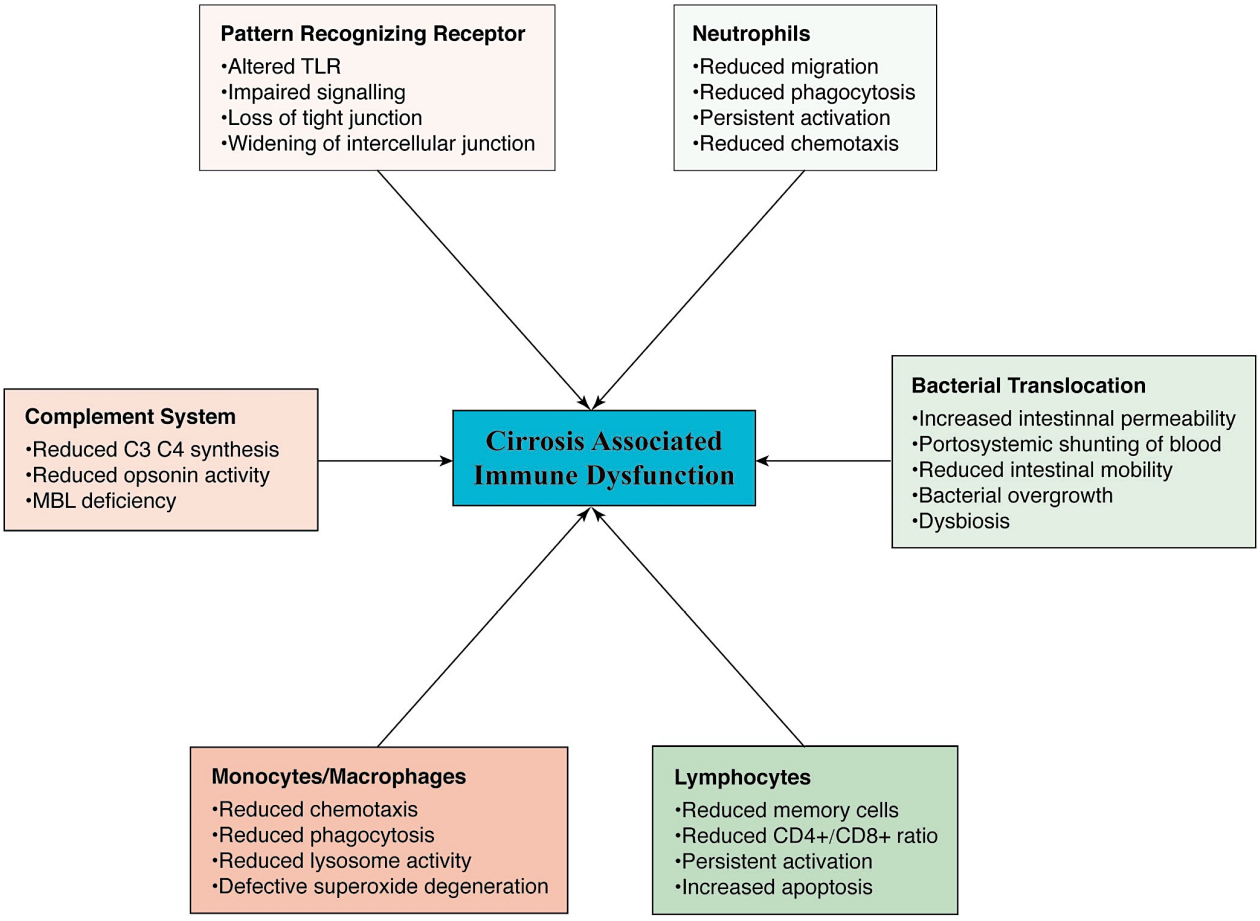

TLR:Toll Like Receptor, MBL:Mannose Binding Lectin

Figure 1: Broad immune dysfunction in patients with liver cirrhosis. Chronic liver inflammation and the associated development of liver cirrhosis are accompanied by a multitude of defects in all aspects of the immune system. Due to the extensive scarring of the hepatic tissue, portal hypertension ensues resulting a in increased gut permeability and the translocation of gut microbiota into the liver. Subsequently, both the innate and the adaptive branch of the immune system are impaired. This is reflected in a defective complement system due to reduced synthesis of complement factors by hepatocytes, as well as impaired function of myeloid cells, such as neutrophils, monocytes and macrophages. Additionally, T and B lymphocytes function is impaired, which is reflected in poor memory cell formation and long-term protection against invading pathogens or after vaccination.

Figure taken from Noor MT, Manoria P. Immune dysfunction in cirrhosis, *J Clin Transl Hepatol* 2017;5(1):50–58.doi: 10.14218/JCTH.2016.00056.

1.3 Reduced vaccination efficacy in patients with liver fibrosis

In addition to contributing to an increased susceptibility to infection, chronic liver inflammation and liver cirrhosis are also associated with decreased vaccine efficacy (Koff, 2001) (Keeffe, 2006). Several studies reported the association between liver cirrhosis and poor antibody responses after Hepatitis B and A virus (HBV) (HAV) vaccination (Keeffe, 2006). Compared to healthy individuals, cirrhosis patients were found to have reduced anti-HBV and HAV titers after vaccination (Loulergue et al. 2009) (Horlander et al. 1999) (Albillos et al. 2014). Cirrhosis patients are recommended to stick to a tighter vaccination schedule compared to persons without co-morbidities, as the immune response to vaccination decreases as liver cirrhosis advances (Leise and Talwalker, 2012) (Koff, 2019). Co-morbidities such as influenza or HAV infection can run a much more severe course in patients already suffering from chronic liver disease; hence extensive research is needed to assess vaccine efficacy in immunocompromised patients (Alter, 2012). Currently, clinicians recommend using inactive or killed-type vaccines instead of live attenuated vaccines in immunocompromised patients to avoid unnecessary risks in cirrhosis patients (Leise and Talwalker, 2012). These data suggest that cirrhosis patients are not only more susceptible to infection, but also may no be receiving the fully benefits of the current vaccination protocols. It therefore remains crucial to fully understand the underlying mechanisms behind the weak response observed in cirrhosis patients or individuals with chronic liver inflammation. This would greatly promote the development of more suitable therapeutic interventions and the design of more efficient vaccination strategies to prevent fatal co-morbidities and associated mortality, as well as improve patient quality of life.

1.4 Murine bile duct ligation model of chronic liver inflammation

Experimental animal models of chronic liver inflammation provide a tool to study the impact of hepatic inflammation on the function of immune cells and their response to vaccination and infection. The most commonly used models of fibrosis are mimicking toxin-induced liver damage by application of carbon tetra-chloride (CCL_4) and bile duct ligation (BDL) (Constandinou et al. 2005) (Tag et al. 2015). Both models feature key hallmarks of liver fibrosis and cirrhosis in patients, which are characterized by leukocyte infiltration into the liver, elevated nitric oxide levels in the serum, as well as overall liver and renal dysfunction, low blood glucose levels and sarcopenia (O'Brien et al. 2015). Ligation of the common bile duct (BDL) in mice represents a model of obstructive cholestasis, in which the healthy liver parenchyma is substituted by scar tissue due to chronic liver inflammation (Tag et al. 2015). Similarly to cirrhosis patients, BDL mice are more susceptible to both bacterial and viral infections and display impaired bacterial clearance of *Escherichia coli* or *Listeria monocytogenes*, which is accompanied by elevated levels of the anti-inflammatory cytokine IL-10 (Abe et al. 2004) (Hackstein et al. 2016).

Upon ligation of the common bile duct, toxic bile salts accumulate in the liver and induce apoptosis of hepatocytes in a Fas dependent manner by day 3 post BDL (Miyoshi et al. 1999). However, even in the absence of Fas signaling, hepatocyte death is induced in a Fas independent manner, albeit with a delay of approximately 7 days (Miyoshi et al. 1999). Hepatocyte damage is accompanied by signs of extensive liver injury, such as elevated levels of alanine aminotransferase (ALT) and aspartate transferase (AST), serum bilirubin and creatinin (O'Brien et al. 2015). The inflammatory conditions induced by hepatocyte death lead to the activation and trans-differentiation of HSCs into myofibroblasts, which are the predominant cell type responsible for laying down ECM components such as α-SMA and type I collagen to initiate a wound healing response (Marra, 1999) (Milani

et al. 1990). This process is initiated by cytokine mediators such as PDGF produced by hepatic KCs or TGFβ with is produced by granulocytes and KCs among others (Nakatsukasa et al. 1990) (Bataller and Brenner, 2005). Fibrogenesis is initiated as early as 8 hours post BDL, based on increased transcript levels of type I collagen, α-SMA and TGFβ (Gerogiev et al. 2008) (Aller et al. 2008). Other inflammatory cytokines such as IL-6 or TNFα accompany fibrogenesis and result in the recruitment of a myriad of immune cells, including monocytes, granulocytes and T and B lymphocytes (Gurjarl et al. 2003) (Baeck et al. 2014) (Georgiev et al. 2008) (Baeck and Tacke, 2014). If the inflammation is not resolved, BDL will results in extensive liver scarring, that mirrors the situation seen in cirrhosis patients (Tag et al. 2015) (O'Brien et al. 2015).

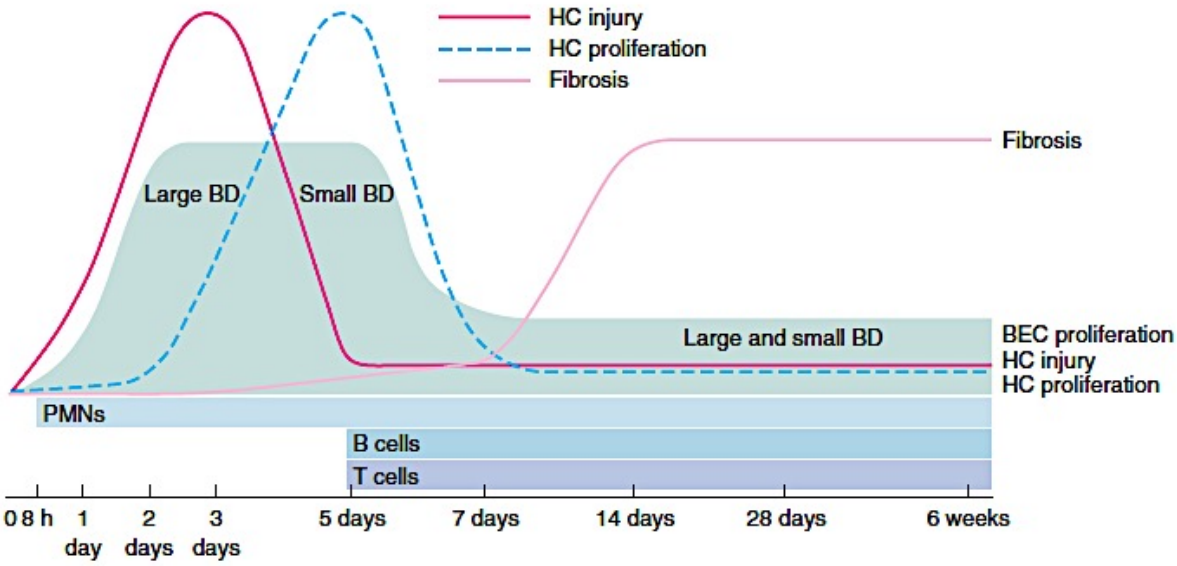

Figure 2: Ligation of the common bile duct disrupts liver homeostasis and function. BDL results in hepatocyte (HC) injury and proliferation upon the release of inflammatory mediators. Liver inflammation after BDL is accompanied by significant infiltration of leukocytes into the liver and biliary epithelial cell (BEC) proliferation in the large and small bile duct (BD), followed by T and B lymphocyte recruitment from day 5 post BDL onwards. Figure taken from Georgiev P., Jochum W., Heinrich S., Jang . H., Nocito A., Dahm F., Clavien P.-A., 2008, Characterization of time-related changes after experimental bile duct ligation, *British Journal of Surgery*, 95:646-56

1.5 The lymphocytic choriomeningitis virus (LCMV)

The lymphocytic choriomenigitis virus (LCMV) is a single stranded RNA virus of the family of *Arenaviridae*. LCMV contains a bi-segmented RNA genome, which is made up of a small (S) and a large (L) RNA segment (Singh et al. 1987). LCMV is one of the best-characterized models to study anti-viral immunity in mice. It is a non-cytopathic virus, whose natural host is the mouse and which is characterized by a strong adaptive immune response dependent on viral load, infection route and strain (Moskophidis et al. 1995). There are several strains of the LCMV, such as LCMV-Armstrong, WE, Docile and clone 13, which are characterized by minor differences in amino acid composition of the glycoprotein that determine cell tropism and the ability of the virus to persist (Moskophidis et al. 1995) (Bocharov, 1998). Infection of adult healthy mice with Armstrong or WE strains of LCMV elicits an effective CD8+ and CD4+ immune response that clears the virus by day 10 post infection (Matloubian et al. 1994) (Brooks et al. 2005). Sterile clearance of the virus is mainly achieved by a strong cytotoxic T lymphocyte (CTL) response (Moskophidis et al. 1995). In contrast, infection with Docile and clone 13 strains results in persistent infection, characterized by low immunopathology and impaired virus-specific CD4+ and CD8+ T cell-mediated immune responses (Brooks et al. 2010). Besides virus-specific CTLs, natural killer (NK) cells and anti-viral antibodies also contribute to the clearance of LCMV infection by killing of infected cells and neutralizing circulating viral particles, respectively (Bacharov, 1998). By these means an acute infection with LCMV-WE is combated and eliminated within 2 weeks of infection in an immunocompetent mouse, without signs of immunopathology and followed by the formation of efficient immunological memory (Moskopidis et al. 1995) (Marsland et al. 2005).

1.6 The innate immune response against LCMV

The innate immune system is a vital part of an organism's defense mechanisms against invading pathogens and provides a first line of defense. It comprises a variety of components, including mechanical barriers such as the skin, gastrointestinal (GI) and respiratory tracts, antimicrobial peptides, as well as various innate cell types (McDonald and Levy, 2019) (Hato and Dagher, 2015). Innate immune cells identify invading pathogens largely via various types of pattern recognition receptors (PRRs), which recognize pathogen-associated molecular patterns (PAMPs) or danger-associated molecular patterns (DAMPs) that arise from cellular stress, damage or cell death in the context of an infection (Abdullah and Knolle, 2014). TLRs, as well as cytosolic PRRs such as RIG-I, MDA5 or STING recognize DNA and RNA fragments of bacterial and viral origin in order to instigate an inflammatory response upon infection (Abdullah and Knolle, 2014). The majority of PRRs induces either inflammasome activation resulting in the production of the pro-inflammatory cytokines IL-1β and IL-18 or the initiation of a strong type I interferon (IFN) response (Abdullah and Knolle, 2014). As a result, a multitude of inflammatory cytokines is expressed to further promote the innate response and up-regulated the expression of PRRs in a positive feedback loop (Abdullah and Knolle, 2014).

In the context of an LCMV infection, viral RNA is sensed by the RIG-like helicases RIG and MDA5, as well as through Toll-like receptor 7 (TLR7) during the innate phase and induces a strong type I IFN response and inflammatory cytokines such as IL-1β, IL-18 and TNF (Zhou et al. 2010) (Macal 2012) (Pythoud et al. 2015). Other key players in the induction of type I IFN through RIG and MDA5 are interferon regulatory factors (IRFs), of which IRF7 has been implicated during LCMV infection, and nuclear factor kB (NF-κB), which have important gene

regulatory functions regarding interferon stimulated genes (ISGs) and further promote anti-viral defense mechanisms (Zhou et al. 2010) (Fitzgerald et al. 2003).

In contrast to an acute infection with LCMV, chronic infection with LCMV leading to high viral load and persistence appears to re-shape the innate immune response and appears to interfere with apoptotic signals via type I IFN levels (Barber et al. 2001) (Pythoud et al. 2015). Congenital infection with LCMV can modulate the anti-viral immune response differently than an acute infection during adulthood (Pythoud et al. 2015). Congenitally infected mice become life long carriers and present with high viral titers, which is achieved by the suppression of the type I IFN response and subsequent interference with the innate defenses (Pythoud et al. 2015) (Saron et al. 1982). In this case, type I IFN is chronically produced at very low levels, suggesting evasion of the innate defenses that allows the virus to persist (Pythoud et al. 2015). Chronic infection with LCMV clone 13 during adulthood on the other hand also results in initially high levels of type I IFN by macrophages and DCs, among others, via MDA5/MAVS-dependent pathways (Clingan et al. 2012) (Zuniga et al. 2015). However, as viral titers remain high during LCMV clone 13 infection, type I IFN levels start to decrease, which is attributable in part to a loss of plasmacytoid DC (pDC) numbers and their production of type I IFN (Zuniga et al. 2008). The loss of type I IFN subsequently interferes with the function of NK cells of the innate immune system and renders the host more vulnerable to subsequent infections, e.g. murine cytomegalovirus (MCMV) (Zuniga et al. 2008). The pro-inflammatory cytokines induced during the innate phase of the anti-viral response are crucial to maintain the infection until the adaptive immune system can be initiated. The innate immune response has therefore an indispensible role during the fight against invading pathogens, in particular since T cell activation and the initiation of the adaptive response takes several days (Janeway et al. 2001).

1.6.1 DCs during LCMV infection

Dendritic cells are a crucial cell population for bridging the gap between the innate and the adaptive immune system by processing and presenting antigen to T lymphocytes and initiating T cell activation and differentiation (Roquilly and Villandangos, 2015) (Eisenbarth, 2018). Clearing an infection with the systemically replicating LCMV requires a strong LCMV-directed CD8+ T cell response, a large part of which is induced by DCs and their innate pathways (Montoya et al. 2005). LCMV gains cellular entry via the alpha-dystroglycan (α-DG) receptor, which is primarily, but not exclusively, expressed on $CD11c^+$ and $DEC\text{-}205^+$ splenic DCs (Sevilla et al. 2000). The affinity of the glycoprotein for α-DG differs among the strains of LCMV and therefore defines the tropism of the virus strain, as well as its overall virulence (Kunz et al. 2001). Upon sensing of the virus, pDCs are activated and produce large amounts of type I IFN within 24 hours of the infection, irrespective of whether LCMV infection is acute or chronic (Dalod et al .2002) (Montoya et al. 2005) (Zuniga et al. 2008). Type I IFN in turn has the potent ability to stimulate T cells directed against LCMV, but also conventional DCs, which further promote the CTL response by initiating cytokine production of TNFα and IL-12 among others (Montoya et al. 2005) (Norris et al. 2013). Type I IFN reaches its peak in the serum around day 2-3 after LCMV infection and plays an essential role in containing and clearing the infection, by promoting DC, as well as T cell-mediated responses against the virus (Biron et al. 2002) (Ou et al. 2001) (Marrack et al. 1999).

Interestingly, there is an inverse correlation between the large amounts of type I IFN being produced by pDCs and their absolute numbers during LCMV infection (Swieki et al. 2011). However, while pDC numbers decline with rising type I IFN levels, their numbers are increasing again by day 3 post infection and are replenished once type I IFN levels return back to baseline (Norris et al. 2013)

(Swieki et al. 2011). DCs can be divided into different subpopulations based on anatomical location, which include conventional DCs (cDCs), which are either CD11b or XCR1 positive, pDCs, monocyte-derived DCs and Langerhans cells (LCs) (Dalod et al. 2014) (Eisenbarth, 2018). While all these DC populations differ slightly in their primary function during viral infection, they all need to functionally mature and up-regulate surface markers such as CD86, CD80 and CD40, to provide sufficient co-stimulatory signaling to T lymphocytes during viral infection.

1.7 T cell-mediated adaptive immune response

The adaptive immune response comes into play, when innate defenses are no longer able to keep an infection in check or the invading pathogen is able to evade innate defenses (Murphy et al. 2012) (Eisen and Chakraborty, 2010). Unlike the innate immune system, the adaptive immune response is characterized by a remarkable degree of pathogen specificity, as well as the ability to establish long-lasting memory enabling faster response rates upon recurrent infections (Wiesel et al. 2009) (Eisen and Chakraborty, 2010). The adaptive immune system is made up of different types of B and T lymphocytes that express cell surface receptors specifically binding pathogen derived peptides (Murphy et al. 2012) (Eisen and Chakraborty, 2010). While B lymphocytes develop and mature in the bone marrow (BM), T lymphocytes undergo maturation in the thymus, where the gene segments of their T cell receptor (TCR) are rearranged to yield a TCR with almost unique antigen specificity (Murphy et al. 2012) (Brändle et al. 1992). The majority of T cells expresses a hetero-dimeric TCR comprised of a paired α- and β-chain, which are each made up of a variable (V), a joining (J), a constant (C) and a diversity (D) (only found in the β-chain) gene segments that are recombined during T cell maturation and selection in the thymus (Toor et al. 2016) (Nikolich-Zugich et al. 2004). TCR diversity is primarily defined by the complementary determining regions (CDRs) located within the recombining gene segments, which are of hypervariable nature and essentially define the binding of peptide to MHCs

(Nikolich-Zugich et al. 2004). Upon infection a small set of T cell clonotypes undergo a proliferative burst, i.e. those T cells specific for the epitopes presented on MHC rapidly expand and develop into effector T cells (Vallejjo et al. 2004) (Yuzefpolskiy et al. 2015).

For sufficient activation and subsequent differentiation into effector cells, T cells require three types of signals. The primary signals requires TCR binding of peptide-MHC, followed by co-stimulatory signals provided by CD28 and CD3 ligand binding and the release of inflammatory cytokines by antigen-presenting cells (APCs) (Murphy et al. 2012) (Yuzefpolskiy et al. 2015). Once the infection is effectively cleared the majority of effector T cells, so called short-lived effector T cells (SLECs) die via apoptosis during the contraction phase of the T cell response (Yuzefpolskiy et al. 2015) (Wiesel et al. 2009). Memory precursor effector T cells (MPECs), which make up roughly 10% of the effector T cells, remain to develop into memory T cells, which are maintained long-term and are able to mount an adaptive immune response considerably faster upon recurrent infection (Yuzefpolskiy et al. 2015) (Joshi et al. 2007).

Upon antigen binding to the TCR multiple downstream signaling cascades are initiated that involve second messengers such as Ca^{2+} and phosphatidylinositol-3-triphosphate (PI3K), as well as kinases such as mitogen-activated protein kinase (MAPK), protein kinase C (PKC) and the serine-threonine kinase Akt, which lead to the downstream activation and translocation to the nucleus of the transcription factors NFAT and NF-κB (Huse, 2009) (Navarro and Cantrell, 2014). As a consequence profound changes in gene expression are initiated, which are essential to the CD8+ T cell-mediated immune response against viruses and other invading pathogens (Huse, 2009) (Navarro and Cantrell, 2014). Effector mechanisms of activated CD8+ T effector cell include cytolysis of infected host cells, as well as the production and secretion of a variety of cytokines, chemokines and microbicidal products that are aimed at promoting the adaptive

immune response (Harty et al. 2000) (Angelosanto et al. 2012). These include the production of antiviral cytokines such as TNFα and IFNγ and cytokines such as IL-2 (Huse, 2009) (Navarro and Cantrell, 2014) (Harty et al. 2000). In order to perform their cytolytic function and lyse infected cells, activated CD8+ T cells also produce cytolytic enzymes such as granzyme B and perforin, which are delivered to infected target cells where they cause apoptotic cell death (Harty et al. 2000) (Harty and Bardović, 2008) (Kulinski et al. 2013).

1.7.1 T cell-mediated immune responses against LCMV

Infection of healthy adult mice with WE or Armstrong strain, known to induce an acute infection, elicits strong CD4+ and CD8+ T cell-mediated responses, of which CD8+ cytotoxic effector T cells (CTLs) make up the predominant effector cell population (Marsland et al. 2005) (Fung-Leung et al. 1991). CD4+ T cells (mainly Th1) also contribute to viral defenses by providing B cell and CTL help, producing inflammatory cytokines and lysing infected cells (Homann et al. 2001). The peak of the CTL-mediated immune response occurs on day 8 during acute LCMV infection, whereas the CD4+ T cell-mediated response is slightly delayed and reaches its peak on day 10 p.i. with a 20-fold lower number of LCMV-specific CD4+ T cells (Homann et al. 2001). The T-cell mediated adaptive immune response against LCMV can be subdivided into three major phases. Upon activation of T lymphocytes, they undergo significant expansion, followed by a contraction phase during which the majority of effector T cells undergoes apoptosis (Zhou et al. 2012). The contraction phase leaves behind a stable pool of memory CD8+ and CD4+ T cells that slowly deteriorates over time, but confers protection and guarantees a more rapid immune response upon recurring infection. Additionally, an acute infection with LCMV is characterized by rapid production of various pro-inflammatory cytokines and antiviral type I IFN (Marsland et al. 2005). Type I IFNs provide potent survival signals to both CD8+ and CD4+ T cells, which are required for sufficient proliferation of LCMV-specific CD8+ T cells, but does not seem to play

a role in effector cell differentiation (Thompson et al. 2006). Upon infection, type I IFN also exerts a crucial effect on splenic DCs, which is required for optimal phenotypic activation and maturation, as well as a subsequent increase in T cell stimulatory capacities, further optimizing the adaptive immune response against LCMV (Montoya et al. 2005). Previous studies using LCMV strains such as clone 13 or Docile on the other hand, have shown the high viral load and spread to be accompanied by clonal deletion of virus-specific CD8+ T cells after initial activation and proliferation (Moskophidis et al. 1993).

1.7.2 T cell exhaustion

Persistent infection and chronic exposure to viral antigen have shown to render virus-specific CD4+ and CD8+ T cells dysfunctional (exhausted), which occurs through a step-wise loss of effector functions such as IL-2, TNFα and IFNγ cytokine production, as well as a loss of proliferative capacity and impaired cytotoxicity after T cell activation (Wherry et al. 2003) (Sanchez-Fueyo and Markmann, 2016). As a consequence of high viral load and spread, virus-specific T cells enter a state of functional exhaustion distinct from functional T effector cells during acute viral infections, in which they fail to elicit a proper anti-viral immune response tolerating the persistence of the virus and can eventually be physically deleted due to a disproportionately high antigen load (Sanchet-Fueyo and Markmann, 2016) (Wherry et al. 2003) (Yi et al. 2010). Exhausted T cells are clearly distinct from T effector or T memory cells, as they fail to mount a robust secondary response upon secondary encounter with the same antigen (Khan et al. 2019) (Angelosanto et al. 2012). However, recently it has been discovered that among the exhausted T cell pool there exists a subpopulation characterized by the expression of the transcription factor Tcf-1 that exhibits memory-like features, with the ability to self-renew and give rise to terminally exhausted Tcf-1- PD-1+ progeny and are responsive to vaccination and checkpoint blockades in the context of tumor therapy (Utzschneider et al. 2016) (Siddiqui et al. 2019). Additionally, it has

been found that T cell exhaustion is also accompanied by epigenetic changes that lead to the formation of exhaustion T cells during chronic viral infection (Alfei et al. 2019) (Khan et al. 2019). The thymocyte selection-associated high mobility group box (Tox) protein is a key driver of these changes and thereby promotes the development and maintenance of exhausted T cells (Alfei et al. 2019) (Khan et al. 2019). Tox is induced via TCR stimulation in the context of high antigen load and correlates with the development of exhausted T cells, while it is only expressed transiently and at low levels during acute viral infections such as LCMV Armstrong (Alfei et al. 2019) (Khan et al. 2019). Deleting Tox from CD8+ T cells results in improved effector functions such as cytokine production, but at the cost of increased immunopathology and a quantitative reduction of Tcf-1+ T cells. (Alfei et al. 2019).

T cell dysfunction and viral persistence can not only be observed in a variety of human infections such as human immunodeficiency virus (HIV) and hepatitis B and C virus infections (HBV) (HCV), but has also been observed in the context of malignancies such as melanoma, non-small-cell lung cancer and renal cell cancer (Wherry et al. 2003) (Hashimoto et al. 2018) (Schietinger and Greenberg, 2014). Another hallmark of exhausted T cells is the disproportionate up-regulation and co-expression of inhibitory receptors such as PD-1, CTLA4, 2B4, TIM3 and LAG3 (Schietinger and Greenberg, 2014) (Barber et al. 2006) (Wherry et al. 2007). Programmed death 1 (PD-1) is a member of the CD28 receptor family and its transient expression on effector T cells promotes the regulation of T cell proliferation and function (Yi et al. 2010) (Barber et al. 2006). While elevated PD-1 expression levels are a hallmark of functionally exhausted T cells, it is no longer found on functional memory T cells after the infection is cleared (Yi et al. 2010) (Wherry et al. 2007). Blocking PD-1 signaling during chronic infection with LCMV clone 13 resulted in augmented CD8+ T cell proliferation, cytokine production and reduced viral burden, identifying the PD-1/PD ligand 1 (PD-L1) signaling axis as a valuable target for therapeutic intervention with respect to T cell exhaustion (Barber

et al. 2006). Inhibition of T cell effector function during functional exhaustion involves a complex network of inhibitory receptors; highlighted by the fact that PD-1 blockade alone does not fully restore function of exhausted T cells (Barber et al. 2006) (Blackburn et al. 2008). Blocking lymphocyte activating-gene 3 (LAG3), an MHC-II ligand up-regulated by exhausted T cells and often co-expressed with PD-1, together with PD-1 appears to have a synergistic effect on augmenting T cell effector functions and dampening of viral load compared to either single blockade (Kahan et al. 2015) (Blackburn et al. 2009). Cytotoxic T-lymphocyte-associated antigen 4 (CTLA4) is another inhibitory receptor of the CD28 receptor family that is associated with T cell exhaustion and blocking antibodies against it are currently used in cancer immunotherapy for melanoma patients and other types of cancer (Schietinger and Greenberg, 2014) (Hodi et al. 2012). The T-cell immunoglobulin and mucin domain-containing protein 3 (TIM3) plays an important role in keeping autoimmune responses in check, while its up-regulation on antigen-specific T cells has also been implicated in a variety of chronic infection such as HIV and HCV in humans and chronic LCMV infections in mice (Yi et al. 2010). The expression levels of TIM3 on exhausted T cells were found to correlate with severity of the exhausted state, while it is also expressed on CD8+ tumor infiltrating T cells (Yie et al. 2010) (Sakuishi et al. 2010). Simultaneous blockade of PD-1 and TIM3 has previously yielded promising results with regard to augmented control of solid tumors in mice (Sakuishi et al. 2010). All these inhibitory receptors serve as a negative feedback mechanism to keep T cell-mediated effector functions in check and prevent immunopathology due to increased T cell-mediated cytotoxicity (Yi et al. 2010) (Patsoukis et al. 2017). However, during persistent antigen exposure exhausted T cells often express high levels of multiple inhibitory receptors simultaneously, interfering with proper cytokine expression, T cell effector functions and subsequent clearance of viral infection or tumor control (Patsoukis et al. 2017). Hence, inhibitory receptors provide valuable targets for augmenting the immune responses against chronic viral infections or malignancies.

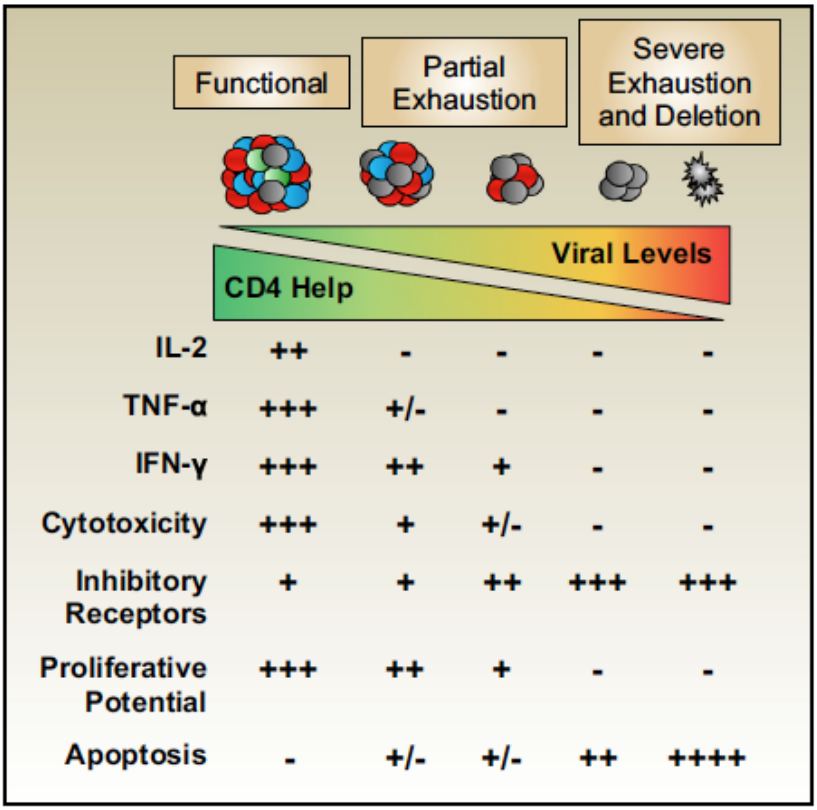

Figure 3: Functional exhaustion in CD8+ T cells is associated with hierarchical loss of effector functions and subsequent deletion during chronic viral infection. During chronic viral persistence and high viral loads CD8+ T cells adopt an exhausted phenotype, characterized by the progressive loss of effector functions and increased expression levels of multiple inhibitory receptors such as PD-1, LAG3, CTLA4 and TIM3. Figure taken from Kahan S. M., Wherry E. J., Zajac A. J., 2014, T cell exhaustion during persistent viral infections, *Virology*, 479-480:180-93

1.7.3 Chronic type I IFN signaling and IL-10 production during viral persistence

Type I IFN signaling has pleiotropic effects on both innate and adaptive immune cells. They are a family of multi-gene cytokines with antiviral activity, which all signal through the same heterodimeric transmembrane receptor (IFNAR) and stimulate the expression of a multitude of genes (IFN-stimulated genes (ISGs)), including cytokine mediators that are crucial in warding off viral infection (Pestka et al. 2004) (McNab et al. 2015). Over the last two decades many studies have

undoubtedly shown that type I IFN signaling has potent T cell independent anti-viral effects by restricting viral replication and spread, however, sustained high levels of type I IFN signaling can also have detrimental effects, such as hyperimmune activation observed during persistence of LCMV clone 13 infection (McNab et al. 2015) (Teijaro et al. 2013). Persisting high levels of type I IFN can lead to tissue damage by inducing large amounts of inflammatory cytokines, thereby exacerbating disease and eventually leading to an immunosuppressive phenotype over time, further promoting the persistence of the pathogen (Davidson et al. 2014) (McNab et al. 2015). Blocking IFNAR signaling however, for example during chronic LCMV infection with clone 13, leads to lower viral titers and reduced PD-1 expression levels (Teijaro et al. 2013). The negative effect on viral control is due to elevated levels of the immunosuppressive cytokine IL-10, which is directly induced by chronic type I IFN signaling during persistent infection and could be decreased after antibody-mediated blockade of interferon receptor signaling (Teijaro et al. 2013) (Hackstein et al. 2016). IL-10 plays a crucial role in dampening inflammatory responses and is also up-regulated during chronic infections such as HIV and HCV in humans (Mannino et al. 2015) (Smith et al. 2018). It directly interferes with cytokine production and inhibits the proliferation of both CD4+ and CD8+ T cells during viral infection (Blackburn and Wherry, 2007). Blocking IL-10 signaling via antibody-mediated IL-10 receptor blockade during the early phase of infection with LCMV clone 13 improves T cell effector functions and leads to viral clearance by day 9 p.i. similar to an acute infection with LCMV Armstrong with the aversion of an exhausted phenotype of virus-specific T cells (Brooks et al. 2006). Hence, IL-10 represents a valuable target to ameliorate T cell exhaustion and promote viral clearance during otherwise chronic viral infections.

1.7.4. Bioenergetic demands of effector T cells during viral infection

As naïve T cells leave their quiescent state after antigen recognition, they undergo profound metabolic changes to meet the metabolic demands of fighting

invading pathogens and uphold effector functions (Buck et al. 2016). While naïve T cells primarily rely on fatty acid oxidation (FAO) and oxidative phosphorylation (OXPHOS) in the mitochondria to support ATP production, T effector cells undergo extensive metabolic reprogramming, which relies on sufficient co-stimulatory signals via CD28, the activation of PI3K and subsequently mTOR signaling to up-regulate aerobic glycolysis (Chao et al. 2017) (Patsoukis et al. 2017). The metabolic switch to aerobic glycolysis involves the synthesis of macromolecules by the tricarboxylic acid (TCA) cycle from metabolites such as pyruvate and glutamine, which provide building blocks for T effector cell proliferation and differentiation, as T cells switch to an anabolic state during activation (van der Windt and Pearce, 2012) (Buck et al. 2006). Once an infection is cleared, memory T cells that remain adopt once again a quiescent and catabolic state utilizing FAO as their main energy source rather than aerobic glycolysis (Buck et al. 2016) (Chao et al. 2017). Memory T cells are characterized by an increased mitochondrial mass, compared to both naïve and effector T cells; the later possessing primarily fragmented mitochondria, possibly to promote the usage of aerobic glycolysis rather than FAO and OXPHOS (Chao et al. 2017).

Mitochondrial dynamics are a means of regulating metabolic pathways in response to alterations in cellular metabolic demands (Chao et al. 2017). They are defined by continuous fission and fusion of mitochondria to adjust mitochondrial mass, mobility, localization and function in response to stimuli such as nutrient availability, growth stimuli or cellular stress (Chao et al. 2017) (Sebastián et al. 2017). Both excess nutrients, as well as cellular dysfunction, can induce mitochondrial fragmentation; the later resulting in the generation of two mitochondria, one with a functional membrane potential and the other one with a low, i.e. dysfunctional, membrane potential, which is then removed by mitophagy (Sebastiaán et al. 2017) (Wai and Langer, 2016). Nutrient depletion can result in mitochondrial elongation and fusion to protect against autophagy and prevent apoptosis (Wai and Langer, 2016). Hence, mitochondrial fusion can promote FAO

by resulting in the formation of supercomplexes of the electron transport chain (ETC) within the inner mitochondrial membrane, which are crucial to maintain an oxidative metabolism in memory T cells (Wai and Langer, 2016) (Chao et al. 2017) (Buck et al. 2016). Mitochondrial fission on the other hand accelerates cell proliferation and can be observed in T effector cells, generating fragmented mitochondria, which allows for the rapid removal of dysfunctional mitochondria via mitophagy (Buck et al. 2016) (Wai and Langer, 2016).

Metabolic insufficiencies and mitochondrial dysfunction have recently been observed in exhausted T cells and appear to contribute to functional exhaustion of effector T cells during infection (Pauken and Wherry, 2015). Bengsch et al. have recently shown that failure to meet bioenergetic demands precedes functional exhaustion in T effector cells during chronic infection with LCMV clone 13 (2016). Exhausted LCMV-specific CD8+ T cells do not up-regulate their glucose metabolism in response to viral infection, as is required to carry out effector functions, and their suppressed bioenergetics state results in a continuous reduction in glucose uptake and use (Buck et al. 2015) (Bengsch et al. 2016). PD-1 is a key driver of suppressed bioenergetics in exhausted T cells during LCMV infection, as it directly represses both glycolysis and OXPHOS at the cost of mitochondrial quality (Bengsch et al. 2016). PD-1 negatively regulates TCR signaling and represses the transcriptional co-activator PGC-1α, which promotes mitochondrial biogenesis (Chao et al. 2017) (Bengsch et al. 2016). Overexpression of PGC-1α results in improved effector function, as well as increased mitochondrial biogenesis and fitness (Chao et al. 2017). In addition, metabolic insufficiencies are also characterized by dysfunctional mitochondria, which have a low membrane potential, produce high levels of reactive oxygen species and fail to uphold a functional ETC to produce ATP and undergo OXPHOS (Ip et al. 2017). In line with the suppressed bioenergetics profile of exhausted T cells during viral infection, Schürich et al. could show that exhausted HBV-specific CD8+ T cells also harbor depolarized, i.e. dysfunctional mitochondria, which is accompanied by a failure to

use OXPHOS to support their energy demand, thereby solely relying on glycolysis further limiting their effector function potential (2016).

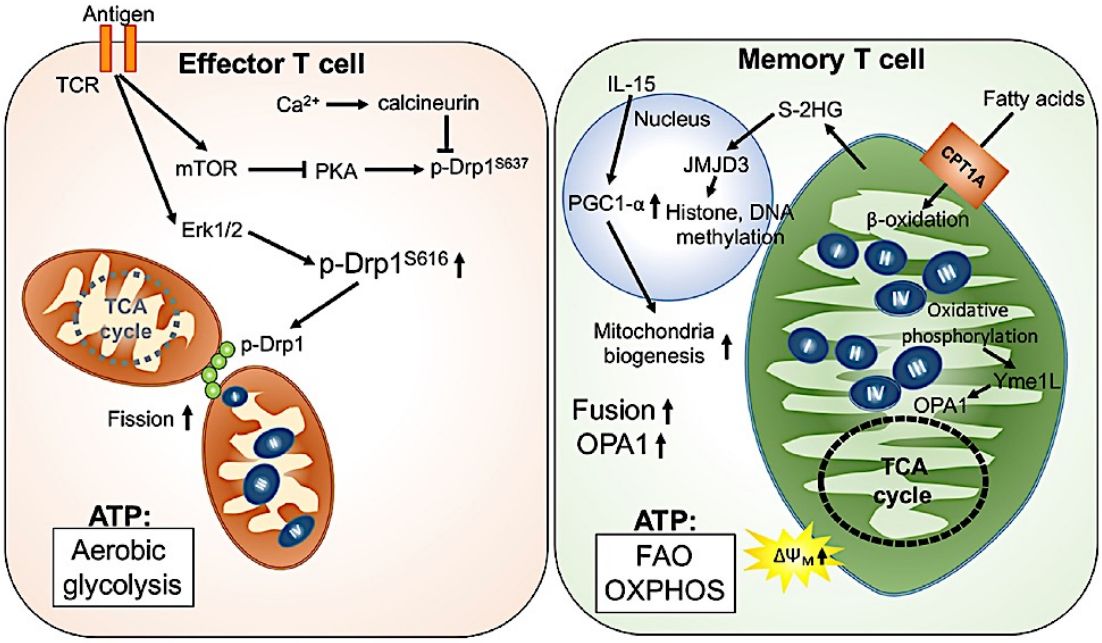

Figure 4: Effector and memory T cells have different metabolic requirements. Activated T effector cells have distinct bioenergetics demands and mitochondrial profile compared to quiescent memory T cells after infection. T effector cells are characterized by fragmented mitochondria and an increase in aerobic glycolysis to produce ATP and leave macromolecules intact to support their rapid proliferation. Memory T cells on the other hand have a much higher mitochondrial mass and are characterized by increased mitochondrial fusion, FAO and rely primarily on OXPHOs to generate ATP. Figure taken from Chao T., Wang H., Ho P.-C., 2017, Mitochondrial control and guidance of cellular activities of T cells, *Frontiers in Immunology*, 8(473):1-7

1.8 Current vaccination strategies against influenza virus infection

Seasonal influenza virus infections are currently estimated to cause up to 650 000 deaths world wide every year, resulting in a significant burden on modern health care systems (Iuliano et al. 2018). Despite the availability of vaccines, influenza virus infections are still causing seasonal epidemics, with people aged over 65 and those suffering from immune suppression being at the highest risk of succumbing to infection (Stöhr, 2002) (Kunisaki and Janoff, 2009) (Petrova and

Russell, 2018). The primary site of influenza A virus (IAV) infection is the epithelium of the lung, which expresses sialic acid on its surface to which hemagglutinin (HA), a surface protein of the influenza virus, can bind initiating the internalization of the virus (Coates et al. 2015). Current influenza vaccines aim at inducing neutralizing antibodies against the HA protein of the virus, the primary target of the adaptive immune response, to confer immune protection (Houser and Subbarao, 2015) (Petrova and Russell, 2018). In addition, influenza vaccines may also include Neuraminidase (NA) components, another surface molecule of the virus essential for releasing viral particles from the cell; however, its contribution to immune protection after vaccination is less well studied (Petrova and Russell, 2018). The influenza virus is an RNA virus that is prone to undergo mutation and allowing for antigenic escape from neutralizing antibodies due to immune selection pressure (Hauser and Subbarao, 2015). Hence, seasonal re-formulation of vaccines is required to provide sufficient communal protection against the currently circulating serotype of influenza (Hauser and Subbarao, 2015). The antigenic drift seen with respect to influenza epitopes presented during infection, necessitates the design of longer lasting and more cross-reactive vaccines which recognize a larger range of serotypes and abolish the need for frequent revaccination (Sridhar et al. 2013) (Houser and Subbarao, 2015). Research going into novel vaccine designs currently aims at targeting CD8+ T cell responses, which, in the context of influenza infection, are largely directed against more conserved proteins of the virus, thereby conferring better cross-reactivity across various serotypes (Lee et al. 2014) (Houser and Subbarao, 2015). However, developing more efficient vaccines requires a better and profound understanding of the determinants rendering peptide epitopes immunogenic, as peptide presentation in the context of MHC molecules alone does not guarantee TCR stimulation and the elicitation of an immune response (Sung et al. 2002). There are many determinants of peptide immunogenicity such as peptide length, peptide-MHC affinity and stability, as well as TCR activation, which all contribute to determining the magnitude of the T cell response elicited and require careful characterization to allow their incorporation

into future vaccines (Zhong et al. 2003) (Ekeruche-Makinde et al. 2013) (Sung et al. 2002).

1.8.1 T cell-mediated adaptive response against influenza infection

Influenza virus infection results in the elicitation of both a strong humoral immune response, as well as cellular immune response mediated by cytotoxic T cells that appears to play an important role in clearance of the virus (Effros et al. 1977) (Rosendahl Huber et al. 2016). Individuals infected with live non-attenuated IAV that mounted a detectable T cell response cleared the infection much more effectively compared to individuals without a clear detectable T cell response, suggesting that T cell-mediated immunity might be a key response for the clearance of influenza infection (McMichael et al. 1983) (Sridhar et al. 2013). Cytotoxic CD8+ T cells contribute to viral clearance by inducing apoptosis of infected cells and producing IFNγ which further promotes the immune response against influenza (Lee et al. 2014). In order to induce a CD8+ T cell response immunogenic peptides from viral proteins such as the nucleoprotein (NP), polymerase acidic protein (PA) or matrix protein 1 (M1), which are usually highly conserved among different serotypes of the IAV, need to be presented on MHC-I molecules (Lee et al. 2014) (Sung et al. 2002). However, out of the large number of peptide epitopes that can theoretically bind any given MHC-I allele to be presented to a T cell receptor (TCR) of a cytotoxic CD8+ T cells during a viral infection, only few elicit detectable CD8+ T cell responses. A key characteristic of CD8+ T cell responses are their immunodominance (ID) hierarchies, in which immunodominant and subdominant epitopes drive CD8+ T cell responses of different magnitudes and quality with respect to effector cytokine production (Zanker et al. 2013) (Ramakus et al. 2012). The majority of the CD8+ T cell-mediated antiviral response is usually driven by one or two immunodominant epitopes, while the remaining epitopes that are being recognized drive subdominant responses (Zhong et al. 2003). Exploiting immunodominant epitopes to develop more efficient vaccines is

a tempting approach, but even though they elicit strong immune responses *in vivo*, they are also often subject to mutations due to immune-driven selection (Rodriguez et al. 2001). Hence, subdominant epitopes provide an additional means to confer reliable, cross-reactive protection against infection when incorporated into vaccines (Rodriguez et al. 2001). Subdominant epitopes have previously been shown to confer protection in the absence of immunodominant epitopes or when they are exogenously boosted and the active suppression on CD8+ T cells specific for subdominant epitopes is lifted (Zhong et al. 2003) (Zanker et al. 2013) (Tscharke et al. 2015) (St Leger et al. 2013). Extensive research is therefore going into analyzing the determinants of peptide immunogenicity and immunodominance hierarchies to be able to biochemically and functionally identify appropriate candidate epitopes for novel vaccines (Zhong et al. 2003) (Wu et al. 2019).

1.9. Hypothesis and aims:

Patients suffering from chronic liver inflammation are well known to be more susceptible to infections due to their innate and adaptive immune system being compromised. While the mechanisms contributing to bacterial infections in patients with liver fibrosis and cirrhosis have received somewhat more attention in the recent years, the exact mechanisms underlying the impaired response against viral infections remain less clear. Since patients with liver fibrosis and cirrhosis are in a general state of immune suppression, they also respond less well to vaccinations compared to healthy individuals. Failure to mount a sufficient immune response in the context of both viral infections and vaccinations can result in accelerated disease progression, severe co-morbidities and higher mortality rates among liver fibrosis and cirrhosis patients. It is therefore crucial to elucidate the mechanisms underlying the impaired T cell-mediated adaptive immune response against viral infections and with respect to vaccinations, in order to develop and implement efficient therapeutic interventions and improve the quality of life of patients. Analyzing the determining factors driving peptide immunogenicity, for instance in

the context of influenza virus infection, provides a means to design more efficient vaccines in the future and contributes to the prevention of morbidity and mortality in patients. The experiments of this thesis therefore aim to gain a better understanding of:

1. The T cell-mediated adaptive response against a systemic infection with LCMV-WE as a model of virus infection in mice with chronic liver inflammation (Chapter 3)

2. The maturation of DCs during LCMV infection in mice suffering from chronic liver inflammation (Chapter 3)

3. The T cell-mediated adaptive response in mice with chronic liver inflammation after vaccination with PolyI:C and OVA (Chapter 4)

4. The differences in peptide immunogenicity during the elicitation of CD8+ T cell responses against PR8 influenza virus infection in mice (Chapter 5)

Chapter 2

Materials and Methods

2.1 Materials

2.1.1 Equipment

Equipment	Manufacturer
Autoclave	Belimed, Cologne, Germany
Benchtop Centrifuge	Eppendorf™ Benchtop Microcentrifuge, Eppendorf, Hamburg, Germany
Capillaries and Pistons for 50 µl displacement pipette	Gilson, Middleton, WI, USA
Cell counting chamber	Neubauer improved; Neubauer, Wertheim; Germany
Cell culture hood	Heraeus, Braunschweig, Germany
Centrifuges	Medicentrifuge; Heraeus, Braunschweig, Germany Centrifuge 5810R, Eppendorf, Hamburg, Germany
Colibri Retractor	Fine Science Tools GmbH, Heidelberg, Germany
Dissection gear/Surgical instruments	Labotec, Göttingen, Germany, Fine Science Tools, GmBH, Heidelberg, Germany
Fine shearing trimmers	Exacta, Aesculap, Suhl, Germany
Flow cytometers	FACS CantoII, Fortessa, LSRII; Beckton, Dickinson & Company, Franklin Lakes, NJ, USA
Freezers (-20°C)	Liebherr, Biberach, Germany
Freezers (-80°C)	Hera freeze, Heraeus, Brauchschweig, Germany
Glass bottles (autoclavable)	100, 250, 500 & 1000 ml; SKS Science, USA
Heating block	ThermoStat plus; Eppendorf, Hamburg, Germany
Heat pad	Eickemeyer, Tuttlingen, Germany
Ice machine	Icematic Scotsman®; Frimont Bettolinc, Pogliano, Italy
Incubators	HERAcell; Heraeus, Braunschweig,

	Germany
IVC mice cages	Tecniplast, Hohenpeißenberg, Germany
ISOFLO Vaporizer	Eickemeyer, Tuttlingen, Germany
Microman E M50E 20-50 µl displacement pipette	Gilson, Middleton, WI, USA
Microscope for cell counting	Leica, Wetzlar, Germany
Mini Centrifuge	Thermo Fisher Scientific, Waktham, MA, USA
Mouse restrainer	University of Bonn, "Hauswerkstatt", Bonn, Germany
PCR Cycler	Eppendorf, Hamburg, Germany
Pipette-Boy	Integra Biosciences, Biebertal, Germany
Pipettes,	Research plus 0.1-2.5, 0.5-10, 2-20, 20-200 and 100-1000 µl, Eppendorf, Hamburg, Germany
Red light bulb/lamp	Infrafil; Phillips, Hamburg, Germany
Refrigerators	Bosch, Suttgart, Germany Liebherr, Bieberach, Germany
Sieves, steel (small)	University of Bonn, Department "Feinmechanik", Bonn, Germany,
Sieves, steel (tall)	University of Bonn, "Hauswerkstatt", Bonn, Germany
Stereo Microscope	Leica, Wetzlar, Germany
Vortex Genie 2	Bender & Hobein, Ismaning, Switzerland
Water bath	TW8; Julabo
Water ion exchanger	EASYPURE®; Thermo Fisher Scientific, Waltham, MA, USA
Workbench, sterile	HERAsage; Heraeus, Braunschweig, Germany

2.1.2 Chemicals and reagents

Chemicals and reagents	Supplier
2-mercaptoethabol	Sigma-Aldrich, St- Louis, MO, USA
2-deoxy-2-[(7-nitro-2,1,3-benzoxadiazol-4-yl)amino]-D-glucose (2-NBDG)	Cayman Chemical Company, Michigan, USA
10x DMEM	Merck (Biochrom), Darmstadt,

	Germany
10x DPBS	Gibco, Thermo Fisher Scientific, Darmstadt, Germany
100 bp DNA ladder	Promega, Madison, WI, USA
Acetic Acetate	Sigma-Aldrich, St. Louis, MO, USA
Agarose	Bioline, Alexandria, NSW, Australia
Ammonium chloride (NH_4Cl)	Merck, Damstadt, Germany
Annexin-V staining kit	BD, Becton, Dickinson and Company, Flanklin Lakes, NJ, USA
Anti-APC beads	Miltenyi, Bergisch Gladbach, Germany
Anti-PE beads	Miltenyi, Bergisch Gladbach, Germany
BD Cytofix/Cytoperm™ Fixation/Permeabilization Solution Kit	BD, Becton, Dickinson and Company, Flanklin Lakes, NJ, USA
Big Dye Terminator v3.1 Kit	Life Technologies, Carlsbad, CA, USA
Bovine serium albumin fraction V (BSA)	Roth, Karlsruhe, Germany
Brefeldin A (1000X)	eBioscience, San Diego, CA, USA
Carprofen (Rimadyl)	Pfizer GmbH, Berlin, Germany
Cell Tracker Violet (CTV)	Life Technologies, Carlsbad, CA, USA
Carboxyfluorescein succinimidyl ester (CFSE)	Life Technologies, Carlsbad, CA, USA
CD4+ T cell Isolation Kit	Miltenyi, Bergisch Gladbach, Germany
CD8a+ T cell Isolationt Kit	Miltenyi, Bergisch Gladbach, Germany
CD11c MicroBeads UltraPure, mouse	Miltenyi, Bergisch Gladbach, Germany
Collagenase from Clostidium histolyticum (Type IV and type VIII)	Sigma –Aldrich, St. Louis, MO, USA
cOmplete™, Mini, EDT-free Protease Inhibitor Cocktail Tablets	Sigma-Aldrich, St. Louis, MO, USA
CountBright™ Absolute Beads	Thermo Fischer Scientific, Waltham, MA, USA
D-Glucose	Applichem GmbH, Darmstadt, Germany
D-Fructose	Roth, Karlsruhe, Germany
Dimethylsulfoxid (DMSO)	Roth, Karlsruhe, Germany
Deoxynucleotide Triphosphate (dNTPs)	Life Technologies, Carlsbad, CA, USA
Disodium hydrogen phosphate (Na_2HPO_4)	Applichem GmbH, Darmstadt, Germany
DMEM	Gibco, Thermo Fisher Scientific, Waltham, MA, USA

DNase	Roche, Basel, Switzerland
DNA Away	Molecular BioProduct, San Diego, CA, USA
DyeEx 96 Kit	Life Technologies, Carlsbad, CA, USA
EasySep™ Mouse T cell isolation kit	StemCell, Cologne, Germany
Ethanol, absolute	Merck, Damstadt, Germany,
Ethylene diamine tetraacetic acid (EDTA)	Merck, Darmstadt, Germany
ExoSAP-IT	Life Technologies, Carlsbad, CA, USA
Fetal calf serum (FCS)	Life Technologies, Carlsbad, CA, USA
Formaldehyde	Roth, Karlsruhe, Germany
FoxP3/Transcription Factor Staining Buffer Set	eBioscience, San Diego, CA, USA
GBSS	PAN Biotech, Aidenbach, Germany
Golgi Plug	BD, Becton, Dickinson and Company, Flanklin Lakes, NJ, USA
HEPES	Roth, Karlsruhe, Germany
Human Recombinant IL-2	Roche, Basel, Switzerland
Ionomycin	Sigma-Aldrich, St- Louis, MO, USA
Isofluorane	AbbVie, Wiesbaden, Germany
LIVE/DEAD™ Fixable Aqua Dead Cell Stain Kit	Life Technologies, Carlsbad, CA, USA
LIVE/DEAD™ Fixable Near-IR Dead Cell Stain Kit	Life Technologies, Carlsbad, CA, USA
L-Alanine	Sigma-Aldrich, St. Louis, MO, USA
L-Asparagine	Applichem GmbH, Darmstadt, Germany
L-Glutamic acid	Sigma-Aldrich, St. Louis, MO, USA
L-Glutamine	Applichem GmbH, Darmstadt, Germany
L-Glutamine (100x)	Gibco, Thermo Fisher Scientific, Waltham, MA, USA
L-Lysine	Sigma-Aldrich, St. Louis, MO, USA
L-Serine	Sigma-Aldrich, St. Louis, MO, USA
L-Threonine	Sigma-Aldrich, St. Louis, MO, USA
Liquid nitrogen	Line, Wiesbaden, Germany
Magnesium chloride ($MgCl_2$)	Roth, Karlsruhe, Germany
Medical Oxygen	Linde, Oberschleißheim, Germany
Methanol	Sigma-Aldrich, St. Louis, MO, USA
Monensin (1000x)	eBioscience, San Diego, CA, USA
NaCl solution (0.9%)	Braun, Melsungen, Germany
Normal goat serum	Life Technologies, Carlsbad, CA, USA
Normal mouse serum	Life Technologies, Carlsbad, CA, USA

PE Annexin V Apoptosis Detection Kit I	BD Pharmingen™, Franklin Lakes, NJ, USA
Penicillin/Streptomycin (P/S)	Gibco, Thermo Fisher Scientific, Waltham, MA, USA
Percoll	GE Healthcare Europe GmbH, Freiburg, Germany
Phosphate-buffered saline (PBS)	Gibco, Thermo Fisher, Scientific, Waltham, MA, USA
Phorbol 12-myristate 13-acetate (PMA)	Sigma-Aldrich, St. Louis, MO, USA
Potassium bicarbonate ($KHCO_3$)	Merck, Darmstadt, Germany
Ptassium chloride (KCl)	VWR (KMF Laborchemie), Darmstadt, Germany
Pyruvate (100x)	Gibco, Thermo Fisher Scientific, Waltham, MA, USA
Red Blood Cell lysis buffer	Sigma-Aldrich, St- Louis, MO, USA
RNase Away® Reagent	Life Technologies, Calrsbad, CA, USA
RNase away spray	VWR, Darmstadt, Germany
RPMI 1640 medium	Invitrogen, Darmstadt, Germany
Sodium azide (NAN_3)	Roth, Karlsruhe, Germany
Sodium hydrogen carbonate ($NaHCO_3$)	Gibco, Thermo Fisher Scientific, Waltham, MA, USA
Sodium dihydrogen phosphate (NaH_2PO_4)	Merck, Darmstadt, Germany
Sodium periodate ($NaIO_4$)	Sigma-Aldrich, St. Louis, MO, USA
Streptavidin, allophycocyanin, crosslinked, conjugate	Life Technologies, Carlsbad, CA, USA
Streptavidin, R-Phycoerythrin Conjugae (SAPE)	Life Technologies, Carlsbad, CA, USA
Superscript III VILO cDNA Syn Kit	Life Technologies, Carlsbad, CA, USA
SybreSafe DNA gel stain	Life Technologies, Carlsbad, CA, USA
Taq DNA polymerade kit	Life Technologies, Carlsbad, CA, USA
Tris	Sigma-Aldrich, St. Louis, MO, USA
Triton X-100	Promega, Madison, WI, USA
Trizol	Life Technologies, Carlsbad, CA, USA
Typan blue (0.4%)	Lonza, Cologne, Germany

2.1.3 Consumables

Consumables	Supplier
48-well plate	Cellstar®, Greiner Bio-One, Kremsmünster, Österreich
96-well U-bottom plates	Cellstar®, Greiner Bio-One, Kremsmünster, Österreich
B cell panning plates	15 cm; Falcon A Corning Brand, Corning, NY, USA
Cap strips for 96 well plates, domed	Eppendorf, Hamburg, Germany
Cotton Swaps	Meditip, Servoprax® GmbH, Wesel, Germany
DNA low bind tube	1.5 ml, Eppdendorf, Hamburg, Germany
DyeEx® 96 Plate	Qiagen, Venlo, Netherlands
FACS tubes	Polystyrene, 12/75 mm; Sarstedt, Nümbrecht, Germany
Filter pipette tips	10 µl, 20 µl, 200 µl, 1000 µl; Axygen®, A Corning Brand, Corning, NY, USA
Gauze, cotton	Medicomp, Paul Hartmann AG, Heidenheim, Germany
Injection Needles	27G, 26G, 25G, 20G; BD Microlance, Becton, Dickinson and Company, Flanklin Lakes, NJ, USA
Kimwipes	Thermo Fisher Scientific, Waltham, MA, USA
LS columns	Miltenyi, Bergisch Gladbach, Germany
Nylon cell strainer	40 µm, 70 µm, 100 µm; Falcon A Corning Brand, Corning, NY, USA
Pasteur pipettes	150mm and 230 mm; Roth, Karlsruhe, Germany
Petri dishes	10 cm; Greiner bio-one, Solingen, Germany
Pipette tips	10 µl, 20 µl, 100 µl; STARLAB, Hamburg
Pipette tips	1000 µl, Greiner bio-one, Frickenhausen, Germany
Silk sutures 6-0	PERMA-HAND Johnson&Johnson Medical GmbH Ethicon Deutschland, Norderstedt, Germany

Plastic Pipettes	5 ml, 10 ml, 25 ml Polypropylene Stripettes, Sarstedt, Nümbrecht, Germany
Tubes	15 ml, 50 ml; Falcon A Corning Brand, Corning, NY, USA
Reaction Tubes	0.5 ml, 1.5 ml, 2 ml, 5 ml; Eppendorf, Hamburg, Germany
Sterile Sorting tubes	5 ml polypropylene Round Bottom Tubes; Falcon A Corning Brand, Corning, NY, USA
Syringes	1 ml, 2 ml, 3 ml, 5 ml, 10 ml, 20 ml BD Discardit™; Becton, Dickinson and Company, Franklin Lakes, NJ, USA
Twin.tec PCR Plate 96, skirted	Eppendorf, Hamburg, Germany

2.1.4 Buffers, media and solutions

Reagent	Ingredients
1x TAE buffer	40 mM Tris, 20 mM acetic acid, 1mM EDTA
1x Perm/Wash buffer	1 part of 10x Perm/Wash buffer (BD), 9 parts of MilliQ Water
Anti-Proteinase buffer	1x PBS, 0.1 % Triton X-100, cOmplete™, Mini, EDTA-free Protease Inhibitor Cocktail
ACK lysis buffer	Deionized water, 8.26 % ammonium chloride, 1 % potassium bicarbonate, 0.037 % EDTA; pH=7.2
Complete RPMI medium	RPMI 1640, 10 % FCS, 2 mM L-glutamine, 1 mM MEM sodium pyruvate, 100 µM MEM non essential amino acids, 5 mM HEPES buffer solution, 50 µM 2-mercaptoethanol, 100 U/ml Penicillin and 100 µg/ml streptomycin
Digestion buffer	RPMI, 1% FCS, 2% Collagenase type IV, 1.5% DNase
FACS buffer	1x PBS, 0.5 % FCS, 0.2 % sodium azide; 1x PBS, 0.5 % BSA, 0.5 % sodium azide
FACS Fix buffer	1x PBS, 2 % FCS, 0.02 % sodium azide, 1 % formaldehyde

MACS buffer	1x PBS, 1 % FCS, 2 mM EDTA; 1x PBS, 0.5 % BSA; 2mM EDTA
T-cell medium	RPMI 1640, 10 % FCS, 1 % P/S, 1 % pyruvate, 1 % 100x L-glutamine, 50 µM 2-mercaptoethanol

2.1.5 Antibodies for flow cytometry analysis

Antigen	Clone	Manufacturer	Conjugated fluorochrome
Annexin-V	N/A	BD Biosciences	PE
B220	RA3-6B2	Biolegend	APC-Cy7 FITC PB
CD3e	145-2C11	eBioscience	APC BV711 eFluor450 FITC PE
CD4	GK1.5	Biolegend	AF700 BV510 FITC
CD5	REA421	Miltenyi Biotec	PerCP-Cy5.5
CD8a	53-6.7	Biolegend	APC BV510 eFluor450 PB PE
CD11b	M1/70	Biolegend	BV711
CD11c	N418	Biolegend	BV605
CD16/32	2.4G2	Made in-house	Unconjugated
CD19	6D5	eBioscience	PB FITC
CD25	3C7	Biolegend	PE
CD44	IM7	Biolegend	BV605 PE-Cy7 eF450 PE
CD45.1	A20	Biolegend	APC PerCP-Cy5.5
CD45.2	104	Biolegend	APC PerCP-Cy5-5
CD62L	MEL:14	eBioscience	PE

			APC-Cy7
CD69	H1.2F3	Biolegend	APC
CD80	16-10A1	Biolegend	AF647
CD86	GL1	eBioscience	FITC
CD107a	1D4B	Biolegend	BV421
CD127	A7R34	eBioscience	PE-Cy7
F4/80	MF48004 BM8	Invitrogen BioLegend	FITC BV421
GranzymeB	GB11	BioLegend	AF647 PE
IFNγ	XMG1.2	Biolegend	PE
IL-2	JES6-5H4	Biolegend	FITC
IL-10R	1B1.3a	BioLegend	PE
KLRG1	2F1	eBioscience	APC
LAG3	eBioC9B7W	Thermo Scientific	PerCP-eF710
Ly6C	HK1.4	Biolegend	PE-Cy7
Ly6G	1A8	Biolegend	APC-Cy7
MHC-II(I-A^b)	AF6-120.1	eBioscience	PB PerCP-eF710
PD-1	29F.1A12	Biolegend	BV421
Rat-IgG1 κ (isotype ctl)	RTK2071	Biolegend	PE-Cy7
Rat-Ig2a κ (isotype ctl)	eBR2a	eBioscience	PE
Rat-IgG2b k (isotype ctl)	2B149/10H5	eBioscience	FITC
TCRb	H57-597	BD Bioscience	APC-Cy7
TIM3	RMT3-23	eBioscience	PE-Cy7
TNFα	MP6-22	Biolegend	PE-Cy7
XCR1	ZET	Biolegend	BV510

2.1.5.1 Antibody to block H-2D^b binding of antigen

Target	Clone	Manufacturer
H-2D^b	28-14-8	BD Pharmingen™, Franklin Lakes, NJ, USA

2.1.5.2 Blocking antibodies for *in vivo* injection

Antigen	Clone	Manufacturer
IFNAR	MAR1-5A3	BioXCell, West Lebanon, NH, USA

2.1.5.3. Cell permeable dyes for flow cytometric analysis

Dye	Manufacturer	Fluorochrome equivalent
Cell Trace Violet	Life Technologies, Carlsbad, CA, USA	PB
Carboxyfluorescein succinimidyl ester (CFSE)	Life Technologies, Carlsbad, CA, USA	FITC
Mitotracker Green (MTG)	Life Technologies, Carlsbad, CA, USA	FITC
Mitotracker Deep Red (MTDR)	Life Technologies, Carlsbad, CA, USA	APC
MitoSox	Life Technologies, Carlsbad, CA, USA	PE
Life/Dead-near I/R	Life Technologies, Carlsbad, CA, USA	APC-Cy7
Life/Dead-Aqua Blue	Life Technologies, Carlsbad, CA, USA	BV510

2.1.6 Synthetic peptides for *in vitro* stimulation

Peptide Names	Amino Acid Sequence	Manufacturer
NAshort	SGPDNGAVAV	GenScript, Hongkong, China
NAlong	SGPDNGAVAVL	GenScript, Hongkong, China
NAshort P4-A	SGPANGAVAV	GenScript, Hongkong, China
NAshort P7-V	SGPDNGVVAV	GenScript, Hongkong, China
NAshort P8-A	SGPDNGAAAV	GenScript, Hongkong, China
NAshort P9-V	SGPDNGAVVV	GenScript, Hongkong, China
NAshort P10-A	SGPDNGAVAA	GenScript, Hongkong, China
NAlong P4-A	SGPANGAVAVL	GenScript, Hongkong, China
NAlong P7-V	SGPDNGVVAVL	GenScript, Hongkong, China
NAlong P9-V	SGPDNGAVVVL	GenScript, Hongkong, China

NAlong P10-A	SGPDNGAVAAL	GenScript, Hongkong, China

2.1.7. Primers used in multiplex assay for TCR repertoire analysis

Primer Names	Primer Sequence	Manufacturer
mTRAV1-Ext	GCACATACAGCACCTCAG	Sigma-Aldrich, St- Louis, MO, USA
mTRAV2-Ext	CCACCAGGGACCACAG	Sigma-Aldrich, St- Louis, MO, USA
mTRAV3-Ext	GGCGAGCAGGTGGAG	Sigma-Aldrich, St- Louis, MO, USA
mTRAV4-Ext	TCTGSTCTGAGATGCAATTTT	Sigma-Aldrich, St- Louis, MO, USA
mTRAV5-1/5-4(D)-Ext	CTTCCYTTGGTATAAGCAAGA	Sigma-Aldrich, St- Louis, MO, USA
mTRAV6-1/6-2-Ext	CAGATGCAAGGTCAAGTGAC	Sigma-Aldrich, St- Louis, MO, USA
mTRAV6-3/6-4(D)-Ext	AAGGTCCACAGCTCCTTC	Sigma-Aldrich, St- Louis, MO, USA
mTRAV6(D)-5-Ext	CTTCTCTGACTGTGAACTGTTC	Sigma-Aldrich, St- Louis, MO, USA
mTRAV6-6-Ext	AGATTCCGTGACTCAAACAG	Sigma-Aldrich, St- Louis, MO, USA
mTRAV6(D/N)-7-Ext	GCCTCAAGGGACAAAGAG	Sigma-Aldrich, St- Louis, MO, USA
mTRAV7-Ext	AGAAGGTRCAGCAGAGCCCAGAATC	Sigma-Aldrich, St- Louis, MO, USA
mTRAV8Ext	TGAAYTGYAGTTACAAGAC	Sigma-Aldrich, St- Louis, MO, USA
mTRAV9-Ext	CTCKSTGSAGCTGAGATGCAA	Sigma-Aldrich, St- Louis, MO, USA
mTRAV10-Ext	GGAGAGAAGGTCGAGCAAC	Sigma-Aldrich, St- Louis, MO, USA
mTRAV11Ext	AAGACCCAAGTGGAGCAG	Sigma-Aldrich, St- Louis, MO, USA
mTRAV12 Ext	GACCCAGAMRGAAGGCCTG	Sigma-Aldrich, St- Louis, MO, USA
mTRAV12-4 Ext	GGGAGGAGCAATGGAGATGG	Sigma-Aldrich, St- Louis, MO, USA
mTRAV13-Ext	TCCTTGGTTCTGCAGG	Sigma-Aldrich, St- Louis, MO, USA
mTRAV14-Ext	GCAGCAGGTGAGACA	Sigma-Aldrich, St- Louis,

	AAG	MO, USA
mTRAV15Ext	CTGSAYTGTTCATATR AGACAAGT	Sigma-Aldrich, St- Louis, MO, USA
mTRAV16Ext	GTACAAGCAAACAGC AAGTG	Sigma-Aldrich, St- Louis, MO, USA
mTRAV17-Ext	CAGTCCGTGGACCAG C	Sigma-Aldrich, St- Louis, MO, USA
mTRAV18 Ext	CAAGATTTCACTGCAC G	Sigma-Aldrich, St- Louis, MO, USA
mTRAV19-Ext	CAAGTTAAACAAAGCT CTCCATC	Sigma-Aldrich, St- Louis, MO, USA
mTRAC21Ext	GTGCACTTGCCTTGTA GC	Sigma-Aldrich, St- Louis, MO, USA
mTRAC Ext	GGCATCACAGGGAAC G	Sigma-Aldrich, St- Louis, MO, USA
mTRAV1-INT	AACGTGAAGGCCAAG C	Sigma-Aldrich, St- Louis, MO, USA
mTRAV2-INT	ACTCTGAGCCTGCCC T	Sigma-Aldrich, St- Louis, MO, USA
mTRAV3-INT	GCCCTCCTCACCTGA G	Sigma-Aldrich, St- Louis, MO, USA
mTRAV5-1/5-4(D)-INT	ATYCGTTCAAATATGG AAAGAAA	Sigma-Aldrich, St- Louis, MO, USA
mTRAV6-1/6-2-INT	GGAGAAGGTCCACAG CTC	Sigma-Aldrich, St- Louis, MO, USA
mTRAV6-3/6-4(D)-INT	CAACTGCCAACAACAA GG	Sigma-Aldrich, St- Louis, MO, USA
mTRAV6(D)-5-INT	CAGTACCCAACCCTG TTCTG	Sigma-Aldrich, St- Louis, MO, USA
mTRAV6-6-INT	ACGGCTGGCCAGAAG	Sigma-Aldrich, St- Louis, MO, USA
mTRAV6(D/N)-7-INT	AAAGGAAGCAGCAGA GG	Sigma-Aldrich, St- Louis, MO, USA
mTRAV7-INT	CAKGRCYTCYYTCAAC TGCAC	Sigma-Aldrich, St- Louis, MO, USA
mTRAV8 INT	TAATCTTAATACGTTC AAATGAG	Sigma-Aldrich, St- Louis, MO, USA
mTRAV9-INT	CAGYTKCTCCTCAAGT ACTAT	Sigma-Aldrich, St- Louis, MO, USA
mTRAV10-INT	GAGGGAGACAGCGCT G	Sigma-Aldrich, St- Louis, MO, USA
mTRAV11-INT	AACAGGACACAGGAA AG	Sigma-Aldrich, St- Louis, MO, USA

mTRAV12-INT	GCTGAACWGCACCTATCAG	Sigma-Aldrich, St- Louis, MO, USA
mTRAV12-4-INT	CAGTGACCCAGAAGGAAGG	Sigma-Aldrich, St- Louis, MO, USA
mTRAV13-INT	TGCAGTGGTTTTACCAA	Sigma-Aldrich, St- Louis, MO, USA
mTRAV14INT	CTCTGACAGTCTGGGAAGG	Sigma-Aldrich, St- Louis, MO, USA
mTRAV15INT	TTAGTGGAGAGATGGTTTT	Sigma-Aldrich, St- Louis, MO, USA
mTRAV16INT	ATTATTCTCTGAACTTTCAGAAGC	Sigma-Aldrich, St- Louis, MO, USA
mTRAV17-INT	TATGAAGGAGCCTCCCTG	Sigma-Aldrich, St- Louis, MO, USA
mTRAV18INT	TACTGGTACCGACAGGTC	Sigma-Aldrich, St- Louis, MO, USA
mTRAV19INT	GCTGACTGTTCAAGAGGGA	Sigma-Aldrich, St- Louis, MO, USA
mTRAV21-INT	AATAGTATGGCTTTCCTGGC	Sigma-Aldrich, St- Louis, MO, USA
mTRAC INT	GCACATTGATTTGGGAGTC	Sigma-Aldrich, St- Louis, MO, USA
mTRBV1Ext	TACCACGTGGTCAAGCTG	Sigma-Aldrich, St- Louis, MO, USA
mTRBV16Ext	CCTAGGCACAAGGTGACAG	Sigma-Aldrich, St- Louis, MO, USA
mTRBV12Ext	GGGGTTGTCCAGTCTCC	Sigma-Aldrich, St- Louis, MO, USA
mTRBV5Ext	GGTATAAACAGAGCGCTGAG	Sigma-Aldrich, St- Louis, MO, USA
mTRBV29Ext	GCTGGAATGTGGACAGG	Sigma-Aldrich, St- Louis, MO, USA
mTRBV20Ext	GGATGGAGTGTCAAGCTG	Sigma-Aldrich, St- Louis, MO, USA
mTRBV13Ext	GCTGCAGTCACCCAAAG	Sigma-Aldrich, St- Louis, MO, USA
mTRBV14Ext	GCAGTCCTACAGGAAGGG	Sigma-Aldrich, St- Louis, MO, USA
mTRBV15Ext	GAGTTACCCAGACACCCAG	Sigma-Aldrich, St- Louis, MO, USA
mTRBV17Ext	GAAGCCAAACCAAGCAC	Sigma-Aldrich, St- Louis, MO, USA
mTRBV19Ext	GATTGGTCAGGAAGG	Sigma-Aldrich, St- Louis,

	GC	MO, USA
mTRBV2Ext	CAGTATCTAGGCCAC AATGC	Sigma-Aldrich, St- Louis, MO, USA
mTRBV23Ext	CTGCAGTTACACAGAA GCC	Sigma-Aldrich, St- Louis, MO, USA
mTRBV24Ext	CAGACTCCACGATAC CTGG	Sigma-Aldrich, St- Louis, MO, USA
mTRBV26Ext	GGTGAAAGGGCAAGG AC	Sigma-Aldrich, St- Louis, MO, USA
mTRBV3Ext	CCCAAAGTCTTACAGA TCCC	Sigma-Aldrich, St- Louis, MO, USA
mTRBV30Ext	CCTCCTCTACCAAAAG CC	Sigma-Aldrich, St- Louis, MO, USA
mTRBV31Ext	CTAACCTCTACTGGTA CTGGCAG	Sigma-Aldrich, St- Louis, MO, USA
mTRBV4Ext	CACGGCTGTTTTCCA GAC	Sigma-Aldrich, St- Louis, MO, USA
mTRBC Ext	CCAGAAGGTAGCAGA GACCC	Sigma-Aldrich, St- Louis, MO, USA
mTRBV1 INT	GTATCCCTGGATGAG CTG	Sigma-Aldrich, St- Louis, MO, USA
mTRBV2 INT	GGACAATCAGACTGC CTC	Sigma-Aldrich, St- Louis, MO, USA
mTRBV3 INT	GATATGGGGCAGATG GTG	Sigma-Aldrich, St- Louis, MO, USA
mTRBV4 INT	CAGGTGGGAAATGAA GTG	Sigma-Aldrich, St- Louis, MO, USA
mTRBV5 INT	GCCAGAGCTCATGTTT CTC	Sigma-Aldrich, St- Louis, MO, USA
mTRBV12 INT	CCAGCAGATTCTCAGT CC	Sigma-Aldrich, St- Louis, MO, USA
mTRBV13 INT	GTACTGGTATCGGCA GGAC	Sigma-Aldrich, St- Louis, MO, USA
mTRBV14 INT	GGTATCAGCAGCCCA GAG	Sigma-Aldrich, St- Louis, MO, USA
mTRBV15 INT	GTGTGAGCCAGTTTC AGG	Sigma-Aldrich, St- Louis, MO, USA
mTRBV16 INT	GAAGCAACTCTGTGG TGTG	Sigma-Aldrich, St- Louis, MO, USA
mTRBV17 INT	GAACAGGGAAGCTGA CAC	Sigma-Aldrich, St- Louis, MO, USA
mTRBV19 INT	GGTACCGACAGGATT CAG	Sigma-Aldrich, St- Louis, MO, USA

mTRBV20 INT	GCTTGGTATCGTCAATCG	Sigma-Aldrich, St- Louis, MO, USA
mTRBV23 INT	GCCAGGAAGCAGAGATG	Sigma-Aldrich, St- Louis, MO, USA
mTRBV24 INT	GCACACTGCCTTTTACTGG	Sigma-Aldrich, St- Louis, MO, USA
mTRBV26 INT	GAGGTGTATCCCTGAAAAGG	Sigma-Aldrich, St- Louis, MO, USA
mTRBV29 INT	GTACTGGTATCGACAAGACCC	Sigma-Aldrich, St- Louis, MO, USA
mTRBV30 INT	GGACATCTGTCAAAGTGGC	Sigma-Aldrich, St- Louis, MO, USA
mTRBV31 INT	CTGTTGGCCAGGTAGAGTC	Sigma-Aldrich, St- Louis, MO, USA
mTRBC Int	CCTCCTTGCCATTCACCCAC	Sigma-Aldrich, St- Louis, MO, USA

2.1.8 Monomers, tetramers and dextramers

Allele	Antigen	Fluorochrome	Manufacturer/Supplier
H2-D^b	LCMV GP 33-41 (KACYNFATM)	APC PE	Immudex, Copenhagen Denmark
I-A^b	LCMV GP 66-77 (DIYKGVYQFKSV)	APC	NIH Tetramer Core Facilit, Atlanta, GA, USA
H2-D^b	IAV NAshort 181-190 monomers (SGPDNGAVAV)	PE	Brooks Laboratory; University of Melbourne, Melbourne, VIC, Australia
H2-D^b	IAV NAlong 181-191 monomers (SGPDNGAVAVL)	APC	Brooks Laboratory; University of Melbourne, Melbourne, VIC, Australia

2.1.9 Virus strains

Virus strain	Description
PR8 Influenza A Virus	A lab adapted strain of the Influenza A Virus with the serotype H1N1. Aliquots were kindly provided by the La Gruta laboratory at Monash University, Melbourne, VIC, Australia.
Lymphocytic Choriomenigitis Virus (LCMV)-WE	The original stock of LCMV-WE was kindly provided by the Fritz Lehmann-Grube laboratory from the Heinrich-Pette-Institute for Experimental Virology and Immunology, University of Hamburg, Germany. The virus was subsequently grown and cultured in the L929 murine fibroblast cell line purchased from Sigma-Aldrich (#85011425).

2.1.10 Mouse strains

The mouse strains described below were all kept and bred (where applicable) under Specific Pathogen Free (SPF) conditions in the House of Experimental Therapy (HET) at the University of Bonn, Germany, according to the German animal welfare guidelines. Mice were transferred to the Institute of Experimental Immunology (IEI) at the University of Bonn, where they were kept under SPF conditions and only for the duration of the experiments. Only female C57BL/6J mice were used for the experiments carried out in Melbourne, VIC, Australia, which were kept under SPF conditions at Monash University according to the animal welfare regulations of Victoria, Australia.

Mouse stain	Description
C57BL/6J	C57BL/6J wildtype non-transgenic mice. For all experiments conducted in Bonn the C57BL/6J wildtype mice were purchased from Janvier (Le Genest-Saint-

	Isle, France) and housed under specific-pathogen free (SPF) conditions at the House of Experimental Therapy (HET) at the University of Bonn according to animal welfare regulations of the state of Nordrhein-Westfalen, Germany. For experiments conducted at Monash University CD57BL/6J mice were purchased from Monash Animal Research Platform (MARP) and kept under SPF conditions at Monash University, according to animal welfare regulations of Victoria, Australia.
CD45.1	B6.SJL-Ptprc^{a} Pepc^{b}/BoyJ mice (Jackson Laboratories, USA) express the congenic leukocyte marker CD45.1, but are otherwise of the same genetic background as C57BL/6J mice. They were kept under SPF conditions at the HET of the University of Bonn and used for cell transfer experiments.
CD45.1/2	These mice were generated by crossing CD45.1 homozygous mice to C57BL/6J mice and are heterozygous for both CD45.1 and CD45.2. These mice were kept under SPF conditions at the HET of the University of Bonn and used for cell transfer experiments.
P14.CD45.1	These mice were generated by crossing P14 mice (B6;D2-Tg(TcrLCMV)327Sdz/JDvsJ) (Jackson Laboratories, USA) and CD45.1 mice. These mice were kept under SPF conditions at the HET of the University of Bonn and used for cell transfer experiments. These mice develop CD8+ T cells that are transgenic for a specific T cell receptor (TCR),

	which is made up of a Va2.3 and a Vb8.1 chain and is specific for the epitope 33-41 of the LCMV glycoprotein.
SMARTA.CD45.1	These mice are a cross bread of SMARTA mice (B6.Cg-*Ptprc*^{a} *Pepc*^{b} Tg(TcrLCMV)1Aox/PpmJ) (Jackson Laboratory) and CD45.1 mice. These mice were kept under SPF conditions at the HET of the University of Bonn and used for cell transfer experiments. These mice develop CD4+ T cells, that are transgenic for a specific TCR that is made up of a Va2.3 and a Vb8.3 chain and is specific for the epitope 61-80 of the LCMV glycoprotein.
OT-I.CD45.1	These mice were generated by crossing OT-I mice (C57BL/6-Tg(TcraTcrb)1100Mjb/J) (Jackson Laboratory, USA) and CD45.1 congenic mice. These mice were kept under SPF conditions at the HET of the University of Bonn and used for cell transfer experiments. These mice develop CD8+ T cells that are transgenic for a TCR, which is made up of the Va2 and the Vb5 chains and is specific for the epitope 257-264 of the ovalbumin peptide.
OT-II.CD45.1	These mice were generated by crossing OT-II mice (B6.Cg-Tg(TcraTcrb)425Cbn/J) (Jackson Laboratory) and CD45.1 congenic mice. These mice were kept under SPF conditions at the HET of the University of Bonn and used for cell transfer experiments. These mice develop CD4+ T cells that are transgenic for a TCR, which is made up of the Va2 and the Vb5 chains and is specific for the epitope 323-339 of the

	ovalbumin peptide. The co-expression of the CD45.1 congenic marker allows for the identification of transferred cells into C57BL/6J mice during cell transfer experiments.

2.1.11 Software

Software	Company
FACS Diva V6.1.1	BD, Becton, Dickinson and Company, Franklin Lakes, NJ, USA
FlowJo V10.0.7	Tree star, Ashland, OR, USA
Illustrator CS6	Adobe Systems, San Jose, CA, USA
IMGT®	IMGT®, the international ImMunoGeneTics information system®
Microsoft Office 2011	Microsoft, Redmond, WA, USA
Photoshop CS6	Adobe Systems, San Jose, CA, USA
Prism10	GraphPad Software, La Jolla, CA, USA

2.2 Methods

2.2.1 Housing of laboratory mice

All laboratory mice were kept under specific pathogen free (SPF) conditions at 24 °C ± 2 °C according to standard housing conditions for laboratory mice and animal welfare guidelines of NRW, Germany or Victoria, Australia. Following the induction of liver fibrosis, mice were monitored daily. Adoptively transferred cells, virus and reagents administered were adjusted in either sterile PBS or 0.9 % NaCl for injection and either injected intraperitoneally (i.p.), intravenously (i.v.), subcutaneously (s.c) or intranasally (i.n.).

2.2.2 Induction of chronic inflammation of the liver by bile duct ligation (BDL)

Male C57BL/6J mice (9-12 weeks of age) were used to induce liver fibrosis by bile-duct ligation. Prior to surgery mice received 0.1 mg/kg Buprenorphine s.c. and their abdomen was shaved using an electrical fur trimmer. Mice were anesthetized using 1.5-2 % isoflurane in 100 % oxygen at 2 L/min. The nose of the mice was placed into a nose cone to deliver 1.5 % of isoflurane in pure oxygen at a continuous flow rate of 2 L/min. Mice were transferred onto an aseptic heat pad set to 37 °C to prevent a drop in core temperature. Using sterile gauze dabbed in a broad-spectrum antiseptic the abdomen was sterilized prior to laparotomy. To confirm sufficient depth of anesthesia, paw pinching was used to confirm absence of reflexes. A 1.5 – 2 cm midline incision in the abdominal skin was made and using moisturized cotton swabs (0.9% saline solution) the skin was carefully separated from the peritoneum. Next, an incision of equal length was made along the *linea alba* using surgical scissors and the peritoneal cavity was spread open by inserting a colibri retractor. The liver and the intestines were carefully moved aside by means of a moisturized cotton swab to not damage the tissue and the common bile duct was separated from the surrounding tissue structures using micro serrated forceps. The bile duct was ligated using two 6-0 silk sutures approximately 0.7 cm apart. The surrounding tissues were moved back into place and mice received 100 µl of 0.9% NaCl directly into the peritoneal cavity to counteract surgery induced dehydration. Both the peritoneal cavity and the skin were sutured back together using 6-0 silk sutures. Mice were placed into a clean cage and left to recover under red light for 5 to 10 minutes before being placed back into their original cage. Mice were administered 0.1 mg/kg Buprenorphin twice daily to counteract post-operative pain, in addition to being monitored twice daily for the entire duration of the experiment. At night mice

2.2.3 Infection with LCMV-WE

Mice were infected with $2x10^4$ PFU/100 µl of sterile PBS or 0.9 % NaCl on day 9 post operation via tail vain injection. Prior to infection mice were put into a new cage and allowed to warm up under red light followed by being placed into a mouse restrainer to immobilize the mice for accurate i.v. injection.

2.2.3.1 Infection with PR8 Influenza A Virus

C57BL/6J female mice aged >7 weeks were infected i.n. with 10^3 PFU of PR8 in 30 µl of sterile PBS/mouse. For the infection procedure mice were anesthetizes with 2-3 % isofluorane at a flow rate of 2 L/min before administration of the virus.

2.2.4 Mouse euthanasia for organ harvest

Mice were euthanized by asphyxiation using 100 % of CO_2 at 2 L/min. To harvest the liver, euthanized mice were subjected to perfusion of the liver via the vena cava using sterile PBS at a flow rate of 4 ml/min for 30-60 seconds. In cases where only the spleen and lymph nodes were required, organs were harvested without any perfusion.

2.2.5 Harvest of Bronchoalveolar Lavage (BAL)

Mice were euthanized by CO_2 asphyxiation and a small incision was made in the trachea, through which a small catheter was inserted. The BAL was harvested by flushing the lung 3x with 1 ml of sterile HBSS, which was collected in a 15 ml tube for further analysis. The BAL was spun down at 1600 rpm for 6 min at 4 °C and re-suspended in complete RPMI (cRPMI) at the required volume. The BAL re-suspended in cRPMI was directly used for surface marker staining or peptide stimulation depending on the experiment.

2.2.5.1 Isolation of lymphocytes from spleen and lymph nodes after influenza infection

Mice were euthanized by CO_2 asphyxiation and prepared for dissection. Spleen, as well as the inguinal, brachial, axial and cervical LNs were harvested either in 4 ml of sterile HBSS buffer. Spleen and LNs were mashed through a sterile 70 µm cell strainer, which was washed with a total of 16 ml of HBSS to create a single cell suspension. Cells were pelleted at 1600 rpm for 6 min at 4 °C and re-suspended in red cell lysis buffer for 4 min. The reaction was quenched with 20 ml of HBSS and spun down. Cells were re-suspended in 5 ml of cRPMI and filtered again through a 70 µm cell strainer prior to further analysis or surface marker staining.

2.2.5.2 Isolation of lymphocytes after LCMV infection

Spleens were harvested in 5 ml of MACS buffer and homogenized through a 100 µm cell strainer using a 5 ml syringe plunger. The cell strainer and plunger were washed with a total of 15 ml MACS buffer, after which cells were centrifuged at 1500 rpm for 5 min at 4 °C. Samples were re-suspended in 7 ml of ACK lysis buffer and incubated at room temperature (RT) for 2 min. Cells were centrifuged, re-suspended in 5 ml of T cell medium (TCM) and filtered through a 40 µm cell strainer prior to counting and surface marker staining.

2.2.5.3 Isolation of liver-associated lymphocytes (LAL)

Livers were harvested after perfusion with sterile PBS via the inferior vena cava at a flow rate of 4 ml/min. Organs were stored on ice in 15 ml Falcon tubes containing 1 ml of DMEM until processing. Liver tissue was homogenized using a 100 µm steel mesh in a sterile petri dish on ice. The mesh and the 5 ml syringe plunger were washed with a total of 14 ml of DMEM and the cell suspension was transferred into a clean 15 ml Falcon tube. Cells were centrifuged at 1500 rpm for

10 min at 4 °C and the pellets re-suspended in 4 ml of 40% Percoll solution. Samples were underlayed with 3 ml of 80% Percoll and centrifuged for 20 min at 1400 g at RT without a break. The first two thirds of the upper Percoll phase was aspirated and discarded, while the interphase containing lymphocytes was collected in a clean 15 ml tube. Cells were washed once in PBS, after which they were re-suspended in 8 ml of ACK lysis buffer and centrifuged at 1500 rpm for 10 min at 4 °C. Cells were re-suspended in 1 ml of TCM for counting and an aliquot taken for in vitro re-stimulation and surface marker staining.

2.2.5.4 Isolation of splenic DCs

To analyze splenic DCs, spleens were harvested into 6-well plates containing digestion buffer. Holding the spleen with forceps, an additional 5 ml of pre-warmed digestion buffer was injected two times. Digestion buffer oozing from the spleen was collected in the well and reused for injection. Spleens were incubated for 15 min at 37 °C in the digestion buffer, followed by transfer into a 70 µm cell strainer and homogenization within the digestion buffer. Following another incubation for 15 min at 37 °C, cell suspensions were transferred into a clean 50 ml tube and the digestion stopped by adding 30 ml of sterile PBS. Cells were centrifuged at 1500 rpm for 5 min at 4 °C, re-suspended in 7 ml of ACK lysis buffer and incubated for 2 min at RT. The reaction was stopped by adding 20 ml of PBS, followed by passing the cell suspension through a 40 µm cell strainer into a fresh 50 ml tube. Cells were centrifuged at 1500 rpm for 5 min at 4 °C and re-suspended in 5 ml of TCM for counting and surface marker staining.

2.2.6 Enrichment of CD11c+ DCs

To isolate CD11c+ cells from the spleen, single cell suspensions were centrifuged at 1500 rpm for 5 min at 4 °C after digestion of the spleen as described above. Cells were re-suspended in 400 µl of MACS buffer per $1x10^8$ of total cells and 100 µl of CD11c MicroBeads per $1x10^8$ of total cells, followed by a 10 min

incubation at 4 °C. Cells were washed by adding 10 ml of MACS buffer per $1x10^8$ of total cells, followed by centrifugation at 1500 rpm for 5 min at 4°C. Pellets were re-suspended in 500 µl of MACS buffer per $1x10^8$ of total cells, while LS columns were equilibrated with 3 ml of MACS buffer. Cell suspensions were passed through individual LS columns, which were washed three times with 3 ml of MACS buffer once the cell suspensions have run through the columns. Columns were placed into new 50 ml tubes and collected cells were flushed out by the addition of 5 ml of MACS buffer. Cell eluates were centrifuged at 1500 rpm for 5 min at 4 °C, re-suspended in 1 ml of MACS buffer, counted and adjusted to $2x10^6$ cells/ml for co-culture experiments.

2.2.7 Isolation of T cells by negative selection

Spleens were processed into single cell suspensions as described above. Cells were centrifuged and re-suspended in 400 µl of MACS buffer and 50 µl of biotin antibody cocktail (Miltenyi; CD4+ and CD8+ T cell isolation kits). Samples were mixed well and incubated at 4 °C for 5 min. A total of 300 µl of MACS buffer and 100 µl of anti-biotin micro beads were added and samples were incubated at 4 °C for another 10 min. The LS columns were calibrated with 3 ml of MACS buffer prior to passing the single cell suspensions through the columns. Columns were washed with an additional 3 ml of MACS buffer. The entire flow through was collected in a clean 50 ml tube and a 200 µl aliquot was taken for a purity check. The remaining sample was pelleted, re-suspended in TCM for counting and the concentration adjusted as needed for cell transfer.

2.2.8 Adoptive cell transfer of T cells

T cells intended for adoptive transfer were washed and re-suspended in sterile PBS to be transferred by tail vein injection using a sterile 27G needle. If adoptively transferred T cells were to be analyzed on day 4 or on day 6 post LCMV infection, a total of $5x10^6$ or $2.5x10^6$ cells respectively, were transferred in 150 µl

per mouse. For adoptively transferred T cells to be analyzed on day 8 post LCMV infection, a total of $5x10^4$ cells were transferred in 100 µl.

2.2.9 Cell trace violet (CTV) labeling of T cells

To analyze cell proliferation, T cells were stained with CTV prior to cell transfer or co-culture with DCs. A single cell suspension was prepared as previously described and stained with 5 µM CTV in PBS for 20 min at 37 °C. The staining was stopped by addition of 20-40 ml of TCM and incubation at 37 °C for 5 min. Cells were centrifuged at 1500 rpm for 5 min at 4 °C and re-suspended in sterile PBS for i.v. injection or in TCM for co-culture with DCs.

2.2.10 Carboxyfluorescein succinimidyl ester (CFSE) labeling of T cells

To analyze cell proliferation, T cells were stained with CFSE prior to cell transfer into mice. A single cell suspension was prepared as previously described and stained with a final concentration of 2 µM of CFSE in PBS for 15 min at 37 °C. The labeling was quenched by the addition of 20 ml of TCM. Cells were washed once and re-suspended in sterile PBS at the required concentration for transfer into mice.

2.2.11 Ovalbumin (OVA) and PolyI:C vaccination

Prior to injection, PolyI:C aliquots were incubated at 65 °C for 10 min and put directly on ice afterwards. A total of 100 µg of PolyI:C and 200 µg of OVA were prepared in sterile PBS for each mouse to be injected i.p..

2.2.12 *In vitro* stimulation of lymphocytes using PMA/Ionomycin

To analyze intracellular cytokines production, CD8+ lymphocytes were incubated with 5 ng/ml of PMA, 200 µg/ml of Ionomycin, as well as Brefeldin A and Monensin at a final dilution of 1/1000 for 3 hrs at 37 °C and 5 % of CO_2. Following

re-stimulation cells were washed in pre-warmed PBS, pelleted and used for surface marker, as well as intracellular cytokine, staining.

2.2.13 Antibody staining of cell surface molecules

To determine the expression of cell surface molecules, single cell suspensions were prepared as described above and an aliquot was taken for analysis. Cells were centrifuged at 1600 rpm for 3 min at 4 °C and re-suspended in 100 µl of FACS or MACS buffer containing the respective fluorochrome-labeled antibodies and Fc-receptor blocking solution at a 1:100 dilution. Cells were stained at 4 °C in the dark for 15-20 min. The antibody staining solution was diluted by addition of 100 µl of buffer, followed by centrifugation at 1600 rpm for 3 min at 4 °C. Cells were re-suspended in MACS buffer or FACS Fix buffer, if cells needed to be fixated for a later analysis.

2.2.13.1 Annexin V apoptosis staining

To determine the proportion of apoptotic cells within an organ, single cell suspensions were prepared as previously described and an aliquot was taken for analysis. Surface molecules were stained as described above in FACS buffer, followed by centrifugation at 1600 rpm for 3 min at 4 °C and a wash with FACS buffer. Cells were washed once with 1x $CaCl_2$ buffer, followed by re-suspension in 100 µl of 1x $CaCl_2$ buffer containing 5 µl of Annexin V according to the manufacturer's instruction. Cells were incubated for 15 min at RT, followed by centrifugation at 1600 rpm for 3 min at 4 °C and washing of cells with 1x $CaCl_2$. Cells were centrifuged at 1600 rom for 3 min at 4 °C again and re-suspended in 200 µl of 1x $CaCl_2$ buffer to be analyzed by flow cytometry within the next 4 hrs.

2.2.13.2 Antibody staining of intracellular cytokines

To determine the expression of intracellular cytokines, single cell suspensions were prepared as described above and an aliquot was taken for analysis. Following the staining of surface molecules cells were centrifuged at 1600 rpm for 3 min at 4 °C and re-suspended in 4 % paraformaldehyde (PFA) and incubated at RT for 10 min. Cells were centrifuged and re-suspended in 100 µl of PERM/Wash and centrifuged directly at 1600 rpm for 3 min at 4 °C. Samples were re-suspended in 50 µl of PERM/Wash containing intracellular cytokine-specific antibodies and incubated for 30 min at 4 °C. The antibody cocktail was diluted by adding 100 µl of PERM/Wash and centrifuging cells at 1600 rpm for 3 min at 4 °C. Cells were re-suspended in 200 µl of FACS buffer for flow cytometric analysis.

2.2.13.3 Antibody staining of intracellular transcription factors

For the staining of intracellular transcription factors the FoxP3/Transcription Factor Staining Buffer kit was used. Single cell suspensions were prepared and cell surface molecules stained as described above. Cells were centrifuged at 1600 rpm for 3 min at 4 °C, re-suspended in 100 µl of Fix/PERM solution and incubated for 20 min at RT. Following fixation and permeabilization of the cells, they were centrifuged at 1600 rpm for 3 min at 4 °C and re-suspended in 50 µl of PERM/Wash containing the transcription factor-specific antibodies. Following incubation for 45 – 60 min at 4 °C, the antibody cocktail was diluted by adding 100 µl of PERM/Wash and centrifuging the cells at 1600 rpm for 3 min at 4 °C. Cells were re-suspended in 200 µl of FACS buffer for flow cytometric analysis.

2.2.13.4 Granzyme B staining

To determine granzyme B production by virus-specific T cells, cell surface molecules were stained as described above. Cells were incubated in 100 µl of Fix/Perm solution (concentrate + diluent at 1:4) for 30 min to 18 hrs. Cells were

centrifuged at 1600 rpm for 3 min at 4 °C, washed in 1x Perm/Wash solution and re-suspended in 100 µl of 1x Perm/Wash containing fluorochrome-coupled antibodies against granzyme B (1:100) and blocking serum (1:100) and incubated for 2 hrs at 4 °C. The staining was stopped with 100 µl of 1x Perm/Wash and cells re-suspended in 200 µl of FACS buffer for flow cytometric analysis.

2.2.13.5 Degranulation assay

To assess degranulation, cells were stained for the marker of secretory lysosome, LAMP1. To this end, wild type splenocytes from a C57BL/6J mouse were isolated to be used as target cells. Target cells were either pulsed with 1 µg/ml of gp33 peptide in TCM for 1 hr at 37 °C or remained un-pulsed as negative control. Isolated splenocytes from infected BDL or Sham mice were co-cultured in TCM at a 1:1 ratio either with non-pulsed target cells and CD107a (LAMP1) antibody (1:100 dilution), or pulsed target cells and CD107a (LAMP1) antibody (1:100 dilution). All co-cultures were supplemented with monensin at a final concentration of 2 µl/ml and centrifuged at 300 g for 1 min at 4 °C. Samples were incubated for 3 hrs at 37 °C and 5 % CO_2. Cells were centrifuged at 1500 rpm for 5 min and the surface markers stained in FACS buffer, as previously described.

2.2.13.6 Cellular mitochondria staining with mitotracker dyes

To assess the mitochondrial fitness of T cells, their mitochondria were stained with the cellular dyes, Mitotracker Green (MTG), Mitotracker Deep Red (MTDR) and Mitosox. Cells were isolated from spleen and liver as previously described and MTG, MTDR and Mitosox were stained together with the required surface antibodies in PBS for 30 min at 37 °C at a final concentration of 250 nM, 250 nM and 5 µM respectively. Cells were washed with PBS and re-suspended in PBS for immediate flow cytometric analysis.

2.2.13.7 Staining of intracellular cytokines after stimulation with the cognate antigen

To assess cytokine production by epitope specific CD8+ T cells, cells were incubated with 1 µM of peptide (or no peptide for negative control) together with 10 U/ml of IL-2 and 1 µg/ml of Golgi stop for 5 hours at 37 °C and 5 % CO2. Following peptide stimulation, cells were centrifuged at 2000 rpm for 3 min at 4 °C and washed with PBS before their surface markers were stained as previously described. To stain intracellular cytokines cells were re-suspended in 100 µl of BD Cytofix/Cytoperm solution and incubated at 4 °C for 20 min. Samples were topped up with 100 µl of cold BD Perm/Wash buffer and centrifuged at 2000 rpm for 3 min at 4 °C. Cells were washed with 200 µl of BD Perm/Wash buffer and centrifuged at 2000 rpm for 3 min at 4 °C. Cells were re-suspended in 50 µl of BD Perm/Wash containing fluorochrome-labeled antibodies raised against cytokines of interest and incubated for 30 min at 4 °C in the dark. Following cytokine staining cells were washed twice in 100 µl of BD Perm/Wash and once in 100 µl of MACS buffer, before being re-suspended in 100 µl of MACS buffer for flow cytometric analysis.

2.2.14 *In vivo* injection of 2-NBDG

To determine cellular glucose uptake *in vivo*, mice were injected i.v. with a fluorescent glucose analogue 30 min prior to organ harvest. A total of 5 mg of 2-NBDG were dissolved in 500 µl of DMSO to yield a stock of 10 mg/ml, of with 10 µl in 100 µl sterile PBS were injected per mouse i.v.. Organs were harvested and processed for flow cytometric analysis as previously described.

2.2.15 Tetramer staining of epitope specific CD8+ T cells

To stain epitope specific CD8+ T cells with specific APC or PE labeled tetramers 100 µl/sample were transferred into round bottom, 96-well plates and centrifuged at 2000 rpm for 3 min at 4 °C. Cells were re-suspended in 50 µl of

tetramer containing MACS buffer (NAshort:PE dilution 1:100; NAlong:APC dilution 1:100) and incubated at RT in the dark for 1 hr. Tetramers were diluted by adding 150 µl of MACS buffer to remove excess tetramers after the staining and cells were centrifuged at 2000 rpm for 3 min at 4 °C. After tetramer staining cells were further processed to access cell surface marker expression.

2.2.16 Tetramer-based enrichment of virus-specific CD8+ T cells

To assess naïve precursor numbers of virus-specific CD8+ T cells prior to infection, naïve precursors were enriched via tetramer-based magnetic enrichment. Spleen and peripheral LNs were harvested in MACS buffer and processed to yield a single cell suspension as previously described. Following red blood cell lysis, a 200 µl aliquot of each sample was set aside to determine total cell numbers prior to enrichment of tetramer-positive CD8+ T cells. Cells were centrifuged at 1600 rpm for 6 min at 4 °C and re-suspended in 100 µl of MACS buffer and an additional 100 µl of Fc-blocking cocktail made up of MACS buffer (1:2 dilution), 2.4G2 supernatant (1:2 dilution), NRS (1:100 dilution) and NMS (1:100 dilution). Each sample was supplemented with 3 µl of NAshort:PE and 3 µl of NAlong:APC tetramer corresponding to 1 µg of each tetramer. Samples were incubated at RT for 1 hr and supplemented with 50 µl of both anti-PE and anti-APC MicroBeads. Cells were incubated at 4 °C for 20-30 min, washed twice with 10 ml of MACS buffer to remove excess unbound MicroBeads and filtered through a 70 µm cell strainer into a new 50 ml tube. Cells were centrifuged and re-suspended in 3 ml of MACS buffer. Samples were passed through an LS column on a magnet to positively enrich tetramer positive cells. The eluate was passed through the column again and the LS column washed with an additional 3 ml of MACS buffer. The positively enriched cell fraction was eluted in 5 ml of MACS buffer into a new 15 ml Falcon. Cells were centrifuged and re-suspended in 90 µl of MACS buffer. A total of 10 µl of PBS containing 10x concentrated viability dye was added and samples incubated for 10 min at RT in the dark. Samples were topped up with 4 ml of PBS

and centrifuged. Cells were re-suspended in 90 µl of MACS buffer and surface markers stained by adding 10 µl of MACS buffer containing 10x concentrated fluorochrome-labeled surface antibodies. Samples were incubated for 20 to 30 min at 4 °C in the dark and topped up with 4 ml of MACS buffer to wash away excess antibodies. Samples were pelleted, re-suspended in a total of 300 µl of MACS buffer and transferred to 5 ml conical tubes for flow cytometric analysis.

2.2.17 Single-cell sort of tetramer positive CD8+ T cells

To assess paired TCR alpha and beta chain expression in tetramer positive CD8+ T cells on day 10 after PR8 influenza infection, single epitope specific CD8+ T cells were sorted based on tetramer binding. Spleen and peripheral LNs from the same mouse were pooled, processed and enriched for tetramer positive CD8+ T cells as described above. Live, single cells positive for tetramer were sorted into single wells of round bottom; half skirted 96-well plates and wells were immediately capped to prevent contamination. Plates containing single cells were stored at -80°C until analysis of their TCR alpha and beta chain usage via multiplex PCR.

2.2.18 Multiplex polymerase chain reaction (PCR) based analysis of paired TCR alpha and beta chains

To determine TCR alpha and beta chain usage of the different epitope-specific CD8+ T cells post PR8 influenza infection, the mRNA of their TCR alpha and beta chains was reverse transcribed into DNA and amplified by multiplex PCR and sequenced, according to the protocol described by Dash et al. 2011, J Clin Invest. Single cells in previously sorted 96-well plates were supplemented with 2.5 µl containing 0.5 µl of 5x Vilo reaction mix, 0.25 µl of 10x Superscript RT, 0.275 µl of 1% Triton X-100 and 1.5 µl of HPLC water and spun down at 2400 rpm for 1 min at 4 °C. The PCR was run according to the following program; 25 °C for 10 min, 42 °C for 120 min and 85 °C for 5 min. The plates were spun down before running the external nested PCR using “external” primers for the alpha and beta regions of the

TCR. Each sample was supplemented with 22.5 µl of PCR mix per well, which was made up of 2.5 µl of 10x PCR buffer + $MgCl_2$, 0.5 µl of 10 mM dNTPs, 0.5 µl each of 5 pmol/µl TRAV Ext, TRAC Ext, TRBV Ext and TRBC Ext primers, 0.15 µl of Tag DNA polymerase and 17.35 µl of HPLC water. Plates were centrifuged at 2400 rpm for 1 min at 4 °C before the PCR was run according to the following program; 95°C for an initial 5 min, 95 °C for 30 sec, 52 °C for 30 sec, 72 °C for 45 sec, which was repeated for 35 cycles and 72 °C for a final 7 min. Plates were spun down before proceeding with the internal nested PCR. A 2.5 µl aliquot of each sample was transferred into two new 96-well plates for their corresponding alpha and beta chains, respectively. Samples in each plate were supplemented with 22.5 µl of internal PCR mix corresponding to their respective alpha or beta chains, according to the reaction mix displayed in the table below.

Reagent	**Volume of a chain mix (µl)**	**Volume of b chain mix (µl)**
10x Coral-Load PCR buffer	2.5	2.5
10mM dNTPs	0.5	0.5
5pmol/µl TRAV Int primers	0.5	-
5pmol/µl TRAC Int primers	0.5	-
5pmol/µl TRBV Int primers	-	0.5
5pmol/µl TRBC Int primers	-	0.5
Taq DNA polymerase	0.15	0.15
HPLC Water	18.35	18.25
Total Volume/ well	**22.5**	**22.5**

Samples were spun down and the internal nested PCR was run according to the conditions described for the external nested PCR described above. Upon completion of the PCR, samples were run on a 2 % agarose gel at 100 V for 30 min to determine the presence of a PCR product. Samples having yielded a PCR product were processed further. A 5 µl aliquot was transferred into a new 96-well plate and supplemented with 1 µl of ExoSAP-IT. Plates were spun down and incubated at 37 °C for 15 min followed by incubation at 80 °C for 15 min. Plates were spun down again and supplemented with 14 µl of PCR mix according to the table below to amplify the alpha and beta chains for sequencing using only the internal reverse primers TRAC Int and TRBC Int, respectively.

Reagent	**Volume of a chain mix (µl)**	**Volume of b chain mix (µl)**
5x Sequencing buffer	4	4
DMSO	1	1
5pmol/µl TRAC Int primer	1	-
5pmol/µl TRBC Int primer	-	1
Big Dye Terminator	1	1
HPLC Water	7	7
Total volume/well	14	14

Each sample was supplemented with 14 µl of either the alpha or beta PCR mix, plates were spun down and the PCR run according to the following parameters; 95 °C for an initial 5 min, 96 °C for 10 sec, 50 °C for 5 sec and 60 °C for 4 min, which was repeated for 30 cycles. All samples were then purified using the Quiagen DyeEx 96 Kit to remove unincorporated terminators. Samples were sequences by the Mircromon Sanger Sequencing facility at Monash University, Clayton, VIC, Australia.

2.2.19 Tetramer dissociation assay

Spleens and LNs were processed into single cell suspension as described above, of which an aliquot was taken to be stained with tetramer in FACS buffer containing 0.2 % sodium azide for 1 hr. Cells were centrifuged, washed in FACS buffer and re-suspended in FACS buffer containing purified anti-H-2D^b and anti-H-2K^b antibody at a 1/20 dilution. Cells were incubated at 37 °C for 0, 5, 10, 15, 30, 45 and 60 min, after which cells samples were transferred to a 96-well plate on ice and diluted with the addition of 150 µl of FACS buffer. After completion of the time course, samples were centrifuged, washed in FACS buffer and surface stained as described above. Cells were analyzed by flow cytometry.

2.2.20 Determining cell numbers

To determine absolute cell counts an aliquot of each cell suspension was diluted in Trypan blue solution at a dilution of 1:10. The diluted cell suspension aliquot was added to a Neubauer counting chamber and viable cells contained in the four large 4x4 squares were counted. The total cell numbers were calculated according to the following formula: cells counted/4 x dilution factor x 10^4 (constant of the counting chamber) = cells/ml cell suspension.

2.2.21 Statistical analysis

To determine statistical significances, a two-tailed unpaired t-test was used, when comparing two different data sets that were expected to have a Gaussian distribution. For comparing two groups of non-parametric data, a Mann-Whitney test was used. For comparing more than two groups a two-way ANOVA was used, as indicated in the figure legends. Analyses were done with Prism 8.0 and p-value of >0.05 was deemed statistically significant.

Chapter 3

Chronic liver inflammation negatively impacts the expansion, effector function and mitochondrial fitness of virus-specific T cells during LCMV infection

3.1 Introduction

Liver fibrosis and chronic inflammation of the liver constitutes a severe health burden worldwide, with an incidence that is continuously rising (Henderson and Iredale, 2007). Liver fibrosis is characterized by the continuous replacement of the healthy liver parenchyma by scar tissue and gradual loss of liver function due to inflammation (Bataller and Brenner, 2005). Liver cirrhosis can develop as a consequence of chronic liver injury and marks the end stage of most liver diseases resulting in organ dysfunction (Bataller and Brenner, 2005) (Marra, 1999). Many insults, such as viral infections like hepatitis B and C, alcoholism, obesity or NASH (non-alcoholic steotohepatitis), can cause chronic inflammation of the liver leading to fibrosis and subsequently to liver cirrhosis, if the liver injury persists (Henderson and Iredale, 2007). Chronic inflammation of the liver is accompanied by extensive production of inflammatory cytokines such as IL-6 and TNFα, as well as ROS, and continuous infiltration of immune cells into the inflamed tissue (Byl et al. 199) (Ramadorie and Saile, 2004) (Karlmark et al. 2008).

A major complication in cirrhosis patients is the increased susceptibility to infections, which is termed cirrhosis-associated immune dysfunction (CAID) and refers to the immunodeficiencies and abnormalities in immune cell function associated with cirrhosis (Albillos et al. 2014). The severe dysfunction of the liver results in impaired innate and adaptive immunity in response to invading pathogens, despite the already established systemic inflammation seen in cirrhosis patients (Tritto et al. 2011). The defect in the innate immune system is highlighted by the reduced phagocytic function of neutrophils present at the site of inflammation in cirrhosis patients (Tritto et al. 2011). In addition, plasma from cirrhosis patients is able to induce phagocytic dysfunction even in healthy neutrophils, when incubated together, suggesting the presence of a soluble factor in the circulation of cirrhosis patients that exerts inhibitory actions on neutrophils, which play a crucial role in combating invading pathogens early during infection

(Tritto et al. 2011). In addition to impaired neutrophil phagocytic function, liver cirrhosis has also been associated with reduced macrophage function, as shown by Gomez et al. (1994), who could show that macrophages from cirrhosis patients are impaired in their ability to clear IgG-coated cells via their Fcγ-receptor. Cirrhosis patients also display severe abnormalities with respect to their CD27+ memory B cell compartment, which were shown to adopt a hyporesponsive state that is characterized by reduced TNFα and IgG production upon activation via CD40 and TLR9 (Doi et al. 2012). The profound changes in immune cell function in cirrhosis patients, abolishes their ability to mount an efficient immune response against bacterial and viral infections, subsequently causing an increase in morbidity and infection-associated mortality (Arvaniti et al. 2010) (Albillos et al. 2014).

To elucidate the underlying mechanisms of the immunosuppressive state of these patients, we combined a well-established mouse model of chronic liver inflammation and fibrosis, together with infection with the lymphocytic choriomeningitis virus (LCMV). The murine bile-duct ligation (BDL) model represents a model of obstructive cholestasis and displays leukocyte infiltration into the liver, elevated nitric oxide levels in the serum, as well as overall liver and renal dysfunction (O'Brien et al. 2016). Recently, our group has shown that mice with liver fibrosis (i.e. BDL-operated mice) are more susceptible to bacterial infections and display impaired clearance of *Listeria monocytogenes* (Hackstein et al. 2016). In these mice we observed elevated levels of the anti-inflammatory cytokine IL-10, which is mirroring the situation in patients with liver fibrosis (Hackstein et al. 2016) (Abe et al. 2004). This is due to elevated levels of type I IFN, which are induced by translocation of gut microbiota during liver fibrosis, which is directly responsible for the up-regulation of IL-10 by myeloid cells upon bacterial infection with *Listeria monocytogenes* (Hackstein et al. 2016).

The aim of this thesis is to unravel the cellular and molecular mechanisms underlying the increased susceptibility to viral infection associated with liver fibrosis. To this end, the murine model of acute infection with the WE strain of LCMV was used, which is characterized by a strong adaptive immune response that leads to sterile clearance of the virus around day 10 post infection (Moskophidis et al. 1995). LCMV-WE infections in mice are effectively cleared by a strong CTL response, which relies on antigen presentation via class I MHC molecules and is not accompanied by any detectable immunopathology in immunocompetent mice (Moskophidis et al. 1995) (Marsland et al. 2005). Our group could previously show that BDL mice are unable to effectively clear an acute infection with LCMV-WE, but rather develop a chronic viral infection that persists until at least day 30 p.i., while healthy control mice clear the virus by day 10 p.i., mirroring the immunocompromised phenotype seen in patients.

To elucidate the underlying mechanism of the immunosuppressive phenotype seen in cirrhosis patients, BDL-operated mice were infected with LCMV-WE and T cell-mediated adaptive immune response was analyzed. To this end both endogenous and adoptively transferred virus-specific T cells were assessed for their ability to produce effector cytokines required for efficient viral clearance, their potential to proliferate and expand upon antigen encounter. Additionally, mitochondrial fitness and expression of inhibitory receptor associated with T cell dysfunction in the context of chronic viral infections were analyzed. Since efficient antigen presentation and priming of T cells by DCs is a determinant of the outcome of the virus-specific T cell responses, the number and maturation status of splenic DCs was investigated. The results of this thesis indicate that chronic liver inflammation affects both the innate and the adaptive branches of the immune system, reflected in impaired DC maturation and failure to launch an efficient T cell response during LCMV infection. Shedding light on the underlying mechanisms of the immunosuppression seen during chronic inflammation of the liver, might open

up new avenues into discovering potentially new therapies to boost the immune system of patients with liver cirrhosis and improve their quality of live.

3.2 Results

3.2.1 Chronic inflammation of the liver is associated with impaired T cell immune responses to acute LCMV infection

Acute LCMV infection of healthy mice is cleared in infected cells by virus-specific CD8+ T cells (Fung-Leung et al. 1991) (Matloubian et al. 1994). If virus-specific T cell immunity is not strong enough within the first 10 days of infection, acute LCMV infection can become chronic (Matloubian et al. 1994). To assess the impact of chronic liver inflammation on the ability of the immune system to clear viral infections, chronic liver inflammation was induced in wild type B6 mice using bile duct ligation (BDL). On day 9 post operation, mice were infected with $2x10^4$ PFU of LCMV (WE strain). In contrast to healthy mice that cleared the acute infection by day 8-10, mice with liver fibrosis failed to control the acute infection (Figure 5, A-C). While viral tiers were identical during the first days after infection, peaked at day 6 and started to decline thereafter in both healthy and BDL-operated mice, viral control at day 8 was not achieved in mice with liver fibrosis. Instead, LCMV infection persisted at high levels in the liver, blood and spleen in mice with liver fibrosis until the end of the experiment at day 30 after infection (Figure 5, A). This indicates a systemic loss of immune control over LCMV infection rather than a local escape of LCMV from clearance in damages liver tissue.

Consistent with the efficient in immune control of LCMV infection at day 8, healthy mice showed a robust LCMV-specific CD8+ T cell response, whereas mice with liver fibrosis had an approximately 10 fold lower number of polyclonal and LCMV-specific CD8+ T cell in the liver (Figure 6, E-H). The observed reduction in the total number of CD8+ T cells in mice with chronic liver inflammation was not due to altered tissue distribution or impaired recruitment of T cells to the livers, as

lower T cell numbers were also found in the spleen of infected BDL mice (Figure 2 A-D). Chronic viral infection is often associated with loss of CD4+ T cell help that is required to sustain CD8+ T cell function and control infection. On day 8 post LCMV infection, the total number of polyclonal and LCMV-specific CD4+ T cells in mice with chronic liver inflammation also showed a significant reduction in numbers compared to control mice (Figure 6 A-B, E-F).

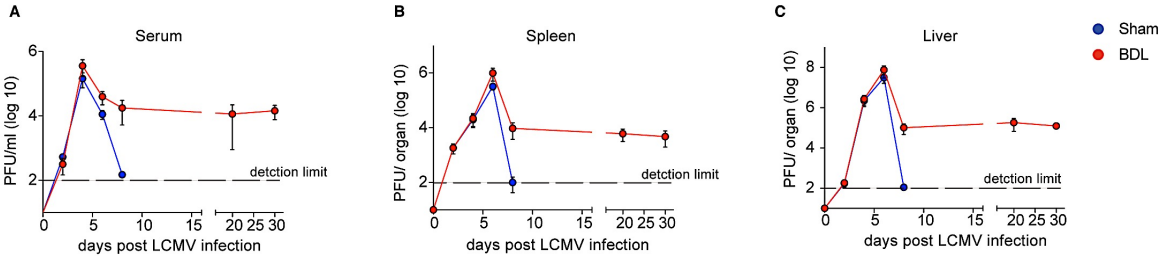

Figure 5: Persistent LCMV infection and high viral titers in BDL-operated mice after LCMV infection. Quantification of virus titers in the serum **(A)**, spleen **(B)** and liver **(C)** of BDL and Sham operated mice after LCMV infection.

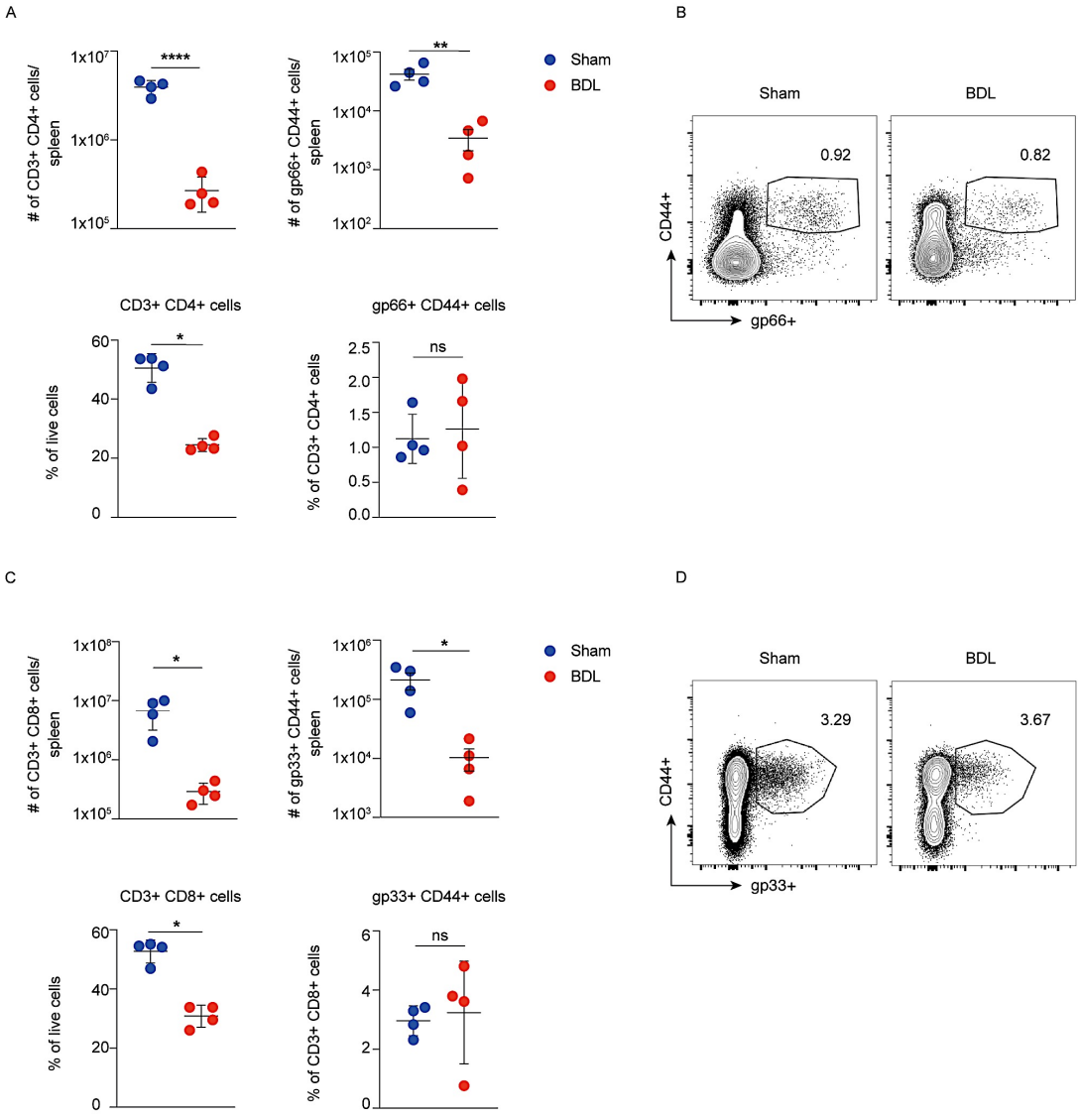
A
# of CD3+ CD4+ cells/ spleen
1x10^7
1x10^6
1x10^5
****
# of gp66+ CD44+ cells/ spleen
1x10^5
1x10^4
1x10^3
1x10^2
**
Sham
BDL
CD3+ CD4+ cells
% of live cells
60
40
20
0
*
gp66+ CD44+ cells
% of CD3+ CD4+ cells
2.5
2.0
1.5
1.0
0.5
0.0
ns
B
Sham
BDL
0.92
0.82
CD44+
gp66+
C
# of CD3+ CD8+ cells/ spleen
1x10^8
1x10^7
1x10^6
1x10^5
*
# of gp33+ CD44+ cells/ spleen
1x10^6
1x10^5
1x10^4
1x10^3
*
Sham
BDL
CD3+ CD8+ cells
% of live cells
60
40
20
0
*
gp33+ CD44+ cells
% of CD3+ CD8+ cells
6
4
2
0
ns
D
Sham
BDL
3.29
3.67
CD44+
gp33+

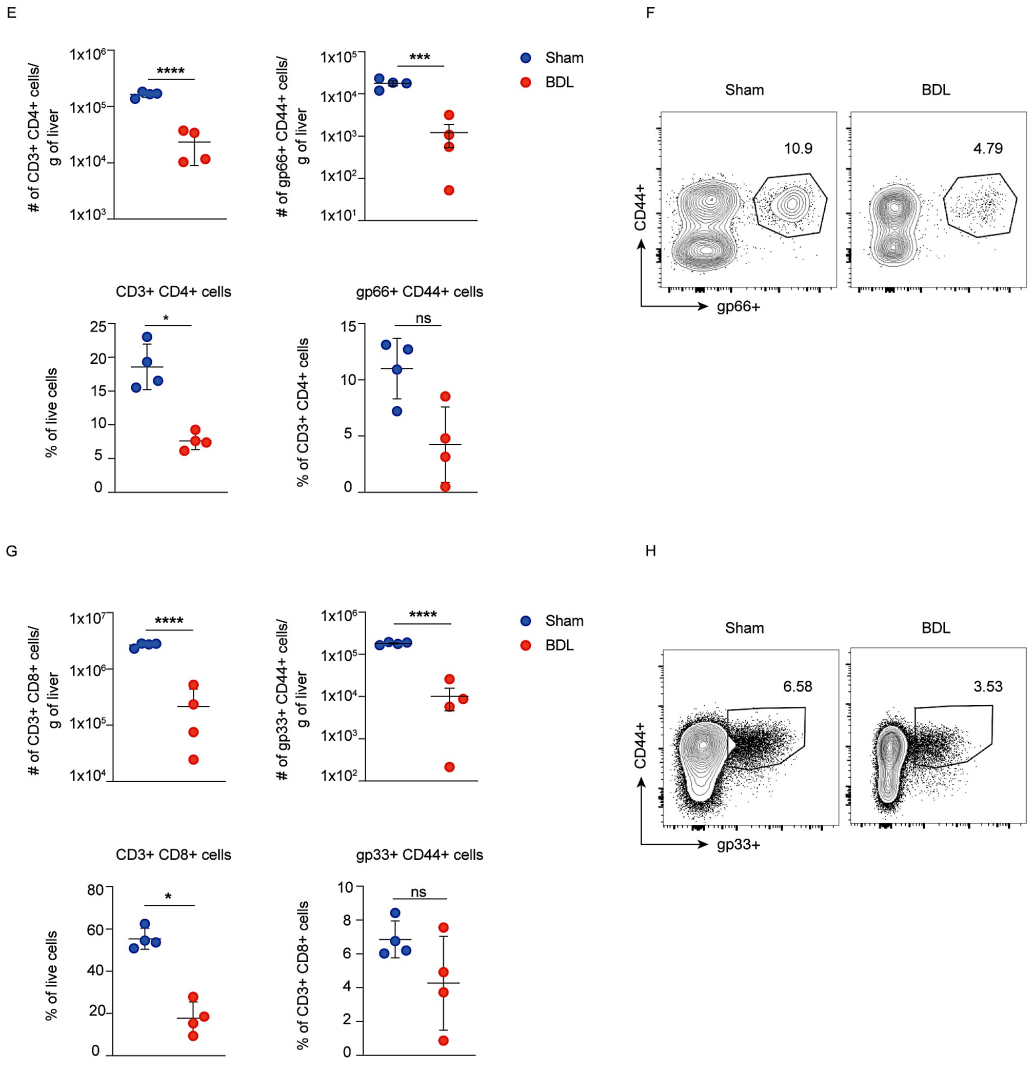

Figure 6: Reduced numbers of LCMV-specific CD4+ and CD8+ T cells in the spleen and liver of BDL-operated mice. Flow cytometric analysis of the liver and spleen of BDL-and Sham-operated mice on day 8 post infection. Total number (upper panel) and frequency (lower panel) of polyclonal CD44^{hi} and gp66-specific CD4+ T cells and CD44^{hi} and gp33-specific CD8+ T cells in the spleen **(A, C)** and liver **(E, G)**. Representative dot plots of CD44hi gp66-specific CD4+ T cells and CD44hih gp33-specific CD8+ T cells in the spleen **(B, D)** and the liver **(F, H)**. Data are representative of 2-3 independent experiments (n=3-5 mice).

3.2.2 Chronic inflammation of the liver renders endogenous virus-specific CD4+ and CD8+ T cells exhausted

During chronic viral infections T cells develop an “exhausted” phenotype characterized by a gradual loss of function and the up-regulation of inhibitory receptors such as PD-1, LAG3, TIM3 and/or CTLA4 (Wiesel et al. 2009) (Kahan et al. 2015). T cell exhaustion is induced by a high antigen load and persistence of the virus that results in the failure to develop and maintain a robust memory T cell compartment (Kahan et al. 2015) (Angelosanto et al. 2012) (Sanchez-Fueyo and Markmann, 2016). Co-expression of PD-1 with inhibitory receptors such as LAG3, TIM3 or CTLA4 was shown to correlate with a higher degree of T cell dysfunction, i.e. exhaustion (Kahan et al. 2015) (Blackburn et al. 2009).

Since BDL mice fail to clear an acute infection with LCMV, the expression of the exhaustion markers PD-1, LAG3 and TIM3 by endogenous LCMV-specific CD4+ and CD8+ T cells in the spleen and liver was analyzed on day 8 p.i.. The results of this experiment showed that gp66+ CD4+ T cells in the spleen and liver of BDL mice contain a significantly higher proportion of cells positive for both PD-1 and LAG3, while the proportion of PD-1 and TIM3 positive cells was similar compared to infected Sham mice (Figure 6 A – B). A similar phenotype can be observed among the gp33+ CD8+ T cells in the spleen and liver of BDL mice. Additionally, there was a higher frequency of PD-1 and LAG3 double positive cells among gp33+ CD8+ T cells from BDL-operated mice compared to LCMV infected Sham-operated mice. However, the proportion of PD-1 and ITM3 double positive gp33+ CD8+ T cells in the spleen and liver of BDL-operated mice was comparable to those from infected Sham-operated mice (Figure 6 C – D). Taken together, these results suggest that chronic inflammation of the liver renders virus-specific T cells at least partially exhausted by day 8 post LCMV infection. Together with the reduction in absolute numbers of LCMV-specific CD4+ and CD8+ T cells, these

data show the negative impact chronic inflammation of the liver has on the T cell-mediated adaptive immune response against viral infection.

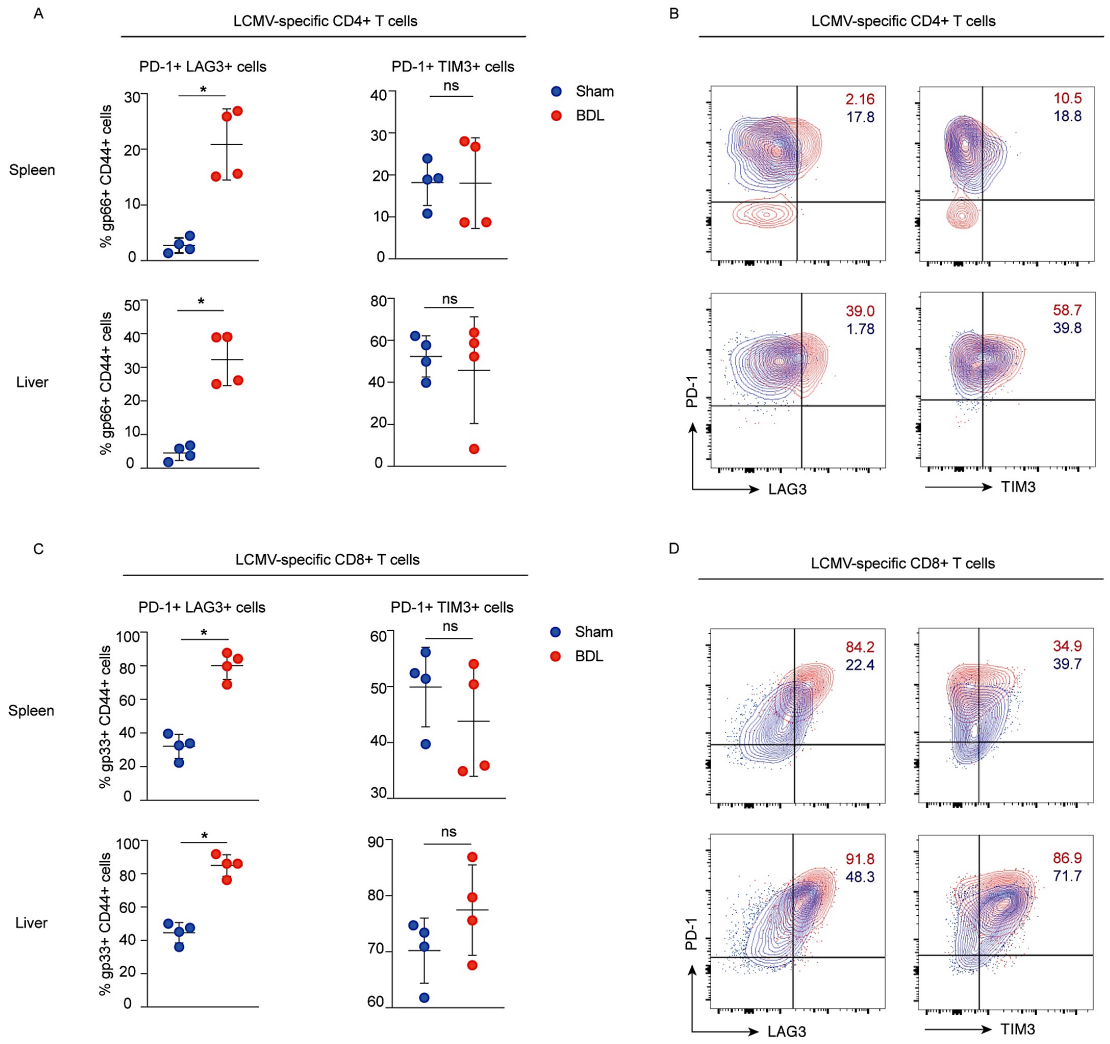

Figure 7: Increased proportion of exhausted LCMV-specific CD4+ and CD8+ T cells in BDL-operated mice after LCMV infection. Flow cytometric analysis of the liver and spleen of BDL-and Sham-operated mice on day 8 post infection. Proportion of PD-1+ LAG3+ and PD-1+ TIM3+ T cells in the spleen and liver among CD44^{hi} gp66+ CD4+ T cells and CD44^{hi} gp33+ CD8+ T cells **(A, C)**. Representative dot plots of PD-1+ LAG3+ and PD-1+ TIM3+ T cells in the spleen and liver among CD44^{hi} gp66 + CD4+ T cells and CD44^{hi} gp33+ CD8+ T cells **(B, D)**. Data are representative of 2-3 independent experiments (n=3-5 mice).

3.2.3 Adoptively transferred LCMV-specific T cells fail to expand after LCMV infection in mice with chronic liver inflammation

To ensure that chronic inflammation of the liver does not affect virus-specific T cell precursors during early development and thymic selection, resulting in the observed dysfunctional phenotype of endogenous virus-specific T cells in BDL-operated mice, naïve LCMV-specific T cells from healthy SMARTA or P14 mice were adoptively transferred. In the transgenic SMARTA and P14 mouse lines 98 % of T cells express T cell receptors (TCRs) specific for the specific for the epitope 61-80 and the epitope 33-41 of the LCMV glycoprotein, respectively (Brooks et al. 2006). Taking advantage of these LCMV-specific T cells enables us to determine how chronic liver inflammation affects the expansion of LCMV-specific T cells during the early phase of the response against LCMV. In contrast to Sham-operated mice that show a distinct increase in SMARTA and P14 T cell number after LCMV infection, SMARTA and P14 T cells fail to expand to the same extent in BDL-operated mice and show significantly lower numbers in the spleen starting on day 4 .p.i. (Figure 8 A, C). SMARTA and P14 T cell numbers remain low also on day 6 and 8 after infection. Similarly, the numbers of SMARTA and P14 t cells in the liver were significantly lower in BDL-operated mice compared to healthy mice at the peak of the T cell-mediated immune response against LCMV, i.e. on day 8 post infection (Figure 9 A, B). This data suggests that the reduced numbers of virus-specific T cells might predominantly be due to reduced proliferation rather than only to a delayed response. Considering the fact that virus-specific SMARTA and P14 T cells numbers increase by a factor of 10 in BDL mice between day 6 and day 8 p.i., while T cells from Sham mice do not show the same increase, the reduction in SMARTA and P14 T cells in BDL mice could be due to a combination of a delayed response, as well as a proliferative defect.

Additionally, the entire polyclonal pool of CD44+ CD4+ and CD8+ T cells was smaller in magnitude starting on day 6 p.i. in BDL-operated mice compared to

Sham-operated mice (Figure 10 A, B). Collectively, chronic inflammation of the liver results in an overall defect within the T cell compartment depicted by lower numbers of polyclonal CD4+ and CD8+ T cells and lower numbers of SMARTA and P14 T cells. These findings indicate that mice suffering from chronic inflammation of the liver already display a defect early on during the expansion phase of the adaptive T cell response against LCMV. This effect cannot be due to a developmental defect established prior to infection in an inflammatory environment, since SMARTA and P14 T cells came from healthy donor mice. Therefore the defect in T cell expansions seems to go beyond the mere inflammatory conditions of this model of liver fibrosis.

In order to elucidate the underlying cause for the lower numbers of SMARTA and P14 T cells seen in BDL-operated mice after infection, SMARTA and P14 T cells were fluorescently labeled with CFSE prior to adoptive transfer. Analysis of SMARTA and P14 T cell proliferation on day 4 p.i. revealed that SMARTA and P14 T cells from BDL-operated mice undergo fewer division cycles after LCMV infection, as indicated by higher levels of CFSE retained in the cells (Figure 11 A, B). These results strongly indicate that reduced numbers of SMARTA and P14 T cells in mice with chronic liver inflammation are due to reduced proliferative potential after LCMV infection during chronic liver inflammation.

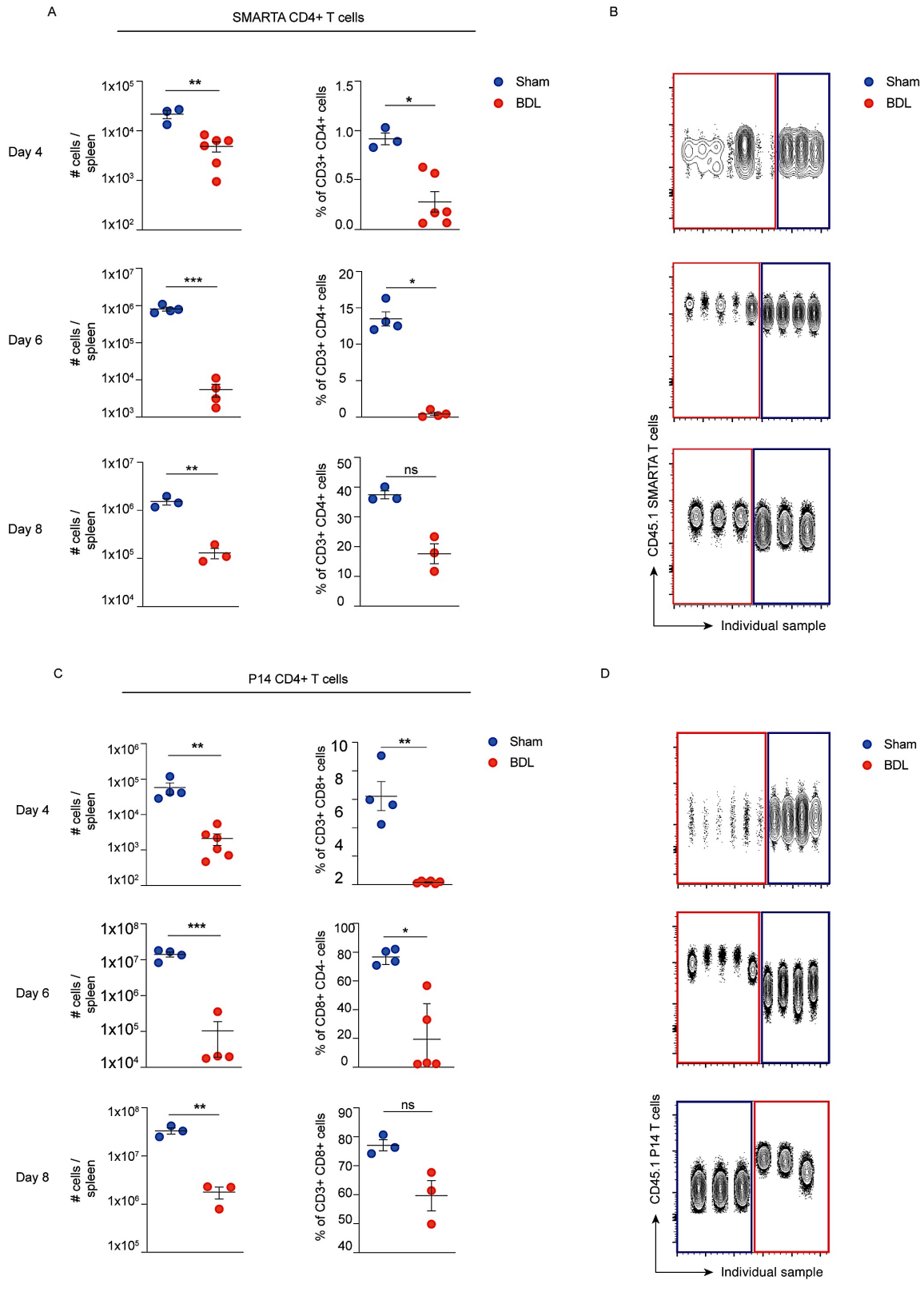
A
SMARTA CD4+ T cells
Day 4
Day 6
Day 8
cells / spleen
% of CD3+ CD4+ cells
Sham
BDL
B
CD45.1 SMARTA T cells
Individual sample
C
P14 CD4+ T cells
% of CD3+ CD8+ cells
% of CD8+ CD4- cells
% of CD3+ CD8+ cells
D
CD45.1 P14 T cells
Individual sample
ns

Figure 8: Reduced number and proportion of transferred LCMV-specific CD4+ (SMARTA) and CD8+ (P14) T cells in the spleen of BDL-operated mice after LCMV infection. Flow cytometric analysis of the spleen of BDL-and Sham-operated mice on day 4, 6 and 8 post LCMV infection. Absolute number and frequency of SMARTA **(A)** and P14 **(C)** T cells from the spleen. Representative dot plots of SMARTA **(B)** and P14 **(D)** T cells from the spleen of different BDL and Sham mice post LCMV infection. Data are representative of 2-4 independent experiments (n=3-6 mice).

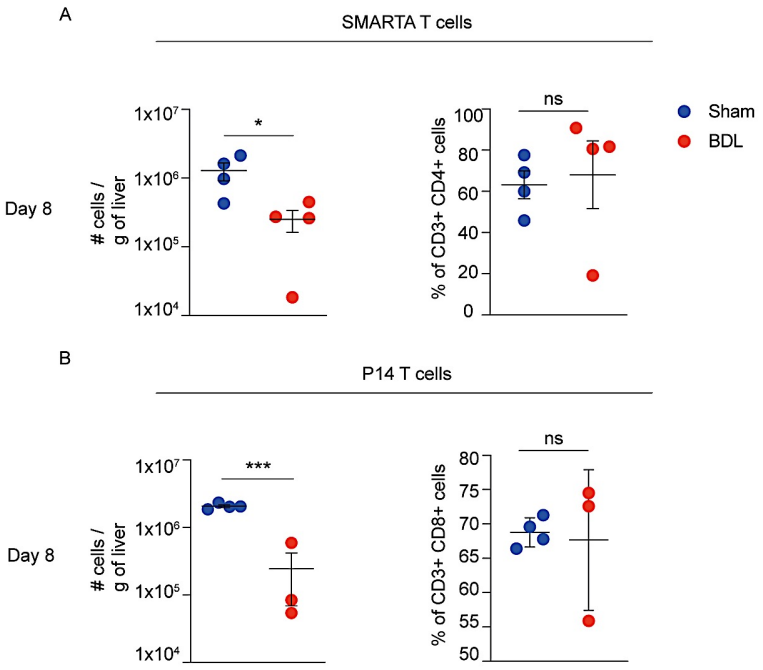

Figure 9: Impaired expansion of transferred SMARTA and P14 T cells in the liver of BDL-operated mice. Flow cytometric analysis of the liver on day 8 post LCMV infection. Total numbers and proportion of SMARTA **(A)** and P14 **(B)** T cells in the liver of BDL-and Sham-operated mice. Data are representative of 3-4 independent experiments (n=3-5 mice).

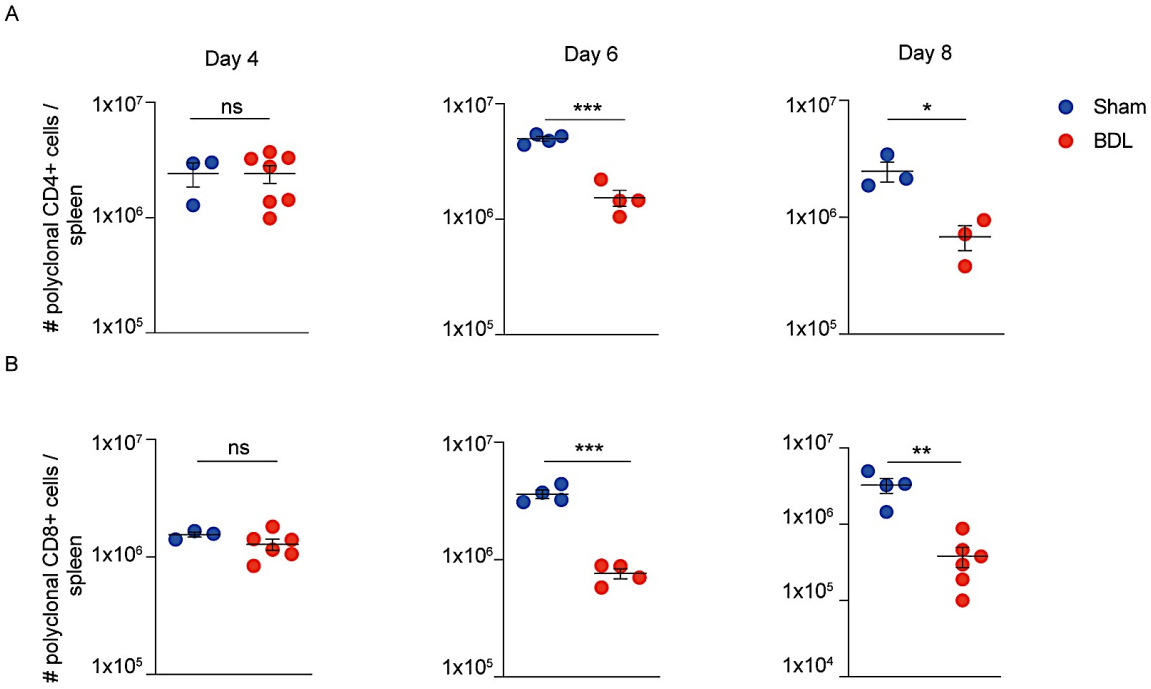

Figure 10: Reduced numbers of polyclonal CD4+ and CD8+ T cells after LCMV infection in mice with liver fibrosis. Flow cytometric analysis of the spleen from BDL- and Sham-operated mice. Total number of polyclonal CD4+ CD44+ **(A)** and CD8+ CD44+ **(B)** T cells on day 4, 6 and 8 post LCMV infection. Data are representative of 2-3 independent experiments (n=3-6 mice).

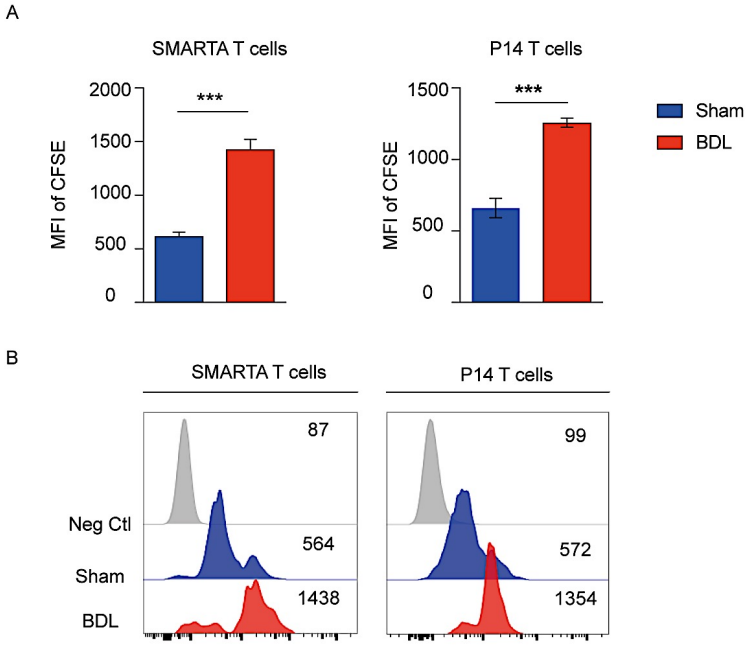

Figure 11: Reduced proliferative potential of transferred SMARTA and P14 T cells in mice with liver fibrosis. Flow cytometric analysis of the spleen of BDL- and Sham-operated mice on day 4 post infection. Intracellular levels of CFSE in SMARTA and P14 T cells **(A)** from the spleen. Representative histograms of CFSE levels in SMARTA and P14 T cells from the spleen **(B)**. Data are representative of 2-3 independent experiments (n=3-5 mice).

3.2.4 SMARTA T cells from BDL-operated mice are more prone to undergo apoptosis after LCMV infection

To determine whether reduced SMARTA and P14 T cell numbers in BDL-operated mice is also in part due to a reduction in survival, the presence phosphatidylserine (PS) on the cell surface, as a early sign of cells undergoing apoptosis, was determined. To this end splenocytes from BDL- and Sham-operated mice were stained with Annexin V, a dye that binds the PS motifs exposed on the cell surface of apoptotic cells, on day 4 post LCMV infection (Leventis and Grinstein, 2010). As shown in Figure 12 A – C SMARTA T cells from the spleen of BDL-operated mice show a significantly higher proportion of Annexin V positive cells, i.e. early apoptotic cells. Therefore, the overall lower numbers of adoptively transferred SMARTA T cells in BDL mice are at least in part due to reduced survival of these cells during LCMV infection in mice suffering from chronic inflammation of the liver.

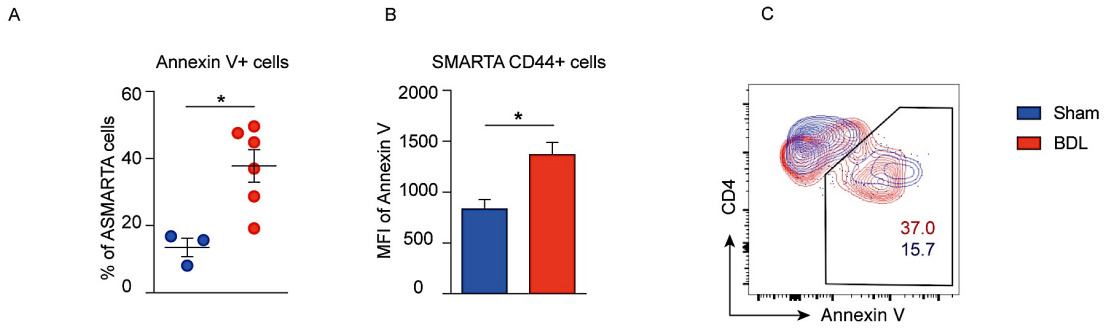

Figure 12: Increased proportion of apoptotic cells among transferred SMARTA T cells in BDL-operated mice at day 4 post LCMV infection. Flow cytometric analysis of the spleen from BDL- and Sham-operated mice after infection. Proportion of Annexin V+ SMARTA T cells **(A)**, as well as the MFI of Annexin V per SMARTA T cell **(B)**. Representative dot plot of Annexin V+ SMARTA T cells in the spleen **(C)**. Data are representative of 2 independent experiments (n=3-6 mice).

3.2.5 SMARTA and P14 T cells display impaired differentiation into short-lived effector T cells in BDL-operated mice after LCMV infection

Upon viral infection both virus-specific CD8+ and CD4+ T cells differentiate into short-lived effector cells (SLECs), as well as memory-precursor effector cells (MPECs) (Marshall et al. 2011) (Yuzefpolskiy et al. 2015). Once the virus is cleared the majority of these effector T cells undergoes apoptosis, while a small subset of MPECs survives to become long-lasting memory T cells and convey protection against recurring viral infection (Yuzefpolskiy et al. 2015).

To determine whether chronic liver inflammation impairs the formation of sufficient numbers of SLECs needed to efficiently combat an acute LCMV infection, SMARTA and P14 T cells were adoptively transferred into BDL- and Sham-operated mice on day 8 post operation and infected with LCMV one day after. Results showed that SLECs, as characterized by the expression of CD44 and KLRG1, together with the lack of CD62L and CD127, are present at a lower proportion, as well as number in both the spleen and the liver of BDL-operated mice on day 8 p.i. (Figure 13 A, B). Taken together, chronic liver inflammation severely affects the ability of transferred virus-specific T cells to differentiation in short-lived effector T cells, explaining in part the impaired T cell mediated response against LCMV in mice with chronic liver inflammation.

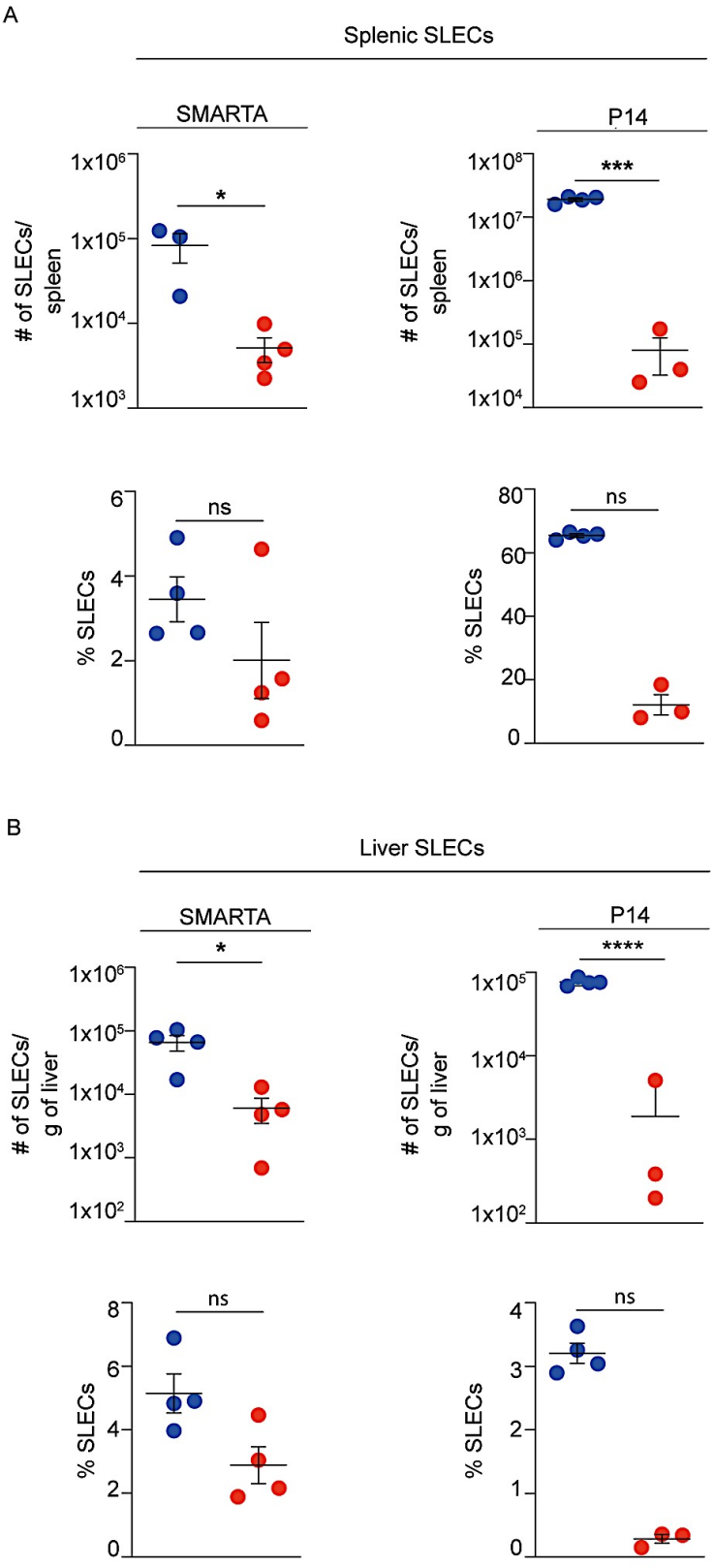
A
Splenic SLECs
SMARTA
P14
# of SLECs/ spleen
1x10^6
1x10^5
1x10^4
1x10^3
*
1x10^8
1x10^7
1x10^6
1x10^5
1x10^4
***
% SLECs
6
4
2
0
ns
80
60
40
20
0
ns
B
Liver SLECs
SMARTA
P14
# of SLECs/ g of liver
1x10^6
1x10^5
1x10^4
1x10^3
1x10^2
*
1x10^5
1x10^4
1x10^3
1x10^2
****
% SLECs
8
6
4
2
0
ns
4
3
2
1
0
ns

Figure 13: Reduced number and proportion of short-lived effector T cells (SLECs) derived from SMARTA and P14 T cells in BDL-operated mice. Flow cytometric analysis of spleen and liver of BDL and Sham operated mice on day 8 post LCMV infection. Absolute numbers and proportion of SLECs derived from SMARTA and P14 T cells from the spleen **(A)** and liver **(B)**. Data are representative of 1-2 independent experiments (n=3-4 mice).

3.2.6 Reduced effector cytokine production in SMARTA and P14 T cells from BDL-operated mice after LCMV infection

A hallmark of an effective immune response against acute viral infections is the ability of virus-specific T cells to produce effector molecules such as IFNγ, TNFα, IL-2 and granzyme B. To assess whether the impaired clearance of the acute strain of LCMV in mice with chronic liver inflammation is due to a decrease in effector cytokine production naïve SMARTA and P14 T cells were adoptively transferred into BDL- and Sham-operated mice one day prior to LCMV infection. As shown in Figure 14 A, C, SMARTA and P14 T cells from the spleen and liver of BDL-operated mice show significantly lower proportions of IFNγ+ cells compared to Sham-operated mice. Likewise, there is lower proportion of IFNγ+ TNFα+ cells among SMARTA and P14 T cells in the spleen and liver of BDL-operated mice compared to infected Sham-operated mice (Figure 14 B, D – F). In line with the high expression of inhibitory receptors, these results further confirm a dysfunctional phenotype of virus-specific T cells during chronic liver inflammation.

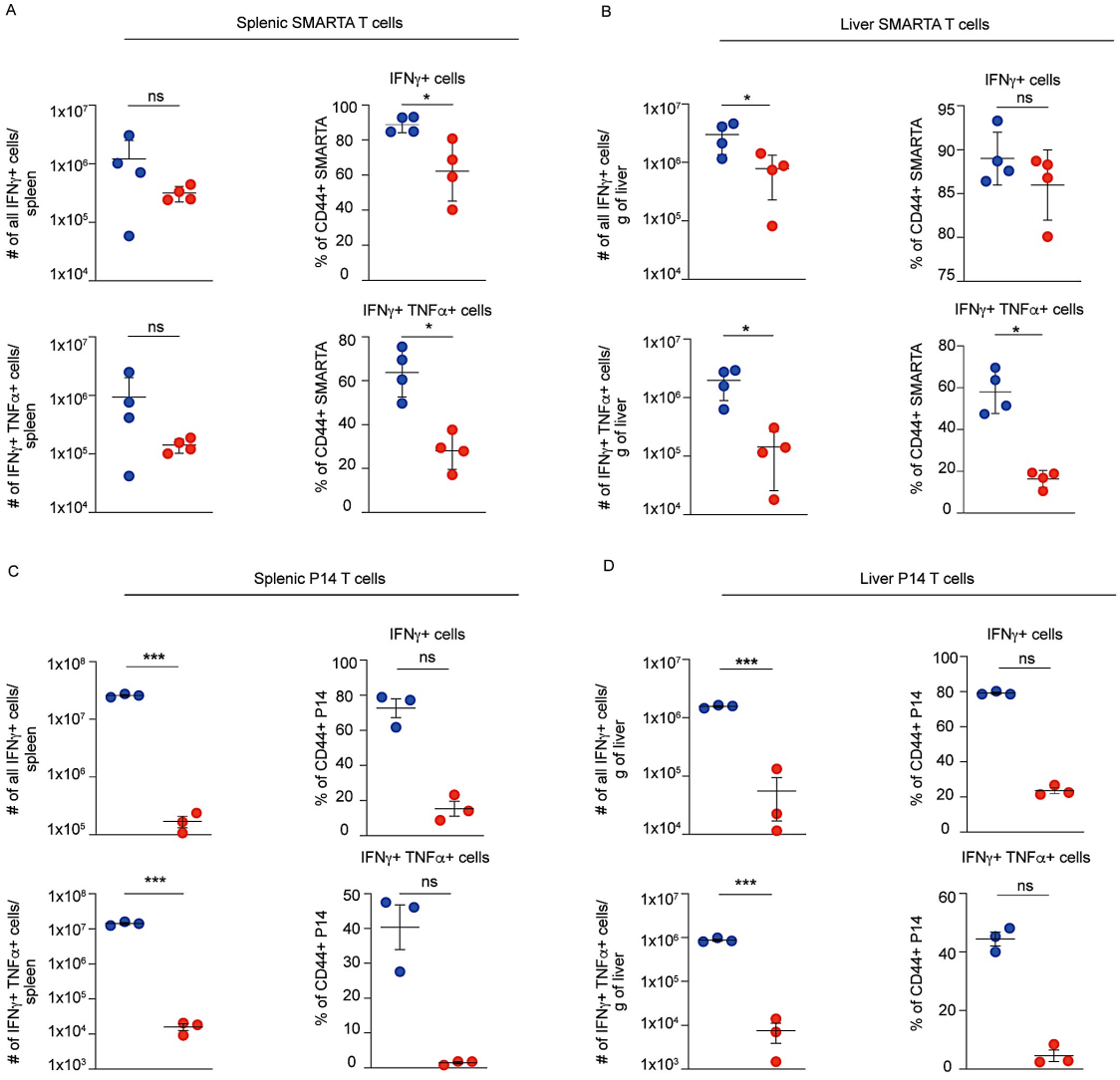
A
Splenic SMARTA T cells
# of all IFNγ+ cells/ spleen
ns
IFNγ+ cells
% of CD44+ SMARTA
*
# of IFNγ+ TNFα+ cells/ spleen
ns
IFNγ+ TNFα+ cells
% of CD44+ SMARTA
*
B
Liver SMARTA T cells
# of all IFNγ+ cells/ g of liver
*
IFNγ+ cells
% of CD44+ SMARTA
ns
# of IFNγ+ TNFα+ cells/ g of liver
*
IFNγ+ TNFα+ cells
% of CD44+ SMARTA
*
C
Splenic P14 T cells
# of all IFNγ+ cells/ spleen
***
IFNγ+ cells
% of CD44+ P14
ns
# of IFNγ+ TNFα+ cells/ spleen
***
IFNγ+ TNFα+ cells
% of CD44+ P14
ns
D
Liver P14 T cells
# of all IFNγ+ cells/ g of liver
***
IFNγ+ cells
% of CD44+ P14
ns
# of IFNγ+ TNFα+ cells/ g of liver
***
IFNγ+ TNFα+ cells
% of CD44+ P14
ns

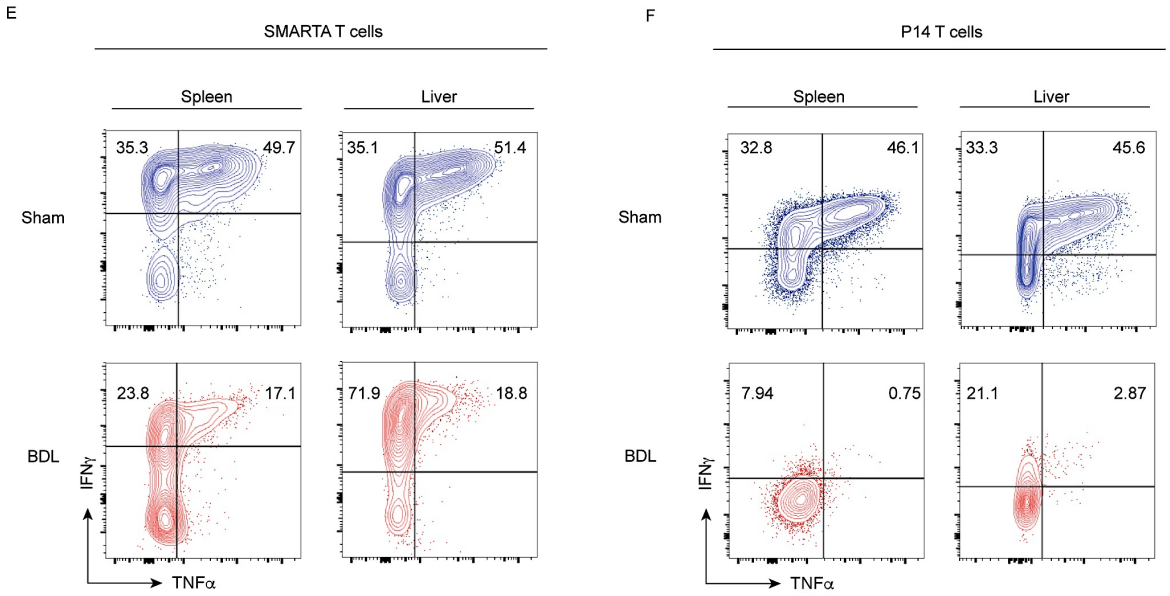

Figure 14: Reduced production of effector cytokines by SMARTA and P14 T cells from BDL-operated mice after LCMV infection. Flow cytometric analysis of the spleen and liver of BDL- and Sham-operated mice on day 8 post infection. Total numbers and proportion of IFNγ+ and TNFα+ SMARTA T cells from the spleen **(A)** and the liver **(B)**. Total number and proportion of IFNγ+ and TNFα+ P14 T cells from the spleen **(C)** and liver **(D)**. Representative dot plots SMARTA **(E)** and P14 **(F)** T cells from the spleen and liver of infected mice. Data are representative of 2 independent experiments (n=3-5 mice).

Next, the ability of SMARTA and P14 T cells to produce the cytotoxic effector molecule granzyme B was determined, which, together with the protein perforin induces death of virally infected cells by DNA fragmentation (Harty et al. 2000). SMARTA and P14 T cell from the spleen of BDL-operated mice displayed a higher proportion of granzyme B producing cells, as well as overall increased levels of granzyme B per cell, compared to Sham-operated mice (Figure 15 A – B). Interestingly, the production of granzyme B does not seem to be impaired by chronic liver inflammation, but instead is enhanced by it. Since cytotoxic CD8+ T cells greatly outnumber cytotoxic CD4+ T cells during viral infections, P14 T cells were more closely focused on to determine whether they can efficiently degranulate and release granzyme B to lyse infected target cells (Marshal and Swain, 2011). The expression of the lysosomal-associated membrane protein-1

(LAMP1), also known as CD107a, on the surface of cytotoxic CD8+ T cells has previously been described as a marker of degranulation in the context of T lymphocyte effector functions, as it is present in the membrane of cytotoxic granules required for the lysis of infected target cells (Betts et al. 2003). Analyzing LAMP1 on the surface of transferred P14 T cells revealed similar proportions of LAMP1 positive cells among P14 T cell from the spleen and the liver of BDL- and Sham-operated mice, but a significant increase in cellular LAMP1 levels in P14 T cells isolated from BDL-operated mice (Figure 15 C). These results indicate that chronic liver inflammation does not impair granzyme B production, but rather results in an increase in granzyme B production, which is accompanied by an increase in LAMP1 levels in P14 T cells from BDL-operated mice.

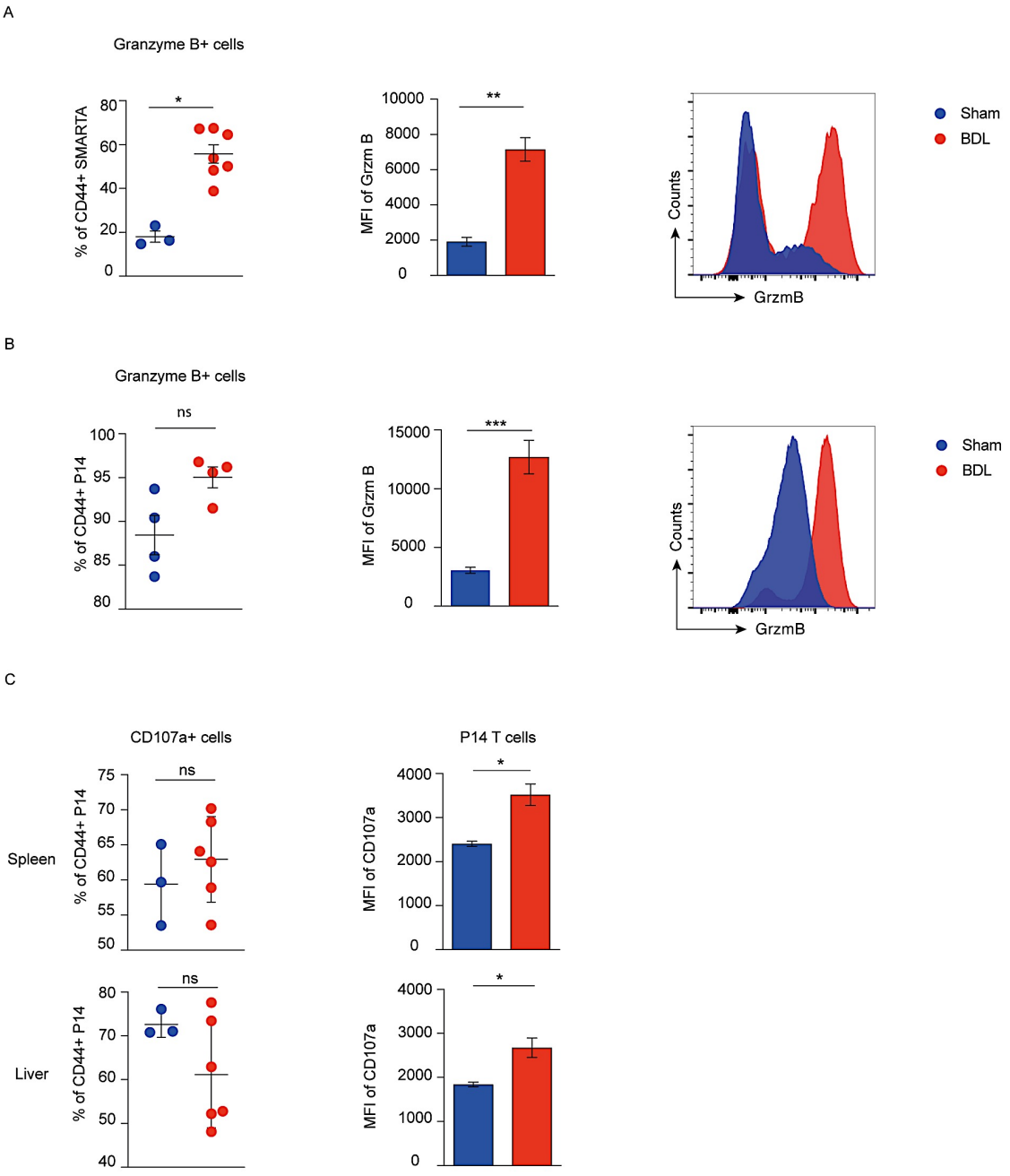

Figure 15: Increased granzyme B and LAMP1 levels in LCMV-specific T cell from BDL-operated mice after LCMV infection. Flow cytometric analysis of the spleen of BDL- and Sham-operated mice on day 8 post LCMV infection. Frequency of granzyme B positive SMARTA **(A)** and P14 **(B)** T cells and the MFI of granzyme B. Proportion of CD107a+ cells and the MFI of LAMP1 among P14 T cells from spleen and liver **(C)**. Data are representative of 1-2 independent experiments (n=3-7 mice).

3.2.7 SMARTA and P14 T cells display enhanced expression of inhibitory markers and an imbalance of t-bet and eomes producing cells in BDL-operated mice after LCMV infection

To determine whether reduced numbers of IFNγ+ and TNFα+ SMARTA and P14 T cells in BDL mice is accompanied by an exhausted, i.e. dysfunctional phenotype of these cells, similar to the phenotype seen in the endogenous virus-specific T cells, the expression of the inhibitory receptors PD-1, LAG3 and TIM3 was analyzed. Results showed an increase in PD-1+ LAG3+ cells among SMARTA and P14 T cells from the spleen and liver of BDL-operated mice, while the proportion of PD-1+ TIM3+ cells remained similar on day 8 after LCMV infection (Figure 16 A-D). SMARTA T cells from the spleen and liver of BDL mice show a significantly higher level of PD-1, LAG3 and TIM3 expression, which is also elevated in P14 T cells, with the exception of TIM3 in P14 T cells from the spleen (Figure 16 E-F). These findings suggest that the impaired antiviral effector function of virus-specific T cells observed in BDL-operated mice could be due to the increased expression of inhibitory receptors, such as PD-1, LAG3 and TIM3, leading to impaired viral clearance in mice with chronic liver inflammation.

T-bet and eomes are transcription factors (TFs) belonging to the family of T-box transcription factors and are crucial for various aspects of the adaptive immune response such as T cell mobilization via CXCR3, cell signaling and the induction of cytolytic signaling molecules such as IFNγ (Knox et al. 2015). While t-bet is crucial for cytotoxic effector differentiation and function, directly up-regulates granzyme B and perforin, eomes is essential for memory cells formation and maintenance (Buggert et al. 2014). Since t-bet and eomes are often deregulated in the context of chronic viral infections and eomes has been shown to be up-regulated in exhausted T cells during chronic LCMV infection in mice, their role in the context of chronic liver inflammation was investigated (Paley et al. 2012).

To investigate whether t-bet and eomes expression is altered in BDL-operated mice after acute infection with LCMV, SMARTA and P14 T cells were transferred on day 8 post operation, followed by LCMV infection one day later. Results showed no apparent difference in the proportion of t-bet+ eomes- and t-bet+ eomes+ cells among SMARTA T cells in the spleen (Figure 17 A). Additionally, the proportion of t-bet+ eomes- cells was significantly decreased in the liver of BDL-operated mice, while the proportion of t-bet+ eomes+ cells is increased, but without reaching statistical significance (Figure 17 A). Likewise, the proportion of t-bet+ eomes- cells among P14 T cells in the spleen and liver of BDL-operate mice is decreased, while the proportion of t-bet+ eomes+ cells among P14 T cells is increased compared to Sham-operated mice, but without showing statistical significance (Figure 17 B). These results show that the balance of t-bet+ eomes- to t-bet+ eomes+ appears to be skewed at least in P14 T cells as a result of chronic liver inflammation. This is in line with the exhausted phenotype of transferred virus-specific T cells that is seen in BDL-operated mice, which has been associated with the up-regulation of eomes and existing literature associating the relapse of lung transplant patients to a reduced t-bet:eomes balance in their CMV-specific CD8+ T cell compartment (Popescu et al. 2014).

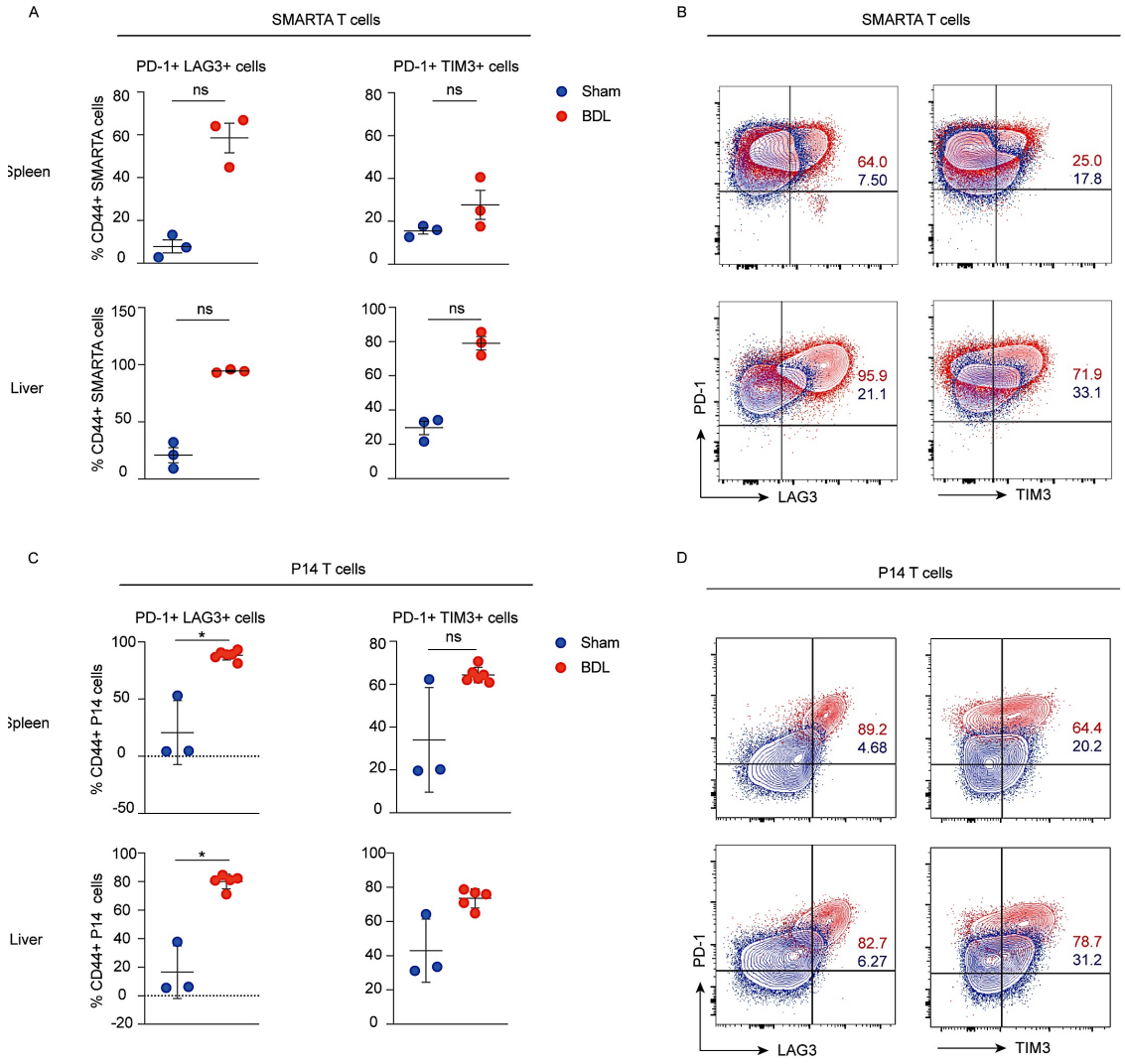
A
SMARTA T cells
PD-1+ LAG3+ cells
PD-1+ TIM3+ cells
Sham
BDL
Spleen
Liver
% CD44+ SMARTA cells
ns
B
SMARTA T cells
64.0
7.50
25.0
17.8
95.9
21.1
71.9
33.1
PD-1
LAG3
TIM3
C
P14 T cells
PD-1+ LAG3+ cells
PD-1+ TIM3+ cells
% CD44+ P14 cells
*
D
P14 T cells
89.2
4.68
64.4
20.2
82.7
6.27
78.7
31.2

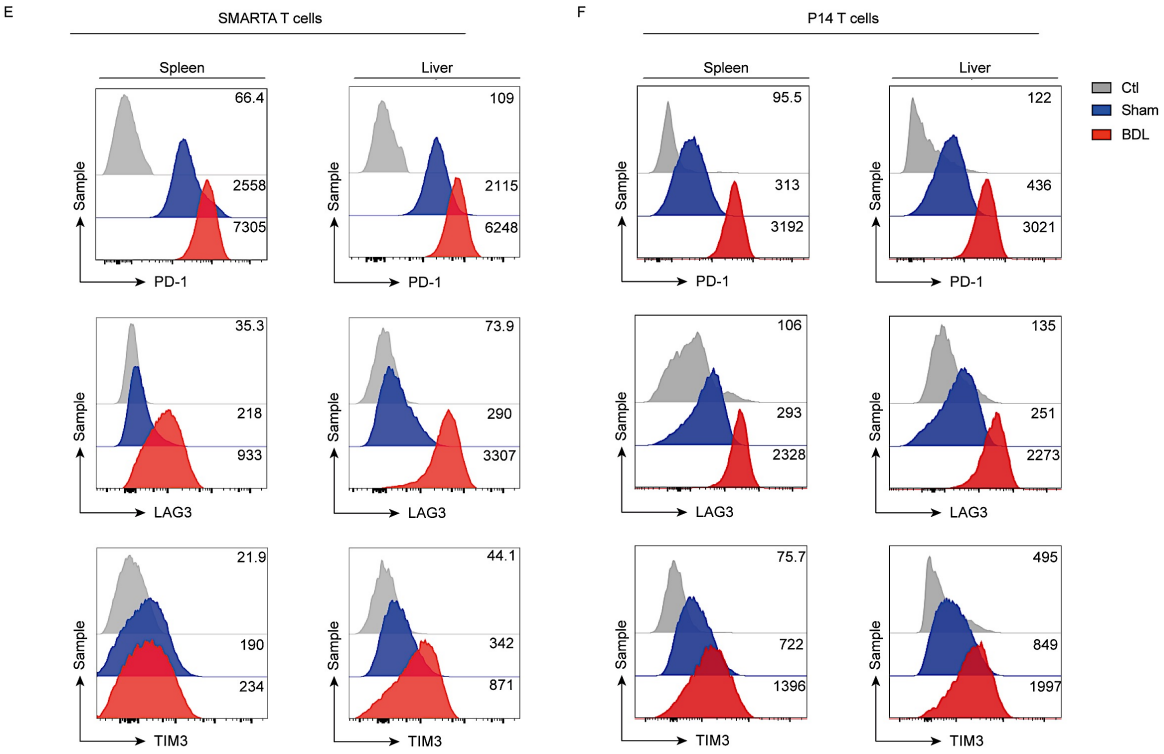

Figure 16: Increased exhaustion marker expression among SMARTA and P14 T cells from BDL-operated mice after LCMV infection. Flow cytometric analysis of the spleen and liver from BDL- and Sham-operated mice on day 8 post infection. Proportion of PD-1+ LAG3+ and PD-1+ TIM3+ cells among SMARTA **(A)** and P14 **(C)** T cells from the spleen and liver after infection. Representative dot plots of PD-1+ LAG3+ and PD-1+ TIM3+ cells among SMARTA **(B)** and P14 **(D)** T cells from the spleen and liver. Representative histograms of the MFI of PD-1, LAG3 and TIM3 among SMARTA **(E)** and P14 **(F)** T cells from the spleen and liver. Data are representative of 2-3 independent experiments (n=3-5 mice).

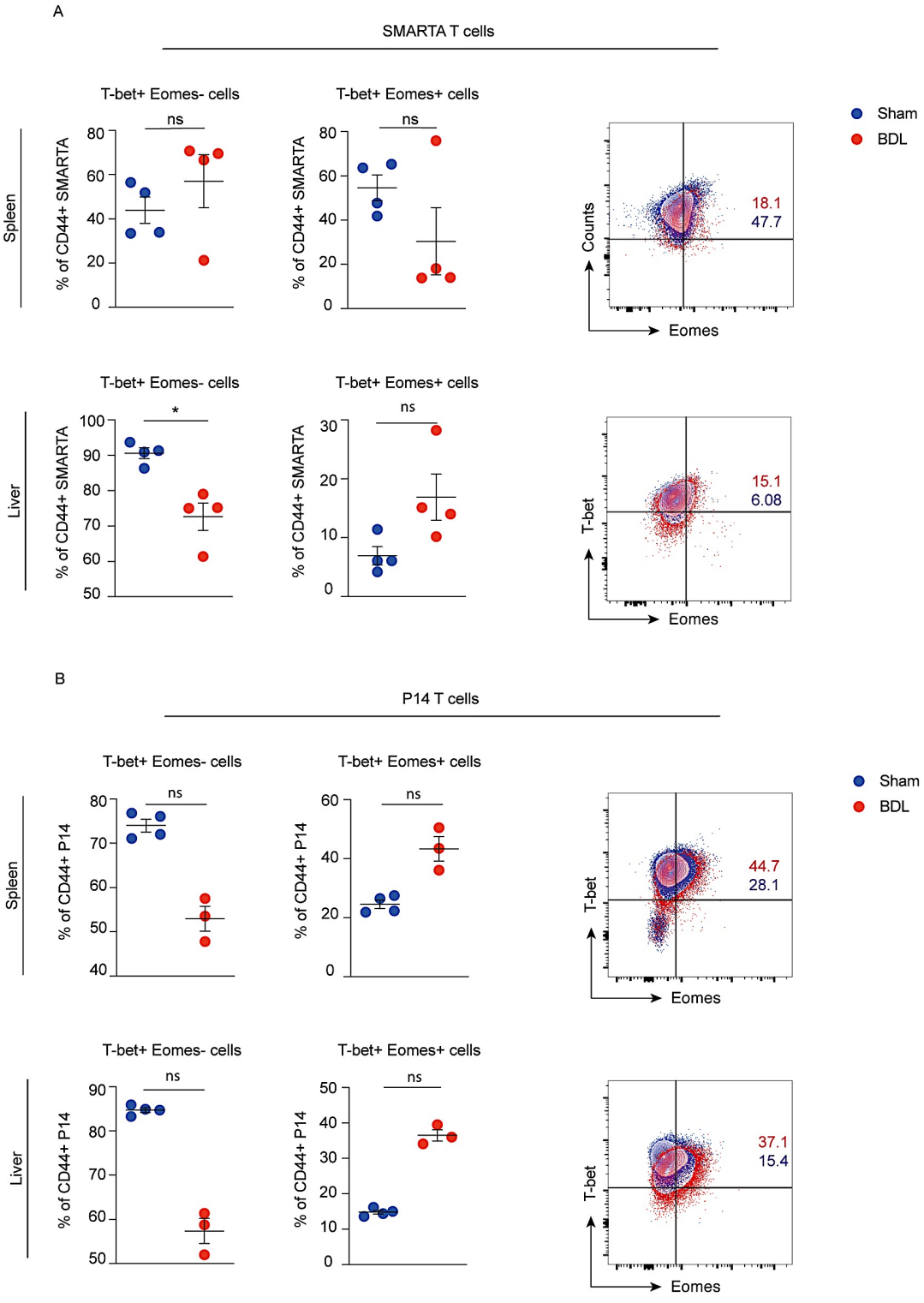
A
SMARTA T cells
T-bet+ Eomes- cells
T-bet+ Eomes+ cells
Spleen
Liver
% of CD44+ SMARTA
ns
*
Counts
Eomes
T-bet
18.1
47.7
15.1
6.08
Sham
BDL
B
P14 T cells
% of CD44+ P14
44.7
28.1
37.1
15.4

Figure 17: Increased proportion of t-bet+ eomes+ cells among SMARTA and P14 T cells in the liver of BDL-operated mice after LCMV infection. Flow cytometric analysis of the spleen and liver of BDL- and Sham-operated mice on day 8 post infection. Proportion of t-bet+ eomes- and t-bet+ eomes+ among SMARTA **(A)** and P14 **(B)** T cells from the spleen and liver, as well as their representative dot plots. Data are representative of 1 independent experiment (n=3-4 mice).

3.2.8 Chronic liver inflammation results in impaired mitochondrial fitness of effector SMARTA and P14 T cells after LCMV infection

Metabolic reprogramming is an essential part of the T cell-mediated adaptive immune response and required by T cells to support appropriate activation and differentiation upon antigen encounter (Chao et al. 2017). Since T cell exhaustion is associated with metabolic insufficiencies and de-regulation of nutrient pathways, we sought to investigate mitochondrial fitness of LCMV-specific T cells from BDL- and Sham-operated mice on day 9 post infection. To this end, we quantified the proportion of cells containing depolarized mitochondria as a means of assessing overall metabolic fitness. These can be identified by co-staining cells with mitotracker green (MTG) dye, which stains mitochondria irrespective of their membrane potential, i.e. functionality, and mitotracker deep red (MTDR), which stains mitochondria with an active, i.e. functional, membrane potential. Depolarized mitochondria stain positive for MTG, but negative for MTDR.

Results showed that SMARTA T cells isolated from the spleen of BDL-operated mice contained a higher proportion of cells with depolarized mitochondria, and an overall increased mitochondrial mass compared to cells from Sham-operated mice (Figure 18 A, B). Interestingly, these differences were less pronounced in SMARTA T cells isolated from the liver (Figure 18 A, B). Likewise, P14 T cells isolated from both the spleen and liver of BDL-operated mice showed an increased proportion of cells with depolarized mitochondria, as well as an

overall increase in total mitochondrial mass compared to cells from Sham-operated mice after infection (Figure 18 C, D).

Another measure of mitochondrial fitness is the level of cellular reactive oxygen species (ROS), which is associated with mitochondrial dysfunction (Sebastián et al. 2017). To further characterize the metabolic phenotype of SMARTA and P14 T cells from BDL mice during LCMV infection, transferred cells were isolated from the spleen and liver on day 8 p.i. and stained with MitoSox dye. Results revealed that SMARTA T cells from the spleen and liver of BDL-operated mice have a higher proportion of cells producing superoxide and higher superoxide levels per cell compared to SMARTA T cells from healthy control mice (Figure 19 A, B). Likewise, P14 T cell isolated from the spleen of BDL-operated mice contain a higher proportion of cells producing superoxide, as well as higher overall levels of superoxide when compared to Sham-operated mice (Figure 19 C, D). Interestingly no difference could be observed in P14 T cells from the liver of BDL-operated mice. Taken together these findings suggest that the mitochondrial fitness of SMARTA and P14 T cells is compromised during chronic inflammation of the liver, which is in line with the previously shown dysfunctional phenotype such as high levels of inhibitory receptors and reduced effector cytokine production.

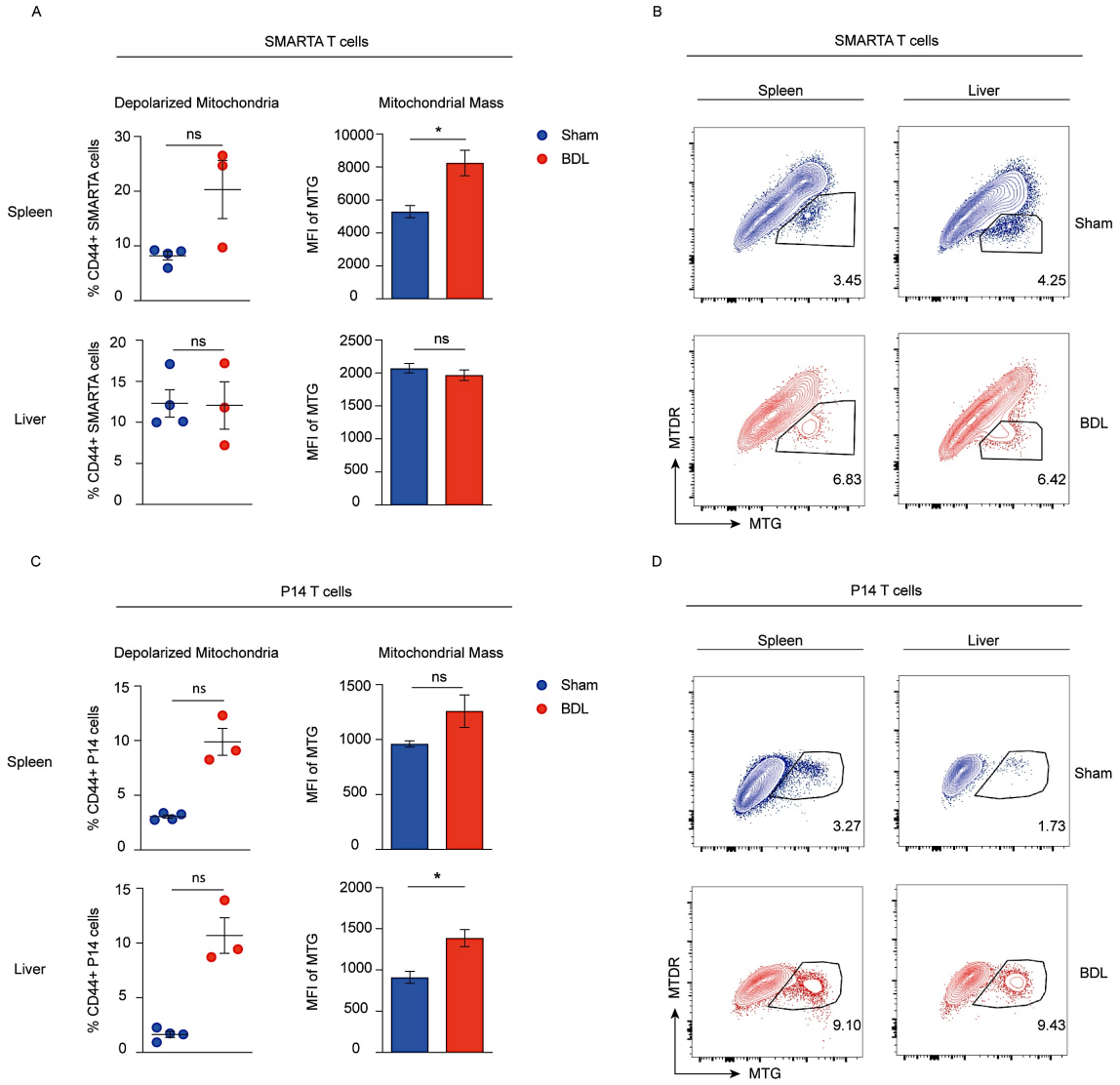

Figure 18: Increased proportion of SMARTA and P14 T cells containing depolarized mitochondria in BDL-operated mice after LCMV infection. Flow cytometric analysis of the spleen and liver of BDL- and Sham-operated mice on day 8 post infection. Proportion of SMARTA **(A)** and P14 **(B)** T cells from the spleen and liver containing depolarized mitochondria and their overall mitochondrial mass based on MFI of MTG. Representative dot plots of SMARTA **(C)** and P14 **(D)** T cells with depolarized mitochondria after infection. Data are representative of 1-2 independent experiments (n=3-4 mice).

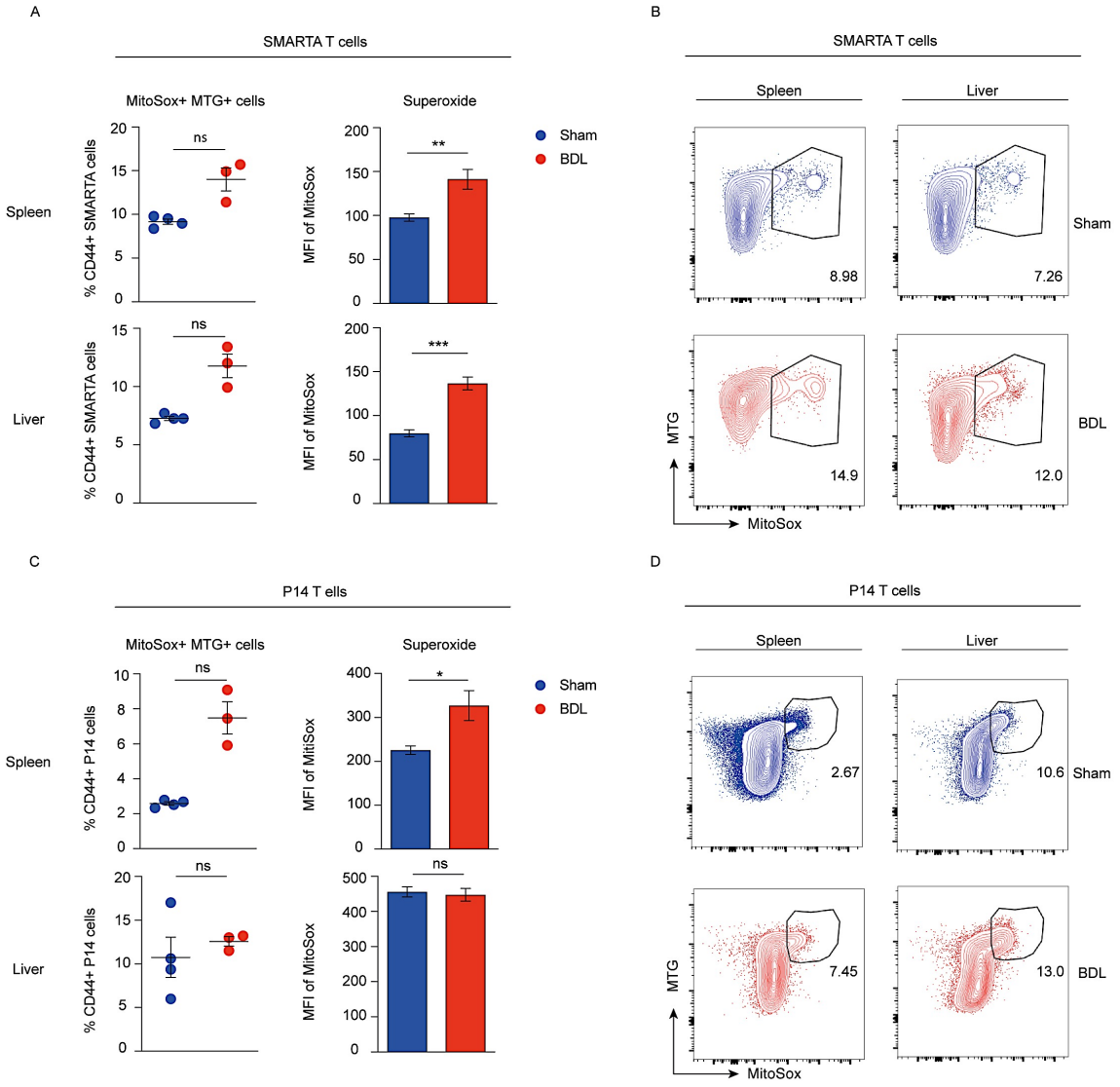

Figure 19: Increased levels of superoxide in SMARTA and P14 T cells from BDL-operated mice after LCMV infection. Flow cytometric analysis of the spleen and liver form BDL- and Sham-operated mice on day 8 post LCMV infection. Proportion of SMARTA **(A)** and P14 **(B)** T cells from the spleen and liver producing superoxide and the MFI of superoxide on a per cell basis. Representative dot plots of SMARTA **(B)** and P14 **(D)** T cells producing superoxide after infection. Data are representative of 1-2 independent experiments (n=3-4 mice).

3.2.9 Chronic liver inflammation impairs mitochondrial fitness in SMARTA and P14 T cells by day 4 post infection

To determine whether mitochondrial fitness of transferred T cells is already impaired during the early phase of the adaptive T cell-mediated response during chronic liver inflammation and whether it potentially precedes T cell exhaustion on day 8, the mitochondrial fitness of SMARTA and P14 T cells from the spleen were assessed on day 4 post LCMV infection.

Results revealed a higher proportion of SMARTA T cells with depolarized mitochondria and an overall increased mitochondrial mass in BDL-operated mice compared to Sham-operated mice after infection (Figure 20 A, B). Conversely, the same effect could not be seen in P14 T cells isolated from the spleen at the same time after LCMV infection. Likewise, SMARTA T cells contained a higher proportion of superoxide producing cells, as well as a significant increase in superoxide levels in BDL-operated mice compared to infected Sham-operated mice (Figure 21 A, B). In contrast, P14 T cells from the spleen of BDL-operated mice contained a similar proportion of superoxide producing cells and overall superoxide levels per cell, when compared to Sham-operated mice (Figure 20 A, B). Taken together, these findings suggest that at least with respect to SMARTA T cells, the mitochondrial fitness of virus-specific T cells is altered as early as day 4 p.i. and potentially precedes T cell exhaustion.

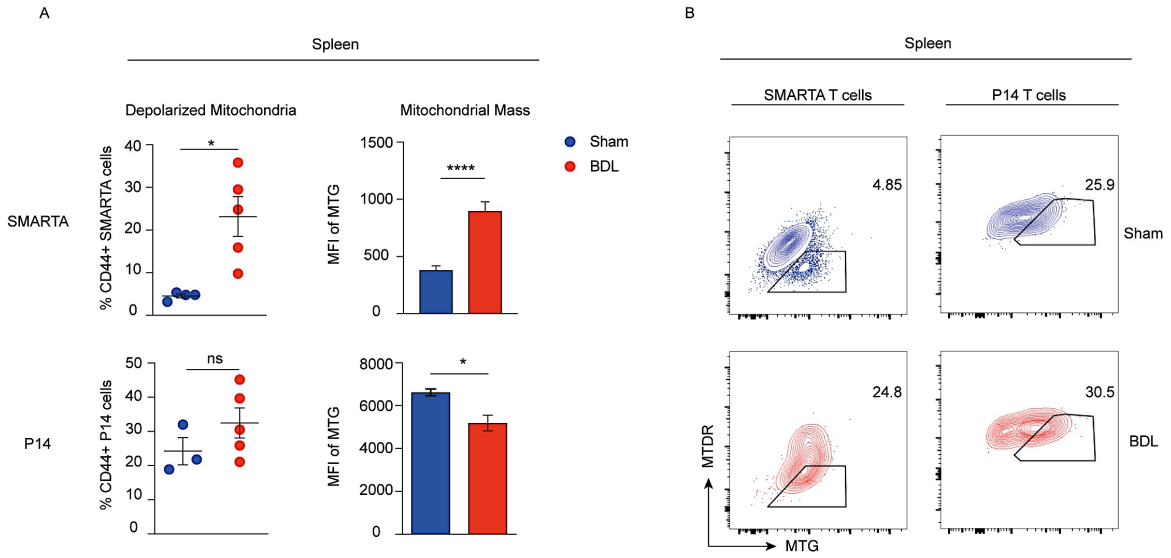

Figure 20: Increased proportion of SMARTA and P14 T cells containing depolarized mitochondria in BDL-operated mice after LCMV infection. Flow cytometric analysis of the spleen on day 4 post infection. Proportion of SMARTA and P14 **(A)** T cells containing depolarized mitochondria and their overall mitochondrial mass based on MFI of MTG. Representative dot plots of cells containing depolarized mitochondria after infection **(B)**. Data are representative of 1-2 independent experiments (n=3-5 mice).

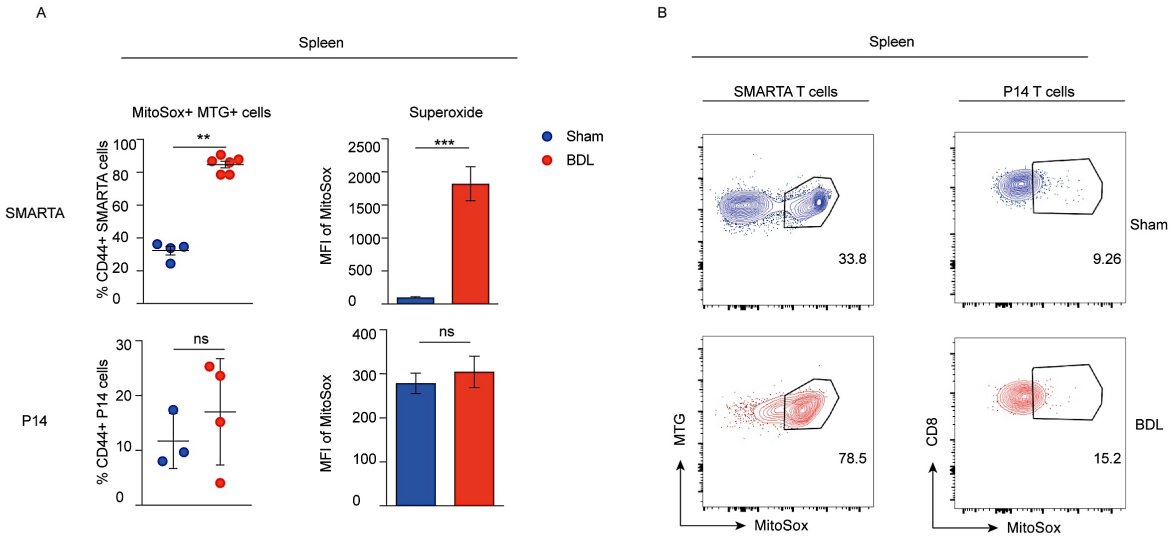

Figure 21: Increased proportion of SMARTA T cells producing superoxide in BDL-operated mice on day 4 after LCMV infection. Flow cytometric analysis of the spleen from BDL- and Sham-operated mice. Proportion of cells among SMARTA and P14 (A) T cells producing superoxide after infection. Representative dot plots of cells producing superoxide in the spleen (B). Data are representative of 1-2 independent experiments (n=3-5 mice).

3.2.10 Chronic liver inflammation results in increased 2-NBDG uptake and an increase in IL-10R expression in SMARTA and P14 T cells after LCMV infection

In order to perform effector functions and make a shift towards aerobic glycolysis upon TCR stimulation, T cells up-regulate their glucose uptake upon activation (Frauwirth et al. 2002) (Jacobs et al. 2008) (Pelletier et al. 2014). To further characterize the metabolic phenotype seen in virus-specific T cells from BDL-operated mice, their glucose uptake was analyzed on day 8 p.i.. Half an hour prior to organ harvest mice were injected intravenously with 100 µg of 2-NBDG; a fluorescent glucose analogue that allows the assessment of glucose uptake per cell. Results revealed that both SMARTA and P14 T cells from the spleen and liver of BDL-operated mice had a much higher glucose uptake than Sham-operated mice (Figure 22 A).

Recently, our group has shown that chronic liver inflammation is accompanied by chronic type I IFN signaling, which leads to increased production of IL-10, an immunosuppressive cytokine, upon infection with *Listeria monocytogenes*, which is not seen in infected control mice (Hackstein et al. 2016). Unpublished work of our group has revealed enhanced expression of INFAR-induced IL-10 expresion after LCMV infection in BDL-operated mice (personal communication Dr Z. Abdullah). To investigate the impact of high IL-10 expression in BDL-operated on the phenotype and effector function of virus-specific T cells, the expression of IL-10R on transferred SMARTA and P14 T cells was first assessed.

Results showed that both SMARTA and P14 T cells isolated from the spleen and liver of BDL-operated mice express higher levels of IL-10R and contain a higher proportion of cells producing IL-10R compared to infected Sham-operated mice (Figure 23 A, B). These finding suggest that adoptively transferred T cells are up-regulating IL-10R expression due to chronic inflammation of the liver and are potentially receptive to anti-IL-10R blockade to determine whether blocking IL-10 signaling improves mitochondrial fitness of exhausted SMARTA and P14 T cells during LCMV infection.

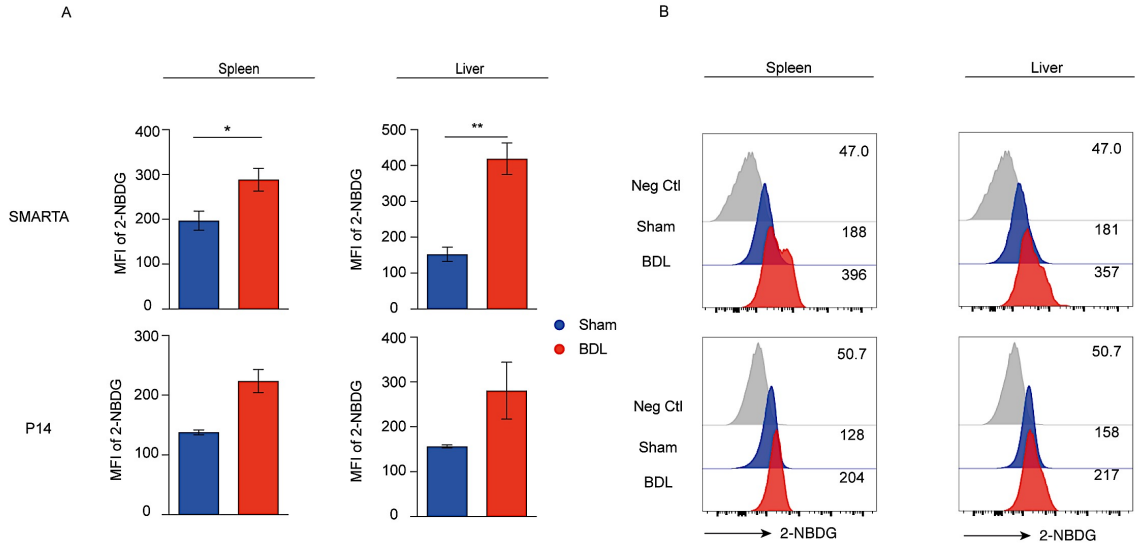

Figure 22: Increased glucose uptake by SMARTA and P14 T cells from BDL-operated mice after LCMV infection. Flow cytometric analysis of the spleen and liver from BDL- and Sham-operated mice on day 8 post infection. MFI of 2-NBDG of SMARTA and P14 T cells from the spleen and liver **(A)**. Representative histograms of 2-NBDG levels in SMARTA and P14 T cells after infection **(B)**. Data are representative of 1 independent experiments (n=3-4 mice).

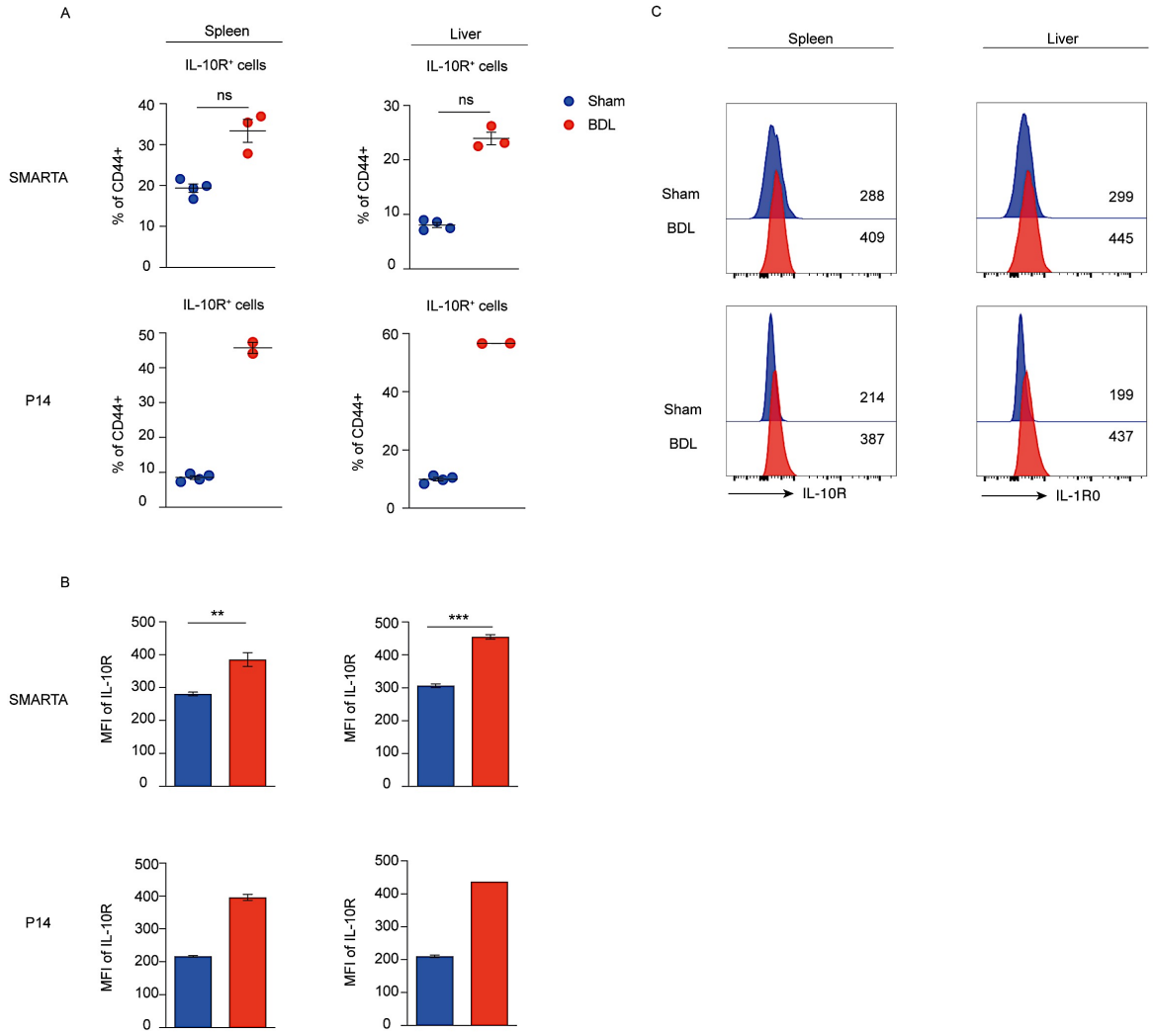

Figure 23: Increased expression of IL-10R by SMARTA and P14 T cells in BDL-operated mice after LCMV infection. Flow cytometric analysis of the spleen and liver of BDL- and Sham-operated mice on day 8 post infection. Proportion of SMARTA and P14 T cell in the spleen and liver expressing IL-10R **(A)**. MFI of the IL-10R of SMARTA and P14 T cells after infection **(B)**. Representative histograms of IL-10R expressing SMARTA and P14 T cells **(C)**. Data are representative of 1-2 independent experiments (n=3-4 mice).

3.2.11 Reduced numbers of DCs in the spleen of mice with chronic liver inflammation after LCMV infection

Effective CD8+ T cell activation depends to a large extent on efficient antigen presentation by DCs. Naïve T cells require three signals for proper activation, expansion and survival, which are cognate antigen presentation in the context of MHC, co-stimulatory molecules such as CD80, CD86 and CD40 and cytokines such as type I IFN, IL-12 and IL-6 among others (Dalod et al. 2014). Activated DCs present antigen in the context of MHC molecules and thereby provide signal 1 of the T cell activation cascade. Since, acute infection with LCMV renders virus-specific T cells dysfunctional in BDL-operated mice already by day 8 post infection, we determined whether chronic liver inflammation negatively impacts DC numbers, potentially interfering with T cell priming during the early phase of the adaptive response. Analyzing IFNγ-producing pDCs, cross-presenting XCR1+ cDCs and CD11b+ cDCs in the spleen of BDL- and Sham-operated mice on day 8 post infection revealed significantly reduced numbers of each DC population in BDL-operated mice (Figure 24 A). Additionally, the proportion of pDCs was much lower in BDL-operated mice, while there was no difference in proportion of XCR1+ and CD11b+ cDCs after infection (Figure 24 B). Collectively, these data suggest that chronic liver inflammation negatively affects DC populations, which could potentially have a negative impact on DC-mediated T cell priming of T cells during liver fibrosis.

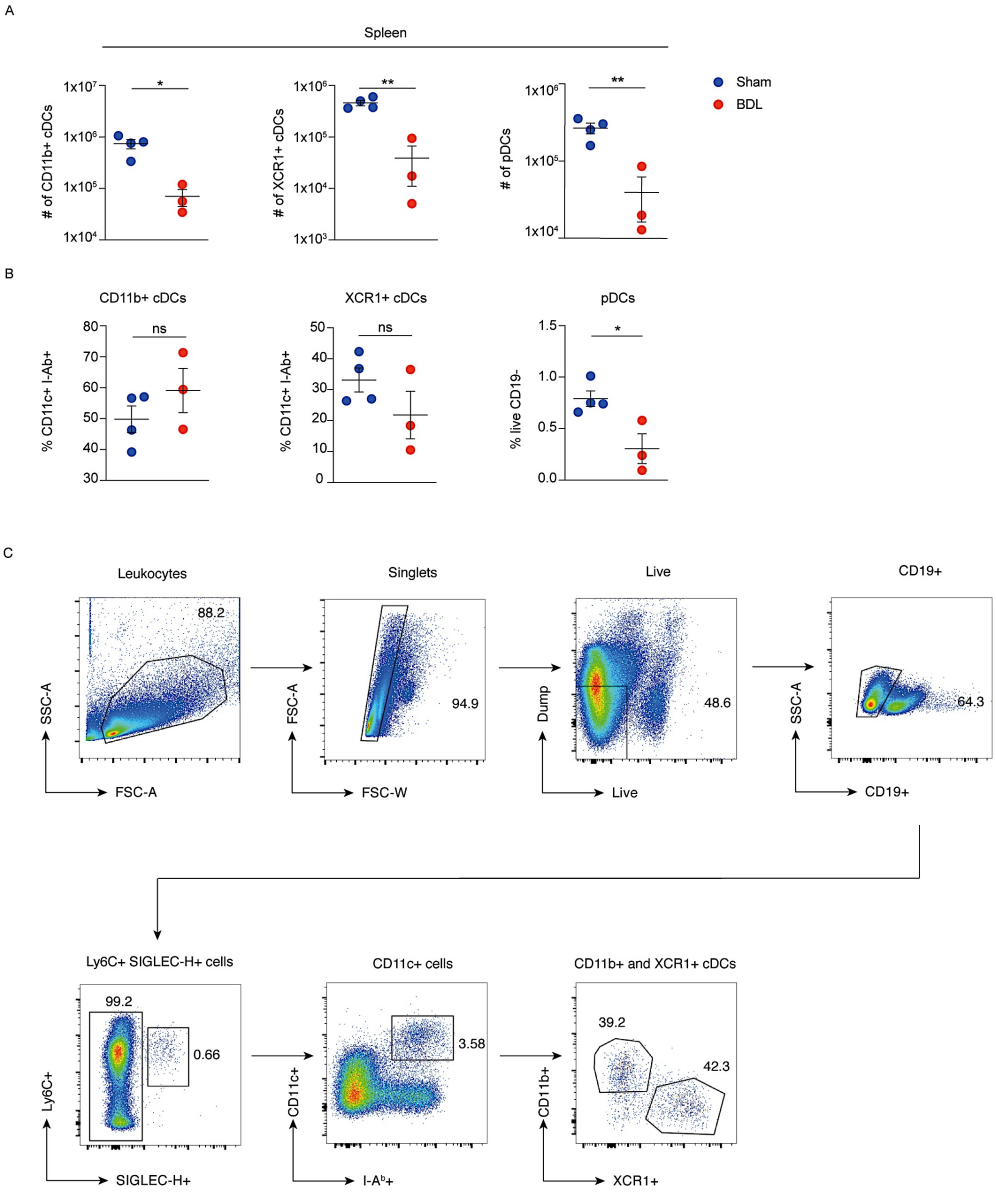

Figure 24: Decreased number of XCR1+ cDCs, CD11b+ cDCs and pDCs in BDL-operated mice after LCMV infection. Flow cytometric analysis of DCs from the spleen of BDL- and Sham-operated mice on day 8 post infection. Total numbers of DCs populations after infection **(A)**. Proportion of XCR1+ cDCs, CD11b+ cDCs and pDCs after infection **(B)**. Representative gating strategy of pDCs, CD11b+ cDCs and XCR1+ cDCs from the spleen of infected mice **(C)**. Data are representative of 2 independent experiments (n=3-4 mice).

3.2.12 Chronic liver inflammation results in impaired maturation of XCR1+ and CD11b+ conventional DCs after LCMV infection

Chronic viral infections, as well as tumors can affect the ability of DCs to mature after antigen uptake and provide co-stimulatory signals to virus-specific T cells (Auffermann-Gretzinger et al. 2001). Here, the extent to which DCs are able to mature after LCMV infection, which is necessary for sufficient T cell priming and providing of co-stimulatory signals, was assessed (Mellman and Seinman, 2001) (Dalod et al. 2014). To this end, total numbers of CD11b+ and XCR1+ cDCs from the spleen were determined 18 hours post LCMV infection. As shown in Figure 25 A and 26 A both cell populations were reduced in infected BDL-operated mice, but not in Sham-operated mice and either uninfected control group. Analyzing the proportion of DCs expressing the maturation marker CD80 and CD86, revealed a decreased proportion of both CD11b+ and XCR1+ cDCs expressing CD80 and CD86 in infected BDL-operated mice (Figure 25 B) (Figure 26 B). Assessing MHC-II producing cells revealed a lower proportion of XCR1+ cDCs expressing MHC-II from both infected and non-infected BDL-operated mice, while nearly all XCR1+ cDCs from infected and non-infected Sham-operated mice were able to express MHC-II (Figure 26 B). Results showed that CD11b+ and XCR1+ cDCs from BLD-operated mice produce significantly lower amounts of CD80, CD86 and MHC-II after infection compared to Sham-operated mice (Figure 25 C-D) (Figure 26 C-D). While there was no difference in maturation marker expression by CD11b+ cDCs between non-infected BDL- and Sham-operated mice, XCR1+ cDCs show lower levels of CD80 and MHC-II expression levels already in non-infected BDL-operated mice compare to the non-infected control group (Figure 26 C-D). Taken together, these findings suggest that chronic liver inflammation negatively affects maturation of CD11b+ and XCR1+ DCs after LCMV infection. This in turn is likely to interfere in T cell priming during the initial phase of the LCMV-directed response, in part explaining why LCMV-specific T cells are present at lower numbers by day 4 post infection and show a lessened effector response.

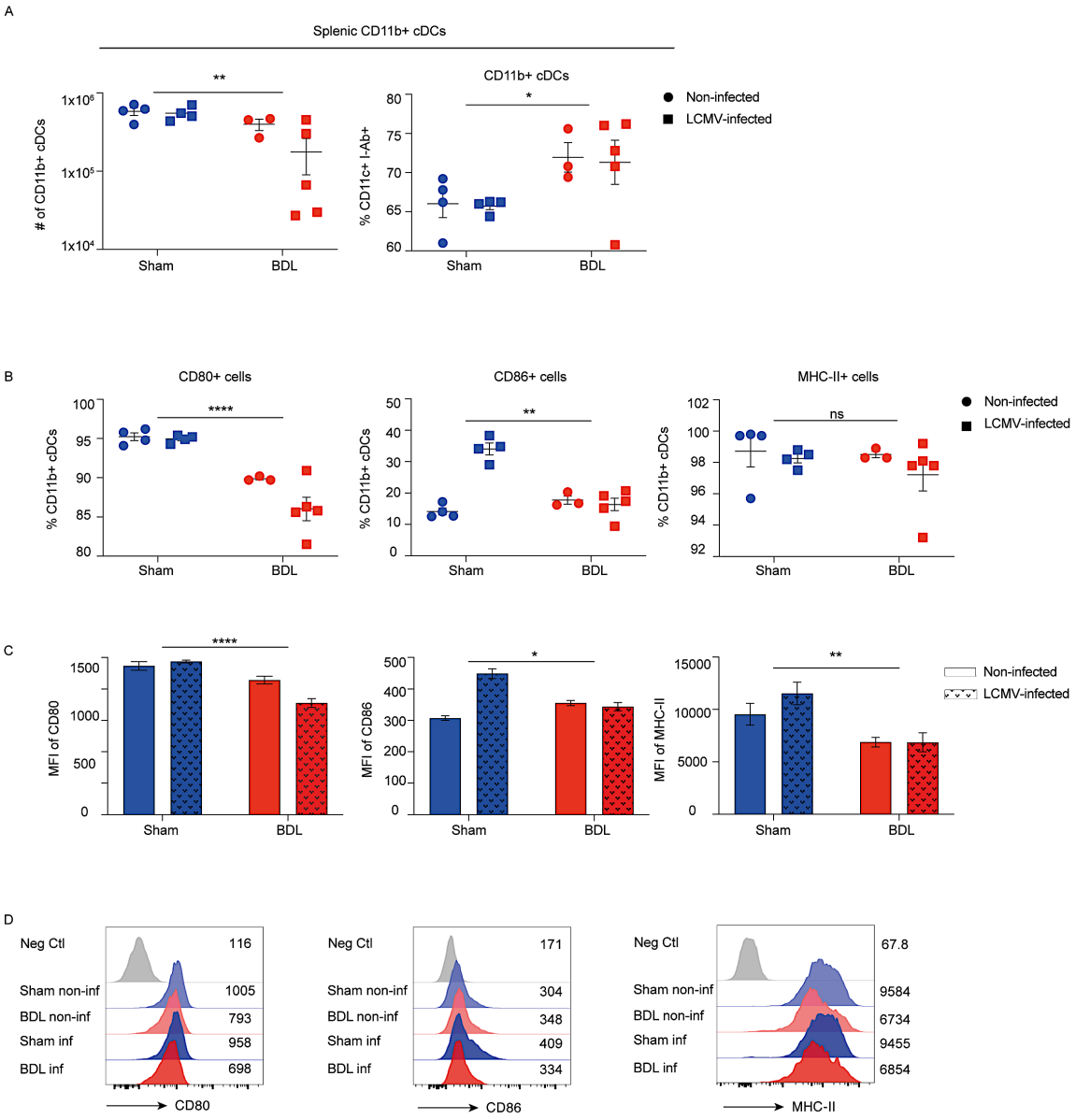

Figure 25: Reduced maturation marker expression by CD11b+ cDCs from BDL-operated mice after LCMV infection. Flow cytometric analysis of the spleen from BDL- and Sham-operated mice 18 hours post infection or without infection. Total numbers and proportion of CD11b+ cDCs in infected and non-infected mice **(A)**. Proportion of CD11b+ cDCs expressing CD80, CD86 and MHC-I with or without infection. A significant effect of LCMV infection on the proportion of CD11b+ cDCs expressing CD86 was detected, $p<0.0002$. **(B)**. MFI of CD80, CD86 and MHC-II expression among CD11b+ cDCs in infected and non-infected mice. A significant effect of LCMV infection on the MFI of CD80 and CD86 was detected, $p<0.05$ and $p<0.0002$, respectively. **(C)**. Representative histograms of CD80, CD86

and MHC-I expression levels among CD11b+ cDCs. **(D)**. Data are representative of 1 independent experiment (n=3-5 mice). Statistical significance was determined using a two-way ANOVA, analyzing LCMV infection and BDL operation as contributing factors. Statistics displayed in graphs **A-C** corresponds to BDL as a factor responsible for the phenotypic differences seen.

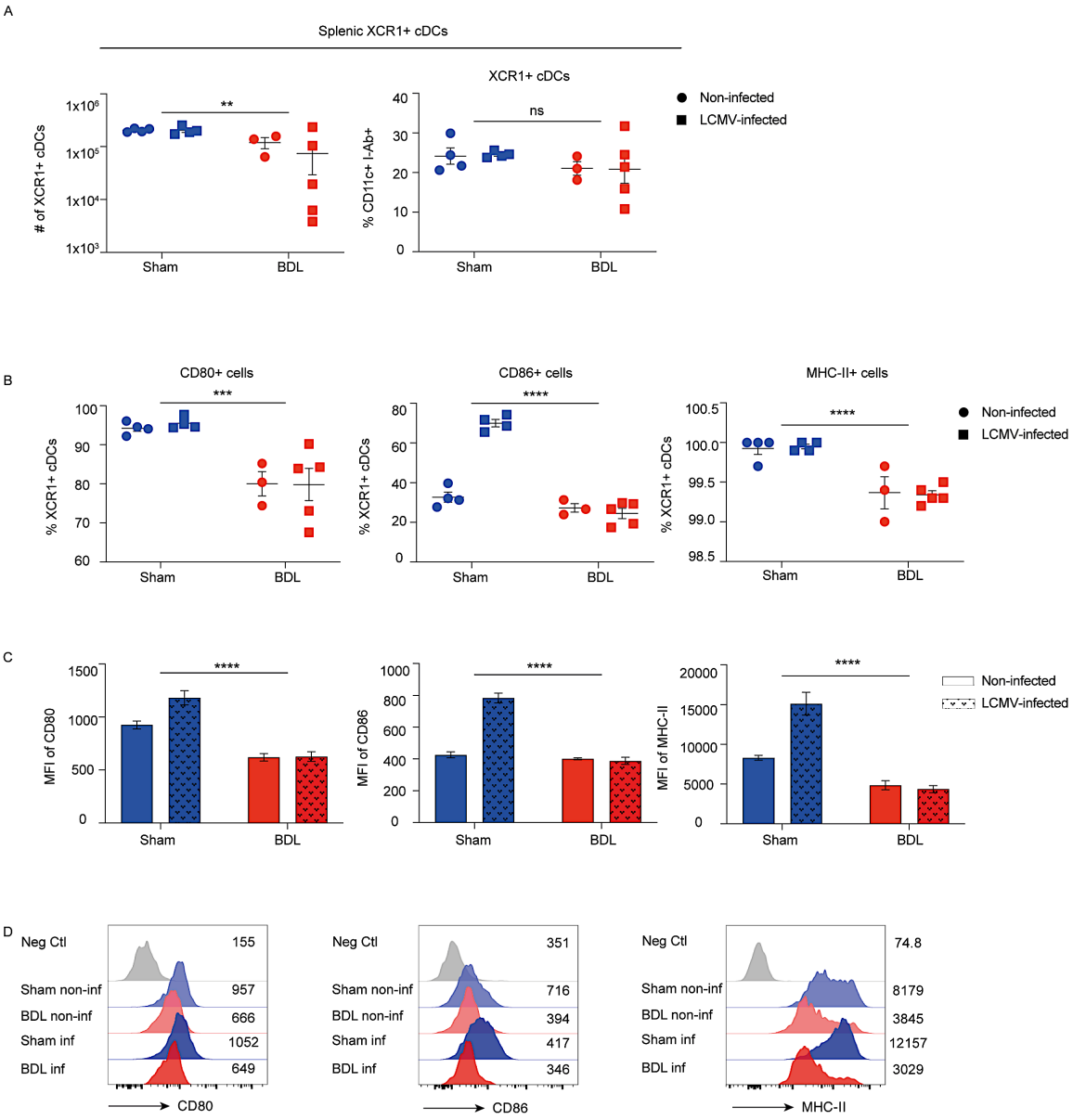

Figure 26: Reduced maturation marker expression by XCR1+ cDCs from BDL-operated mice after LCMV infection. Flow cytometric analysis of the spleen from BDL- and Sham-operated mice 18 hours post infection or without infection. Total numbers and proportion of XCR1+ cDCs in infected and non-infected mice **(A)**. Proportion of XCR1+ cDCs expressing CD80, CD86 and MHC-I with or without infection. A significant effect of LCMV infection on the proportion of XCR1+ cDCs expressing CD86 was detected, $p<0.0001$ **(B)**. MFI of CD80, CD86 and MHC-II expression among XCR1+ cDCs in infected and non-infected mice. A significant effect of LCMV infection on the MFI of CD80, CD86 and MHC-II was detected, $p<0.05$, $p<0.0001$ and $p<0.0021$ respectively **(C)**. Representative histograms of CD80, CD86 and MHC-I expression levels among XCR1+ cDCs **(D)**. Data are representative of 1 independent experiment (n=3-5 mice). Statistical significance was determined using a two-way ANOVA, analyzing LCMV infection and BDL operation as contributing factors. Statistics displayed in graphs **A-C** corresponds to BDL as a factor responsible for the phenotypic differences seen.

3.3 Discussion

The experiments described in this chapter aim to elucidate the underlying mechanisms of the impaired T cell mediated immune response in the context of viral infections in mice. To this end mice were subjected to the induction of chronic liver inflammation, followed by viral infection with the model virus LCMV. One day prior to infection mice received an adoptive transfer of LCMV-specific CD4+ and CD8+ T cells, which were analyzed at different time points post LCMV infection to monitor their activation, expansion and effector function throughout the infection. In addition, the maturation state of DCs was investigated to determine, whether they are potentially able to sufficiently prime LCMV-specific T cells in the context of chronic liver inflammation.

By enumerating absolute numbers of adoptively transferred LCMV-specific CD4+ and CD8+ T cells, it could be seen that their expansion is impaired as early as day 4 post LCMV infection. These findings provide the first indication as to why the T cell-mediated response against viral infections is diminished in the context of chronic liver inflammation. Virus-specific T cells are not expanding to the same extent as those from healthy mice, providing inadequate protection against the

virus, likely allowing it to persist. The reason why LCMV-specific T cells from mice with chronic liver inflammation do not expand to the same extent as those from healthy mice, is at least in part due to a reduction in proliferative potential. The reduced proliferation after LCMV infection could be due to poor DC-mediated priming of T cells as a result of the inflammatory environment in the liver. The fact that DC populations such as XCR1+ cDCs, as well as CD11b+ cDCs are less mature after the induction of chronic liver inflammation further supports this hypothesis, as the DCs are required to mature after antigen acquisition in order to functionally prime T cells and induce the adaptive immune response (Drutman and Trombetta, 2010).

Investigating the ability of LCMV-specific T cells to produce effector cytokines at the peak of the T cell mediated immune response, revealed a negative impact of chronic liver inflammation on the production of IFNγ and TNFα. These findings are in line with the exhausted phenotype seen during chronic infection with LCMV clone 13, during which a high antigen load is associated with the formation of exhausted, i.e. dysfunctional T cells and the progressive loss of effector cytokines such as IL-2, TNFα and eventually IFNγ (Wherry et al. 2007) (Kahan et al. 2015). During persistent infections with LCMV clone 13 endogenous virus-specific T cells display high levels of inhibitory receptors, or exhaustion markers, such as PD-1, LAG3 and 2B4 by day 8 post infection compared to LCMV-specific T cells during an acute infection with LCMV Armstrong (Wherry et al. 2007). Exhaustion marker levels were still elevated by day 60 p.i. compared to an acute infection with LCMV, and their high expression levels were associated with poor formation of memory T cells (Angelosanto et al. 2012). Interestingly, a similar phenotype can be observed during LCMV-WE infection in mice with chronic liver inflammation. Diseased mice infected with LCMV-WE fail to clear the virus by day 8-10 post infection and there are high viral loads detectable in their livers by day 30 p.i. still (data not shown). Consistent with the persistence of the virus in BDL-operated mice, LCMV-specific T cells from these mice exhibit a significantly higher

up-regulation of inhibitory receptors such as PD-1 and LAG3, characteristic of chronic viral infections (Wherry et al. 2007). In contrast, there is a higher proportion of LCMV-specific T cells producing granzyme B in mice with chronic liver inflammation, including elevated levels of granzyme B per cell, as well as elevated levels of LAMP1; indicating their ability to degranulate and release granzyme B. The elevated production of granzyme B could be a direct result of continuously high levels of type I IFN, which accompanies chronic inflammation of the liver, and can induce granzyme B production (Hackstein et al. 2016) (Urban et al. 2016). Another reason could be that exhausted T cells are “prioritizing” the killing of infected cells rather than the production of effector cytokines such as IFNγ, TNFα or IL-2 to make the most of their limited resources during the inflammatory conditions they are in.

T cell exhaustion was previously shown to be associated with an imbalance in metabolic pathways usage and utilization of metabolites for either aerobic glycolysis or OXPHOS (Patsoukis et al. 2017). While naïve T cells, as well as memory T cells rely largely on OXPHOS and FAO for ATP production, effector T cells need to make a switch to aerobic glycolysis and up-regulate their glucose uptake in order to meet their bioenergetics demands and sustain their rapid proliferation and effector functions (Chang et al. 2013) (Buck et al. 2016). Results have shown that LCMV-specific T cells from mice with chronic liver inflammation have a much higher proportion of cells containing depolarized, i.e. dysfunctional, mitochondria, which indicates mitochondrial dysfunction and impaired metabolic fitness. Additionally, LCMV-specific T cells from diseased mice produce higher levels of superoxide, a sign of cellular stress, supporting the hypothesis that chronic liver inflammation negatively impacts on metabolic fitness, thereby exacerbating T cell dysfunction and allowing the virus to persist.

The experiments described in this chapter have shown that chronic liver inflammation impairs T cell function during viral infection, initially by interfering with

their proliferation upon antigen exposure and also by rendering them exhausted by the peak of the adaptive response against LCMV. Despite LCMV-WE being an acute strain, the infection persists in mice with chronic liver inflammation due to virus-specific T cells being rendered exhaustion and loosing their ability to produce effector cytokines such as IFNγ and TNFα. While virus-specific T cells maintain their potential to produce and release granzyme B, their mitochondrial function appears to be impaired, which is in line with their exhausted phenotype. These results contribute to elucidating the reason as to why chronic liver inflammation causes persistence of otherwise acute viral infections and may provide new approaches for future therapeutic interventions.

Chapter 4

Chronic liver inflammation impairs the expansion and functionality of antigen-specific T cells after OVA/PolyI:C vaccination

4.1 Introduction

Patients suffering from chronic inflammation of the liver are at a much higher risk of contracting infectious diseases further increasing the morbidity and mortality associated with chronic liver diseased (Cheruvattath and Balan, 2007) (Albillos et al. 2014) (Buchorntavakul et al. 2016). Patients with chronic liver disease were reported to elicit insufficient protective immunity after vaccination and primary infection was indicated by antibody titers below the detection limit (Loulergue et al. 2009) (Buchorntavakul et al. 2016). Generally speaking, the more advanced the chronic liver disease, the more reduced the immunogenicity of the vaccine, e.g. after hepatitis A, hepatitis B or influenza vaccination (Koff, 2019) (Bunchorntavakul et al. 2016). Hence, it is crucial to make existing vaccines more effective in patients with chronic liver diseases to prevent potentially lethal co-morbidities and provide these patients with sufficient immunological protection against infections such as hepatitis A and B, as well as influenza or pneumococcal infection. To this end it is crucial to understand how chronic inflammation of the liver impairs the protective immune response after vaccination. To model chronic liver inflammation associated with chronic liver disease, the murine BDL model was used, followed by OVA and PolyI:C vaccination after establishment of the disease. Results showed that on the peak of the T-cell mediated immune response post vaccination there are fewer endogenous OVA-specific CD8+ T cells present in the spleen of BDL- compared to Sham-operated mice. Additionally, both OVA-specific CD8+ T cells from the spleen and liver of BDL mice display an exhausted phenotype after vaccination. Likewise, adoptively transferred OT-II and OT-I T cells, which are specific peptide sequence 323-339 and 257-64 (SIINFEKL) of the OVA protein, respectively, are also exhibiting an exhausted phenotype after vaccination, as well as lower effector cytokine production.

4.2 Results

4.2.1 Impaired T cell immune responses to OVA/PolyI:C vaccination in mice with chronic liver inflammation

Chronic liver inflammation is associated with decrease vaccination efficacy and reduced long-term protection against infection. To assess the impact of chronic liver inflammation on the ability of the immune system to mount a detectable and sufficient T cell response upon vaccination, BDL- and Sham-operated mice were vaccinated with 100 µg OVA and 200 µg of PolyI:C on day 9 post operation. PolyI:C, a potent adjuvant and TLR3 agonist known to activate innate cells such a NK cells and DCs, can also act directly on T cells and was used to boost the antigenic response (Salem et al. 2009). On day 8 post vaccination the magnitude of the OVA-specific CD8+ T cell response was assessed and found to be significantly diminished in the spleen of fibrotic mice compared to healthy control mice (Figure 27 A). In line with these finding is the increased frequency of PD-1+ LAG3+ and PD-1+ TIM3+ cells among OVA-specific CD8+ T cells in the spleen as well as the liver of BDL-operated mice compared to healthy control mice (Figure 28 A). The increased expression levels of PD-1, LAG3 and TIM3 of OVA-specific CD8+ T cells suggest a functional impairment of antigen-specific T cells that resembles that of LCMV-specific T cells after infection with the acute strain WE of LCMV during chronic liver fibrosis (Figure 28 B). Despite the antigen load being lower during vaccination compared to an infection with a replicating infection with a virus such as LCMV, chronic liver inflammation prevents proper expansion of antigen-specific effector CD8+T cells and renders them exhausted.

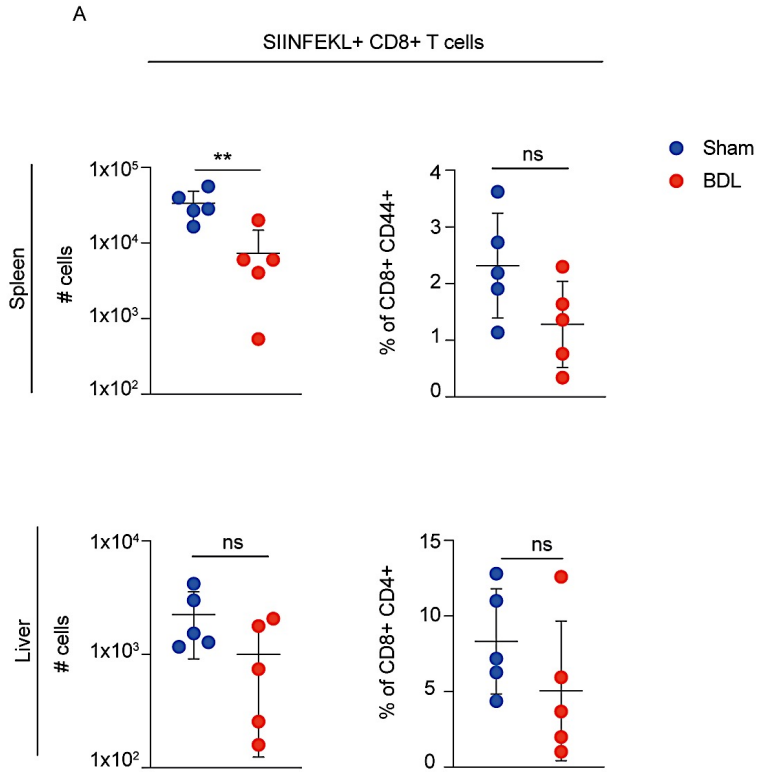

Figure 27: Reduced number of OVA+ CD8+ T cells in BDL-operated mice after OVA/PolyI:C vaccination. Flow cytometric analysis of the spleen and liver of BDL- and Sham-operated mice on day 8 post vaccination. Total numbers and proportion of endogenous SIINFEKL+ CD8+ T cells. Data are representative of 2 independent experiments (n=4-5 mice).

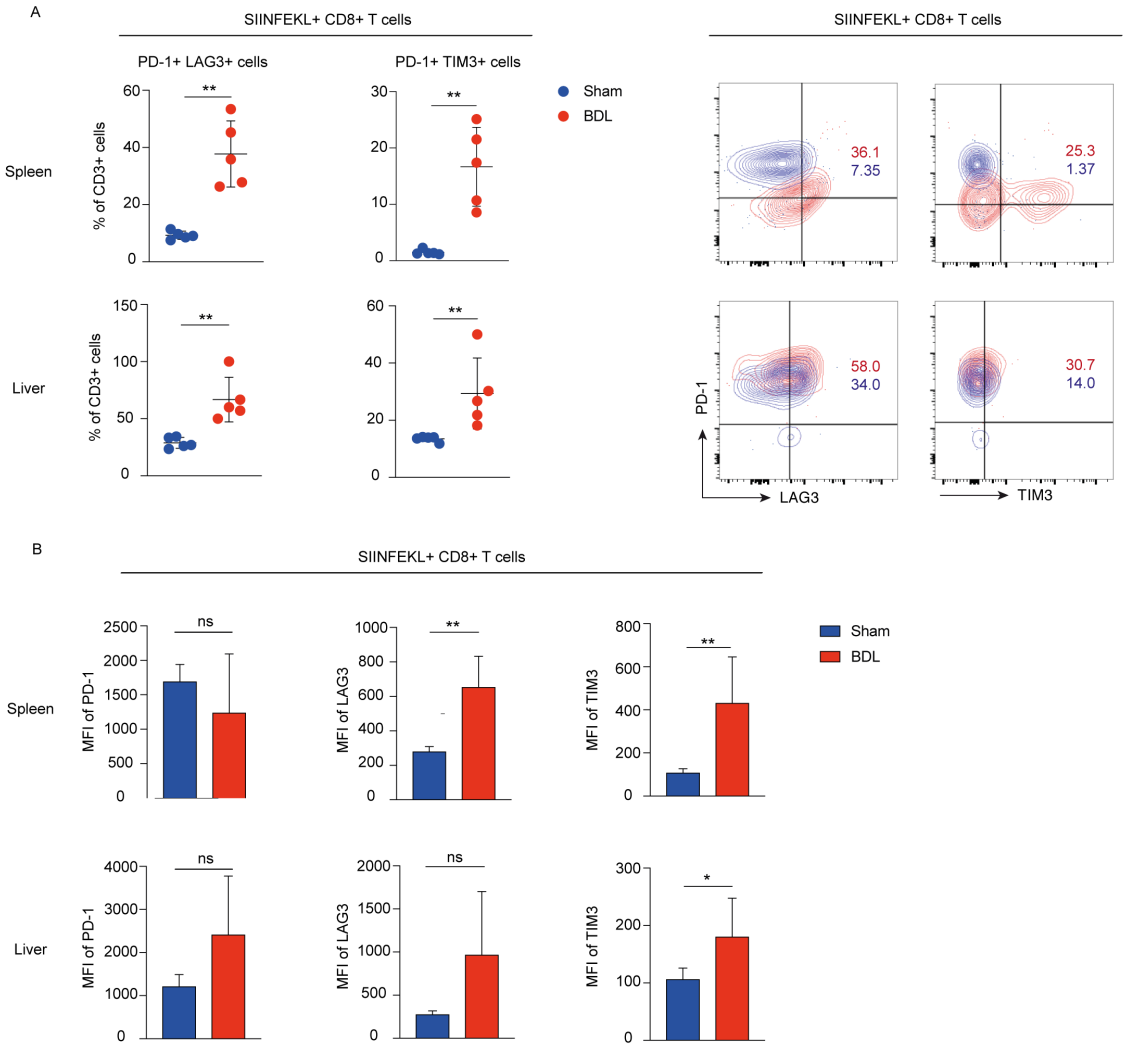

Figure 28: Increased proportion of exhausted OVA-specific CD8+ T cells in BDL-operated mice after OVA/Polyl:C vaccination. Flow cytometric analysis of the spleen and liver of BDL- and Sham-operated mice on day 8 post vaccination. Proportion of PD-1+ LAG3+ and PD-1+ TIM3+ cells among SIINFEKL+ CD8+ T cells **(A)**. MFI of PD-1, LAG3 and TIM3 of SIINFEKL+ CD8+ T cells **(B)**. Representative dot plot of PD-1+ LAG3+ and PD-1+ TIM3+ cells among SIINFEKL+ CD8+ T cells **(C)**. Data are representative of 2 independent experiments (n=5 mice).

4.2.2 Chronic liver inflammation is associated with reduced numbers of transferred OT-I T cells and elevated levels of inhibitory receptor expression after OVA/PolyI:C vaccination

To ascertain that the lower number of OVA-specific CD8+ T cells seen in BDL-operated mice after vaccination were not due to developmental impairment during thymic selection in the context of liver inflammation, transgenic OVA-specific CD8+ T cells (OT-I) were transferred prior to vaccination. OT-I T cells isolated on day 8 post OVA/PolyI:C vaccination were lower in number and proportion in BDL-operated mice than in their healthy counterparts, recapitulating the situation seen in the endogenous OVA-specific CD8+ T cell compartment (Figure 29 A). The reduced number of OT-I T cells was seen in both the spleen and the liver of BDL-operated mice. Among these OT-I T cells there was a higher proportion of PD-1+ LAG3+ and PD-1+ TIM3+ cells, while OT-I T cells from BDL-operated mice also show higher levels of PD-1, TIM3 and LAG3 after vaccination (Figure 30 A-C). These findings suggest that even though OT-I T cells were transferred in BDL- and Sham-operated mice only one day prior to vaccination, chronic liver inflammation seams to render antigen-specific CD8+ T cells exhausted after antigen encounter, likely interfering with their effector function, potentially explaining why T cell immunity is diminished after vaccination in the context of liver inflammation

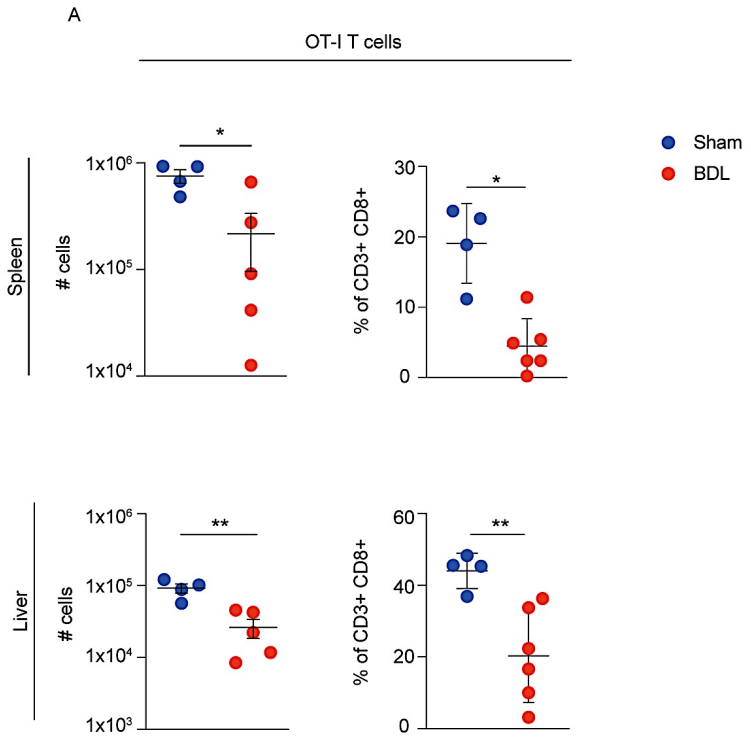

Figure 29: Reduced number of OT-I T cells in BDL-operated mice after OVA/PolyI:C vaccination. Flow cytometric analysis of the spleen and liver of BDL- and Sham-operated mice on day 8 post vaccination. Total numbers and proportion of OT-I T cells **(A)**. Data are representative of 2 independent experiments (n=3-5 mice).

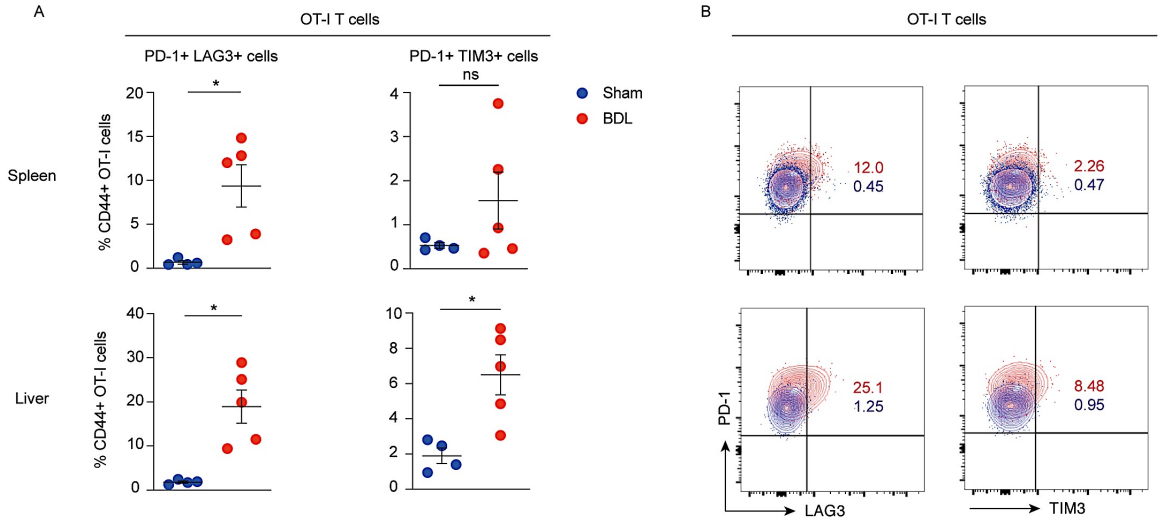

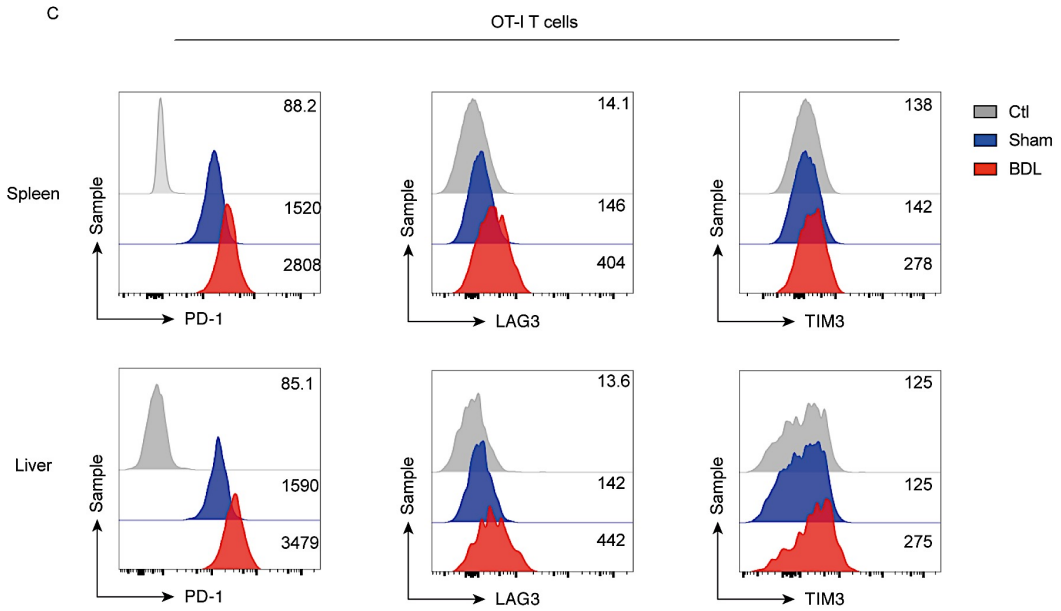

Figure 30: Increased expression of inhibitory receptors by OT-I T cells in BDL-operated mice after OVA/PolyI:C vaccination. Flow cytometric analysis of the liver and the spleen of BDL- and Sham-operated mice on day 8 post vaccination. Proportion of PD-1+ LAG3+ and PD-1+ TIM3+ cells among OT-I T cells **(A)**. Representative dot plots of PD-1+ LAG3+ and PD-1+ TIM3+ cells among OT-I T cells after vaccination **(B)**. MFI of PD-1, LAG3, TIM3 of OT-I T cells from the spleen and liver **(C)**. Data are representative of 2 independent experiments (n=3-5 mice).

4.2.3 Impaired effector cytokine production by OVA-specific CD8+ T cells after OVA/PolyI:C vaccination in mice with chronic liver inflammation

To determine whether the reduced expansion of OT-I T cells during chronic inflammation of the liver, as well as their up-regulation of inhibitory receptors, is accompanied by a qualitative change in their effector response, the effector cytokine production of adoptively transferred OT-I T cells was assessed. BDL- and Sham-operated mice received OT-I T cells one day prior to OVA/PolyI:C vaccination on day 9 post operation, which were isolated 8 days later. Results showed a decreased proportion of IFNγ+ TNFα+, as well as IFNγ+ IL-2+ cells among OT-I T cells from the spleen and liver of BDL-operated mice (Figure 31 A, B). Likewise, the proportion of total IFNγ+ cells was also significantly lower in BDL-

operated mice post vaccination (Figure 31 A). Collectively, these data show that antigen-specific CD8+ T cells are severely impaired in their effector cytokine production after vaccination in mice with fibrosis, which is accompanied by an exhausted phenotype could at least in part explain why so many cirrhosis patients respond poorly to vaccination and fail to develop long lasting T cell immunological memory (Keeffe, 2006).

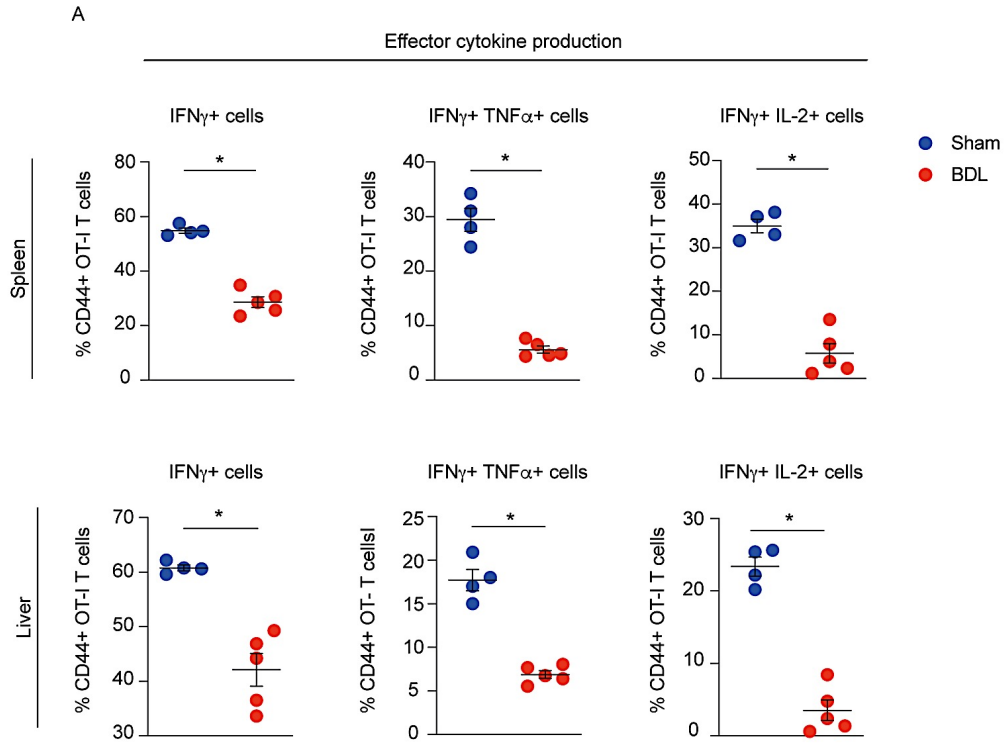

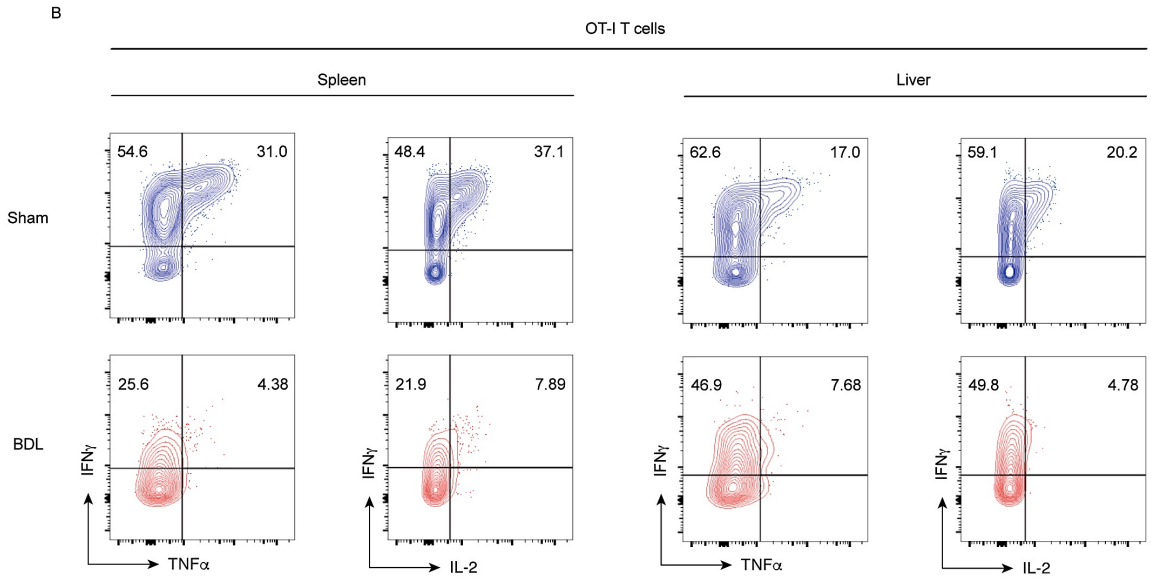

Figure 31: Reduced effector cytokine production by OT-I T cells in BDL-operated mice after OVA/PolyI:C vaccination. Flow cytometric analysis of the spleen and liver of BDL- and Sham-operated mice on day 8 post vaccination. Proportion of IFNγ+, IFNγ+ TNFα+ and IFNγ+ IL-2+ cells among OT-I T cells **(A)**. Representative dot plots of IFNγ+ TNFα+ and IFNγ+ IL-2+ cells among OT-T cells after vaccination **(B)**. Data are representative of 2 independent experiments (n=3-5 mice).

4.2.4 Chronic liver inflammation impairs OT-II T cell expansion and effector cytokine production and causes partial exhaustion after OVA/PolyI:C vaccination

To determine whether OVA-specific CD4+ T cells are also affected by chronic liver inflammation, they were co-transferred with OT-I T cells into BDL- and Sham-operated mice on day 8 post operation, i.e. one day prior to vaccination. Results showed reduced total numbers of OT-II T cells in both the spleen and liver on day 8 post infection (Figure 32 A). Effector cytokine production was impaired in OT-II T cells from the liver, as shown by a lower proportion of OT-II T cells producing IFNγ and TNFα, or IFNγ together with IL-2 (Figure 32 B). Interestingly, there was no difference in IFNγ+ TNFα+ and IFNγ+ IL-2+ cells among OT-II T cells isolated from the liver, while the absolute number of IFNγ+ cells was even

increased in BDL-operated mice (Figure 32 B). However, when considering that OT-II T cells recruited to the liver are low during vaccination to begin with and 10 fold lower than those present in the spleen, the difference in cytokine production might only be apparent in the secondary lymphoid organs. To assess whether the impaired production of effector cytokines was accompanied by an exhausted phenotype in BDL-operated mice, PD-1, LAG3 and TIM3 expression levels were analyzed. Interestingly, there was a higher proportion of PD-1+ LAG3+ cells among OT-II T cells in the spleen of BDL-operated mice, but not the liver (Figure 33 A). While TIM3 could not be detected at all in OT-II T cells from either BDL- or Sham-operated mice, LAG3 expression levels were significantly up-regulated in OT-II T cells from the spleen of BDL-operated mice compared to health Sham mice (Figure 33 B). Collectively, these results show, that while OT-II T cells are also impaired with respect to expansion and cytokine production, they appear less exhausted than their CD8+ T cell counterparts. However, even so this partially exhausted phenotype and reduced effector cytokine production could have consequences for CD8+ memory T cell formation after vaccination and explain in part why cirrhosis patients to develop no strong immunological memory after vaccination.

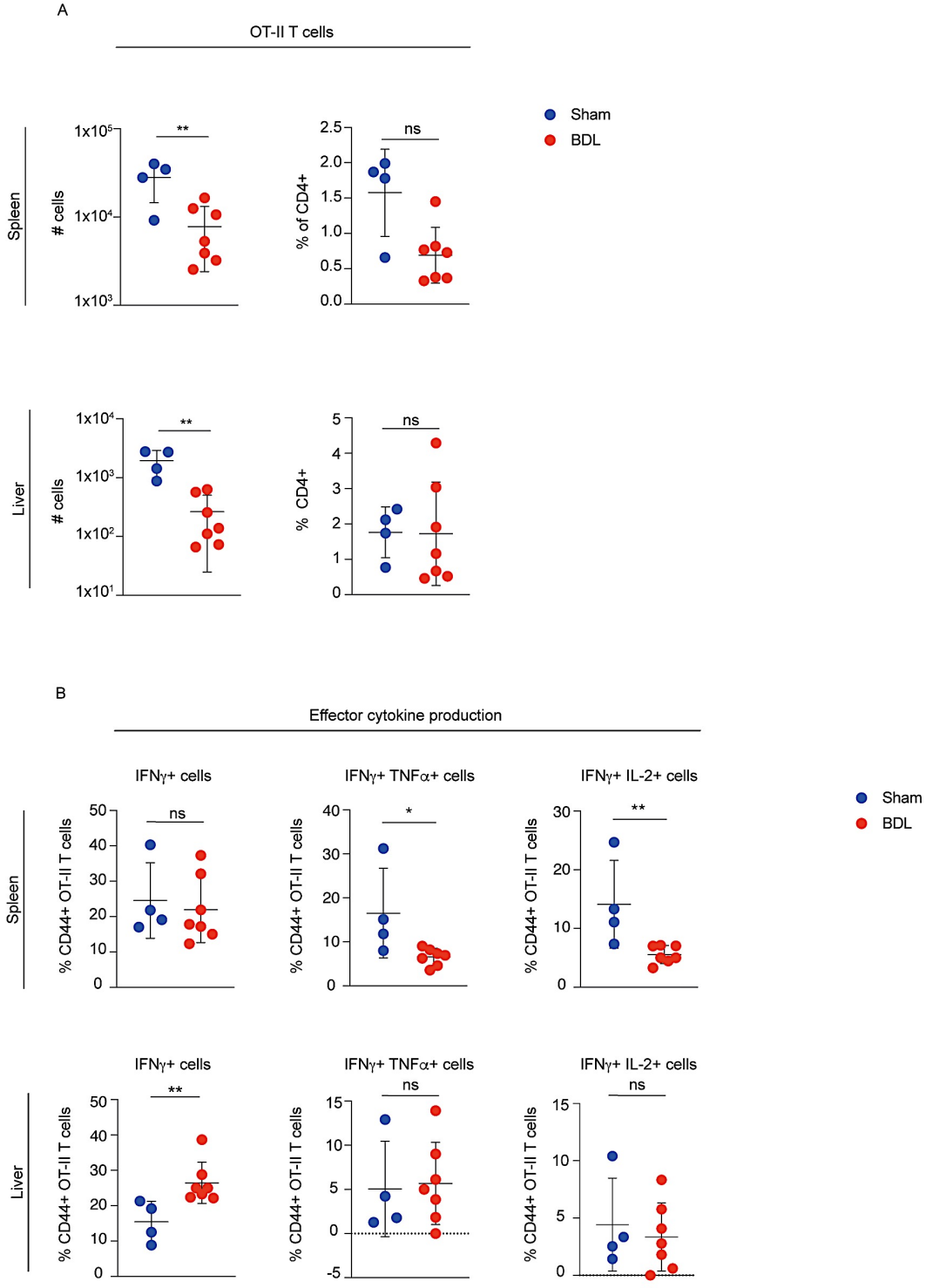
A
OT-II T cells
Sham
BDL
Spleen
cells
1x10⁵
1x10⁴
1x10³
**
% of CD4+
2.5
2.0
1.5
1.0
0.5
0.0
ns
Liver
cells
1x10⁴
1x10³
1x10²
1x10¹
**
% CD4+
5
4
3
2
1
0
ns
B
Effector cytokine production
IFNγ+ cells
IFNγ+ TNFα+ cells
IFNγ+ IL-2+ cells
Sham
BDL
Spleen
% CD44+ OT-II T cells
50
40
30
20
10
0
ns
40
30
20
10
0
*
30
20
10
0
**
Liver
IFNγ+ cells
IFNγ+ TNFα+ cells
IFNγ+ IL-2+ cells
% CD44+ OT-II T cells
50
40
30
20
10
0
**
15
10
5
0
-5
ns
15
10
5
0
ns

Figure 32: Reduced number of OT-II T cells and effector cytokine production in BDL-operated mice after OVA/PolyI:C vaccination. Flow cytometric analysis of the spleen and liver of BDL- and Sham-operated mice on day 8 post vaccination. Total number and proportion of OT-II T cells after vaccination **(A)**. Proportion of IFNγ+, IFNγ+ TNFα+ and IFNγ+ IL-2+ cells among OT-I T cells **(B)**. Data are representative of 1 independent experiments (n=4-7 mice).

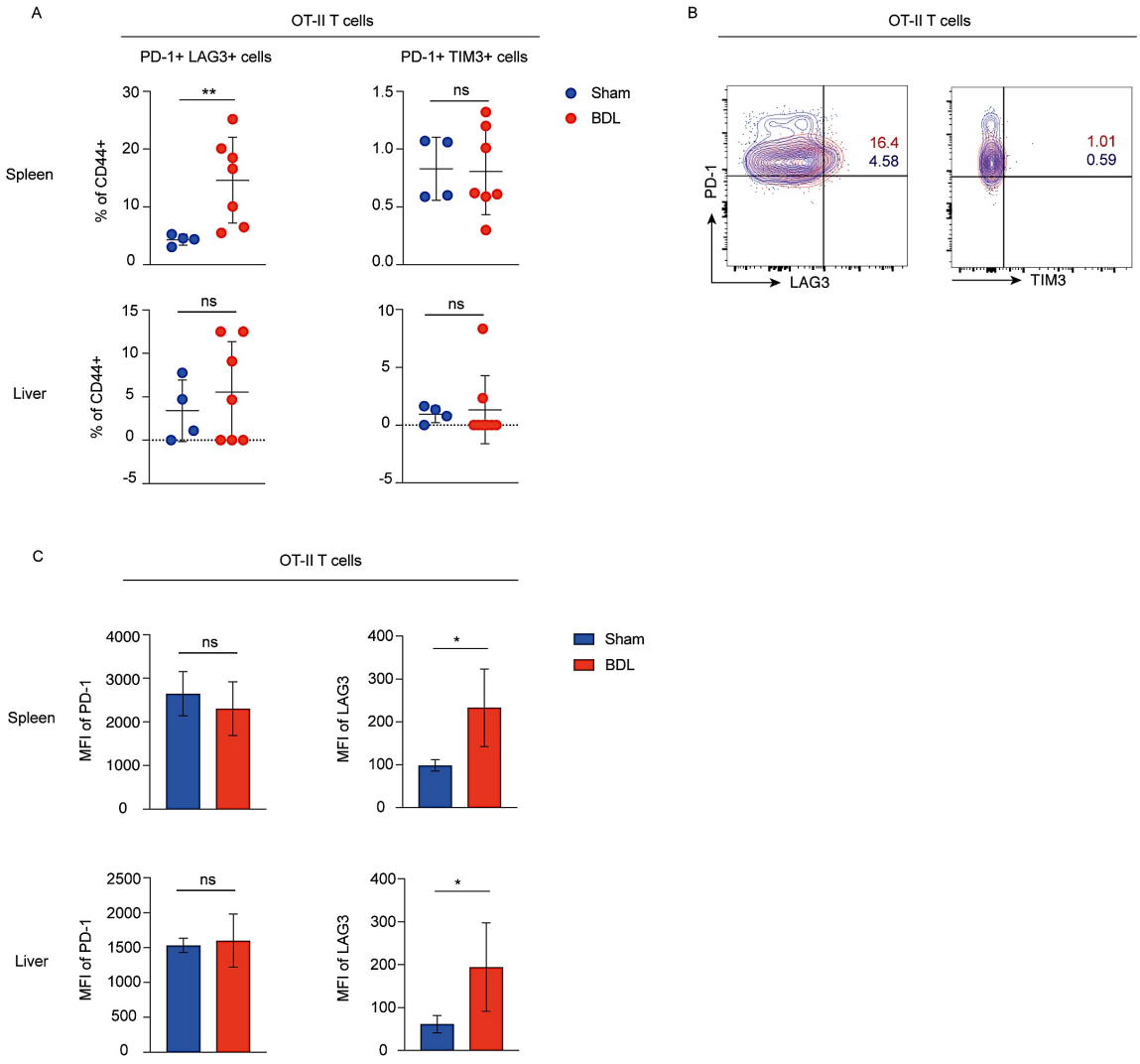

Figure 33: Increased expression of inhibitory receptors by OT-II T cells in BDL-operated mice after OVA/PolyI:C vaccination. Flow cytometric analysis of the spleen and liver of BDL- and Sham-operated mice on day 8 post vaccination. Proportion of PD-1+ LAG3+ and PD-1+ TIM3+ cells among OT-I T cells after vaccination **(A)**. Representative dot plots of PD-1+ LAG3+ cells among OT-I T cells **(B)**. MFI of PD-1 and MAG3 of OT-I T cells isolated from BDL- and Sham operated mice **(C)**. Data are representative of 1 independent experiments (n=4-7 mice).

4.2.5 Chronic inflammation of the liver does not affect absolute numbers of adoptively transferred T cells by day 4 post transfer, but renders them more prone to undergo apoptosis

To determine whether the lower numbers of adoptively transferred T cells seen after vaccination or infection, were due to chronic inflammation of the liver as such or additional antigen-mediated activation of T cells, OT-I and OT-II T cells were co-transferred into BDL- and Sham-operated mice and enumerated 4 days later. Type I IFNs are cytokines crucial for the inflammatory response against acute infections, but previous findings have shown sustained high levels of type I IFNs (as seen during chronic viral infections) to have a negative, immunregulatory effect on T cell immunity and viral clearance (Teijaro et al. 2013) (Wilson et al. 2013). Our group could previously show that chronic liver inflammation in mice is associated with a strong up-regulation of type I IFN and its downstream targets (Hackstein et al. 2016). To ascertain the effect of chronic type I IFN on survival of antigen-specific T cells during chronic liver inflammation, one group of BDL-operated mice was treated with IFNAR blocking antibody on the day of cell transfer and two days later. Results showed no differences in absolute numbers of both OT-I and OT-II T cells between Sham-operated mice and BDL-operated mice with or without IFNAR blocking antibody (Figure 34 A). However, while total numbers are similar by day 4 post transfer, OT-I and OT-II T cells from BDL-operated mice show first signs of apoptosis compared to healthy control mice (Figure 34 B). While IFNAR blockade resulted in a significantly lower proportion of apoptotic OT-II T cells, when comparing only BDL-operated mice, the proportion of apoptotic OT-II T cells did not reach the level of apoptotic OT-II T cells found in Sham-operated mice (Figure 34 B). These findings suggest that while absolute numbers of OT-I and OT-II T cells are similar between Sham- and BDL-operated mice by day 4, they might be lower in BDL-operated mice at later time points, as they are already showing early signs of apoptosis.

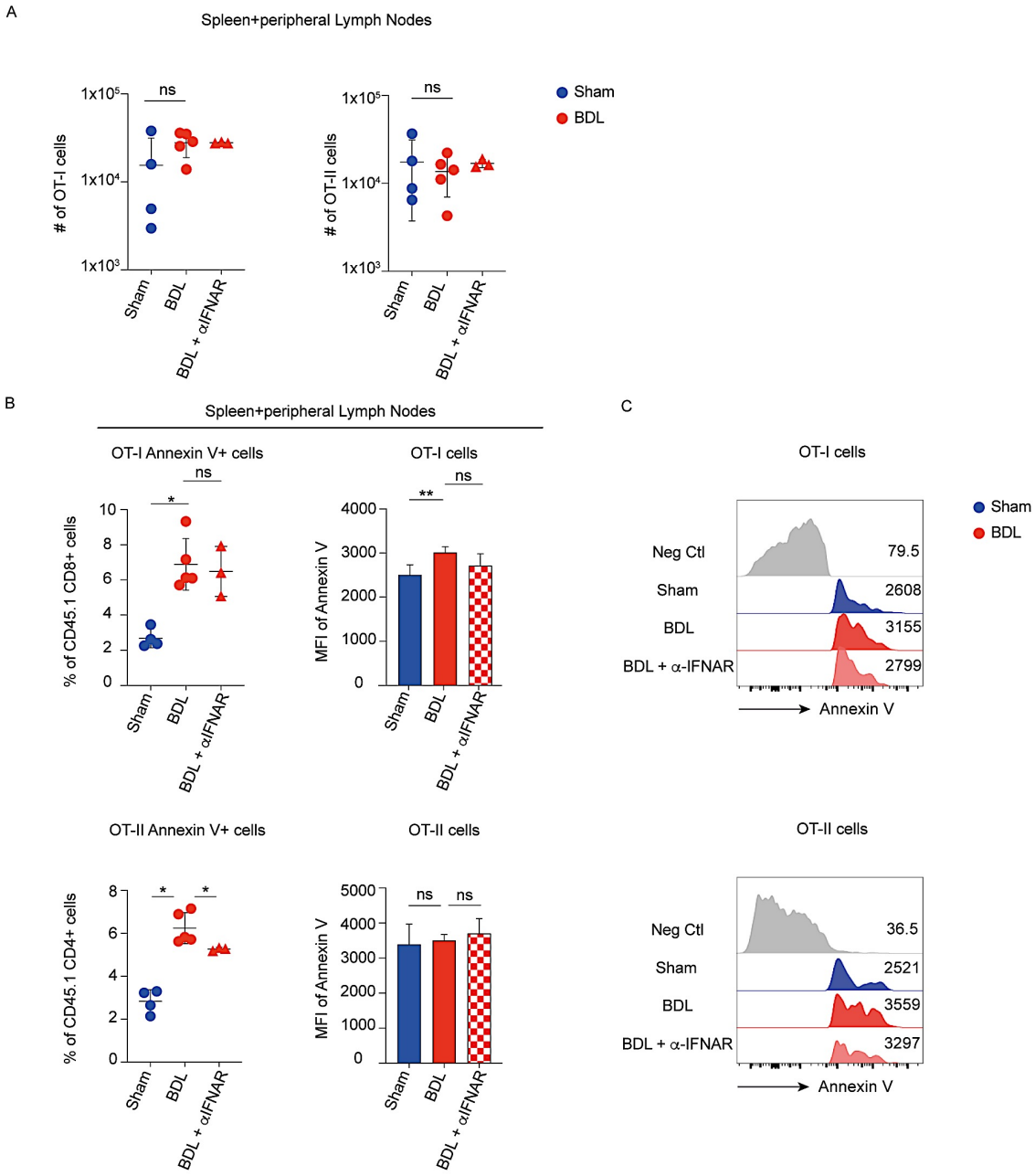

Figure 34: Peripheral maintenance of OT-I and OT-I T cells in naïve BDL- and Sham-operated mice. Flow cytometric analysis of the spleen and brachial, axial and inguinal LNs from BDL- and Sham-operated mice with or without anti-IFNAR blocking antibodies. Total number of OT-I and OT-II T cells in the spleen and peripheral LNs **(A)**. Proportion of Annexin V+ cells among OT-I and OT-II T cells, as well as MFI of Annexin V **(B)**. Representative histograms MFI of Annexin V of OT-I and OT-II T cells in BDL- and Sham-operated mice **(C)**. Data are representative of 1 independent experiments (n=3-5 mice).

4.3 Discussion

The experiments presented in this chapter aim to elucidate the underlying mechanisms of the impaired T cell response upon vaccination of in the context of chronic liver inflammation. Patients suffering from chronic liver disease and inflammation have a severely impaired immune system resulting in diminished immune responses that fail to contain and eliminated invading pathogens; irrespective of whether they are of viral or bacterial origin. Since the T cell-mediated immune response against LCMV in mice with chronic liver inflammation is insufficient both with respect to magnitude and quality of the response, this chapter investigates whether T cells are also rendered exhausted, i.e. dysfunctional, after vaccination with PolyI:C and OVA. There is a significantly higher proportion of individuals not responding to vaccination and failing to mount a detectable immune response among patients with chronic liver disease compared to healthy individuals (Koff, 2019). Exploiting PolyI:C and OVA vaccination as a model system provides a valuable tool to investigate T cell responses to vaccination in the context of chronic liver fibrosis in mice. Understanding the underlying mechanisms of the diminished immune response to vaccination will provide the next step in implementing more efficient vaccines for patients with an impaired immune system.

Results have shown that endogenous OVA-specific CD8+ T cells are present in significantly lower numbers in the spleen of diseased mice on day 8 after PolyI:C and OVA vaccination. Interestingly, no significant difference in numbers could be detected in the liver of diseased mice. This could be due to the number of T cells available to circulate is not impaired, in contrast to the total amount of T cells available in the secondary lymphoid organs such as the spleen. However, when analyzing the quality of antigen-specific CD8+ T cells, it becomes apparent that there is a higher proportion of exhausted T cells in diseased mice, compared to healthy mice. These findings are of particular interest, when considering the fact

that the antigen load administered during vaccination is finite, as opposed to an increasing antigen load during an infection with a replicating virus such as LCMV.

To make sure that antigen-specific T cells have not been impaired during their development in the thymus in mice with chronic liver inflammation prior to vaccination, OT-II and OT-I were adoptively transferred one day prior to vaccination. Interestingly, the absolute numbers of OT-II and OT-I T cells were significantly lower in both the spleen and the liver of diseased mice compared to healthy control mice. Additionally, even though OT-I T cells were only transferred one day prior to vaccination, they were equally exhausted by day 8 post vaccination as their endogenous counterparts, while OT-II T cells only showed signs of exhaustion in the spleen of diseased mice, but not in the liver. The lower antigen load during vaccination, compared to a viral infection, might explain the different impact on CD4+ and CD8+ T cells. Additionally, the effector cytokine response is more strongly impaired in OT-I T cells by day 8 post vaccination in diseased mice than in OT-II T cells. Chronic liver inflammation results in a much lower proportion of OT-I T cells producing INFγ, IFNγ and TNFα and IFNγ together with IL-2 in diseased mice compared to healthy control mice. These findings suggest that chronic liver inflammation on its own seems to negatively impact antigen-specific T cells in such a way that upon antigen encounter T cells fail to be sufficiently activated. Instead of performing their effector function, they are rendered exhausted and dysfunctional, failing to form an immunological memory and long-term protection upon vaccination. Considering that chronic liver inflammation is already accompanied by a myriad of inflammatory cytokine mediators, it is tempting to speculate that antigen-specific T cells are continuously exposed to signal 3 cytokines, which will interfere with the required order of activation signals upon antigen encounter (Sckisel et al. 2015). While this might be the reason why T cells are rendered exhausted and dysfunctional even after vaccination with a finite antigen load in the context of chronic liver disease, further experiments are required to undoubtedly prove this hypothesis.

To determine to what extent chronic liver inflammation by itself impairs the survival of adoptively transferred T cells. OT-I and OT-II T cells were transferred on day 8 post operation and isolated from the spleen and peripheral LNs 4 days after. Absolute numbers of both OT-I and OT-II T cells were similar between mice with chronic liver inflammation and healthy control mice. However, T cells isolated from diseased mice contained a higher proportion of apoptotic cells. These findings suggest that at least until day 4 post transfer chronic liver inflammation does not affect absolute numbers of adoptively transferred T cells. However, considering the higher proportion of T cells prone to undergo apoptosis, it is likely that with disease progression the inflammatory conditions of the liver will have a negative impact on T cell peripheral maintenance over time.

The experiments described in this paper shed light on how the T cell-mediated immune response is altered and impaired by chronic liver inflammation after vaccination. While providing valuable insights into the mechanisms failing during the T cell-mediated response during chronic liver inflammation, these findings raise further questions that when answered will help implement new and more efficient vaccine designs for patients already suffering from a compromised immune system.

Chapter 5

Overlapping peptides elicit distinct T cell responses during influenza A virus infection

5.1 Introduction

Effector CD8+ T cells play a crucial role in driving the adaptive immune response against a variety of intracellular pathogens and tumors (Cox and Zajac, 2010). Antigen specificity is determined by their individual heterodimeric TCRs, which are generated through DNA rearrangement of individual gene segments during clonal selection in the thymus (Welsh et al. 2010). CD8+ T cells generally recognize antigenic peptides of 8-11 amino acids in lengths, which are presented in the context of self-MHCs on APCs (Zhong et al. 2003). Upon peptide-MHC binding of TCRs, CD8+ T cells undergo clonal expansion to mount an efficient immune response against the respective pathogen, followed by a contraction phase, during which up to 95% of the antigen-specific CD8+ T cells undergo apoptosis and the formation of a small set of memory CD8+ T cells, which are maintained long-term (Cox and Zajac, 2010) (Kaech and Ahmed, 2001) (Mescher et al. 2006). Out of the large number of peptide epitopes that can theoretically bind any given MHC allele to be presented to CD8+ T cells during viral infections, comparatively few peptides are able to elicit a detectable T cell response (Raué and Slifka, 2009). Hence, extensive research has gone into analyzing the determinants of peptide immunogenicity to be able to biochemically and functionally identify appropriate candidate epitopes for novel and more efficient vaccines (Zhong et al. 2003). There is a multitude of algorithms allowing for the *in silico* prediction of immunogenic peptides, based on already know peptide binding motifs and the results of previously performed *in vivo* peptide binding assays, which aid in the identification of potential immunogenic epitopes, but fall short in providing a true reflection of the *in vivo* situation (Davenport et al. 1995) (Altuvia and Margalit, 2004). Previous approaches involved testing the reactivity of T cells against overlapping peptide panels spanning the entire length of proteins of interest (Tobery et al. 2001). For peptides that elicit CD8+ T cell responses, the minimal epitope is then defined as the shortest peptide able to elicit a response,

with longer versions of the peptide thought to be processed down to the minimal epitope *in vivo* (Tong et al. 2006).

Recent assessment of influenza A virus (IAV)-derived peptides following *in vitro* infection of dendritic cell (DC) and epithelial cell lines by mass spectrometry, identified 21 immunogenic peptides, 7 of which were novel, which were able to elicit a detectable CD8+ T cell response following IAV infection in mice (Wu et al. 2019). Among these immunogenic peptides, two were overlapping peptides derived from the neuraminidase protein $NA_{181-190}$ (NA10) and $NA_{181-191}$ (NA11) of the PR8 strain of influenza A virus, both of which were presented in the context of H2-D^b. While the NA11 peptide has previously been identified in the context of influenza A virus infection in mice, the NA10 peptide is completely novel (Zanker et al. 2013). Both peptides were detectable via both direct and cross-presentation; however the longer peptide was presented at 3-10-fold higher levels following infection of DC or lung epithelial cell lines (Wu et al. 2019). The fact that these highly similar peptides are both normally processed and presented following IAV infection offers a unique opportunity to dissect the endogenous CD8+ T cell response to these peptides to understand the extent to which similarity in epitope amino acid sequence was reflected in the corresponding CD8+ T cell populations elicited. Therefore the different CD8+ T cell populations elicited by the overlapping NA10 and NA11 peptides presented on H2-D^b were extensively analyzed. Results showed that even though these peptides only differ in length by the addition of one leucine residue at the C-terminus of the NA11 peptide, they induce entirely distinct CD8+ T cell populations with no evidence of cross-reactivity. Analysis of naïve epitope-specific T cell frequency, TCR $\alpha\beta$ repertoire, as well as magnitude and quality of the T cell responses, give further evidence that they are functionally distinct populations driven by a single amino acid addition on the NA11 peptide.

5.2 Results

5.2.1 Influenza A virus infection elicits distinct NA10- and NA11-specific CD8+ T cell populations in the spleen and BAL of mice

In order to validate *in vivo* the overlapping influenza A virus (IAV) peptides NA10 (SGPDNGAVAV) and NA11 (SGPDNGAVAL), which our group had previously identified in an unbiased mass spectrometry approach *in vitro* (Wu et al. 2019), female B6 mice were infected intranasally (i.n.) with 10^3 PFU PR8 influenza A virus to analyzed NA10- and NA11-specific CD8+ T cell populations on day 10 post infection (p.i.). Day 10 marks the peak of the CD8+ T cell response after influenza infection in mice (Zhong et al. 2003) and allowed the analysis of the NA10- and NA11-specific CD8+ T cells present in both the bronchoalveolar lavage (BAL) and spleen in response to influenza infection. Since peptide presentation in the context of MHC, does not in itself guarantee sufficient stimulation of TCR (Sung et al. 2002), we needed to validate that the NA10 and NA11 peptides identified by mass spectrometry are able to induce detectable CD8+ T cell populations *in vivo*. On day 10 p.i. dual NA10 and NA11 tetramer staining showed two distinct peptide-specific CD8+ T cell populations in both the BAL and the spleen of all infected mice analyzed (Figure 35 A). Additionally, both populations were present at similar magnitudes, when quantifying absolute numbers in both tissues (Figure 35 B). Hence, the overlapping NA10 and NA11 peptides constitute two immunogenic peptides that elicit distinct and subdominant, CD8+ T cell populations that are detectable both in the BAL and the spleen of influenza infected mice.

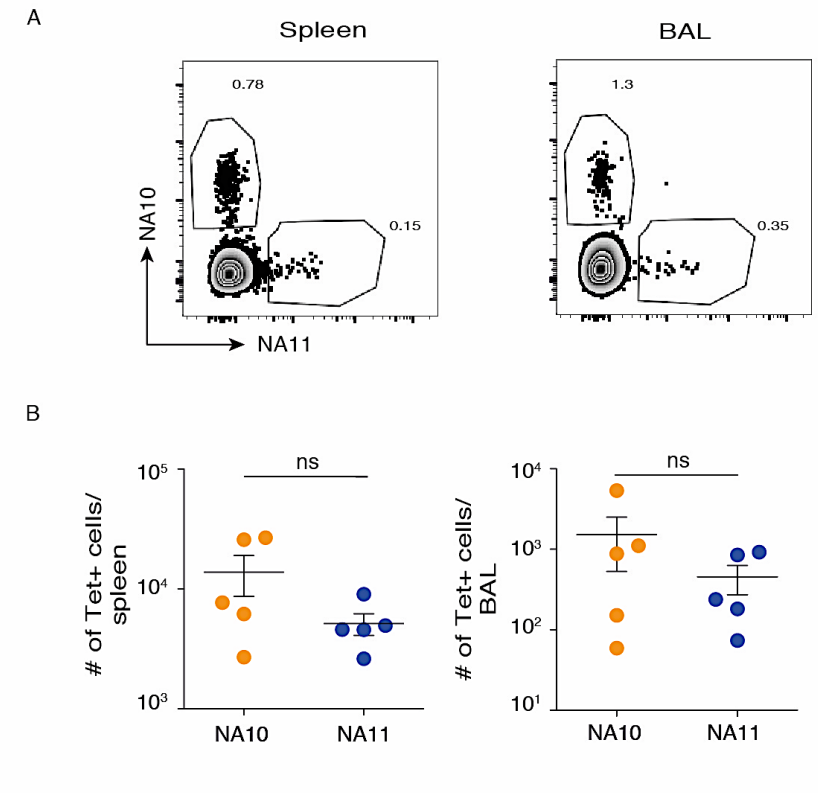

Figure 35: Enumeration of NA10- and NA11-specific CD8+ T cells in the spleen and BAL post PR8 infection. Female C57BL/6J mice were infected intranasally (i.n.) with 10^3 PFU of PR8 influenza virus. On day 10 post infection (p.i.) the spleen and the bronchoalveola lavage (BAL) were harvested for analysis and subsequent dual tetramer staining with NA10 and NA11 tetramers. **A)** Dual tetramer staining with NA10- and NA11-specific tetramers in the spleen and BAL of infected mice. Gates were set on live and CD19-, F4/80-, I-A^b- (dump) cells, followed by gating on CD4-, TCRβ+, CD8+, CD44+ T cells to identify the proportion of tetramer positive cells. **B)** Absolute numbers of NA10- and NA11-specific CD8+ T cells in the spleen and BAL of infected mice. Data are representative of 2-3 independent experiments and were analyzed using a parametric-paired *t*-test (n=5-6).

5.2.2 Lack of cross-reactivity between NA10- and NA11-specific CD8+ T cells after influenza infection

NA10- and NA11- specific CD8+ T cells identified after influenza infection present as two clearly distinct populations after influenza infection, with no detectable dual positive CD8+ T cells in a dual tetramer staining. To further

analyze the extent to which these populations were mutually exclusive and to determine whether there was preferential binding of one tetramer over the other we carried out dual tetramer staining, in which the concentration of one tetramer was kept constant, while the other was titrated. Flow cytometric analysis revealed that even at low concentration of either tetramer both NA10- and NA11-specific CD8+ T cell populations remained distinct (Figure 36 A, B). These findings confirm that the two populations are mutually exclusive, even though their peptide specificities differ only by the addition of one C-terminal leucine amino acid residue within the NA11 peptide sequence.

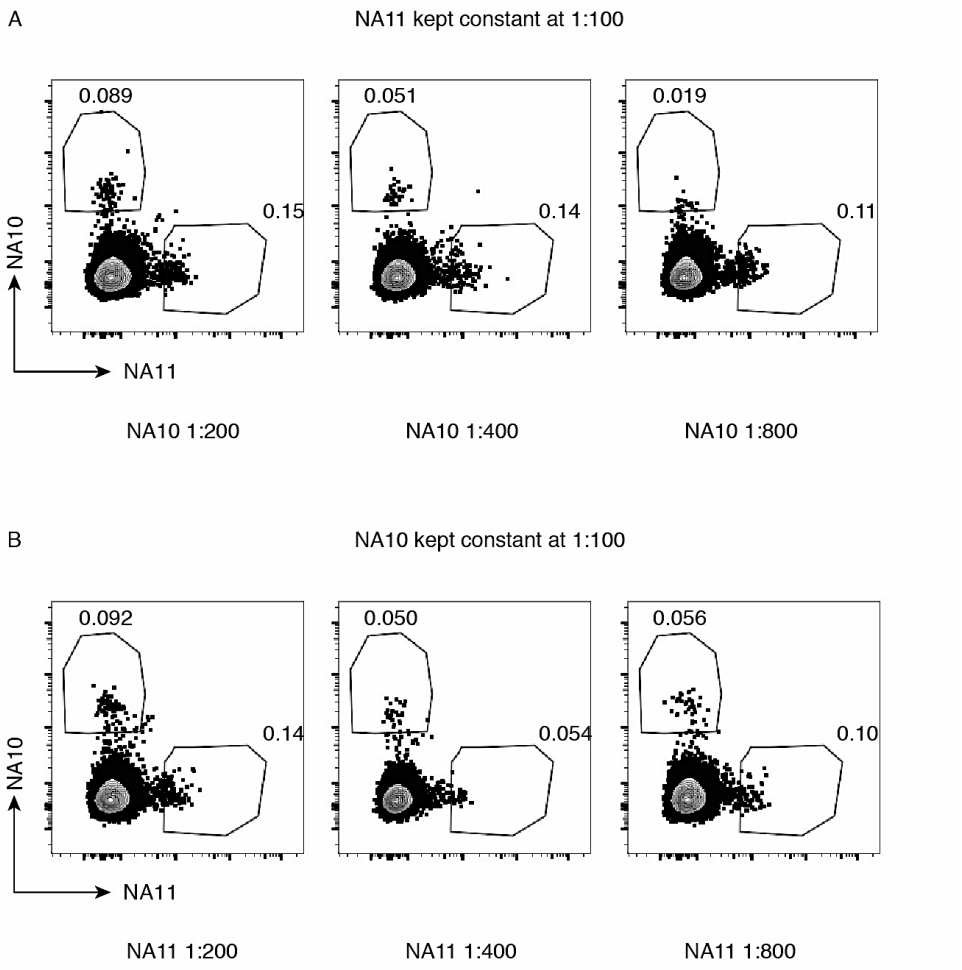

Figure 36: Assessment of cross-reactivity of NA10- and NA11-specific CD8+ T cells after either tetramer titration. Female C57BL/6J mice were infected i.n. with 10^3 PFU of PR8 influenza virus. On day 10 p.i. the spleens were harvested

for analysis and subsequent dual tetramer staining with NA10 and NA11 tetramers. **A)** Representative dot plots of NA10- and NA11-specific CD8+ T cells, in which the NA11 tetramer was kept constant (1:100) and the NA10 tetramer was titrated (1:200, 1:400, 1:800). **B)** Representative dot plot of NA10- and NA11-specific CD8+ T cells after infection, where the NA10 tetramer was kept constant and the NA11 tetramer was titrated (1:200, 1:400, 1:800). Gates were set on live and CD19-, F4/80-, I-A^b- (dump) cells, followed by gating on CD4-, TCRβ+, CD8+, CD44+ T cells to identify NA10- and NA11-specific CD8+ T cells after infection. Data are representative of 2-3 independent experiments.

5.2.3 Cytokine production by NA10- and NA11-specific CD8+ T cells after influenza infection

To assess whether there are any qualitative differences between NA10- and NA11-specific CD8+ T cells after influenza infection with respect to their effector cytokine production, lymphocytes from BAL and spleen were isolated and *in vitro* stimulated with NA10 and NA11 peptides for a total of 5 hours. IFNγ production has previously been used as a read-out to assess the number of peptide-specific CD8+ T cells (La Gruta et al. 2004). Identifying the proportion of IFNγ positive cells able to also produce additional effector cytokines such as TNFα and IL-2 was used to analyze the quality of the cytokine response. Peptide stimulation of lymphocytes isolated from the BAL and spleen revealed similar proportions of IFNγ CD8+ T cells able to produce TNFα and IL-2 after NA10 and NA11 peptide stimulation, with the exception of lymphocytes from the spleen that were stimulated with the NA11 peptide, as they showed an increase in the proportion of IFNγ+ cells that were also TNFα positive (Figure 37 A, B, C, D). These findings show that effector cytokine production by both NA10- and NA11-specific CD8+ T cells is similar with the exception of TNFα-producing lymphocytes isolated from the spleen. This phenomenon could be explained by a shortening of the NA11 peptide down to the same length of the NA10 peptide, allowing TCR-stimulation of both cell populations in our *in vitro* culture.

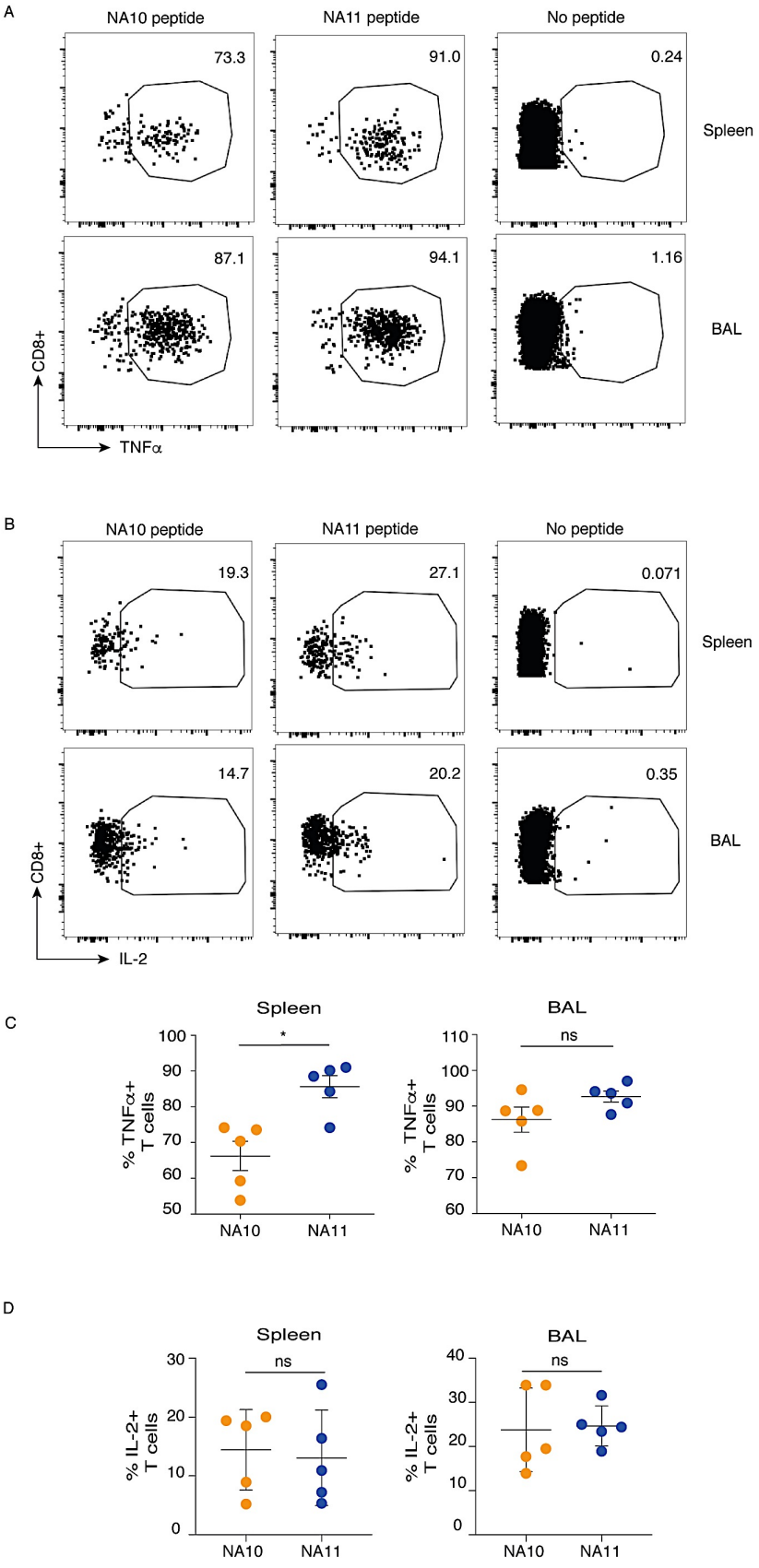
A
NA10 peptide
NA11 peptide
No peptide
73.3
91.0
0.24
Spleen
87.1
94.1
1.16
BAL
CD8+
TNFα
B
NA10 peptide
NA11 peptide
No peptide
19.3
27.1
0.071
Spleen
14.7
20.2
0.35
BAL
CD8+
IL-2
C
Spleen
BAL
% TNFα+ T cells
*
ns
NA10
NA11
D
Spleen
BAL
% IL-2+ T cells
ns
NA10
NA11

Figure 37: Qualitative analysis of the cytokine response after *in vitro* peptide stimulation of lymphocytes. Female C57BL/6J mice were infected i.n. with 10^3 PFU of PR8 influenza virus. On day 10 p.i. the spleen and the BAL were harvested and processed for *in vitro* peptide stimulation. **A)** Representative dot plots of TNFα+ cells after peptide stimulation. Gates were set on live, CD4-, CD8+ and IFNγ+ cells. **B)** Representative dot plots of IL-2+ cells after peptide stimulation. Gates were set on live, CD4-, CD8+ and IFNγ+ cells. **C)** Proportion of TNFα+ cells out of all IFNγ+ cells in the spleen and BAL of infected mice. **D)** Proportion of IL-2+ cells out of all IFNγ+ cells in the spleen and BAL of infected mice. Data are representative of 2-3 independent experiments and were analyzed using a non-parametric Mann-Whitney *t*-test (n=5-6 mice).

5.2.4 NA10- and NA11-specific CD8+ T cells display distinct TCR avidities after influenza infection

Peptide length is one of the major determinants of peptide-MHC stability, which consequently impacts greatly on TCR binding and stability, thereby influencing the magnitude of the CD8+ T cell response (Ekeruche-Makinde et al. 2013) (Zhong et al. 2003). Hence, we decided to assess whether the overlapping NA10 and NA11 peptides bond to MHC display different TCR avidities after influenza infection. To this end we isolated lymphocytes from BAL and spleen, fluorescently labeled NA10- and NA11-specific CD8+ T cells in a dual tetramer staining, followed by incubation with an H-2D^b blocking antibody for various time periods to prevent re-binding of tetramers upon dissociation. Assessing NA10 and NA11 tetramer dissociation over time allowed us to determine the overall TCR avidity of each peptide. NA10-specific CD8+ T cells were shown to have an overall higher TCR avidity which was statistically significant in NA10-specific CD8+ T cells isolated from BAL, while the same trend was observed in lymphocytes isolated from the spleen ($p>0.05$) (Figure 38 A, B).

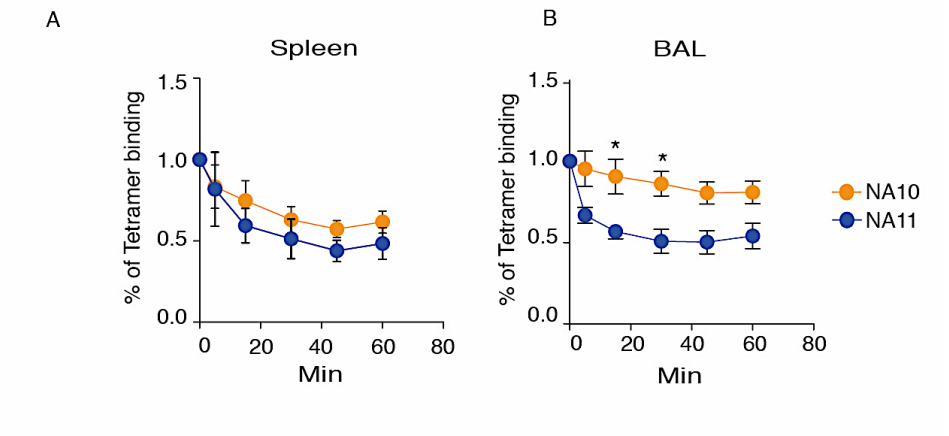

Figure 38: Assessment of the TCR avidity of NA10- and NA11-specific CD8+ T cells post PR8 infection. Female C57BL/6J mice were infected i.n. with 10^3 PFU of PR8 influenza virus. On day 10 p.i. the spleen and the BAL were harvested and processed. Following dual tetramer staining, re-binding of the tetramers was inhibited by co-incubation with an anti-H-2D^b antibody at 37°C, during which the signal intensity of the tetramers was analyzed at various different time points. Proportion of the total NA10- and NA11-specific CD8+ T cells from the spleen **(A)** and BAL **(B)** still binding tetramer at various time points after co-incubation with anti-H-2D^b antibody. Data are representative of only one experiment and were analyzed using a non-parametric Mann-Whitney *t*-test (n=5 mice).

5.2.5 NA10- and NA11-specific CD8+ T cells display distinct TCR repertoire usage after influenza infection

In order to unravel the unique reactivities of NA10- and NA11-specific CD8+ T cell populations and to understand how these populations differ at the structural level of clonotypic composition, NA10- and NA11-specific CD8+ T cells were single cell sorted on day 10 after influenza infection. We performed multiplex TCR analysis and sequenced their paired TCR α- and β-chains. Importantly, TCR α- and β-sequence analysis was performed on NA10- and NA11-specific populations from the same mice. TCR analysis revealed distinct TCR usage between the NA10- and NA11-specific CD8+ T cell populations, as well as expansion of individual T cell clones after infection (Figure 39 A, B). Each population is binding TCRs made up of a different α- and β-chain composition, while their distinct reactivities are also reflected in their different complementarity-determining region

3 (CDR3) loops, which confers peptide binding specificity (Figure 40 A, B). NA10-specific TCRs are predominantly made up of TRAV12-3, TRAV9 and TRBV5 or TRBV2 across the three different mice that were analyzed (Figure 38 A, B). In contrast, NA11-specific TCRs are made up of TRAV10, TRAV6-7, TRAV7-4 and TRBV12-1, TRBV12-2 or TRBV13-1 (Figure 38 A, B). Likewise, there are distinct CDR3 regions among NA10- and NA11-specific TCRs that are predominating, which are evidence of clonal expansion and thereby evidence of distinct TCR reactivities among NA10- and NA11-specific CD8+ T cells (Figure 40 A, B).

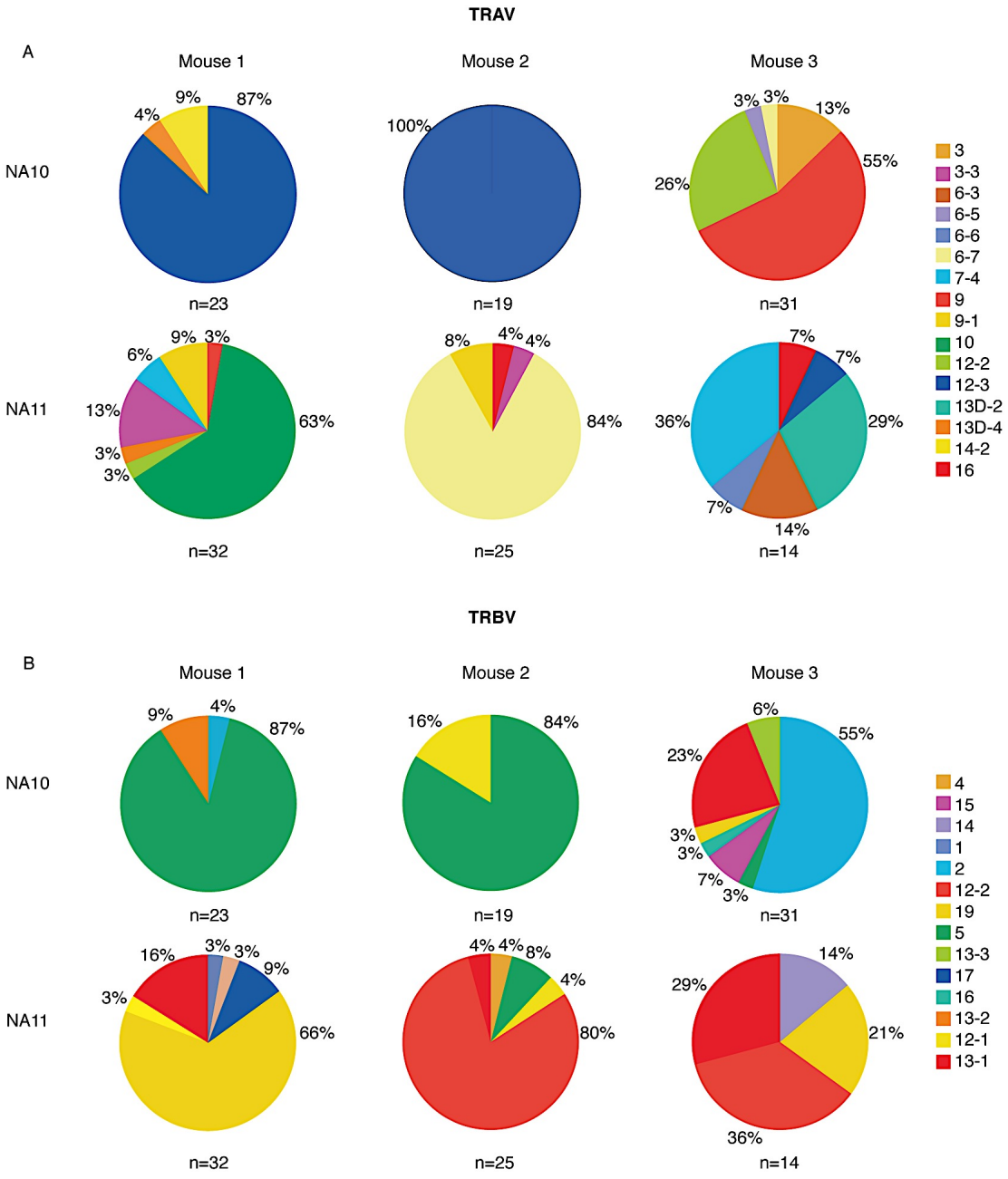

Figure 39: Characterization of CD8+ NA10- and NA11-specific TCR repertoires after infection. Female C57BL/6J mice were infected i.n. with 10^3 PFU of PR8 influenza virus. On day 10 p.i. the spleen and the peripheral lymph nodes (LNs) were harvested and magnetically enriched for CD8+ T cells. Individual NA10- and NA11-specific CD8+ T cells were single cell sorted for subsequent multiplex analysis of their paired TCR α- and β-chains. TRAV **(A)** and TRBV **(B)** gene segments used by NA10- and NA11-specific CD8+ T cells after infection.

NA10- and NA11-specific CD8+ T cell repertoires were characterized from the same mice (n=3 mice).

A

Epitope	Mouse Number	TRAV	CDR3 sequence	TRAJ	Frequency
NA10	1	13D-4	APLSGSFNKL	4	4.4
NA10	1	14-2	PGTQVVGQL	5	8.7
NA10	1	12-3	RTQVVGQL	5	82.6
NA10	1	12-3	TRQVVGQL	5	4.4
NA10	2	12N-3	RTQDVGQL	5	5.3
NA10	2	12N-3	RTQVVGHL	5	5.3
NA10	2	12N-3	RTQVVGQF	5	5.3
NA10	2	12N-3	RTQVVGQL	5	84.2
NA10	3	6-5	ANNTNTGKL	27	3.2
NA10	3	12-2	IPDTNAYKV	30	22.6
NA10	3	9	KGGSALGRL	8	3.2
NA10	3	9	QAGTGGLSGKL	3	3.2
NA10	3	9	RMAQVVGQL	5	3.2
NA10	3	12-2	RSNYNVL	21	3.2
NA10	3	9	SAGTGGLSDKL	2	3.2
NA10	3	9	SAGTGGLSGKL	2	22.6
NA10	3	9	SAGTGGLSGNL	2	3.2
NA10	3	9	SAGTGGVSGKL	2	3.2
NA10	3	9	SANTGGLSGKL	2	3.2
NA10	3	9	SAPNTGGLSGKL	2	3.2
NA10	3	3	SEGTQVVGQL	5	12.9
NA10	3	9	SGGAGNTGKL	37	3.2
NA10	3	9	SGGSGNTGKL	37	3.2
NA10	3	6-7	VYTGGLSGKL	2	3.2
NA11	1	13D-4	HLSGSFNKL	4	3.1
NA11	1	12D-2	SALTGSGGKL	44	3.1
NA11	1	9-1	SAMDSNYQL	33	9.4
NA11	1	9	SANSGTYQ	13	3.1
NA11	1	7-4	SEGAITES	31	3.1
NA11	1	3-3	YNQGKL	23	12.5
NA11	1	10	YPGDNSKL	38	65.6
NA11	2	3-3	RNSNNRI	31	4
NA11	2	6-7	RPTGGSNAKL	44	80

NA11	2	6-7	RPTGGSNAKV	44	4
NA11	2	9-1	SHNYAQGL	26	8
NA11	2	16	SMATGGNNKL	56	4
NA11	3	13-D2	RGFGGSNAKL	42	7.1
NA11	3	13-D2	RGSGGSNAKL	42	21.4
NA11	3	12-3	SEDGSSGNKL	32	7.1
NA11	3	16	SLMATGGNNKL	56	7.1
NA11	3	6-3	SLTGFASAL	35	14.2
NA11	3	7-4	SPVGDNSKL	38	35.7
NA11	3	6-6	YMGYKL	9	7.1

B

Epitope	Mouse Number	TRBV	CDR3 sequence	TRBJ	Frequency
NA10	1	13-2	GEETDPSGNTL	1-3	8.7
NA10	1	2	SQDAGDSDY	1-2	4.3
NA10	1	5	SQDRDTDV	1-1	13
NA10	1	5	SQDRDTEV	1-1	69.7
NA10	1	5	SQDTDTEV	1-1	4.3
NA10	2	12-1	SLDRDTEV	1-1	15.8
NA10	2	5	SQDRDAEV	1-1	5.3
NA10	2	5	SQDRDTEV	1-1	78.9
NA10	3	19	RGTEV	1-1	3.2
NA10	3	13-1	SDAKDSAETL	2-3	3.2
NA10	3	13-3	SDDRYEQ	2-7	3.2
NA10	3	13-1	SDDWGGAGDTQ	2-5	19.4
NA10	3	13-3	SDHNSYNSPL	1-6	3.2
NA10	3	15	SFRVSKERL	1-4	3.2
NA10	3	15	SFRVSNERL	1-4	3.2
NA10	3	16	SLLGGYSQNTL	2-4	3.2
NA10	3	5	SQAGGDSDY	1-2	3.2
NA10	3	2	SQDNGDSDY	1-5	16.1
NA10	3	2	SQEEGNSDY	1-2	6.5
NA10	3	2	SQEGGDSDY	1-2	3.2
NA10	3	2	SQESGDSDY	1-2	29
NA11	1	1	SEGGAEQ	2-1	3.1
NA11	1	13-1	SGGLGGNTGQL	2-2	15.6
NA11	1	19	SPGGITGQL	2-2	65.6

NA11	1	12-1	SPTKNTEV	1-1	3.1
NA11	1	17	SRVRTGGKDTQ	2-5	9.3
NA11	1	4	SSTGGAETL	2-3	3.1
NA11	2	13-1	SEQWGYYAEQ	2-1	4
NA11	2	4	SFGGKRDTQ	2-5	4
NA11	2	12-2	SPWGVEQ	2-7	84
NA11	2	5	SQDPWGSQNTL	2-4	8
NA11	3	13-1	GDSYAEQ	2-1	7.1
NA11	3	19	RDTNSGNTL	1-3	14.2
NA11	3	13-1	SESLGVYYEQ	2-7	7.1
NA11	3	14	SFGRGNAEQ	2-1	14.4
NA11	3	19	SINNTGQL	2-2	7.1
NA11	3	12-2	SLETGDGNTL	1-2	35.7
NA11	3	13-1	TESMGVSYEQ	2-7	7.1
NA11	3	13-1	TESMGVTYEQ	2-7	7.1

Table 40: Identification of CDR3 sequences of individual a- and b-chains of NA10- and NA11-specific CD8+ T cells after infection. Female C57BL/6J mice were infected i.n. with 10^3 PFU of PR8 influenza virus. On day 10 p.i. the spleen and the peripheral lymph nodes (LNs) were harvested and magnetically enriched for CD8+ T cells. Individual NA10- and NA11-specific CD8+ T cells were single cell sorted for subsequent multiplex analysis of their paired TCR α- and β-chains. CDR3 sequences from α- **(A)** and β-chains **(B)** of NA10- and NA11-specific T cells after infection. NA10- and NA11-specific CD8+ T cell repertoires were characterized from the same mice (n=3 mice).

5.2.6 Mutating the same individual residues within the NA10 and NA11 peptides differentially affects NA10- and NA11-specific CD8+ T cells

To further strengthen our hypothesis that the CD8+ T cell populations induced by the NA10 and NA11 peptides during influenza infection are mutually exclusive, we mutated single amino acid residues within the sequence and determined to what extent these mutated peptides are still able to induce IFNγ production in NA10- and NA11-specific CD8+ T cells after influenza infection. We hypothesized that, if the NA10- and NA11-specific CD8+ T cell populations are mutually exclusive, this is likely due to a different structural basis of NA10 and NA11 recognition and mutations of the same amino acid residue within the

NA10/NA11 sequence would affect TCR binding differently. Therefore we isolated lymphocytes from BAL and spleen on day 10 p.i. and *in vitro* stimulated them with a variety of mutated NA10 and NA11 peptides to analyze how single amino acid mutations affect the proportion of IFNγ positive cells they induce, i.e. affect their overall TCR binding ability. Results showed that only the single amino acid mutation at position 4 made a difference in terms of proportion of IFNγ positive cells in the spleen, whereas there was no detectable difference in proportion of IFNγ positive cells, when stimulating lymphocytes isolated from BAL (Figure 40 A, B).

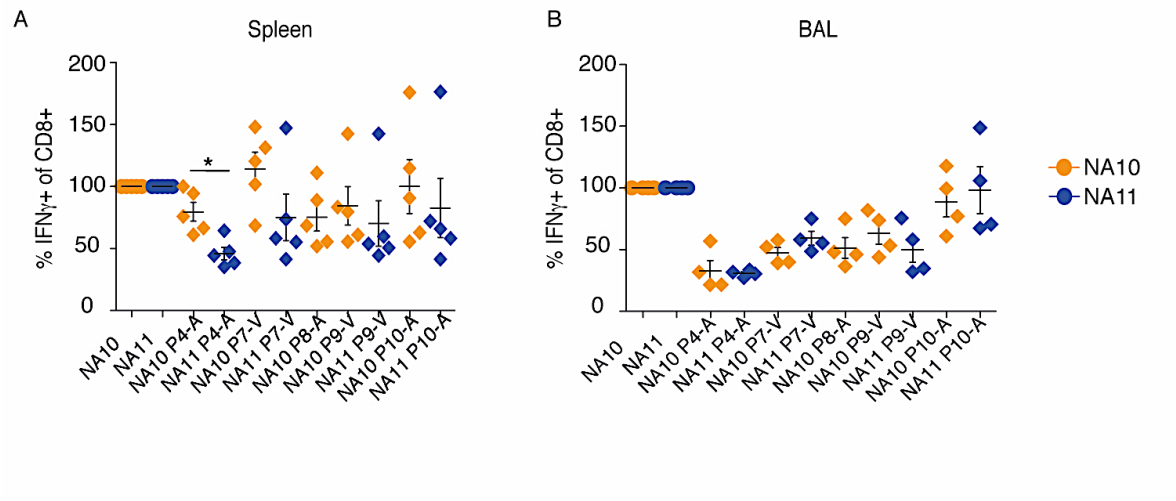

Figure 40: Analysis of IFNγ cytokine production after *in vitro* stimulation with mutated NA10 and NA11 peptides. Female C57BL/6J mice were infected i.n. with 10^3 PFU of PR8 influenza virus. On day 10 p.i. the spleen and the BAL were harvested and processed for *in vitro* stimulation with wild type and mutated peptides. **A)** Proportion of IFNγ+ cells among all CD8+ T cells from the spleen after peptide stimulation *in vitro*. **B)** Proportion of IFNγ+ cells among all CD8+ T cells from the BAL after peptide stimulation. Data are representative of only one experiment and were analyzed using a non-parametric Mann-Whitney *t*-test (n=5 mice)

5.2.7 Absence of cross-reactivity in naïve NA10- and NA11-specific CD8+ T cell precursors prior to influenza infection

To determine whether NA10- and NA11-specific CD8+ T cells are uniquely reactive prior to influenza infection or whether the distinct NA10- and NA11-specific CD8+ T cells arise from a largely cross-reactive pool of naïve CD8+ T cells, we carried out dual tetramer-based magnetic enrichment of NA10- and NA11-specific CD8+ T cells, which were analyzed by flow cytometry. Results showed that prior to influenza infection NA10- and NA11-specific CD8+ T cells isolated from the spleen and peripheral LNs of uninfected mice do not display any cross-reactivity between NA10 and NA11 peptides (Figure 41 A). Additionally, the magnitude of the naïve NA10- and NA11-specific precursor pools was similar, indicating that the NA10- and NA11-specific CD8+ T cell populations detectable during influenza infection have expanded to similar extents and have arisen from a distinct, non-cross reactive precursor pool (Figure 41 B). We also assessed CD5 expression of naïve NA10- and NA11-specific CD8+ T cells as a measure of TCR surface levels and reactivity (Azzam et al. 1998). Results showed no significant difference in CD5 expression between the different populations, suggesting their TCR affinity does not differ prior to infection.

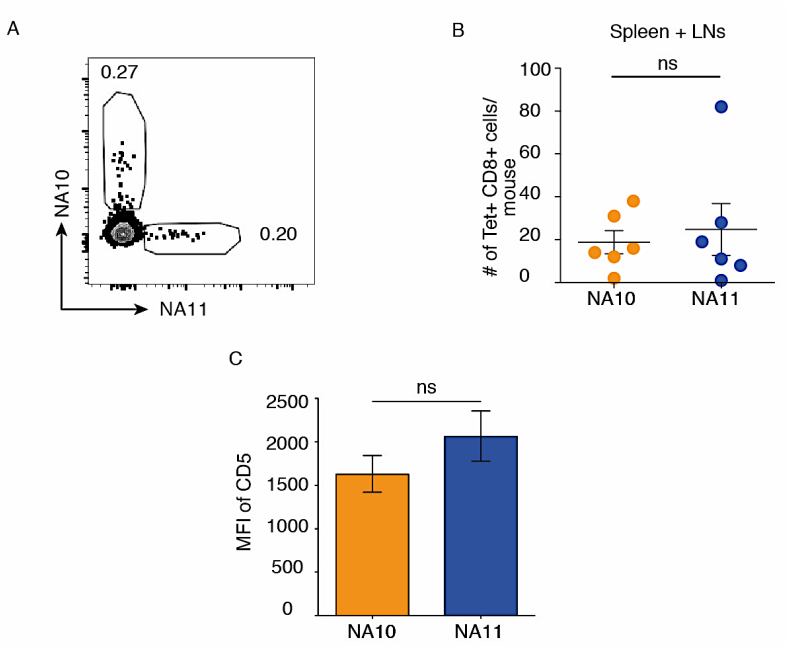

Figure 41: Magnitude and reactivity of naïve NA10- and NA11-specific CD8+ T cell precursor populations prior to infection. The spleen and peripheral LNs of naïve female C57BL/6J mice were harvested, processed and enriched for naïve NA10- and NA11-specific CD8+ T cells. **A)** Representative dot plot of NA10- and NA11-specific CD8+ T cell precursors in the spleen and peripheral LNs, showing no cross-reactivity in a dual tetramer staining. **B)** Number of naïve NA10- and NA11-specific CD8+ T cell precursors in the spleen and peripheral LNs. Gates were set on live, B220-, I-A^b, F4/80-, CD4-, CD44- and CD8+ cells. **C)** MFI of CD5 of naïve NA10- and NA11-specific CD8+ T cell precursors from the spleen and peripheral LNs. Data are representative of 3 different experiments and were analyzed by a parametric-unpaired *t*-test (n=5-6 mice).

5.3 Discussion

The experiments presented in this chapter aim to shed light on the extent to which a single amino acid extension can result in two distinct CD8+ T cell responses after PR8 influenza infection in mice. Influenza A virus infection constitutes a severe health burden worldwide, with 650 000 deaths per year and still causes seasonal epidemics, even though protective vaccines are available (Iuliano et al. 2018) (Guerche-Séblain et al. 2019). A shortcoming of the currently available influenza vaccines, however, is the fact that they provide poor cross-

reactivity across different serotypes of the influenza virus, necessitating annual reformulation of the vaccine to provide protection against the currently circulating viral serotype (Doherty and Kelso, 2008) (Hauser and Subbarao, 2015). A way to achieve higher cross-reactivity could be to incorporate peptide components targeted at CD8+ T cell responses, as these are often directed against more conserved protein regions of the virus (Lee et al. 2008) (Doherty and Kelso, 2008). CD8+ T cell responses are characterized by immunodominant hierarchies, meaning only a limited number of peptide epitopes elicits a detectable anti-viral T cells response, while others remain silent (Sercarz et al. 1993) (Cukalac et al. 2014) (Connelley et al. 2016). Understanding which epitopes are presented during the immune response against influenza infection, i.e. understanding the factors driving peptide immunogenicity, is a crucial step towards incorporating CD8+ T cell responses into new, more cross-reactive vaccines (Sette et al. 1994).

Here, we could show that the NA10 and the NA11 peptides presented on H-2D^{b} during PR8 influenza infection in mice elicit distinct CD8+ T cell populations in both the spleen and BAL of infected mice. NA10 and NA11 tetramer positive CD8+ T cells remained distinct populations, even when the concentration of either tetramer was titrated, excluding the possibility of preferential binding of one tetramer over the other and supporting the claim that these populations are truly independent of one another. Hence, the single amino acid extension of one leucine residue at the C-terminus of the NA11 peptide is most likely sufficient to change the peptide conformation to the extent that it elicits distinct CD8+ T cell populations. In fact, this is in line with previous findings in the context of *Theileria parva* infection, where the overlapping peptides Tp_{49-59} and Tp_{50-59} were found to elicit two distinct CD8+ T cell populations, despite differing only by one additional lysine residue at the N-terminus (Connelley et al. 2016). In this case, the single amino acid addition appeared to result in a conformational change altering the anchorage of the peptide within the MHC-I binding groove (Connelley et al. 2016).

Within the immunodominance hierarchy of CD8+ T cell responses directed against the PR8 influenza virus, the NA10- and NA11-specific CD8+ T cell populations make up subdominant responses of similar overall magnitude. However, with respect to the quality of the NA10- and NA11-specific immune response there are minor differences visible. Peptide length appears to be a crucial factor determining peptide-MHC and TCR binding, as well as the downstream TCR signaling (Ekeruche-Makinde et al. 2013). A phenomenon that has previously been described with respect to superimposed peptides found during HIV infection in human. In their studies the authors could show that the overlapping peptides RW8 (RYPLTFGW) and RW10 (RYPLTFGWCF) derived from the HIV Nef protein are presented in the context of HLA-A, but elicit distinct CTL responses during infection (Sun et al. 2014). Despite only differing by the extension of 2 amino acid residues, their respective CD8+ T cell responses are characterized by distinct TCR repertoire usage (Sun et al. 2014). It is therefore likely that the extension by one leucine residue in the case of the NA10 and NA11 peptides affects their TCR, which could potentially affect the magnitude of the effector response. In contrast to this stands the fact that N10-specific CD8+ T cells from the BAL appear to have a significantly higher TCR affinity on day 10 post PR8 infection than NA11-specific CD8+ T cells. The same trend can be observed in the spleen of infected mice, but does not show any statistical difference.

To further support the claim that NA10- and NA11-specific CD8+ T cells are truly distinct populations during PR8 infection, their TCR repertoires were analyzed on a single cell basis. Indeed, NA10- and NA11-specific CD8+ T cell populations contain distinct TCR repertoires across at least three different mice. Analyzing their CDR3 sequences, which is the major determinant driving peptide specificity, revealed clearly distinct sequences and confirmed clonal expansion of NA10- and NA11-specific CD8+ T cells (Danska et al. 1990). These findings are in line with those of Connelley et al. (2016), who could also demonstrate that the reason why the Tp_{49-59}- and Tp_{50-59}-specific CD8+ T cells elicit distinct populations during

Theileria parva infection is due to a different TCR repertoire usage. Additionally, single residue mutations of the NA10 and N11 peptide sequence seems to affect TCR binding differently with respect to position 4 of the peptide sequence. Mutating residue 4 from an Aspartic Acid (D) to an Alanine (A) resulted in a significantly lower proportion of IFNγ positive cells among NA11-specific CD8+T cells compared to NA10-specific CD8+ T cells. These results suggest that that NA10 and NA11 peptides bind different TCRs, as mutating the same residue affect TCR binding differently among NA10- and NA11-specific CD8+ T cell populations.

To determine whether NA10- and NA11-specific CD8+ T cells are uniquely reactive prior to infection, their naïve precursor numbers were analyzed. Results revealed distinct populations of naïve NA10 and NA11 precursors, which were present at similar magnitudes and showed similar TCR avidity towards ligand bound MHC, based on similar expression of the surface protein CD5 (Azzam et al. 1998). Hence, NA10- and NA11-specific CD8+ T cells are already uniquely reactive prior to PR8 influenza infection. The peptide-binding groove of MHC-I molecules is closed at either end resulting in MHC-I primarily binding peptides of 8-10 amino acids in length (Wieczorek et al. 2017). In order to accommodate peptides longer than 10 amino acids the peptide termini are maintained as MHC-I anchors, which leaves the central amino acids to protrude from the binding site and bind the TCR (Wieczorek et a. 2017). Taken together these findings therefore support the hypothesis that by one amino acid extension the conformation of the binding region of the NA10 and N11 epitopes is altered and subsequently affects MHC-I binding and TCR specificity in such a way that it results in two distinct, non cross-reactive CD8+ T cell populations, which display individual TCR repertoire usage during PR8 influenza infection.

Chapter 6

Concluding remarks

6.1.1 Chronic liver inflammation is associated with an increased risk of infection

Chronic liver damage as a consequence of hepatic inflammation regardless of etiology, is clinically linked to enhanced susceptibility to bacterial and viral infections, as well as weak immune responses to vaccination, for which no mechanistic explanation has been found so far (Henderson and Iredale, 2007). Roughly 29 million people are suffering from chronic liver disease in Europe alone, causing up 170 00 deaths annually, which are directly attributable to complications of liver cirrhosis; the end stage of chronic liver inflammation (Blachier et al. 2013). The incidence of people suffering from immune-mediated liver damage due to chronic viral hepatitis and liver damage due to alcohol-induced steatohepatitis (ASH) or non-alcoholic steatohepatitis (NASH) is steadily increasing across the globe (Henderson and Iredale, 2007) (Herkel et al. 2005) (Byun and Yi, 2017).

Previously, we have shown that chronic type I IFN induced by translocation of gut microbiota during liver fibrosis triggers the production of IL-10 by myeloid cells upon infection with intracellular pathogens such as *Listeria monocytogenes* (Hackstein et al. 2016). We have identified a key role of type I IFN as a molecular trigger and IL-10 as an execution mechanism affecting innate immune responses to bacterial infections during chronic liver damage. In this thesis, the bile duct ligation model, a preclinical model of chronic liver damage, was used to unravel the cellular and molecular underpinnings of the malfunctioning of adaptive immunity in response to viral infections and vaccination during chronic liver inflammation (Geerts et al. 2008). Using the well-defined lymphocytic choriomeningitis virus (LCMV), as well as OVA/PolyI:C vaccination, we could show that chronic liver damage is associated with impaired viral clearance, loss of effector T cell immune responses to viral infection and vaccination, effective maturation of antigen-presenting DCs and compromised mitochondrial fitness of antigen-specific CD4+ and CD8+ T cells. To our knowledge, this is the first time so far that chronic liver

fibrosis has been shown to affect the T cell-mediated immune response to viral infection and vaccination.

6.1.2 Chronic liver inflammation induces immune exhaustion of virus-specific T cells

An infection with the WE strain of LCMV constitutes an acute infection, which healthy, immunocompetent mice can clear within 8-10 days without considerable symptoms or immunopathology (Fung-Leung et al. 1991). Mice suffering from chronic liver inflammation however, show signs of viral persistence, including high viral titers post day 9 of infection, as well as impaired effector functions, which is commonly seen during infections with chronic strains of LCMV such as clone 13 (Wherry et al. 2007) (Allan et al. 1997) (Teijaro et al. 2013). Chronic infection with LCMV clone 13 is characterized by high antigen load and viral titers, rendering virus-specific T cells functionally exhausted, which closely resembles the phenotype observed in BDL mice after acute infection with LCMV-WE (Teijaro et al. 2013) (Wilson et al. 2013). Previous studies investigating the underlying cause of viral persistence during clone 13 infection revealed a key role of chronic type I IFN signaling in mediating immune suppression and antigen-specific T cell dysfunction, a phenomenon that we could also observe in BDL-operated mice infected with the acute strain WE of the LCMV (Teijaro et al. 2013) (Wilson et al. 2013) (Hackstein et al. 2016).

Acute infection with LCMV-WE leads to defects in the adaptive T cell compartment only in BDL-operated mice, which manifest as significantly reduced number of both endogenous and transferred LCMV-specific CD4+ and CD8+ T cells at the peak of the antiviral T cell response. The effect was visible in both the spleen and liver of infected BDL-operated mice and constitutes a systemic defect in the magnitude of the LCMV-directed T cell response, which is further supported by the fact that overall cellularity of polyclonal CD44+ CD4+ and CD44+ CD8+ T

cells was reduced. Our results are in agreement with existing literature that describes a reduction in antigen-specific T cell numbers and their effector functions during various chronic viral infections in both mice and humans, such as LCMV clone 13 infection or HIV or HCV infections (Wilson et al. 2013) (Brockman et al. 2009) (McMahan et al. 2010). The aforementioned chronic infections were characterized by elevated PD-1 expression levels, in addition to the co-expression of TIM3 in the case of HCV-specific CD8+ T cells, driving the exhausted phenotype observed during infection (McMahan et al 2010) (Wilson et al. 2013) (Brockman et al. 2009). PD-1, LAG3 and partially TIM3 expression, was an attribute common to LCMV-specific T cells in mice with chronic liver fibrosis, providing a potential mechanism through which T cell numbers and function are suppressed.

Another key characteristic of chronic viral infection is sustained type I IFN signaling, which is associated and commonly observed together with elevated exhaustion marker expression such as PD-1. While type I IFN signaling is crucial for the clearance of acute LCMV infection, as proven by the fact that IFNAR-/- mice fail to clear an acute infection with LCMV Armstrong, it negatively impacts virus-specific T cell function during chronic LCMV infection via the up-regulation of the immunosuppressive cytokine IL-10 (Wilson et al. 2013) (Teijaro et al. 2013). Even though negative immune regulatory factors such as IL-10 and PD-1 can also be found during acute LCMV infection, they are present at elevated levels during chronic LCMV infection, exerting a negative effect on viral control (Wilson et al. 2013) (Teijaro et al. 2013). Studies blocking type I IFN signaling during chronic LCMV infection could show improved viral clearance in a CD4+ T cell-dependent manner (Teijaro et al. 2013). Here, we could show that exhaustion markers such as PD-1, LAG3 and TIM3 are up-regulated in SMARTA and P14 T cells during chronic liver inflammation, which is in line with existing literature and ties in with the strong type I IFN signature present in BDL-operated mice due to microbial translocation form the gut, which we could previously show (Hackstein et al. 2016).

Taking into account chronic type I IFN signaling, as well as microbial translocation in BDL-operated mice prior to LCMV infection, it is tempting to hypothesize that LCMV-specific T cells are exposed to inflammatory cytokines, i.e. signal 3 of the T cell activation cascade prior to encountering their cognate antigen. Signal 3 stimulation prior to TCR engagement (signal 1) and co-stimulation via CD28 (signal 2), would likely interfere with normal T cell priming and result in the profound proliferative and functional defects upon LCMV infection (Sckisel et al. 2015). The phenomenon of T cells paralysis was previously describes by Sckisel et al., who demonstrated that immune stimulation, i.e. out-of-sequence signal 3, in the form of anti-CD40 and rhIL-2 renders primary CD4+ T cells paralyzed and suppressed their function and differentiation into memory T cells via SOCS3 inhibition of STAT5b signaling (2015). However, whether a similar mechanism is at play in the context of chronic liver inflammation requires additional experiment to be proven.

By adoptively transferring LCMV-specific SMARTA and P14 T cells prior to LCMV infection, we could exclude that chronic liver inflammation negatively conditioned LCMV-specific T cells prior to infection. SMARTA and P14 T cells were likewise reduced in numbers in BDL-operated mice after LCMV infection starting as early as day 4 post infection. These results suggest that, rather than a developmental defect, the presence of a soluble unknown factor associated with chronic liver inflammation is responsible to subduing the T cell-mediated response against LCMV, as SMARTA and P14 T cells were otherwise functional prior to transfer into diseased mice. These findings are of particular interest when considered in the context of previous findings which have shown that adoptively transferred virus-specific T cells are able to clear an already established persistent viral infection (Brooks et al. 2006). Moreover, studies investigating HIV-specific CD8+ T cell maintenance during chronic infection, could establish a direct link between PD-1 expression levels on HIV-specific CD8+ T cells and their sensitivity to apoptosis (Petroval et al. 2008). By blocking the PD-1/PD-L1 signaling axis the

authors could show that HIV-specific CD8+ T cells were better at surviving, as well as proliferating; an effect which was indirectly associated with increased proportion of cytokine producing cells (Petrova et al. 2006). As PD-1 levels are significantly increased in SMARTA and P14 T cells in BDL-operated mice, it is likely playing a role in the reduced T cells numbers and cytokine production during LCMV infection; however, the fact that SMARTA and P14 T cell numbers are reduced during the early phase of the LCMV-directed response suggest that there are additional factors at play subduing the T cell-mediated response early on in fibrotic mice.

We could show that lower numbers of SMARTA and P14 T cells in BDL-operated mice are in part due to a weakened proliferative capacity during the early expansion phase of the adaptive T cell numbers, which is likely affecting their absolute numbers also at the peak of the response around day 8 post infection (Laidlaw et al. 2016) (Openshaw and Tregoning, 2005). This is in line with the finding that functionally impaired virus-specific T cells are eliminated by apoptosis during chronic viral persistence, as seen in the case of the high affinity NP396-specific CD8+ T cells during LCMV clone 13 infection (Wherry et al. 2003) (Cornberg et al. 2013). Indeed, chronic liver inflammation seems to induce apoptosis in a higher proportion of SMARTA T cells after LCMV infection when compared to otherwise healthy mice. These findings are in agreement with previous literature suggesting that an excessive uptake of apoptotic bodies from dying hepatocytes by liver macrophages (Kupffer cells) enhances the expression of death ligands, such as Fas ligand, as well as TNFα, which might further potentiate T cell death during chronic liver inflammation through deregulation of apoptotic mechanism (Guicciardi and Gores, 2005) (Askenasy et al. 2005).

In conjunction with waning T cell function, chronic viral infection is also associated with impaired generation of long lasting memory T cells (Wherry et al. 2007) (Brooks et al. 2006). During acute infection virus-specific T cells undergo a

contraction phase following viral clearance, during with approximately 5% of T cells are maintained as memory T cells to confer long-term protection (Homan et al. 2001). In contrast, during chronic viral infection such as LCMV clone 13, the formation of a stable memory T cell pool is deregulated (Angelosanto et al. 2012). Here, we could show that at the peak of the T cell mediated response against LCMV BDL-operated mice display a reduction in number as well as proportion of short-lived effector T cells (SLECs), characterized by CD44 and KLRG1 expression and lack of CD62L and CD127 (Joshi et al. 2007). These findings provide another possible reason as to why LCMV is poorly controlled in BDL-operated mice and raises the possibility that subsequent memory T cell formation from the pool of effector T cells in equally impaired during the contraction phase of the T cell response.

Taking a closer look at the effector cytokine response of LCMV-specific T cells revealed a significant reduction in IFNγ+ TNFα+ cells among SMARTA and P14 T cells from BDL-operated mice. In addition, the proportion of PD-1+ LAG3+, as well as PD-1+ TIM3+ cells among SMARTA and P14 T cells was increased in BDL-operated mice, alongside their ability to produce granzyme B and subsequently degranulate. These findings are key attributes of T cell exhaustion during chronic LCMV infection, but not usually found during acute LCMV infection in immunocompetent mice (Pauken and Wherry, 2015). While higher levels of granzyme B seem counter-intuitive, considering it is a cytotoxic effector molecule promoting the elimination of virally infected target cells, higher granzyme B levels have previously been described during chronic LCMV infection and are in line with the reduction in effector cytokine production such as IFNγ, TNFα and IL-2 (Wherry et al. 2007). Therefore our findings fit in with the existing literature showing viral persistence to be linked with diminished virus-specific CD4+ and CD8+ T cell responses due to high viral titers and antigen load characterized by the progressive loss of T cell function (Allan et al. 1997) (Cornberg et al. 2013) (Wherry et al. 2007).

T-bet is a transcription factor essential for CD8+ T cell differentiation into SLECs (Wiesel et al. 2012). It is closely linked to the function of the transcription factor eomes, which is essential for the formation of memory precursor effector cells (MPECs), which subsequently give rise to long-lived memory T cells (Buggert et al. 2014). A finely tunes balance between t-bet and eomes expression levels is essential for proper formation of effector and memory T cell compartments, however, previous findings have show this balance to be deregulated in the context of chronic viral infection (Kaech and Cul, 2012) (Buggert et al. 2014). In the context of HIV infection in humans, Buggert et al. were able to show such deregulation of t-bet and eomes expression, proven by the fact that HIV-specific CD8+ T cells were almost exclusively $eomes^{high}$, while CMV-specific CD8+ T cells in comparison showed balanced distribution of t-bet and eomes expression (2014). $Eomes^{high}$ HIV-specific CD8+ T cells were shown to be associated with an exhausted phenotype, as well as poor effector function capabilities (Buggert et al. 2014). In the context of chronic liver inflammation we could also observe a deregulation of t-bet and eomes expressing cells among P14 and SMARTA T cells after LCMV infection, associated with viral persistence. Our findings show that the balance between t-bet and eomes expressing cells is skewed, potentially explaining the reduced proportion of SLECs among SMARTA and P14 T cells from BDL-operated mice. Up-regulation of eomes expression was previously shown to be associated with the expression of various inhibitory receptors, which is in line with the exhausted phenotype observed in the context of chronic liver inflammation (Buggert et al. 2014). Likewise, persistent antigen load, which is also seen in BDL-operated mice after LCMV infection, results in reduced levels of t-bet expression exacerbating the associated exhausted CD8+ T cell phenotype (Kao et al. 2011).

Collectively, these findings strongly suggest that chronic liver inflammation drives virus-specific CD4+ and CD8+ T cells towards a terminally differentiated phenotype with clear signs of T cell exhaustion. This phenotype includes: I) overall

reduction in T cell numbers, II) loss of the ability to produce IFNγ and TNFα, III) up-regulation of inhibitory receptors such as PD-1, LAG3 and TIM3, IV) increased expression of granzyme B and V) de-regulation of t-bet and eomes expressing T cells.

6.1.3 Mitochondrial dysfunction in LCMV-specific T cells during chronic liver inflammation

Upon antigen engagement of the TCR, T cells undergo a metabolic switch towards aerobic glycolysis, favoring anabolism and leaving macromolecules intact to sustain their rapid proliferation and to carry out effector functions (van der Windt et al. 2012) (Buck et al. 2016) (Chao et al. 2017) (Patsoukis et al. 2017). While naïve T cells primarily rely on catabolic metabolism and utilize mitochondrial OXPHOS for their ATP production, differentiation into functional effector T cells requires metabolic reprogramming and the up-regulation of aerobic glycolysis to sustain cellular demands for ATP (Patsoukis et al. 2017) (van der Windt et al. 2012). In contrast, memory T cells primarily make use of OXPHOS and rely on FAO, which are channeled into the mitochondrial TCA cycle to produce ATP (Krauss et al. 2001).

Exhausted T cells that fail to sustain effector functions have previously been shown to also display impaired metabolic reprogramming and mitochondrial fitness (Bengsch et al. 2016). Indeed, exhausted SMARTA and P14 T cells isolated from BDL-operated mice after LCMV infection displayed higher proportions of cells containing depolarized, i.e. dysfunctional, mitochondria, as well as increased levels of superoxide levels. These findings are indicative of impaired mitochondrial fitness and could be observed in SMARTA T cells from the spleen and liver, as well as P14 T cells isolated from the spleen of BDL mice on day 8 p.i.. Additionally, the same effect could be seen in SMARTA T cells isolated from the spleen of BDL mice as early as day 4 p.i., but not in P14 T cells. Impaired mitochondrial fitness is

likely to contribute to the dysfunctional T cell phenotype during chronic liver inflammation, and might even precede functional exhaustion with respect to LCMV-specific CD4+ T cells. These results are in agreement with current literature, describing a link between high levels of PD-1 expression in exhausted T cells and an altered glycolytic and mitochondrial profile, via the repression of the metabolic regulator PGC1-α driving mitochondrial biogenesis (Bengsch et al. 2016). Additional inhibitory receptors such as CTLA4, TIM3 and LAG3 have been implicated in deregulating the metabolic reprogramming of T cells after activation resulting in reduced aerobic glycolysis, impaired amino acid metabolism and metabolic fitness (Patsoukis et al. 2015) (Patsoukis et al. 2017).

Another rate-liming step of the metabolic switch towards aerobic glycolysis after T cell activation is the uptake of sufficient amounts of glucose (Pearce and Pearce, 2013). GLUT1 is the primary glucose transporter in T cells and its expression, as well as trafficking to the cell surface is up-regulated upon T cell activation via the PI3K/Akt signaling pathway (Jacobs et al. 2008). Up-regulation of GLUT1 occurs early during T cell activation and in its absence T effector function and proliferation cannot be sustained and cellular metabolism is impaired (McIntyre et al. 2014) (Siska et al. 2016). Interestingly, SMARTA and P14 T cells isolated from spleen and liver of BDL-operated mice, take up significantly more glucose at day 8 post LCMV infection than T cells from Sham mice, indicative of higher levels of GLUT1 expression. Schürich et al. have previously shown that exhausted T cells isolated from patients chronically infected with HBV express increased levels of the GLUT1 transporter compared to virus-specific T cells isolated from patients with an acute CMV infection (2016). There seems to be a correlation between the expression of the inhibitory receptor PD-1 and GLUT1 in dysfunctional HBV-specific T cells (Schürich et al. 2016). Further analyses are require to ascertain whether GLUT1 expression in SMARTA and P14 T cells is really increased at protein level, however, the glucose uptake is not impaired, but rather increased after chronic inflammation of the liver. Glucose uptake as such does not contribute

to the altered mitochondrial fitness of SMARTA and P14 T cells after LCMV infection. Instead, the increase in glucose uptake by transferred LCMV-specific T cells might be an attempt to channel enough glucose towards the glycolytic pathway to sustain bioenergetics demands during the effector response and subsequent failure of glucose to be used for glycolysis, but rather OXPHOS. However, to undoubtedly determine whether virus-specific T cells from mice with chronic liver inflammation show a shift towards OXPHOS away from aerobic glycolysis, the extent to which they utilize either pathway needs to be elucidated by measuring their lactate production, a byproduct of glycolysis, and their respective oxygen consumption rates, a byproduct of OXPHOS (Windt and Pearce, 2012).

Chronic liver inflammation and fibrosis are accompanied by a strong type I IFN signature which is due to the continuous translocation of gut microbiota into the liver after the development of portal hypertension (Hackstein et al. 2016) (Giannelli et al. 2014). Type I interferon signaling is induced through continuous TLR stimulation via DAMPS and PAMPS derived from the gut microbiota (Hackstein et al. 2016). This state of chronic inflammation and activation of innate immune cells results in up-regulation of the anti-inflammatory cytokine IL-10 upon subsequent infection with *Listeria monocytogenes*, dampening the pathogen-directed immune response and resulting in a high proportion of infection-associated mortality (Hackstein et al. 2016). Type I IFN have been shown to directly up-regulate IL-10 production to dampen the inflammatory response under many different contexts such as LPS-stimulated BMDMs or persistent infection with LCMV clone 13 (Chang et al. 2010) (Teijaro et al. 2013). IL-10 expression is increased both after infection with LCMV clone 13, as well as after acute LCMV infection in mice with chronic liver inflammation and can be suppressed after blockade of type I IFN signaling via the IFNAR1 (Teijaro et al. 2013) (unpublished data). The expression of the IL-10 receptor is significantly up-regulated in SMARTA and P14 T cells transferred into BDL mice after LCMV infection, making them receptive to anti-inflammatory IL-10 signaling and suggesting a negative feed back

loop dampening T effector function. Since IL10 is known to negatively regulate the metabolic switch to glycolysis and the expression of glycolytic genes after TLR stimulation, blockade of IL-10 signaling provides a potential target to improve T effector function with respect to both mitochondrial fitness, as well as inhibitory receptor expression (Ip et al. 2017).

6.1.4 Alteration of splenic DC populations and their maturation during chronic inflammation

DCs are important for the induction of T cell mediated immunity, as they are the most effective type of APC able to induce functional T cell activation (Roquilly and Villandangos, 2015) (Lim et al. 2012). DCs need to functionally mature and up regulate co-stimulatory receptors such as CD86, CD80 and CD40, as well as MHC-II molecules prior to T cell activation; either in response to DAMPs and PAMPs or inflammatory cytokine signaling (Merad et al. 2013) (Roquilly and Villandagos, 2015) (Boes et al. 2002) (Alter et al. 2010). During chronic liver inflammation CD11b+ and XCR1+ cDCs, as well as pDCs are present in lower numbers in the spleen during the peak of the T cell response against LCMV. DC have a circulating life span of roughly a week suggesting that chronic liver inflammation impairs either the recruitment of DC precursors and their differentiation into mature antigen-presenting cells, or favors their deletion in the context of chronic inflammation and infection (Roquilly and Vallidangos, 2015).

PDCs have previously been shown to produce great amounts of type I IFNs during infection, which promotes pDC activation and subsequently their decline in numbers via the induction of apoptosis (Swieki et al. 2011). There is an inverse correlation between high levels of type I IFN being produced and a decline in pDC numbers during infections associated with high levels of type I IFN production (Swieki et al. 2011). Furthermore, it is known that both acute and persistent strains of LCMV induce high levels of type I IFNs in the initial phase of the response and

subsequently a reduction in pDC numbers with disease progression (Zuniga et al. 2008). Considering that chronic liver inflammation is accompanied by chronic type I IFN signaling in itself, the reduction in pDC numbers at the peak of the T cell response might be explained by the continuously high levels of type I IFN due to both chronic liver inflammation, as well as LCMV infection. Additionally, pDC depletion during LCMV infection was shown previously by Swieki and Colonna to have no effect on CD8+ T cell mediated effector cytokine production and cellular cytotoxicity (2010). It's contribution to viral control and clearance of LCMV in the context of chronic liver inflammation is therefore likely to be minimal.

Since, DC-mediated T cell priming is essential for functional adaptive T cell responses, the effect of chronic liver inflammation on the maturation of CD11b+ and XCR1+ cDCs was determined during the early phase of LCMV infection. CD11b+ and XCR1+ cDCs are reduced in numbers in BDL-operated mice as early as 18 hours post infection, when compared to non-infected control mice and infected Sham-operated mice. Additionally, CD11b+ and XCR1+ cDCs show significantly lower levels of maturation marker expression such as CD80, CD86 and MHC-II in BDL-operated mice after infection, suggesting impaired maturation, which might directly impact on antigen-presentation, T cell interaction and co-stimulation. Moreover, shuttling of MHC-II molecules to the cell surface, a requirement for proper antigen-presentation and part of the maturation process appears altered in mice with chronic liver inflammation. These findings are in agreement with previous literature describing a reduction in DC maturation in response to maturation stimuli in patients with chronic HCV (Auffermann-Gretzinger et al. 2001). In their study, Auffermann-Gretzinger et al. compared DCs derived from patients with chronic HCV and resolved HCV and could show that monocyte-derived DCs from chronic HCV patients maintained an immature phenotype in response to maturation stimuli and continued to uptake antigen, which was not seen in patients with resolved HCV infection (2001).

Interestingly, both DC subsets display minor differences in proportion of CD80+ cDCs in BDL-operated mice even prior to infection, suggesting a negative effect of the chronic inflammatory environment in itself, potentially interfering with the proper differentiation of immature circulating DCs from progenitor cells. Considering the highly inflammatory milieu in BDL-operated mice, raises the question of whether DCs have been functionally paralyzed by continuous stimulation with inflammatory TLR ligands impairing their ability to mature fully and prime T cells sufficiently upon pathogen encounter (Roquilly and Villandangos, 2015). The phenomenon of DC paralysis or dysfunction, has previously been described in the context of murine cytomegalovirus (MCMV) infection, which infects DCs and results in down regulation of maturation markers such as CD86, CD80, MHC-I and MHC-II, CD40 and CD54 (Andrews et al. 2001). The down regulation of maturation markers in DCs interferes with DC function and provides a means to induce immunosuppression of the virus (Andrews et al. 2001). Type I IFN might additionally impair the maturation of DCs during chronic viral inflammation. Longman et al. could previously show that the timing of type I IFN signaling is crucial for DC-mediated T cell activation via cross-presentation (2007). More specifically, they could show that exposure of immature DCs to type I IFN negatively affects DC-mediated T cell activation via cross-presentation, while “late” exposure to type I IFN, i.e. when DC had already taken up antigen and matured, enhances DC-mediated T cells activation (Longman et al. 2007). Supporting their findings was the work of Sevilla et al. 2004, who could show that DCs infected during LCMV clone 13 infection displayed a reduced exhaustion marker expression (CD86, CD80, CD40, MHC-I and MHC-II) and antigen-presentation (2004). Moreover, they could show that this effect was largely due to type I IFN signaling, as DCs deficient for the IFNAR were able to mature fully despite LCMV clone 13 infection (Sevilla et al. 2004). Taking into account the presence of chronic type I IFN during chronic liver inflammation in mice, type I IFN signaling is likely suppress DC maturation after LCMV-WE infection.

6.1.5 Compromised T cell immune responses to vaccination

Similar to the impaired anti-viral immune response, cirrhosis patients show low response rates to vaccinations, making it increasingly difficult to confer immune protection against common viruses such as influenza, HBV and HAV, for which immunization are readily available and effective (Loulergue et al. 2009). To elucidate the mechanisms underlying the poor immune response during chronic liver disease, BDL-operated mice were vaccinated with OVA and PolyI:C and antigen-specific T cells analyzed on day 8 post immunization. Interestingly endogenous OVA-specific CD8+ T cells were present at much lower numbers in the spleen of mice with chronic liver inflammation. In addition, OVA-specific CD8+ T cells from the spleen and liver showed a much higher proportion of PD-1+ LAG3+ and PD-1+ TIM3+ cells in BDL-operated mice, characteristic of an exhaustion phenotype. This is particularly interesting considering the fact that the antigen load during vaccination is finite, as opposed to the antigen load during viral persistence.

In order to exclude that endogenous antigen-specific T cells from BDL-operated mice were functionally impaired during their development prior to vaccination, OT-I T cells were transferred prior to OVA/PolyI:C vaccination. Interestingly, OT-I T cells were similarly impaired with regards to the up-regulation of the inhibitory receptors PD-1, TIM3 and LAG3, when isolated from mice with chronic liver inflammation. In addition, absolute numbers of OT-I T cells are much lower in the spleen and liver of BDL-operated mice after vaccination. These findings suggest that the inflammatory milieu these cells enter during chronic liver disease is enough to impair the induction of an effective adaptive T cell response, negatively regulating T cell function, as seen by the reduction in effector cytokine production by OT-I T cells from the spleen and liver.

OT-II T cells transferred and isolated from the spleen and liver after vaccination were likewise reduced in BDL-operated mice, suggesting impaired CD4+ T cell help and function, potentially exacerbating the defect in the adaptive CD8+ T cell response. Indeed, the proportion of IFNγ+ TNFα+ cells, as well as IFNγ+ IL-2+ cells among transferred OT-II T cells is significantly lower in the spleen of BDL mice, whereas the same effect could not be detected in OT-II T cells recovered from the spleen. These data suggest that, at least with respect to CD4+ T cells, those antigen-specific cells circulating to the liver out of the secondary lymphoid organs retain their function to produce effector cytokines such as IFNγ, TNFα and IL-2. Additionally, transferred OT-II T cells from the spleen and liver of BDL mice expressed increased levels of the inhibitory receptor LAG3 and similar levels of PD-1. The inhibitory receptor PD-1 expression is transiently induced in effector T cells upon activation in acute infection, however, the additional increase in LAG3 levels in mice suffering from chronic liver inflammation suggest functional exhaustion of these T cells, which is in line with their reduced effector cytokine production (Yi et al. 2010).

To determine whether chronic liver inflammation and chronic type I IFN signaling negatively impacts on T cell viability and might be responsible, at least in part, for the lower numbers of transferred T cells, OT-I and OT-II T cells were co-transferred and analyzed 4 days later. To elucidate the impact chronic type I IFN signaling has on cell viability, part of the BDL-operated mice received IFNAR blocking antibodies (anti-IFNAR) to shut down the IFNAR signaling pathway. Interestingly, the inflammatory milieu in BDL mice does not seem to impact peripheral maintenance by day 4 post transfer, but renders transferred OT-I and OT-II T cells more prone to undergo apoptosis, suggesting that at later time points of chronic liver inflammation peripheral maintenance might start to be reduced. With respect to OT-II T cells this could be due to chronic type I IFN signaling, as the proportion of apoptotic cells decreases after anti-IFNAR administration, when

compared to untreated BDL mice. Type I IFN stimulates a multitude of downstream genes (interferon stimulated genes (ISGs)), including genes promoting apoptosis including TNFα related apoptosis inducing ligand (TRAIL) or the Fas ligand (Chawla-Sarkar et al. 2003). Sustained type I IFN signaling in the context of chronic viral infection has also been shown to promote NK cell-mediated cellular cytotoxicity, which could explain why adoptively transferred T cells are more prone to undergo apoptosis in BDL mice (Oh et al. 2019).

These findings raise the important question to what extent the inflammatory milieu imprints on antigen-specific T cells and inhibits the proper activation and effector function of these T cells. T cells from mice with chronic liver inflammation are likely to receive cytokine signals prior to antigen binding and co-stimulatory signals, which might potentially interfere with the signaling cascade and proper T cell activation after antigen encounter, resulting in impaired effector function and T cell exhaustion.

Collectively, the results of this thesis will give insight not only into the cellular and molecular mechanisms that promote viral persistence during chronic liver inflammation, but also the consequence of hepatic inflammation on protective immunity after primary infection or immunization. Moreover, the findings of this project will be the groundwork for generating novel options for treatments of viral infections and vaccinations in patients with liver fibrosis. Our results identify potential targets for immune therapy of infections occurring in patients with chronic liver damage. The mechanistic understanding of host-factors that determine loss of T cell protection against infection may apply well beyond the particular model of organ damage described here. Our findings have made a start at unraveling a new paradigm that links morbidities of chronic liver damage to compromised T cell immunity for which there are no effective treatments currently available. Mechanism-based development of future host-targeted immune therapies may

greatly improve disease outcome of patients suffering from liver fibrosis that contracted an additional viral infection.

6.1.6 Overlapping peptides induce distinct CD8+ T cell populations during PR8 influenza infection in mice

Only few distinct peptide epitopes elicit detectable CD8+ T cell responses, considering the vast number of peptides that could theoretically bind any given MHC-I allele to be presented to T lymphocytes. They can be classified into immunodominant and subdominant epitopes, based on the magnitude and quality of the T cell response they elicit, i.e their ID hierarchies, both of which could be exploited for future vaccine design against influenza virus infections (Zanker et al. 2013) (Ramakus et al, 2012) (Tscharke et al. 2015) (St Leger et al. 2013). Hence, it is crucial to determine the driving factors of peptide immunogenicity in order to fully exploit their characteristic for future effective and long lasting influenza vaccines inducing protective CD8+ T cell immunity.

Recently, two peptides derived from the influenza neuraminidase (NA) protein of the murine PR8 virus were identified, one of which is completely novel, which differ only by the extension of one C-terminal leucine amino acid residue (Wu et al. 2019). These NA10 and NA11 epitopes are derived from the neuraminidase protein and presented in the context of H-2D^{b} and appear to elicit two entirely distinct and non cross-reactive CD8+ T cell populations during PR8 infection. To determine to what extent a single amino acid extension drives different CD8+ T cell populations with respect to magnitude, function and TCR repertoire specificity, mice were infected with PR8 virus and NA10 and NA11 specific CD8+ T cell isolated from the BAL and spleen were analyzed by dual tetramer staining at the peak of the antiviral-response. Indeed, the NA10 and NA11 epitopes elicit two entirely distinct CD8+ T cell populations of similar magnitude during PR8 infection. To make sure that these populations were truly distinct and

there was no preferential binding of one tetramer over the other, a tetramer titration assay was done, where the concentration of tetramer was kept constant, while the other was titrated. Results showed no shift of either one NA10- or NA11-specific CD8+T cell population towards the other, suggesting truly distinct populations. Hence, the extension by one additional leucine residues appear to make the difference with respect to TCR binding specificities, resulting in a conformational change in the part of the epitope that binds the TCR pocket.

While the magnitude of the NA10- and NA11-specific CD8+ T cell responses are fairly similar, their quality in terms of effector cytokine production might still differ. However, while there is a significant increase on proportion of NA11-specific T cells isolate from the spleen that can make TNFα in addition to IFNγ, the same effect cannot be seen in NA11-specific T cells isolated from the BAL of infected mice. However, this might be explained by the fact that there are enough cytokine producing cells recruited to the lung, i.e. the site of infection, whereas the initial pool of cytokine producing cells to recruit from in the secondary lymphoid organs is much smaller in the case of NA10-specific CD8+ T cells. Additionally, the same effect could not be observed with respect to IL-2 production in addition to IFNγ production, suggesting that the NA10- and NA11-specific T cell populations fairly similar concerning effector cytokine production.

To determine whether the NA10- and NA11-specific T cell populations have a different TCR usage base on the additional leucine residue and whether their TCR avidities differ as a consequence, their TCR repertoires were sequenced and their respective TCR avidities assessed after infection. Interestingly, the NA10-specific T cells isolated from the BDL of infected mice appear to have a significantly higher TCR avidity compared to NA11-specific T cells. While the same trend could be observed in the spleen, it did not reach statistical significance. These findings suggest that there is indeed a difference in TCR binding based on the addition of a C-terminal leucine residue in the NA11 epitope. Likewise, single

cell sequencing of paired TCR α- and β-chains of NA10- and NA11-specific CD8 + T cells revealed distinct TCR repertoire usage, even between NA10- and NA11-specific CD8+ T cell isolated from the same mouse, including distinct CDR3 regions, which confer the peptide binding specificity of a TCR (Nikolich-Zugich et al. 2004) (Rosati et al. 2017). Hence, it is likely that the addition of one leucine amino acid residue changes the conformation of the core amino acid residues of the NA11 peptide and consequently alters its TCR binding specificities. To further support the hypothesis that the additional leucine residue results in different TCR specificities, individual core amino acid residues of the NA10 and NA11 epitopes, thought to be involved in TCR binding, were mutated. Subsequently, lymphocytes isolated from BAL and spleen were stimulated with the mutated peptides and their ability to engage in TCR binding was assessed base on IFNγ production. In principle, if the NA10 and NA11 peptides bind their respective TCRs in a different manner, then mutating the same amino acid residue within the peptide sequence should affect TCR binding differently for each peptide. Interestingly only mutating position 4 within the peptide sequence resulted in a significant difference in IFNγ production in cells isolated from the spleen, but not the BAL. Taken together these results are in line with previous findings by Sun et al. (2014), who showed that two superimposed HIV epitopes are able to elicit distinct T cell populations based on different TCR specificities. Taken together these findings support the notion that peptide length is crucial in determining TCR binding specificity based on different peptide confirmations (Sun et al. 2014).

Lastly, the naïve precursors of NA10- and NA11-specific T cells were quantified to determine whether they were uniquely reactive prior to infection or whether the distinct NA10- and NA11-specific CD8+ T cells arise from a cross-reactive pool of naïve CD8+ T cells. Indeed, NA10- and NA11-specific T cells appear to arise from a uniquely reactive pool of naïve precursors, which appear to have similar TCR specificities as indicated by similar CD5 surface expression

levels prior to infection, since CD5 expression reflects the avidity of the TCR of positively selected T lymphocytes in the thymus (Azzam et al. 1998)

Taken together these findings highlight the importance of peptide length for TCR binding specificities and stress the need to properly characterize the determinants of peptide immunogenicity in order to effectively incorporate them into future influenza vaccines.

Chapter 7

References

1. Abdullah Z., Knolle P. A., 2014, Scaling of immune responses against intracellular bacterial infection, *The EMBO Journal*, 33(20):2283-2294

2. Abe T., Arai T., Ogawa A., Hiromatsu T., Masuda A., Matsuguchi T., Nimura Y., Yoshikai Y., 2004, Kupffer Cell-Derived Interleukin 10 is Responsible for Impaired Bacterial Clearance in Bile Duct-Ligated Mice, *Hepatology*, 40(2):414-423

3. Albillos A., Lario M., Álvarez-Mon M., 2014, Cirrhosis-associated immune dysfunction: Distinctive features and clinical relevance, *Journal of Hepatology*, 61:1385-1396

4. Allan J. Z., Blattman J. N., Murali-Krishna K., Sourdive D. J. D., Suresh M., Altman J. D., Ahmed R., 1997, Viral immune evasion due to persistence of activated T cells without effector function, *J. Exp. Med.,*188(12):2205-2213

5. Aller M.-A., Arias J.-L., García-Domínguez J., Arias J.-I., Durán M., Aria J., 2008, Experimental obstructive cholestasis: the wound-like inflammatory liver response, *Fibrogenesis and Tissue Repair*, 1(6): doi:10.1186/1755-1536-1-6

6. Alter M. J., 2012, Vaccinating patients with chronic liver disease, *Gastroenterology and Hepatology*, 8(2):120-122

7. Alter G., Kavanagh D., Rihn S., Luteijn R., Brooks D., Oldstone M., van Lunzen J., Altfeld M., 2010, IL-10 induces aberrant deletion of dendritic cells by natural killer cells in the context of HIV infection, *The Journal of Clinical Investigation*, 120(6):1905-1913

8. Altuvia Y., Margalit H., 2004, A structure-based approach for prediction of MHC-binding peptides, *Methods*, 454-459

9. Alfei F., Kanev K., Hofmann M., Wu M., Ghoneim H. E., Roelli P., Utzschneider D. T., von Hoesslin M., Cullen J. G., Eisenberg V., Wohlleber D., Steiger K., Merkler D., Delorenzi M., Knolle P. A., Cohen C. J., Thimme R., Youngblood B., Zehn D., 2019, TOX reinforces the phenotype and longevity of exhausted T cells in chronic viral infection, *Nature*, 571:265-288

10. Andrews D. M., Andoniou C. E:, Granucci F., Ricciardi-Castagnoli P., Degli-Esposti M. A., 2001, Infection of dendritic cells by murine cytomegalovirus induces functional paralysis, 2(11):1077-1084

11. Angelosanto J. M., Blackburn S. D., Crawford A., Wherry E. J., 2012, Progressive loss of memory T cell potential and commitment to exhaustion during chronic viral infection, *Journal of Virology*, 86(15);8161-8170

12. Askenasy N., Yolcu A. S., Yaniv I., Shirwan H., 2005, Induction of tolerance using Fas ligand: a double-edged immunomodulator, *Blood*, 105:1396-1404

13. Asrani S. K., Devarbhavi H., Eaton J., Kamath P. S., 2019, Burden of liver disease in the world, *Journal of Hepatology*, 70(1):151-171

14. Auffermann-Gretzinger S.,Keefe E. B., Levy S., 2001, Impaired dendritic cell maturation in patients with chronic, but not resolved, hepatitis C virus infection, *Blood*, 97:3171-3178

15. Avaniti V., D'Amico G., Fede G., Manousou P., Tsochatzis E., Pleguezuelo M., Burroughs A. K., 2010, Infections in Patients with Cirrhosis Increase Mortality Four-Fold and Should Be Used in Determining Prognosis, *Gastroeneterology*, 139:1246-1256

16. Azzam H. S., Grinberg A., Lui K., Shen H., Shores E. W., Love P. E., 1998, CD5 expression is developmentally regulated by T cell receptor (TCR) signals and TCR avidity, *Journal of Experimental Medicine*, 188(12):2301-2311

17. Beack C., Wei X., Bartneck M., Pech V., Heymann F:, Gassler N., Hittatiya K., Eulberg D., Luedde T., Trautwein C., Tacke F., 2014, Pharmacological inhibition of the chemokine C-C motif chemokine ligand 2 (Monocyte chemoattractant protein 1) accelerates liver fibrosis regression by suppressing Ly-6C+ macrophage infiltration in mice, *Hepatology*, 59:1060-1072

18. Baeck C., Tacke F., 2014, Balance of inflammatory pathways and interplay of immune cells in the liver during homeostasis and injury, *EXCLI Journal*, 13:67-81

19. Barber G. N., 2001, Host defense, viruses and apoptosis, *Cell Death and Differentiation*, 8:113-126

20. Barber D. L., Wherry E. J., Masopust D., Zhu B., Allison J. P., Sharpe A. H., Freeman G. J., Ahmed R., 2006, Restoring function in exhausted CD8 T cells during chronic viral infection, *Nature Articles*, 439:682-687

21. Bartoletti M., Giannella M., Lewis R. E., Viale P., 2016, Bloodstream infections in patients with liver cirrhosis, *Virulence*, 7(3):309-319

22. Bataller R., Brenner D. A., 2005, Liver fibrosis, *The Journal of Clinical Investigation*, 115(2):209-218

23. Bayram A., Özkur A., Erkilic S., 2009, Prevalence of human cytomegalovirus co-infected in patients with chronic viral hepatitis B and C: A comparison of clinical and histological aspects, *Journal of Clinical Virology*, 45:212-217

24. Bengsch B., Johnson A. L., Kurachi M., Odorizzi P. M., Pauken K. E., Attanasio J., Stelekati E., McLane L. M., Paley M. A., Delgoffe G. M., Wherry E. J., 2016, Bioenergetic insufficiencies due to metabolic alterations regulated by the inhibitory receptor PD-1 are an early driver of CD8+ T cell exhaustion, *Immunity*, 45:358-373

25. Betts M. R., Brechley J. M., Price D. A., De Rosa S. C., Douek D. C., Roederer M., Koup R. A., 2003, Sensitive and viable identification of antigen-specific CD8+ T cells by a flow cytometric assay for degranulation, *J Immunol Methods*., 1;281(1-2):65-78

26. Blachier M., Leleu H., Peck-Radosavljevic M., Valla D.-C., Roudot-Thoraval F., 2013, The burden of liver disease in Europe, *European Association for the study of the liver*, 1-64

27. Blackburn S. D., Wherry E. J., 2007, IL-10, T cell exhaustion and viral persistence, *Trends in Microbiology*, 15(4):143-146

28. Bocharov G. A., 1998, Modelling the dynamic of LCMV infection in mice: Conventional and exhaustive CTL response, *J. Theor. Bio.,* 192:283-308

29. Boes M., Cerny J., Massol R., den Brouw M. O., Kirchhausen T., Chen J., Ploegh H. L., 2002, T-cell engagement of dendritic cells rapidly rearranges MHC class II transport, *Letters to Nature*, 418:983-988

30. Booty M. G., Nunes-Alves C., Carpenter S. M., Jayaraman P., Behar S. M., 2016, Multiple inflammatory cytokines converge to regulate CD8+ T cell expansion and function during tuberculosis, *J Immunol*, 196:1822-1831

31. Bone R. C., Grodzin C. J., Balk R. A., 1997, Sepsis: A new hypothesis for pathogenesis of the disease process, *CHEST*, 112:235-243

32. Brändle D., Müller C., Rülicke T., Hengartner H., Pircher H., 1992, Engagement of the T-cell receptor during positive selection in the thymus down-regulates RAG-1 expression, *Proc. Natl. Acad. Sci. USA*., .89:9529-9533

33. Brion C. A., Nguyen K. B. Oien G. C., 2002, Innate immune responses to LCMV infections: Natural Killer cells and cytokines, In: Oldstone M. B. A. (eds) Arenaviruses II. Currents Topics in Microbiology and Immunology, vol 263. *Springer,* Berlin, Heidelberg

34. Brockman M. A., Kwon D. S., Tighe D. P., Pavlik D. F., Rosato P. C., Sela J., Porichis F., Le Gall S., Waring M. T., Moss K., Jessen H., Pereyra F., Kavanagh D. G., Walker B. D., Kaufmann D. E., 2009, IL-10 is up-regulated in multiple cell types during viremic HIV infection and reversibly inhibits virus-specific T cells, *Blood*, 114:346-356

35. Brooks D. G., McGavern D. B., Oldstone M. B. A., 2006, Reprogramming of antiviral T cells prevents inactivation and restores T cell activity during persistent viral infection, *The Journal of Clinical Investigation*, 116(6):1875-1885

36. Brooks D. G., Teyton K., Oldstone M. B. A., McGavern D. B., 2005, Intrinsic functional dysregulation of CD4 T cells occurs rapidly fullowing persistent viral infection, *Journal of Virology*, 79(16):10514-10527

37. Brooks D. G., Trifilo M. J., Edelmann K. H., Teyton L., McGavern D. B., Oldstone M. B. A., 2006, Interleukin-10 determines viral clearance or persistence in vivo, *Nature Medicine*, 12(11):1301-1309

38. Brooks D. G., Walsh K. B., Elsaesser H., Oldstone M. B. A., 2010, IL-10 directly suppresses CD4 but not CD8 T cell effector and memory responses following acute viral infection, *PNAS*, 107(7):3018-3023

39. Buck M. D., O'Sullivan D., Klein Geltink R. I., Curtis J. D., Chang C.-H., Sanin D. E., Qui J., Kretz O., Braas D., van der Windt G. J. W., Chen Q., Huang S. C.-C., O'Neill C. M., Edelson B. T., Pearce E. J., Sesaki H., Huber T. B., Rambold A. S., Pearce E. L., 2016, Mitochondrial dynamics controls T cell fate through metabolic programming, *Cell*, 166:63-76

40. Buck M. D., Sowell R. T., Kaech S. M., Pearce E. L., 2017, Metabolic instruction of immunity, *Cell,* 169:570-586

41. Buck M. D., O'Sullivan D., Pearce E. L., 2015, T cell metabolism drives immunity, *J. Exp. Med.,* 212(9):1345-1360

42. Buggert M., Tauriainen J., Yamamoto T., Frederiksen J., Ivarsson M. A., Michaëlsson J., Lund O., Hejdeman B., Jansson M., Sönnerborg A., Koup R. A., Betts M. R., Karlsson A. C., 2014, T-bet and eomes are differentially linked to the exhausted phenotype of CD8+ T cells in HIV infection, *PLOS Pathogen*, 10(7);e1004251

43. Bunchorntavakul C., Chamrronkul N., Chavalidhamrong D., 2016, Bacterial infections in cirrhosis: A critical review and practival guidance, *World J Hepatol*, 8(6):307-321

44. Byl B., Roucloux I., Crusiaux A., Dupont E., Devière J., 1993, Tumor necrosis factor alpha and interleukin 6 plasma levels in infected cirrhotic patients, *Gastroenterology*,104(5):1492-1497

45. Byun J.-S., Yi H.-S., 2017, Hepatic immune mircroenvironment in alcoholic and non-alcoholic liver disease, *BioMed Research International*, 217: Article ID 6862439, 12 pages, https://doi.org/10.1155/2017/6862439

46. Chang C.-H., Curtis J. D., Maggi L. B. Faubert B., Villarino A. V., O'Sullivan D., Huang S. C.-C., van der Windt G. J. W., blagih J., Qui J., Weber J. D., Pearce W. J., Jones R. G., Pearce E. L., 2013, Posttranscriptional control of T cell effector function by aerobic glycolysis, *Cell*, 153:1239-51

47. Chang E. Y., Guo B., Doyle S. E., Cheng G., 2010, Cutting edge: Involvement of the type I IFN production and signaling pathway in lipopolysaccharide-induced IL-10 production, *J Immunol*., 178:6705-6709

48. Chao T., Wang H., Ho P.-C., 2017, Mitochondrial control and guidance of cellular activities of T cells, *Frontiers in Immunology*, 8(473):1-7

49. Chaplin D. D., 2010. Overview of the immune response, *J Allergy Clin Immunol*., 125:2-23

50. Chawla-Sarkar M., Lindner D. J., Liu Y.-F., Williams B. R., Sen G. C., Silverman R. H., Borden E. C., 2003, Apoptosis and interferons: Role of interferon-stimulated genes as mediators of apoptosis, *Apoptosis*, 8:237-249

51. Cheruvattath R., Balan V., 2007, Infections in patients with end-stage liver disease, *J Clin Gastroenterol*, 41(4):403-411

52. Clingan J. M., Ostrow K., Hosiawa K. A., Chen Z. J., Matloubian M., 2012, Differential roles for RIG-I-like receptors and nucleic acid-sensing TLR pathways in controlling a chronic viral infection, *The Journal of Immunology*, 188:4432-4440

53. Coates B. M., Staricha K. L., Wiese K. M., Ridge K. M., 2015, Influenza A virus infection, innate immunity, and childhood, *JAMA Pediatrics*, 169(10):956-963

54. Connelley T. K., Li X., MacHugh N., Colau D., Graham S. P., van der Bruggen P., Tarracha E. L., Gill A., Morrison W. I., 2016, CD8 T-cell responses against the immunodominant Theileria parva peptide $Tp2_{49-59}$ are composed of two distinct populations specific for overlapping 11-mer and 10-mer epitopes, *Immunology*, 149:172-185

55. Constandinou C., Henderson N., Iredale J. P., 2005, Modeling liver fibrosis in rodents, *Methods in Molecular Medicine*, 117:237-250

56. Cornberg M., Kenney L. L., Chen A. T., Waggoner S. N., Kim S-K., Dienes H. P., Welsh R. M., Selin L. K., 2013, Clonal exhaustion as a mechanism to protect against severe immunopathology and death from an overwhelming CD8 T cell response, *Frontiers in Immunology*, 5(475):1-8

57. Cox M. A., Zajac A. J.M., 2010, Shaping successful and unsuccessful CD8+ T cell responses flowing infection, *Journal of Biomedicine and Biotechnology*, Article ID 159152; doi:10.1155/2010/159152

58. Cukalac T., Chadderton J., Zeng W., Cullen J. G., Kan W. T., Doherty P. C., Jackson D. C., Turner S. J., La Gruta N. L., 2014, The influenza virus-specific CTL immunodominance hierarchy in mice is determined by the relative frequency of high-avidity T cells, *J Immunol*, 192:4061-4068

59. Dalod M., Chelbi R., Malissen B., Lawrence T., 2014, Dendritic cell maturation: functional specialization through signaling specificity and transcriptional programming, *The EMBO Journal*, 33(10):1104-1116

60. Danska J. S., Livingstone A. M., Paragas V., Ishihara R., Fathman C. G., 1990, The predumptive CDR3 regions of both T cell receptor α and β chains determine T cell specificity for myoglobin peptides, *J. Exp. Med*., 173:27-33

61. Dash P., McClaren J. L., Oguin lll T. H., Rothwell W., Todd B., Morris M. Y., Becksfort J., Reynolds C., Brown S. A., Doherty P. C., Thomas P. G., 2011, Paired analysis of the TCRα and TCRβ chains at the single-cell level in mice, *J Clin Invest*., 121(1):288-295

62. Davenport M. P., Ho Shon I. A. P., Hill A. V. S., 1995, An empirical method for the prediction of T-cell epitopes, *Immunogenetics*, 42:392-397

63. Davidson S., Crotta S., McCabe T. M., Wack A., 2014, Pathogenic potential of interferon $\alpha\beta$ in acute influenza infection, *Nature Communications*, 5:3864, DOI: 10.1038/ncomms4864

64. Doherty P. C., Kelso A., 2008, Toward a broadly protective influenza vaccine, *The Journal of Clinical Investigation*, 118(10):3273-3275

65. Doi H., Iyer T. K., Carpenter E., Li H., Chang K.-M., Vonderheide R. H., Kaplan D. E., 2012, Dysfunctional B-cell activation in cirrhosis resulting from hepatitis C infection associated with disappearance of CD27-positive B-cell population, *Hepatology*, 55:709-719

66. Drutman S. B., Trombetta E. S., 2010, Dendritic cells continue to capture and present antigens after maturation in vivo, *J Immunol*., 185(4):2140-2146

67. Duchini A., Vuerbes E., Nyberg L. M., Hendry M., Pockros P. J., 2000, Hepatic decompensation in patients with cirrhosis during infection with influenza A, *Arch Intern Med*, 160:113-115

68. Dumot J. A., Barnes D. S., YOunossi Z., Gordon S. M., Avery R. K., Domen R. E., Henderson M., Carey W. D., 1999, Immunogenicity of hepatitis A vaccine in decompensated liver disease, *Am. Coll. of Gastroenterology*, 94(6):1601-1604

69. Effros R. B., Doherty P. C., Gerhad W., Bennink J., 1997, Gerneration of both cross-reactive and virus-specific T-cell populations after immunization with serologically distinct influenza A viruses, *Journal of Experimental Medicine*, 145:557-568

70. Eisenbarth S. C., 2018, Dendritic cell subsets in T cell programming: location dictates function, *Nature Reviews*, 19:89.103

71. Eisen H. N., Chakraborty A. K., 2010, Evolving concepts of specificity in immune reactions, *PNAS*, 107(52):22373-22380

72. Ekeruche-Makinde J., Miles J. J., van den Berg H. A., Skowera A., Cole D. K., Dolton G., Schauenburg A. j. A., Tan M. P., Pentier J. M., Llewellyn-Lacey S., Miles K. M., Bulek A. M., Clement M., Williams T., Trimby A., Bailey M., Rizkallah P., Rossjohn J., Peakman M., Price D. A., Burrows S. R., Sewell A. K., Wooldridge L., 2013, Peptide length determines the outcome of TCR/peptide-MHCI engagement, *Blood*, 121(7):1112-1123

73. Fernández J., Gustot T., 2012, Management of bacterial infections in cirrhosis, *Journal of Hepatology*, S1-S12

74. Fernández J. Navasa M., Gómez J., Colmenero J., Vila J., Arroyo V., Rodés J.,

2002, Bacterial infections in cirrhosis: Epidemiological changes with invasive procedures and norfloxacin prophylaxis, *Hepatology*, 35(1):140-148

75. Frauwirth K. A., Riley J. L., Harris M. H., Parry R. V., Rathmell J. C. Plas D. R., Elstrom R. L., June C. H., Thompson C. B., 2002, The CD28 signaling pathway regulates glucose metabolism, *Immunity*, 16:769-777

76. Fung-Leung W.-P., Künding T. M., Zinkernagel R. M., Mak T. W., 1991, Immune response against lymphocytic choriomeningitis virus infection in mice without CD8 expression, *J. Exp. Med*., 174:1425-1429

77. Gairin J. E., Mazarguil H., Hudrisier D., Oldstone M. B. A., 1995, Optimal lymphocytic choriomeningitis virus sequences restricted by H-2D^{b} major histocompatibility complex class I molecules and presented to cytotoxic T lymphocytes, *Journal of Virology*, 69(4):2297-2305

78. Geerts A. M., Vanheule E., Praet M., Vlierberghe H. V., De Vos M., Colle I., 2008, Comparison of three research models of portal hypertension in mice: macroscopic, histological and portal pressure evaluation, *Int. J. Exp. Path.,* 89:251-263

79. Georgiev P., Jochum W., Heinrich S., Jang J. H., Nocito A., Dahm F., Clavien P.-A., 2008, Characterization of time-related changes after experimental bile duct ligation, *British Journal of Surgery*, 95:646-656

80. Geruche-Séblain C. E., Caini S., Paget J., Vanhems P., Schellevis F., 2019, Epidemiology and timing of seasonal influenza epidemics in the Asia-Pacific region, 2010-2017: implications for influenzy vaccination programs, *BMC Public Health*, 19(331):1-10

81. Giannelli V., Gregorio V. D., Iebba V., Giusto M., Schippa S., Merli M., Thalheimer U., 2014, Microbiota and the gut-liver axis: Bacterial translocation, inflammation and infection in cirrhosis, *World J Gastroenterol*., 20(45):16795-16810

82. Gomez F,, Ruiz P., Schreiber A. D., 1994, Impaired function of macrophage Fcy receptors and bacterial infection in alcoholic cirrhosis, *N Engl J Med*., 331:1122-1128

83. Guerche-Séblain C. E., Caini S., Paget J., Vanhems P., Schellevis F., 2019, Epidemiology and timing of seasonal influenza epidemics in the Asia-Pacific region, 2010-2017: implications for influenza vaccination programs, *BMC Public Health*, 19:331 https://doi.org/10.1186/s12889-019-6647-y

84. Guicciardi M. E., Gores G. J., 2005, Apoptosis: A mechanism of acute and chronic liver injury, *Gut*, 54:1024-1033

85. Guidotti L. G., Borrow P., Brown A., McClary H., Koch R., Chisari F. V., 1999, Noncytopathic clearance of lymphocytic choriomeningitis virus from the hepatocyte, *J Exp. Med*., 189(10):1555-1564

86. Gujral J. S., Farhood A., Bajt M. L., Jaeschke H., 2003, Neutrophils aggravate acute liver injury during obstructive cholestasis in bile duct-ligated mice, *Hepatology*, 38:355-363

87. Hackstein C.-P., Assmus L. M., Welz M., Klein S., Schwandt T., Schultze J., Förster I.,Gondorf F., Beyer M., Kroy D., Kurts C., Tribecka J., Kastenmüller W., Knolle P. A., Abdullah Z., 2016, Gut microbial translocation corrupts myeloid cell function to control bacterial infection during liver cirrhosis, *Gut*, 66:507-518

88. Harty J. T., Badovinac V. P., 2008, Shaping and reshaping CD8+ T-cell memory, *Nature Reviews*, 8:107-119

89. Harty J. T., Tvinnereim A. R., 2000, CD8+ T cell effector mechanisms in resistance to infection, *Annu. Rev. Immunol*., 18:275-308

90. Hashimoto M. Kamphorst A. O., Im S. J., Kissick H. T., Pillai R. N., Ramalingam S. S., Araki K., Ahmed R., 2018, CD8 T cell exhaustion in chronic infection and cancer: Opportunities for interventions, *Annu. Rev. Med.,* 69:301-318

91. Hato T., Dagher P. C., 2015, How the innate immune system senses trouble and causes trouble, *Clin J Am Soc Nephrol*., 10:1459-1469

92. Henderson N. C., Iredale J. P., 2007, Liver fibrosis: cellular mechanisms of progression and resolution, *Clinical Science*, 112:265-289

93. Herkel J., Schuchmann M., Tiegs G., Lohse A. W., 2005, Immune-mediated liver injury, *Journal of Hepatology*, 42:920-923

94. Hernandes-Gea V., Friedmann S. L., 2011, Pathogenesis of liver fibrosis, *Annu. Rev. Pathol. Mech. Dis.,* 6:425-456

95. Heymann F., Peusquens J., Ludwig-Portugall I., Kohlhepp M., Ergen C., Niemietz P., Martin C., van Rooijen N., Ochando J. C., Randolph G. J., Luedde T.,Ginhoux F., Kurts C., Trautwein C., Tacke F., 2015, Liver inflammation abrogates immunological tolerance induced by Kupffer cells, *Hepatology,* 62:279-291

96. Hodi F. S., O'Day S. J., McDermott D. F., Weber R. W., Sosman J. A., Haanen J. B., Gonzalez R., Robert C., Schadendort D., Hassel J. C., Akerley W., van den Eertwegh A. J. M., Lutzky J., Lorigan P., Vaubel J. M., Linette G. P., Hogg D., Ottensmeier C. H., Lebbé C., Peschel C., Quirt I., Clark J. I., Colchok J. D., Weber J. S., Tian J., Yellin M. J., Nichol G. M., Hoos A., Urba W. J., 2010, Improved survival with ipilimumab in patients with metastatic melanoma, *N Engl J Med*, 363(8):711-723

97. Homann D., Teyton L., Oldstone M. B. A., 2001, Differential regulationof antiviral T-cell immunity results in stable CD8+ but declining CD4+ T-cell memory, *Nature Medicine*, 7(8):913-919

98. Homann C., Varming K., Høgåsen K., Mollnes T. E., Graudal N., Thomson A. C., Garred P., 1997, Acquired C3 deficiency in patients with alcoholic cirrhosis predisposes to infection and increased mortality, *Gut*, 40:544-49

99. Horlander J. C., Boyle N. Manam R., Schenk M., Herring S., Kwo P. Y., Lumeng L., Chalasani N., 1999, Vaccination against Hepatitix B in patients with chronic liver disease awaiting liver transplantation, *The American Journal of the Medical Sciences*, 318(5):304-307

100. Houser K. and Subbarao K., 2015, Influenza Vaccines: Challenges and Solutions, *Cell Host Microbe*, 11;17(3):295-300

101. Huppa J. B., Davis M. M., 2003, T-cell-antigen recognition and the immunological synapse, *Nature Reviews*, 3:973-983

102. Huse M., 2009, The T-cell-receptor signaling network, *Journal of Cell Science*, 122:1269-1273

103. Ip W. K. E., Hoshi N., Shouval D. S., Snapper S., Medzhitov R., 2017, Anti-inflammatory effect of IL-10 mediated by metabolic reprogramming of macrophages, *Science*, 356:513-519

104. Iuliano A. D., Roguski K. M., Chang H. H., Muscatello D. J., Palekar R., Tempia S., Cohen C., Gran J. M., Schanzer D., Cowling B. J., Wu P., Kyncl J., Ang L., Park M., Redlberger-Fritz M., Yu H., Espenhain L., Krishan A., Emukule G., van Asten L., Pereira de Silva S., Aungkulanon S., Buchholz U., Widdowson M-A., Bresee J. S., 2018, Estimates of global seasonal influenza-associated respiratory mortality: a modeling study, *Lancet*, 391:1285-1300

105. Jacobs S. R., Herman C. E., MacIver N. J., Wofford J. A., Wieman H. K., Hammen J. J., Rathmell J. C., 2008, Glucose uptake is limiting in T cell activation and requires CD28-mediated Akt-dependent and independent pathways, *J Immunol*, 180:4476-4486

106. Jacobs R. J., Meyerhoff A. S., Saab S., 2005, Immunization needs of chronic liver disease patients seen in primary care versus specialist settings, *Digestive Disease and Sciences*, 50(8):1525-1531

107. Janeway Jr C. A., Travers P., Walport M., Shlomchik M. J., 2001, Immunobiology: The Immune system in health and disease, 5th edition, *Garland Science*, ISBN-10: 0-8153-3642-X

108. Joshi N. S., Cui W., Chandele A., Lee H. K., Urso D. R., Hagman J., Gapin L., Kaech S. M., 2007, Inflammation directs memory precursor and short-lived effector CD8+ T cell fates via the graded expression of T-bet transcription factor, *Immunity*, 27:281-295

109. Kaech S. M., Ahmed R., 2001, Memory CD8+ T cell differentiation: initial antigen encounter triggers a developmental program in naïve cells, *Nature*, 2(5):415-422

110. Kaech S. M., Cul W., 2012, Transcriptional control of effector and memory CD8+ T cell differentiation, *Nat Rev Immunol*, 12(11):749-761

111. Kahan S. M:, Wherry E. J., Zajac A. J., 2015, T cell exhaustion during persistent viral infections, *Virology*, 479-480:180-193

112. Kamimura D., Atsumi T., Stofkova A., Nishikawa N., Ohki T., Suzuki H., Katsunuma K., Jiang J-J., Bando H., Meng J., Sabharwal L., Ogura H., Hirano T., Arima Y., Murakami M., 2015, Naïve T cell homeostasis regulated by stress responses and TCR signaling, *Frontier in Immunology*, 6(638):1-5

113. Kao C., Oestreich K. J., Paley M. A., Crawford A., Angelosanto J. M., Ali M.-A., Intlekofer A. M., Boss J. M., Reiner S. L., Weinmann A. S., Wherry E. J., 2011, Transcription factor T-bet represses expression of inhibitory receptor PD-1 and sustains virus-specific CD8+ T cell responses during chronic infection, *Nature Immunology*, 12(7):663-672

114. Karlmark K. R., Wasmuth H. E., Trautwein C., Tacke F., 2008, Chemokine-directed immune cell infiltration in acute and chronic liver disease, *Expert Rev. Gastroenterol. Hepatol*., 2(2):233-242

115. Keeffe E. B, 1995, Is hepatitis A more severe in patients with chronic hepatitis B and other chronic liver disease?, *Am J Gastroenterol*, 90(2):201-205

116. Keeffe E. B., 2006, Hepatitis A and B superimposed on chronic liver disease: Vaccine-preventable diseases, *Transactions of the American Clinical and Climatological Association*, 117:227-238

117. Khan O., Giles J. R., McDonald S., Manne S., Ngiow S. F., Patel K. P., Werner M. T., Huang A. C., Alexander K. A., Wu J. E., Attanasion J., Yan P., George S. M., Bengsch B., Staupe R. P., Donahue G., Xu W., Amaravadi R. K., Xu X., Karakousis G. C., Mitchell T. C., Schuchter L. M., Kaye J., Berger S. L., Wherry E. J., 2019, TOX transcriptionally and epigenetically programs CD8+ T cell exhaustion, *Nature*, 571:211-234

118. Knolle P. A., Thimme R., 2014, Hepatic immune regulation and its involvement in viral hepatitis infection, *Gastroenterology*, 146:1193-1207

119. Knox J. J., Cosma G. L., Betts M. R., McLane L. M., 2015, Characterization of T-bet and Eomes in pheripheral human immune cells, *Frontiers in Immunology*, 5(217);1-13

120. Koff R. S., 2001, , Risks associated with hepatitis A and hepatitis B in patients with hepatitis C*, J Clin Gastoeneterol*., 33(1):20-26

121. Koff R. S., 2019, Immunizations for patients with chronic liver disease, *UpToDate Wolters Kluwer,* 1-12

122. Krauss S., Brand M. D., Buttgereit F., 2001, Signaling takes a breath – New quantitative perspectives on bioenergetics and signal transduction, *Immunity*, 15:497-502

123. Kulinski J. M., Tarakanova V. L., Verbsky JJ., 2013, Regulation of antiviral CD8 T-cell responses, *Critical Reviews in Immunology*, 33(6)477-488

124. Kunisaki K. M., Janoff E. N., 2009, Influenza in immunosuppressed populations: A Review of infection frequency, morbidity, mortality and vaccine responses, *Lancet Infect Dis*., 9(8):493-504

125. Kunz S., Sevilla N., McGavern D. B., Campbell K. P., Oldstone M. B. A., 2001, Molecular analysis of the interaction of LCMV with its cellular receptor a-dystroglycan, *Journal of Cell Biology*, 155(2):301-310

126. La Gruta N. L., Turner S. J., Doherty P. C., 2004, Hierarchies in cytokine expression profiles for acute and resolving influenza virus-specific CD8+ T cell responses: correlation of cytokine profile and TCR avidity, *The Journal of Immunology*, 172:5553-5560

127. Laidlaw B. J., Craft J. E., Kaech S. M., 2016, The multifaceted role of CD4+ T cells in CD8+ T cell memory, *Nature Reviews Immunology*, 16:102-111

128. Lim T. S., Go J. K. H., Mortellaro A., Lim C. T., Hämmerling G. J., Ricciardi-Castagnoli P., 2012, CD80 and CD86 differentially regulate mechanical interactions of T-cells with antigen-presenting dendritic cells and B-cells, PLOS ONE, 7(9):e45185 doi:10.1371/journal.pone.0045185

129. Lee Y-T., Kim K-H., Ko E-J., Lee Y-N., Kim M-C., Kwon Y-M., Tang Y., Cho M-K., Lee Y-J., Kang S-M., 2014, New vaccines against influenza virus, *Clin Exp Vaccine Res*, 3:12-28

130. Lee L Y.-H., Ha D. L. A., Simmons C., de Jong M. D., Chau N. V. V., Schumacher R., Peng Y. C., McMichael A. J., Farrar J. J., Smith G. L., Townsend A. R. M., Askonas B. A., Rowland-Jones S., Dong T., 2008, Memory T cells established by seasonal human influenza A infection cross-react with

avian influenza A (H5N1) in healthy individuals, *J. Clin. Invest.*, 118(10):3478-3490

131. Leise M. D., Talwalkar J. A., 2013, Immunizations in chronic liver disease: What should be done and what is the evidence, *Curr Gastroenterol Rep*, 15(300):1-7

132. Leventis P. A., Grinstein S., 2010, The distribution and function of phosphatidylserine in cellular membranes, *Annu. Rev. Biophys*., 39:407-427

133. Lepiller Q., Tripathy M. K., Di Martino V., Kantelip B., Herbein G., 2011, Increased HCMV seroprevalence in patients with hepatocellular carcinoma, *Virology Journal*, 8(485):1-10

134. Longman R. S., Braun D., Pellegrini S., Rice C. M., Darnell R. B., Albert M. L., 2007, Dendritic-cell maturation alters intracellular signaling networks, enabling differential effects of IFN-a/b on antigen cross-presentation, *Blood*, 109:1113-1122

135. Loulergue P., Pol, S., Mallet V., Sogni P., Launay O., 2009, Why actively promote vaccination in patients with cirrhosis? *Journal of Clinical Virology*, 46:206-209

136. Macal M., Lewis G. M., Kunz S., Flavell R., Harker J. A., Zuniga E. I., 2012, Plasmacytoid dendritic cells are productively infected and activated through TLR-7 early after arenavirus infection, *Cell Host & Microbe*, 11:617-630

137. MacIntyre A. N., Gerriets V. A., Nichols A. G., Michalek R. D., Rudolph M. C., Deollveira D., Anderson S. M., Abel E. D., Chen B. J., Hale L. P., Rathmell J. C., *Cell Metab*., 20(1):61-72

138. Mannino M. H., Zhu Z., Xiao H., Bai Q., Wakefield M. R., Fang Y., 2015, The paradoxical role of IL-10 in immunity and cancer, *Cancer Letters*, 367(2):103-107

139. Marra F., 1999, Hepatic stellate cells and the regulation of liver inflammation, *Journal of Hepatology*, 31:1120-1130

140. Marrack P., Kappler J., Mitchell T., 1999, Type I interferon keep activated T cells alive, *J. Exp. Med*., 189(3):512-529

141. Marshall H. D., Chandele A., Jung Y. W., Meng H., Poholek A. C., Parish I. A., Rutishauser R., Cui W., Kleinstein S. H., Craft J., Kaech S. M., 2011, Differential Expression of Ly6C and T-bet distinguish Effector and Memory Th1 CD4+ Cell Properties during Viral Infection, *Immunity*, 35,633-646

142. Marshall N. B., Swain S. L., 2011, Cytotoxic CD4 T cells in Antiviral Immunity, *Journal of Biomedicine and Biotechnology*, Article ID 954602, 8 pages

143. Marsland B. J., Nembrini C., Schmitz N., Abel B., Krautwald S., Bachmann M. F., Kopf M., 2005, Innate signals compensate for the absence of PKC-Θ during in vivo CD8+ T cell effector and memory responses, *PNAS*, 102(40):14374-14379

144. Matloubian M., Concepcion R. J., Ahmed R., 1994, CD4+ T cells are required to sustain CD8+ cytotoxic T-cell responses during chronic viral infection, *J Virol*., 68(12):8056-8063

145. McDonald D. R., Levy O., 2019, Clinical Immunology: Principles and

Practice (5th Ed.) Chapter 3 – Innate Immunity, *Elsevier*, 39-51.e1

146. McMahan R. H., Golden-Mason L., Nishimura M. I., McMahon B. J., Kemper M., Allen T. M., Gretch D. R., Rosen H. R., 2010, Tim-3 expression on PD-1+ HCV-specific human CTLs is associated with viral persistence, and its blockade restores hepatocyte-directed in vitro cytotoxicity, *J Clin Invest*., 120(12):4546-4557

147. McMichael A. J., Gotch F. M., Noble G. R:, Beare P. A. S., 1983, Cytotoxic T-cell immunity to influenza, *N Engl J Med*., 309:13-17

148. McNab F., Mayer-Barber K., Sher A., Wack A., O'Garra A., 2015, Type I interferons in infectious disease, *Nature Reviews*, 15:87-103

149. Mellman I., Steinman R. M., 2001, Dendritic Cells: Specialized and regulated antigen processing machines, *Cell*, 106:255-258

150. Merad M., Sathe P., Helft J., Miller J., Mortha A., 2013, The dendritic cell lineage: Ontogeny and function of dendritic cells and their subsets in the steady state and the inflamed setting, *Annu. Rev. Immunol.,* 31:563-604

151. Mescher M. F., Curtsinger J. M., Agarwal P., Casey K. A., Gerner M., Hammerbeck C. D., Popescu F., Xiao Z., 2006, Signals required for programming effector and memory development by CD8+ T cells, *Immunological Reviews*, 211:81-92

152. Milani S., Herbst H., Schuppan D., Kim K. Y., Riecken E. O., Stein H., 1990, Procollagen expression by non-parenchymal rat liver cells in experimental biliary fibrosis, *Gastroenterology*, 98:175-184

153. Miyoshi H., Rust C., Roberts P. J., Burgart L. J., Gores G. J., 1999, Hepatocyte apoptosis after bile duct ligation in the mouse involves Fas, *Gastroenterology*, 117:669-677

154. Montoya M., Edwards M. J., Reid D. M., Borrow P., 2005, Rapid activation of spleen dendritic cell subsets following lymphocytic choriomeningitis virus infection of mice: Analysis of the involvement of type I IFN, *J Immunol*., 174:1851-1861

155. Moskophidis D., Battegay M., van den Broek M., Laine E., Hoffmann.Rohrer U., Zinkernagel R., M., 1995, Role of virus and host variables in virus persistence or immunophathological disease caused by a non-cytolytic virus, Journal of General *Virology*, 76:381-391

156. Murphy, K., 2012, Janeway's Immuno Biology, 8th edition, *Garland Science*, ISBN:978-0-81534243-4

157. Nakatsukasa H., Nagy P., Evarts R. P., Hsis C.-C., Marsden E., Thorgeirsson S. S:, 1990, Cellular distribution of transforming growth factor-b1 and procollagen types I, III, IV transcripts in carbon tetrachloride-induced rat liver fibrosis, *J. Clin. Invest*., 85:1833-1843

158. Navarro M. N., Cantrell D. A., 2014, Serine-threonine kinases in TCR signaling, *Nature Immunology*, 15(9):808-814

159. Nikolich-Zuhich J., Slifka M. K., Messaoudi I., 2004, The many important facets of T-cell repertoire diversity, *Nature Reviews*, 4:123-132

160. Noor M. T., Manoria M., 2017, Immune dysfunction in cirrhosis, *Journal of Clinical and Translational Hepatology*, 5:50-58

161. Norris B. ., Uebelhoer L. D., Nakays H. I., Price A. A., Grakoui A., Pulendran B., 2013, Polyphasic innate immune responses to acute and chronic LCMV infection: Innate immunity to acute and chronic viral infection, *Immunity*, 38(2): doi:10.1016/j.immuni.2012.10.022

162. Nusrat S., Khan M. S., Fazili J., Madhoun M. F., 2014, Cirrhosis and its complications: Evidence based treatment, *World J Gastroenterol*, 20(18):5442-5460

163. O'Brien A. J., Fullerton J. N., Massey K. A., Auld G., Sewell G., James S., Newson J., Karra E., Winstanley A., Alazawi W., Garcia-Martinez R., Cordoba J., Nicolaou A., Gilroy D. W., 2014, Immunosuppression in acutely decompensated cirrhosis is mediated by prostaglandin E_2, *Nature Medicine*, 20(5):518-525

164. O'Brien A., China L., Massey K. A., Nicolaou A., Winstanley A., Newson J., Hobbs A., Audzevich T., Gilroy D. W., 2015, Bile duct-ligated mice exhibit multiple phenotypic similarities to acute decompensation patients despite histological differences, *Liver Int.,* 36:837-846

165. Oh J. H., Kim M. J., Choi S. J., Ban Y. H., Lee H. K., Shin E.-C., Lee K.-M., Ha S.-J., 2019, Sustained type I IFN reinforces NK-mediated cancer immunosurveillance during chronic virus infection, *Cancer Immunol Res*, 7(4):584-599

166. Openshaw P. J. M., Tregoning J. S., 2005, Immune Responses and Disease Enhancement during Respiratory Syncytial Virus Infection, *Clinical Microbiology Reviews*, 18(3):541-555

167. Ou R., Zhou S., Huang L., Morskophidis D., 2001, Critical role for alpha/beta and gamma interferons in persistence of lymphocytic choriomeningitis virus by clonal exhaustion of cytotoxic T cells, *J Virol*., 75(18):8407-8423

168. Paley M. A., Kroy D. C., Odorizzi P. M., Johnnidis J. B., Dolfi D. V., Barnett B. E., Bikoff E. K., Robertson E. J., Lauer G. M., Reiner S. L., Wherry E. J., 2012, Progenitor and terminal subsets of CD8+ T cells cooperate to contain chronic viral infection, *Science*, 338(6111);1220-1225

169. Patsoukis N., Bardhan K., Chatterjee P., Sari D., Liu B., Bell L. N., Karoly E. D., Freeman G. J., Petkova V., Seth P., Li L., Boussiotis V. A., 2015, PD-1 alters T-cell metabolic reprogramming by inhibiting glycolysis and promoting lipolysis and fatty acid oxidation, *Nature Communications*, DOI: 10.1038/ncomms7692

170. Patsoukis N., Weaver J. D., Strauss L., herbel C., Seth P., Boussiotis V. A., 2017, Immunometabolic regulations mediated by co-inhibitory receptors and their impact on T cell immune responses, *Frontiers in Immunology*, 8(330):1-19

171. Pauken K. E., Wherry E. J., 2015, Overcoming T cell exhaustion in infection and cancer, *Trends in Immunology*, http://dx.doi.org/10.1016/j.it.2015.02.008

172. Pearce E. L., Pearce E. J., 2013, Metabolic pathways in immune cell activation and quiescence, *Immunity*, 38:633-643

173. Pelletier M., Billingham L. K., Ramaswamy M., Siegel R. M., 2014, Extracellular flux analysis to monitor glycolytic rates and mitochondrial oxygen consumption, *Methods in Enzymology*, 542:125-149

174. Pestka S., Krause C. D., Walter M. R., 2004, Interferons, interferon-like

cytokines, and their receptors, *Immunological Reviews*, 202:8-32

175. Petrovas C., Casazza J. P., Brenchley J. M., Price D. A., Gostick E., Adams W. C., Precopio M. L., Schacker T., Roederer M., Douek D. C., Koup R. A., 2006, PD-1 is a regulator of virus-specific CD8+ T cell survival in HIV infection, *J Ex Med*., 203(10):2281-2292

176. Petrova V. N., Russell C. A., 2018, The evolution of seasonal influenza viruses, *Nature Reviews*, 16:47-60

177. Popescu I., Pipeling M. R., Shah P. D., Orens J. B., McDyer J. F., 2014, T-bet:Eomes balance, effector function, and proliferation of cytomegalovirus-specific CD8+ T cells during primary infection differentiates the capacity for durable control, *The Journal of Immunology*, 193:5709-5722

178. Propst-Graham K. L., Preheim L C., Vander Top E. A., Snitily M. U., Gentry-Nielsen M. J., 2007, Cirrhosis-induced defects in innate pulmonary defense against Streptococcus pneumoniae, *BMC Microbiology*, 7:94 doi:10.1186/1471-2180-7-94

179. Pythoud C., Rothenberger S., Martínez-Sobrido L., de la Torre J. C., Kunz S., 2015, Lymphocytic choriomeningitis virus differentially affects the virus-induced type I interferon response and mitochondrial apoptosis mediated by RIG-I/MAVS, *Journal of Virology*., 89(12):6240-6250

180. Rajkovic I. A., Williams R., 1986, Abnormalities of neutrophil phagocytosis, intracellular killing and metabolic activity in alcoholic cirrhosis and hepatitis, *Hepatology*, 6(2):252-262

181. Ramadori G., Saile B., 2004, Inflammation, damage repair, immune cells,

and liver fibrosis: Specific of nonspecific, this is the question, *Gastroenterology*, 127(3):997-1000

182. Ramakus S., Rubio D., Ma X., Sette A., Sigal L. J., 2012, Memory CD8+ T cells specific for a single immunodominant or subdominant determinant induced by peptide-dendritic cell immunization protect from an acute lethal viral disease, Journal of Virology, 86(18):9748-9759

183. Raué H.-P., Slifka M. K., 2009, CD8+ T cell immunodominance shifts during the early stages of acute LCMV infection independently from functional avidity maturation, *Virology*, 390:197-204

184. Rigamonti E., Chinetti-Gbaguidi G., Staels B., 2008, Regulation of macrophage functions by PPAR-a, PPAR-g, and LXRs in mice and men, *Arterioscler Thromb Vasc Biol*, 28:1050-1059

185. Robinson M. W., Harmon C., O'Farrelly C., 2016, Liver immunology and its role in inflammation and homeostasis, *Cellular and Molecular Immunology*, 13:267-276

186. Roquilly A., Villadangos J. A., 2015, The role of dendritic cell alterations in susceptibility to hospital-acquired infections during critical-illness related immunosuppression, *Molecular Immunology*, 68:120-123

187. Rosati E., Dowds C. M., Liaskous E., Hendriksen E. K. K., Karlsen T. H., Franke A., 2017, Overview of methodologies for T-cell receptor repertoire analysis, *BMC Biotechnology*, 17(61):1-16

188. Rosendahl Huber S. K., Luimstra J. J., van Beek J., Hoppes W., Jacobi R. H. J., Hendriks M., Kapteijn K., Ouwerkerk C., Rodenko B., Ovaa H., de Jonge

JJ., 2018, Chemical modification of influenza CD8+ T-cell epitopes enhances their immunogenicity regardless of immunodominance, *PLoS One*, 11(6): e0156462. doi:10.1371/journal.pone.0156462

189. Sakuishi K., Apetoh L., Sullivan J. M., Blazar B. R., Kuchroo V. K., Anderson A. C., 2010, Targeting Tim-3 and PD-1 pathways to reverse T cell exhaustion and restore anti-tumor immunity, *J. Exp. Med*., 207(10):2187-94

190. Salem M. L., Diaz-Montero M., El-Naggar S. A., Chen Y., Moussa O., Cole D. J., 2009, The TLR3 agonist poly(I:C) targets CD8+ T cells and augments their antigen-specific responses upon their adoptive transfer into naïve recipient mice, *Vaccine*, 27(4):549-557

191. Sanchez-Fueyo A., Markmann J. F., 2016, Immune Exhaustion and Transplantation, *American Journal of Transplantation*, 16(7):1953-1957

192. Saron M.-F., Riviere Y., Hovanessian A. G., Guillon J.-C., 1982, Chronic production of interferon in carrier mice congenitally infected with lymphocytic choriomeningitis virus, *Viology*, 117:253-256

193. Schietinger A., Greenberg P. D., 2014, Tolerance and Exhaustion: Defining mechanisms of T cell dysfunction, *Trends Immunol*., 35(2):51-60

194. Schuppan D., Afdahl N. H., 2008, Liver cirrhosis, *Lancet*, 371(9615):838-851

195. Schürich A., Pallett L. J., Jajbhay D., Wijngaarden J., Otano I., Gill U. S., Hansi N., Kennedy P. T., Nastouli E., Gilson R., Frezza C., Henson S. M., Maini M. K., 2016, Distinct metabolic requirements of exhausted and functional virus-specific CD8 T cells in the same host, *Cell Reports*, 16:1243-1252

196. Sckisel G. D., Bouchlaka M. N., Monjazeb A. M., Crittenden M., Curt B. D., Wiklins D. E. C., Alderson K. A., Sungur C. M., Ames E., Mirsoian A., Reddy A., Alexander W., Soulika A., Blazar B. R., Longo D. L., Wiltrout R. H., Murphy W. J., 2015, Out-of-sequence signal 3 paralyzes primary CD4+ T-cell-dependent immunity, *Immunity*, 43:240-250

197. Sebastián D., Palacín M., Zorrano A., 2017, Mitochondrial dynamics: Coupling mitochondrial fitness with healthy aging, *Trends in Molecular Medicine*, 23(3):201-215

198. Seki E., Schnabl B., 2012, Role of innate immunity and the microbiota in liver fibrosis: crosstalk between the liver and gut, *J Physiol*., 590(3):447-458

199. Sercarz E. E., Lehmann P. V., Ametani A., Benichou G., Miller A., Moudgil K., 1993, Dominance and cyrypticity of T cell antigenic determinants, *Annu. Rev. Immunol*., 11:729-766

200. Sette A., Vitiello A., Reherman B., Fowler P., Nayersina R., Kast W. M., Melief C. J., Oseroff C., Yuan L., Ruppert J., Sidney J., del Guercio M. F., Southwood S., Kubo R. T., Chesnut R. W., Grey H. M., Chisari F. V., 1994, The relationship between class I binding affinity and immunogenicity of potential cytotoxic T cell epitopes, *J Immunol*., 153(12): 5589-5592

201. Sevilla N., Kunz S., Holz A., Lewicki H., Homann D., Yamada H., Campbell K. P., de la Torre J. C., Oldstone M. B. A., 2000, Immunosuppression and Resultant Viral Persistence by Specific Viral Targeting of Dendritic Cells, *J. Exp. Med*., 192(9):1249-1260

202. Sevilla N., McGavern D. B., Teng C., Kunz S., Oldstone M. B. A., 2004, Viral targeting of hematopoietic progenitors and inhibition of DC maturation as a dual strategy for immune subversion, *J Clin Invest*., 113(5):737-745

203. Siddiqui I., Schaeuble K., Chennupati V., Fuertes Marraco S. A., Calderon-Copete S., Ferreira S. P., Carmona S. J., Scarpellino L., Gfeller D., Pradervand S., Luther S. A., Speiser D. E., Held W., 2019, Intratumoral Tcf1+PD-1+CD8+ T cells with stem-like properties promote tumor control in response to vaccination and checkpoint blockade immunotherapy, *Immunity*, 50:195-211

204. Singh M., Fuller-Pace F. V., Buchmeier M. J., Southern P. J., 1987, Analysis of the genomic L RNA segment from lymphocytic choriomenigitis virus, *Virology*, 161:448-456

205. Siska P. J., van der Windt G. J. W., Kishton R. J., Cohen S., Eisner W., MacIver N. J., Kater A. P., Weinberg J. B., Rathmell J. C., 2016, Suppression of Lut1 and glucose metabolism by decreased Akt/mTORC1 signaling drives T cell impairment in B cell leukemia, *J Immunol*, doi:10.4049/jimmunol.1502464

206. Smith L. K., Boukhaled G. M., Condotta S. A., Mazouz S., Guthmiller J. JJ., Vijay R., Butler N. S., Bruneau J., Shoukry N. H., Krawczyk C. M., Richer M. J., 2018, Interleukin-10 directly inhibits CD8+ T cell function by enhancing N-glycan branching to decrease antigen sensitivity, *Immunity*, 48:299-312

207. Sridhar S., Begom S., Bermingham A., Hoschler K., Adamson W., Carman W., Bean T., Barclay W., Deeks J. J., Lalvani A., 2013, Cellular immune correlates of protection against symptomatic pandemic influenza, *Nature Medicine*, 19(10):1305-1312

208. St Leger A. J., Jeon S., Hendricks R. L., 2013, Broadening the repertoire of functional herpes simplex virus type 1 (HSV-1)-specific CD8+ T cells reduces viral reactivation from latency in sensory ganglia, *J Immunol*., 191(5):2258-2265

209. Stöhr K., 2002, Influenza – WHO cares, *The Lancet*, 2:517

210. Sun X., Fujiwara M., Shi Y., Kuse N., Gatanaga H., Appay V., Gao G. F:, Oka S., Takiguchi M., 2014, Superimposed epitopes restricted by the same HLA molecule drive distinct HIV-specific CD8+ T cell repertoires, *The Journal of Immunology*, 193:77-84

211. Sung M-H., Zhao Y., Martin R., Simon R., 2002, T-cell epitope prediction with combinatorial peptide libraries, *Journal of Computational Biology*, 9(3):527-539

212. Swieki M., Colonna M., 2010, Unraveling the functions of plasmacytoid dendritic cells during viral infections, autoimmunity, and tolerance, *Immunological Reviews*, 234:142-162

213. Swieki M., Wang Y., Vermi W., Gilfillan S., Schreiber R. D., Colonna M., 2011, Type I interferon negatively controls plasmacytoid dendritic cell numbers in vivo, *J. Exp. Med*., 208(12):2367-2374

214. Tacke F., Zimmermann H. W., 2013, Macrophage heterogeneity in liver injury and fibrosis, *Journal of Hepatology*, 60:1090-1096

215. Tag C. G., Sauer-Lehnen S., Weiskirchen S., Borkham-Kamphost E., Tolba R. H., Tacke F., Weiskirchen R., 2015, Bile duct ligation in mice: Induction of inflammatory liver injury and fibrosis by obstructive cholestasis, *J. Vis. Exp.,* 96: e52438, doi:10.3791/52438

216. Takeda K., Kaisho T., Akira S., 2003, Toll-like receptors, *Annu. Rev. Immunol*., 21:335-376

217. Tanaka S., Toh Y., Minagawa H., Mori R., Sugimachi K., Minamishima Y., 1992, Reactivation of cytomegalovirus in patients with cirrhosis: Analysis of 122 cases, *Hepatology*, 16(6):1409-1414

218. Teijaro J. R., Ng C., Lee A. M., Sullivan B. M., Sheehan K. C. F., Welch M., Schreiber R. D., de la Torre J. C., Oldstone M. B. A., 2013, Persistent LCMV infection is controlled by blockade of type I interferon signaling, *Science*, 340:207-211

219. Teltschik Z., Wiest R., Beisner J., Nuding S., Hofmann C., Schoelmerich J., Bevins C. L., Stange E. F., Wehkamp J., 2012, Intestinal bacterial translocation in rats with cirrhosis is related to compromised paneht cell antimicrobial host defense, *Hepatology*, 55:1154-1163

220. Thompson M. R., Kaminski J. J., Kurt-Jones E. A., Fitzgerald K. A., 2011, Pattern recognition receptors and innate immune response to viral infection, *Viruses*, 3:920-940

221. Tobery W. W., Wang S., Wang X-M., Neeper M. P., Jansen K. U., McClements W. L., Caulfied M. J., 2001, A simple and efficient method for the monitoring of antigen-specific T cell responses using peptide pool arrays in a modified ELISpot assay, *Journal of Immunological Methods*, 254:59-66

222. Toor A. A., Toor A. A., Rahmani M., Manjili M. H., 2016, On the organization of human T-cell receptor loci: log-periodic distribution of T-cell receptor gene

segments, *J. R. Soc. Interface*., 13: 20150911.http://dx.doi.org/10.1098/rsif.2015.0911

223. Tong J. C., Tan T. W., Tanganathan S., 2006, Methods and protocols for prediction of immunogenic epitopes, *Briefings in Bioinformatics*, 8(2):96-108

224. Tritto G., Bechlis Z., Stadlbauer V., Davies N., Francés R., Shah N., Mookerjee R. P., Such J., Jalan R., 2011, Evidence of neutrophil functional defect despite inflammation in stable cirrhosis, *Journal of Hepatology*, 55:574-581

225. Tscharke D. C., Croft N. P., Doherty P. C., La Gruta N., 2015, Sizing up the key determinants of the CD8+ T cell response, *Nature Reviews*, 15:705-716

226. Urban S. L., Berg L. J., Welsh R. M., 2016, Type I interferon licenses naïve CD8+ T cells to mediate anti-viral cytotoxicity, *Virology*, 493:52-59

227. Utzschneider D. T., Charmoy M., Chennupati V., Pousse L., Ferreira D. P., Calderon-Copete S., Danilo M., Alfei F., Hofmann M., Wieland D., Pradervand S., Thimme R., Zehna D., Held W., 2016, T cell factor 1-expressing memory-like CD8+ T cells sustain the immune response to chronic viral infections, *Immunity*, 45:415-427

228. Vallejo A. N., Weyand C. M., Goronzy J. J., 2004, T-cell senescence: a culprit of immune abnormalities in chronic inflammation and persistent infection, *Trends in Molecular Medicine*, 10(3):121-124

229. van der Windt G. J., W., Pearce E. L., 2012, Metabolic switching and choice during T-cell differentiation and memory development, *Immunological Reviews*, 249:27-42

230. van der Windt G. J. W., Everts B., Chang C.-H., Curtis J. D., Freitas T. C., Amiel E., Pearce E. J., Pearce E. L., 2012, Mitochondrial respiratory capacity is a critical regulator of CD8+ T cell memory development, *Immunity*, 36:68-78

231. Varani S., Lazzarotto T., Margotti M., Masi L., Gramantieri L., Bolondi L., Landini M. P., 2000, Laboratory signs of acute or recent cytomegalovirus infection are common in cirrhosis of the liver, *Journal of Medical Virology*, 63:25-28

232. Wai T., Langer T., 2016, Mitochondrial dynamics and metabolic regulation, *Trends in Endocrinology & Metabolism*, 27(2):105-117

233. Ward N. S., Casserly B., Ayala A., 2008, The compensatory anti-inflammatory response syndrome (CARS) in critically ill patients, *Clin Chest Med*., 29(4):617-viii

234. Welsh R. M., Che J., W., Brehm M. A., Selin L. K., 2010, Heterologous immunity against viruses, *Immunological Review*, 235:244-266

235. Wherry E. J., Blattman J. N., Murali-Krishna K., van der Most R., Ahmed R., 2003, Viral persistence alters CD8 T-cell immunodominance and tissue distribution and results in distinct stages of functional impairment, *Journal of Virology*, 77(8):4911-4927

236. Wherry E. J., Ha S.-J., Kaech S. M., Haining W. N., Sarkar S., Kalia V., Subramaniam S., Blattman J. N., Barber D. L., Ahmed R., 2007, Molecular signature of CD8+ T cell exhaustion during chronic viral infection, *Immunity*, 27:670-684

237. Whynn T. A., Chawla A., Pollard J. W., 2013, Macrophage biology in development, homeostasis and disease, *Nature*, 496:445-455

238. Wieczorek M., Abualrous E. T., Sticht J., Álvaro-Benito M-. Stolzberg S., Noé F., Freund C., 2017, Major histocompatibility complex (MHC) class I and MHC class II proteins: Conformational plasticity in antigen presentation, *Frontiers in Immunology*, 8(292): doi: 10.3389/fimmu.2017.00292

239. Wiesel M., Crouse J., Bedenikovic G., Sutherland A., Joller N., Oxenius A., 2012, Type-I IFN drives the differentiation of short-lived effector CD8+ T cells in vivo, *Eur. J. Immunol*., 42:320-329

240. Wiesel M., Walton S., Richter K., Oxenius A., 2009, Virus-specific CD8 T cells: activation, differentiation and memory formation, *The Authors Journal Compilation (AMPIS),* 117:356-381

241. Wiest R., Garcia-Tsao G., 2005, Bacterial translocation (BT) in cirrhosis, *Hepatology*, 41(3):422-433

242. Wilson E. B., Yamada D. H., Elsaesser H., Herskovitz J., Deng J., Cheng G., Aronow B. J., Karp C. L., Brooks D. G., 2013, Blockade of chronic type I interferon signaling to control persistent LCMV infection, *Science*, 340(6129):202-207

243. Wu T., Guan J., Handel A., Tscharke D. C., Sidney J., Sette A., Wakim L. M., Sng X. Y. X., Thomas P. G., Croft N. P., Purcell A. W., La Gruta N. L., 2019, Quantification of epitope abundance reveals the effect of direct and cross-presentation on influenza CTL responses, *Nature Communications*, 10(2846): https://doi.org/10.1038/s41467-019-10661-8

244. Yi J. S., Cox M. A., Zajay A. J., 2010, T-cell exhaustion: characteristics, causes and conversion, *Immunology*, 129:474-478

245. Yuzefpolskiy Y., Baumann F. M., Kalia V., Sarkar S., 2015, Early CD8 T-cell memory precursors and terminal effectors exhibit equipotent in vivo degranulation, *Cellular & Molecular Immunology*, 12, 400-408

246. Zanker D., Waithman J., Yewdell J. W., Chen W., 2013, Mixed proteasomes function to increase viral peptide diversity and broaden antiviral CD8+ T cell responses, *Journal of Immunology*, 191:000-000, doi:10.4049/jimmunol.1300802

247. Zhong W., Reche P. A., Lai C-C., Reinhold B., Reinherz E. L., 2003, Genome-wide characterization of a viral cytotoxic T lymphocyte epitope repertoire, *The Journal of Biological Chemistry*, 278(46);14:45135-45144

248. Zhou S., Cerny A. M., Zacharia A., Fitzgerald K. A., Kurt-Jones E. A., Finberg R. W., 2010, Induction and inhibition of type I interferon responses by distinct components of lymphocytic choriomeningitis virus, *Journal of Virology*, 84(18):9452-9462

249. Zhou W.-C., Zhang Q.-B., Qiao L., 2014, Pathogenesis of liver cirrhosis, *World J Gastroenterol*., 20(23):7312-7324

250. Zhou X., Ramachandran S., Mann M., Popkin D. L., 2012, Role of Lymphocytic Choriomenigitis Virus (LCMV) in Understanding Viral Immunology: Past, Present and Future, *Viruses*, 4:2650-2669

251. Zuniga E. I., Liou Li-Y., Mack L., Mendoza M., Oldstone B. A., 2008, Persistent virus infection inhibits type I interferon production by plasmacytoid

dendritic cells to facilitate opportunistic infections, *Cell Host and Microbe*, 4:374-386

252. Zuniga E. I., Macal M., Lewis G. M., Harker J. A., 2015, Innate and adaptive immune regulation during chronic viral infections, *Annu Rev Virol*., 2(1):573-597

Curriculum Vitae – Lisa Mareike Assmus

Publications

Hackstein[*] C.-P., Assmus[*] L. M., Welz M., Klein S., Schwandt T., Schultze J., Förster I., Gondorf F., Beyer M., Kroy D., Kurts C., Jonel T., Kastenmüller W., Knolle[#] P. A., Abdullah[#] Z., 2016, Gut microbial translocation corrupts myeloid cell function to control bacterial infection during liver cirrhosis, *Gut*, 0:1–12. doi:10.1136/gutjnl-2015-311224

Namineni S., O'Connor T., Faure-Dupuy S., Johansen P., Riedl T., Liu K., Xu H., Shinde P., Li F., Pandyra A., Sharma P., Ringelhan M., Muschaweckh A., Borst K., Blank P., Lamapl S., Durantel D., Farhat R., Weber A., Lenggenhager D., Kundig T. M., Staeheli P., Protzer U., Wohlleber D., Holzmann B., Binder M., Breuhahn K., Assmus L. M., Nattermann J., Abdullah Z., Rolland M., Dejardin E., Lang P. A., Lang K. S., Karin M., Lucifora J., Kalinke U., Knolle P., Heikenwaelder M., 2019; A dual role for hepatocyte-intrinsic canonical NF-κB signaling in virus control, *Journal of Hepatology*, accepted

*Equal contribution
[#] Senior authors